



Process Design and Economics for the Conversion of Lignocellulosic Biomass to Hydrocarbons: Dilute-Acid and Enzymatic Deconstruction of Biomass to Sugars and Biological Conversion of Sugars to Hydrocarbons

R. Davis, L. Tao, E.C.D. Tan, M.J. Bidy,
G.T. Beckham, and C. Scarlata
National Renewable Energy Laboratory

J. Jacobson and K. Cafferty
Idaho National Laboratory

J. Ross, J. Lukas, D. Knorr, and P. Schoen
Harris Group Inc.

**NREL is a national laboratory of the U.S. Department of Energy
Office of Energy Efficiency & Renewable Energy
Operated by the Alliance for Sustainable Energy, LLC.**

This report is available at no cost from the National Renewable Energy
Laboratory (NREL) at www.nrel.gov/publications.

Technical Report
NREL/TP-5100-60223
October 2013

Contract No. DE-AC36-08GO28308

Process Design and Economics for the Conversion of Lignocellulosic Biomass to Hydrocarbons:

Dilute-Acid and Enzymatic Deconstruction of Biomass to Sugars and Biological Conversion of Sugars to Hydrocarbons

R. Davis, L. Tao, E.C.D. Tan, M.J. Bidy,
G.T. Beckham, and C. Scarlata
National Renewable Energy Laboratory

J. Jacobson and K. Cafferty
Idaho National Laboratory

J. Ross, J. Lukas, D. Knorr, and P. Schoen
Harris Group Inc.

Prepared under Task No. BB07.2410

**NREL is a national laboratory of the U.S. Department of Energy
Office of Energy Efficiency & Renewable Energy
Operated by the Alliance for Sustainable Energy, LLC.**

This report is available at no cost from the National Renewable Energy Laboratory (NREL) at www.nrel.gov/publications.

NOTICE

This report was prepared as an account of work sponsored by an agency of the United States government. Neither the United States government nor any agency thereof, nor any of their employees, makes any warranty, express or implied, or assumes any legal liability or responsibility for the accuracy, completeness, or usefulness of any information, apparatus, product, or process disclosed, or represents that its use would not infringe privately owned rights. Reference herein to any specific commercial product, process, or service by trade name, trademark, manufacturer, or otherwise does not necessarily constitute or imply its endorsement, recommendation, or favoring by the United States government or any agency thereof. The views and opinions of authors expressed herein do not necessarily state or reflect those of the United States government or any agency thereof.

This report is available at no cost from the National Renewable Energy Laboratory (NREL) at www.nrel.gov/publications.

Available electronically at <http://www.osti.gov/bridge>

Available for a processing fee to U.S. Department of Energy and its contractors, in paper, from:

U.S. Department of Energy
Office of Scientific and Technical Information
P.O. Box 62
Oak Ridge, TN 37831-0062
phone: 865.576.8401
fax: 865.576.5728
email: <mailto:reports@adonis.osti.gov>

Available for sale to the public, in paper, from:

U.S. Department of Commerce
National Technical Information Service
5285 Port Royal Road
Springfield, VA 22161
phone: 800.553.6847
fax: 703.605.6900
email: orders@ntis.fedworld.gov
online ordering: <http://www.ntis.gov/help/ordermethods.aspx>

Cover Photos: (left to right) photo by Pat Corkery, NREL 16416, photo from SunEdison, NREL 17423, photo by Pat Corkery, NREL 16560, photo by Dennis Schroeder, NREL 17613, photo by Dean Armstrong, NREL 17436, photo by Pat Corkery, NREL 17721.



Printed on paper containing at least 50% wastepaper, including 10% post consumer waste.

Executive Summary

The U.S. Department of Energy (DOE) promotes the production of a range of liquid fuels and fuel blendstocks from lignocellulosic biomass feedstocks by funding fundamental and applied research that advances the state of technology in biomass collection, conversion, and sustainability. As part of its involvement in this program, the National Renewable Energy Laboratory (NREL) investigates the conceptual production economics of these fuels.

Between 1999 and 2012, NREL conducted a campaign to quantify the economic implications associated with measured conversion performance for the biochemical production of cellulosic ethanol, with a formal program between 2007–2012 to set cost goals and to benchmark annual performance toward achieving these goals, namely the pilot-scale demonstration by 2012 of biochemical ethanol production at a price competitive with petroleum gasoline based on modeled assumptions for an “*n*th” plant biorefinery. This goal was successfully achieved through NREL’s 2012 pilot plant demonstration runs, representing the culmination of NREL research focused specifically on cellulosic ethanol, and a benchmark for industry to leverage as it commercializes the technology. This important milestone also represented a transition toward a new Program focus on infrastructure-compatible hydrocarbon biofuel pathways, and the establishment of new research directions and cost goals across a number of potential conversion technologies.

This report describes in detail one potential conversion process to hydrocarbon products by way of biological conversion of lignocellulosic-derived sugars. The pathway model leverages expertise established over time in core conversion and process integration research at NREL, while adding in new technology areas primarily for hydrocarbon production and associated processing logistics. The overarching process design converts biomass to a hydrocarbon intermediate, represented here as a free fatty acid, using dilute-acid pretreatment, enzymatic saccharification, and bioconversion. Ancillary areas—feed handling, hydrolysate conditioning, product recovery and upgrading (hydrotreating) to a final blendstock material, wastewater treatment, lignin combustion, and utilities—are also included in the design. Detailed material and energy balances and capital and operating costs for this baseline process are also documented.

This benchmark case study techno-economic model provides a production cost for a cellulosic renewable diesel blendstock (RDB) that can be used as a baseline to assess its competitiveness and market potential. It can also be used to quantify the economic impact of individual conversion performance targets and prioritize these in terms of their potential to reduce cost. The analysis presented here also includes consideration of the life-cycle implications of the baseline process model, by tracking sustainability metrics for the modeled biorefinery, including greenhouse gas (GHG) emissions, fossil energy demand, and consumptive water use.

Building on prior design reports for biochemical ethanol production in 1999, 2002, and 2011, NREL, together with the Harris Group Inc., performed a feasibility-level analysis for a plausible conversion pathway to RDB to meet an intermediate DOE cost goal of \$5/gallon gasoline equivalent (GGE) by 2017. The modeled biorefinery processes 2,205 dry ton biomass/day and achieves an RDB selling price of \$5.10/GGE in 2011\$ as determined by modeled conversion targets and “*n*th-plant” project costs and financing, associated with a process RDB yield of 45.4 GGE/dry ton. In addition, the report includes a high-level discussion on improvements needed to achieve a final 2022 DOE target of \$3/GGE moving forward, focused on coproducts from lignin.

Biological Renewable Diesel Blendstock (RDB) Process Engineering Analysis

Dilute Acid Pretreatment, Enzymatic Hydrolysis, Hydrocarbon (FFA) Bioconversion, Hydrotreating to Paraffins (RDB)

All Values in 2011\$

Minimum Fuel Selling Price (MFSP): \$5.35 /gal
MFSP (Gasoline-Equivalent Basis): \$5.10 /GGE

Contributions:	Feedstock	\$1.85 /gal (\$1.76/GGE)
	Enzymes	\$0.39 /gal (\$0.37/GGE)
	Non-Enzyme Conversion	\$3.11 /gal (\$2.96/GGE)
	RDB Production	31.3 MMgal/yr (at 68 °F) (32.9 MM GGE/yr)
	RDB Yield	43.3 gal / dry U.S. ton feedstock (45.4 GGE/ton)
	Bioconversion Metabolic Yield	0.284 kg FFA/kg total sugars (79% of theoretical)
	Feedstock + Handling Cost	\$80.00 /dry U.S. ton feedstock
	Internal Rate of Return (After-Tax)	10%
	Equity Percent of Total Investment	40%

Capital Costs	
Pretreatment	\$51,400,000
Neutralization/Conditioning	\$2,200,000
Enzymatic Hydrolysis/Conditioning/Bioconversion	\$75,400,000
On-site Enzyme Production	\$12,400,000
Product Recovery + Upgrading	\$26,600,000
Wastewater Treatment	\$60,100,000
Storage	\$3,400,000
Boiler/Turbogenerator	\$76,000,000
Utilities	\$8,800,000
Total Installed Equipment Cost	\$316,300,000
Added Direct + Indirect Costs	\$266,400,000
(% of TCI)	46%
Total Capital Investment (TCI)	\$582,700,000
Installed Equipment Cost/Annual Gallon	\$10.09
Total Capital Investment/Annual Gallon	\$18.59
Loan Rate	8.0%
Term (years)	10
Capital Charge Factor (Computed)	0.135
Carbon Retention Efficiencies:	
From Hydrolysate Sugar (Fuel C / Sugar C)	49.5%
From Biomass (Fuel C / Biomass C)	26.2%
Maximum Yields (100% of Theoretical) ^a	
FFA Production (U.S. ton/yr)	172,465
Current FFA Production (U.S. ton/yr) ^b	117,587
Current Yield (Actual/Theoretical)	68.2%

^a Complete conversion of biomass carbohydrates to C16 fatty acid

^b Recovered FFA yield after concentration, sent to hydrotreating
 (Theoretical yields above do not consider refining to final RDB product, as refining yield varies with catalyst and conditions)

Manufacturing Costs (cents/gal RDB product)	
Feedstock + Handling	184.9
Sulfuric Acid	6.2
Ammonia (pretreatment conditioning)	3.6
Caustic	6.5
Glucose (enzyme production)	21.7
Hydrogen	8.4
Other Raw Materials	19.2
Waste Disposal	4.5
Net Electricity	-16.3
Fixed Costs	44.9
Capital Depreciation	58.7
Average Income Tax	34.1
Average Return on Investment	158.5

Manufacturing Costs (\$/yr)	
Feedstock + Handling	\$57,900,000
Sulfuric Acid	\$1,900,000
Ammonia (pretreatment conditioning)	\$1,100,000
Caustic	\$2,000,000
Glucose (enzyme production)	\$6,800,000
Hydrogen	\$2,600,000
Other Raw Materials	\$6,000,000
Waste Disposal	\$1,400,000
Net Electricity	-\$5,100,000
Fixed Costs	\$14,100,000
Capital Depreciation	\$18,400,000
Average Income Tax	\$10,700,000
Average Return on Investment	\$49,600,000

Specific Operating Conditions	
Enzyme Loading (mg/g cellulose)	10
Saccharification Time (days)	3.5
Bioconversion Time (days)	2.9
Bioconversion FFA titer (wt%)	9%
Excess Electricity (kWh/gal)	2.6
Plant Electricity Use (kWh/gal)	11

Figure ES-1. Economic summary for diesel blendstock production

Table of Contents

Executive Summary	i
Acronyms	v
1 Introduction.....	1
1.1 Background and Motivation	1
1.2 Process Overview	3
1.3 Techno-Economic Analysis Approach	6
1.4 About n^{th} -Plant Assumptions.....	7
1.5 About the NREL Aspen Model.....	8
2 Design Basis and Conventions.....	9
2.1 Plant Size	9
2.2 Feedstock Composition.....	9
2.3 Updated Modeling Basis	10
2.4 Design Report Conventions	11
2.4.1 Units	11
2.4.2 Total Solids Loading.....	11
2.4.3 Product Density and Heating Value	11
3 Process Design and Cost Estimation Details	12
3.1 Area 100: Feedstock Storage and Handling	12
3.1.1 Overview	12
3.1.2 Design Basis	15
3.1.3 Cost Estimation	16
3.2 Area 200: Pretreatment and Conditioning.....	16
3.2.1 Overview	16
3.2.2 Design Basis	18
3.2.3 Cost Estimation	21
3.2.4 Achieving the Design Case	22
3.3 Area 300: Enzymatic Hydrolysis, Hydrolysate Conditioning, and Bioconversion	23
3.3.1 Overview	23
3.3.2 Design Basis	24
3.3.3 Cost Estimation	36
3.3.4 Achieving the Design Case.....	37
3.3.4.1 Biomass Deconstruction (Pretreatment + Enzymatic Hydrolysis).....	38
3.3.4.2 Bioconversion.....	39
3.3.4.3 Low-Cost Media	42
3.4 Area 400: Cellulase Enzyme Production	42
3.4.1 Overview	42
3.4.2 Design Basis	43
3.4.3 Cost Estimation	45
3.4.4 Enzyme Cost Discussion	46
3.5 Area 500: Product Recovery and Upgrading	47
3.5.1 Overview	47
3.5.2 Design Basis	48
3.5.3 Cost Estimation	52
3.6 Area 600: Wastewater Treatment	53
3.6.1 Overview	53
3.6.2 Design Basis	55
3.6.3 Cost Estimation	57
3.7 Area 700: Product and Feed Chemical Storage	58
3.7.1 Overview	58
3.7.2 Design Basis	58
3.7.3 Cost Estimation	59
3.8 Area 800: Combustor, Boiler, and Turbogenerator.....	59
3.8.1 Overview	59
3.8.2 Design Basis	59

3.8.3	Cost Estimation	60
3.9	Area 900: Utilities	60
3.9.1	Overview	60
3.9.2	Design Basis	61
3.9.3	Cost Estimation	63
4	Process Economics	64
4.1	About Cost-Year Indices	64
4.2	Total Capital Investment	65
4.3	Variable Operating Costs	67
4.4	Fixed Operating Costs	69
4.5	Discounted Cash Flow Analysis and the Minimum Selling Price of Fuel.....	70
4.5.1	Discount Rate.....	70
4.5.2	Equity Financing.....	71
4.5.3	Depreciation	71
4.5.4	Taxes.....	72
4.5.5	Construction Time	72
4.5.6	Start-Up Time	73
4.5.7	Working Capital	73
5	Analysis and Discussion	76
5.1	Carbon and Water Balances	76
5.2	Sustainability Metrics for 2017 Base Model.....	79
5.3	Cost Sensitivity Analysis	82
5.3.1	Single-Point Sensitivity Analysis	82
5.3.2	Evaluation of Alternative Metabolic Pathways	85
6	Paths Forward to \$3/GGE	88
6.1	Lignin Utilization: Technical Context	89
6.2	Lignin Utilization: TEA Modeling/Analysis.....	93
6.3	Lignin Utilization: Sustainability Analysis	97
7	Concluding Remarks.....	102
7.1	Summary.....	102
7.2	Future Work	103
	References	105
	Appendix A. Individual Equipment Cost Summary	113
	Appendix B. Discounted Cash Flow Rate of Return Worksheet.....	120
	Appendix C. Process Parameters/Operating Summary.....	122
	Appendix D. Aspen Plus Properties.....	123
	Appendix E. Process Flow Diagrams.....	128

Acronyms

BETO	Bioenergy Technologies Office	MM	million
BFW	boiler feed water	MVR	mechanical vapor recompression
BLS	Bureau of Labor Statistics	MYPP	BETO's Multi-Year Program Plan
CBP	consolidated bioprocessing	NPV	net present value
CIP	clean-in-place	NREL	National Renewable Energy Laboratory
COD	chemical oxygen demand	OTR	oxygen transfer rate
CSL	corn steep liquor	OUR	oxygen uptake rate
DAP	diammonium phosphate	PFD	process flow diagram
DCFROR	discounted cash flow rate of return	PSA	pressure swing adsorption
DCO	decarboxylation	RDB	renewable diesel blendstock
DOE	U.S. Department of Energy	SCFM	standard cubic feet per minute
FCI	fixed capital investment	SHF	separate (or sequential) hydrolysis and fermentation
FFA	free fatty acid	SOT	annual State of Technology case
FGD	flue gas desulfurization	SSCF	simultaneous saccharification and co-fermentation
GBT	gravity belt thickener	TAN	total acid number
GGE	gallon gasoline equivalent	TCI	total capital investment
GHG	greenhouse gas	TDC	total direct cost
HDO	hydrodeoxygenation	TEA	techno-economic analysis
HHV	higher heating value	TS	total solids
HMF	5-hydroxymethyl furfural	VOC	volatile organic compound
INL	Idaho National Laboratory	VVM	volume (of gas) per volume (of liquid) per minute
IS	insoluble solids	WWT	wastewater treatment
IRR	internal rate of return		
ISBL	inside battery limits (of the plant)		
LCA	life cycle assessment		
LHV	lower heating value		
MESP	minimum ethanol selling price		
MFSP	minimum fuel selling price		

1 Introduction

1.1 Background and Motivation

The U.S. Department of Energy (DOE) Bioenergy Technologies Office (BETO) promotes the production of liquid fuels from lignocellulosic feedstocks by sponsoring programs in fundamental and applied research that aim to advance the state of biomass conversion technology. These programs include laboratory research to develop improved cellulose hydrolysis enzymes and metabolic conversion microorganisms through synthetic biology, detailed engineering studies of potential processes, and construction of pilot-scale demonstration and production facilities. This research is conducted by national laboratories, universities, and private industry in conjunction with engineering and construction companies.

To support the DOE program, the National Renewable Energy Laboratory (NREL) investigates the process design and economics of cellulosic biofuel manufacturing in order to develop an absolute plant-gate price for fuels and fuel blendstocks based on process and plant design assumptions consistent with applicable best practices in engineering, construction, and operation. This plant-gate price is referred to as the *minimum fuel selling price* or MFSP. The MFSP can be used by DOE to assess the cost-competitiveness and market penetration potential of a given cellulosic biofuel technology pathway in comparison with petroleum-derived fuels and established biofuel technologies such as starch- or sugar-based ethanol.

The techno-economic analysis (TEA) effort at NREL also helps to direct biomass conversion research by examining the sensitivity of the MFSP to process alternatives and research advances. Proposed research and its anticipated results can be translated into a new MFSP that can be compared to the benchmark case documented in this report. Such comparison helps to quantify the economic impact of core research targets at NREL and elsewhere and to track progress toward meeting competitive cost targets. It also allows DOE to make more informed decisions about research proposals that claim to reduce MFSP.

For more than 10 years, NREL has developed design case models and associated reports that document process and cost targets for ethanol production from cellulosic feedstocks via biochemical conversion (e.g., deconstruction to monomeric sugars followed by fermentation to ethanol), based on the best understanding of the technology and equipment costs at the time. Early reports were established in 1999 [1] and in 2002 [2] to establish a target model aimed initially at producing ethanol at a price competitive with traditional corn-based ethanol. Over the following 9 years, a great deal of progress was made to better quantify R&D conversion performance and process economics (namely equipment costs) for a commercial-scale cellulosic biorefinery. To reflect these learnings, NREL revisited the biochemical ethanol design report in detail in 2011 to incorporate recent research progress in the conversion areas (pretreatment, conditioning, enzymatic hydrolysis, and fermentation), optimizations in product recovery, and an increased understanding of the ethanol plant's back end (separation, wastewater, and utilities), in conjunction with an engineering subcontractor (Harris Group Inc.) to refine cost estimates based on more thorough vendor feedback. This updated report detailed a more rigorous and robust pathway model with a new minimum ethanol selling price (MESP) target of \$2.15/gal [3], intended to approximate cost competitiveness with *petroleum gasoline* (versus corn grain ethanol) consistent with new DOE cost targets for 2012 [4] (see Figure 1). Subsequently, NREL did meet the important milestone of demonstrating achievement of the \$2.15/gal MESP target

based on a modeled 2,000 dry metric ton/day integrated “nth-plant” facility using process performance data garnered from NREL pilot-scale demonstration runs in 2012 [5, 6].

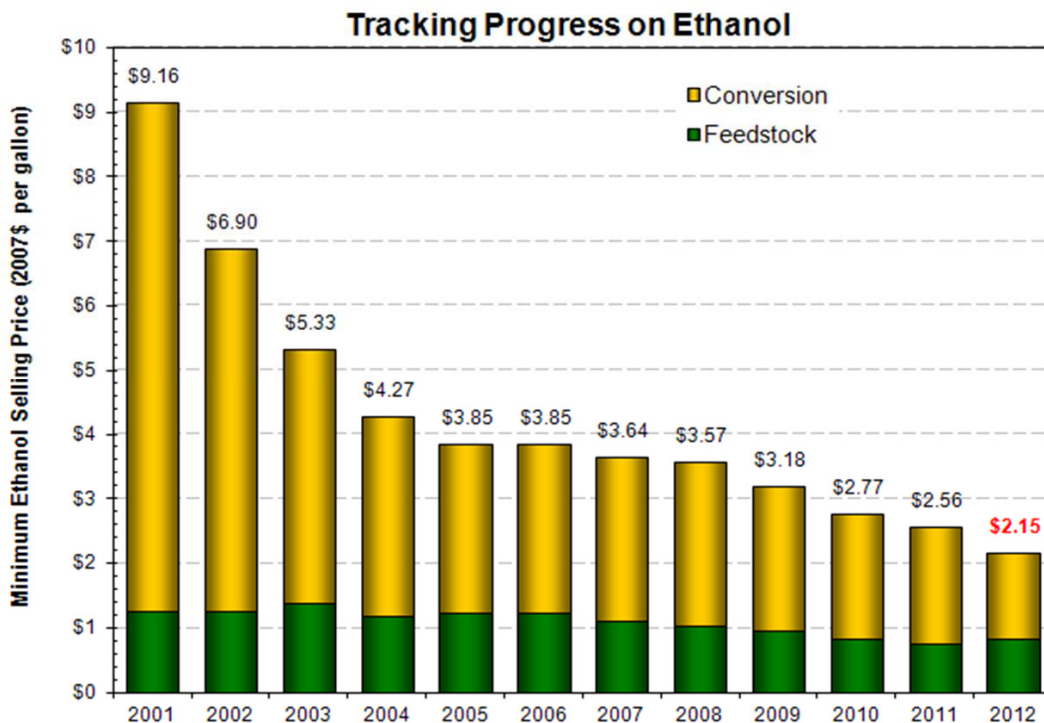


Figure 1. Ethanol State of Technology, 2001–2012, using updated 2011 model framework [3, 7–9]

While further room for improvement exists to continue reducing ethanol costs, the achievement of the 2012 MESP target represented the culmination and closeout of NREL’s primary charter to demonstrate technology improvements required to de-risk the technology in support of moving it toward commercialization, and to provide a benchmark for private industry to expand upon. Moving forward, DOE-BETO is transitioning its core platform focus from ethanol to hydrocarbon fuel and blendstock products (fungible/infrastructure-compatible fuels), including a new pathway MFSP cost target of \$3/gallon gasoline equivalent (GGE) in 2022 for the biological sugar conversion platform, with an interim target of \$5/GGE in 2017 [10]. The focus of this report is to document a plausible pathway model for biological conversion of cellulosic sugars to hydrocarbon blendstock products in the diesel boiling range, primarily to enable achieving the 2017 interim cost goal, but with additional insight provided for a path forward to ultimately meet the 2022 target of \$3/GGE.

This analysis leverages the decades of experience that NREL has established in biochemical conversion research, primarily with respect to the front end of the process for biomass pretreatment and enzymatic deconstruction to sugars, which largely remain the same as previously documented but with more aggressive targets. Likewise, the work also builds upon NREL’s earlier models, including the 2011 ethanol design model, as well as continuing the practice of consulting with vendors through the assistance of an engineering company to assist in design and cost estimation for critical unit operations. For the present report, NREL worked with Harris Group to provide engineering support primarily for new or modified unit operations

relative to the 2011 ethanol basis, which is based in large part on vendor quotations. Thus, the economics of this conceptual process uses the best available equipment and raw material costs and an “*n*th-plant” project cost structure and financing. The projected 2017 *n*th-plant MFSP computed in this report is \$5.10/GGE (\$5.35/gal) in 2011\$.

Modifications to the conceptual process design presented here will be reflected annually through NREL’s State of Technology (SOT) reports. These ensure that the process design and its cost benchmarks incorporate the most current data from equipment vendors, NREL, and other DOE-funded research.

Similar to caveats noted in prior NREL design reports, we stress that this design report serves to describe a *single, feasible* biological conversion process and to transparently document the assumptions and details that went into its design. This report is not meant to provide an exhaustive survey of process alternatives or cost-sensitivity analyses. Furthermore, it is important to note that the various technologies and metabolic pathways to diesel-range hydrocarbon products from biomass are generally less well-understood and more complex than cellulosic ethanol production (which is supported by decades of research), and thus intrinsically carry a higher degree of uncertainty in the model inputs and assumptions utilized here. Moving forward, as the science and technology progress for less well-defined areas of the process such as metabolic conversion and lignin deconstruction and upgrading, the process models and economic tools developed for this report may be updated in a similar fashion as the ethanol design report iterations have evolved.

1.2 Process Overview

The process described here uses preprocessing (deacetylation) and co-current dilute-acid pretreatment of lignocellulosic biomass (primarily corn stover), followed by enzymatic hydrolysis (saccharification) of the remaining cellulose, followed by hydrolysate conditioning and bioconversion of the resulting hexose and pentose sugars to diesel-range fatty acids. The process design also includes feedstock handling and storage, product purification, product upgrading (hydrotreating) to straight-chain paraffin blendstocks, wastewater treatment (WWT), lignin combustion, product storage, and required utilities. The process is divided into nine areas (see Figure 2).

Area 100: Feed handling. The feedstock, in this case milled corn stover blended with switchgrass, is delivered to the feed handling area from a uniform-format feedstock supply system. Only minimum storage and feed handling are required. From there, the biomass is conveyed to the pretreatment reactor (Area 200).

Area 200: Pretreatment and conditioning. In this area, the biomass is processed in an alkaline deacetylation step to solubilize and remove acetate and other non-fermentable components, then drained and treated with dilute sulfuric acid catalyst at a high temperature for a short time to liberate the hemicellulose sugars and break down the biomass for enzymatic hydrolysis. Ammonia is then added to the whole pretreated slurry to raise its pH to ~5 for enzymatic hydrolysis.

Area 300: Enzymatic hydrolysis, hydrolysate conditioning, and bioconversion. Enzymatic hydrolysis is initiated in a high-solids continuous reactor using a cellulase enzyme prepared

onsite. The partially hydrolyzed slurry is next batched to one of several parallel bioreactors. Hydrolysis is completed in the batch reactor with a total hydrolysis time of 3.5 days between the continuous and batch steps. The slurry is then fed to a vacuum filter press to remove insoluble solids (namely lignin), and the remaining soluble sugar stream is split into a small fraction that is sent directly to the fed-batch bioreactors to initiate conversion and a larger fraction that is concentrated in a vacuum evaporation system to concentrate the sugar components. The solids fraction exiting the filter press is sent to the combustor (Area 800). The concentrated sugar slurry exiting the evaporators is cooled and inoculated with the generic bioconversion microorganism. The conversion step proceeds in fed-batch mode under aerobic reactor conditions. After a total of 2.9 days of conversion in the bioreactor, most of the cellulose and xylose have been converted to free fatty acids (FFAs). The resulting broth is sent to the product recovery train (Area 500).

Area 400: Cellulase enzyme production. The on-site enzyme production section was maintained in this design, consistent with the details provided in the 2011 ethanol report. Purchased glucose (corn syrup) is the primary carbon source for enzyme production. Media preparation involves a step in which a portion of the glucose is converted to sophorose to induce cellulase production. The enzyme-producing fungus (modeled after *Trichoderma reesei*) is grown aerobically in fed-batch bioreactors. The entire fermentation broth, containing the secreted enzyme, is fed to Area 300 to carry out enzymatic hydrolysis.

Area 500: Product recovery and upgrading. The FFA product is secreted from the organism during the conversion step in A300 and is phase-separated from water via decantation and centrifugation. The heavy liquid (water) phase is sent to WWT (Area 600), while the recovered FFA product (> 99% purity) is sent to product upgrading in an on-site hydrotreating facility (including reactors, fresh and recycle gas compressors, flash columns, and product fractionation, utilizing purchased hydrogen). The primary product from the hydrotreating section is a diesel-range paraffinic product suitable as a diesel blendstock. The hydrotreating section also includes a pressure swing adsorption (PSA) unit in the recycle gas loop to remove carbon dioxide (CO₂) generated during decarboxylation.

Area 600: Wastewater treatment. Plant wastewater streams are treated by anaerobic and aerobic digestion. The methane-rich biogas from anaerobic digestion is sent to the combustor (Area 800), where sludge from the digesters is also burned. The treated water is suitable for recycling and is returned to the process.

Area 700: Storage. This area provides bulk storage for chemicals used and produced in the process, including corn steep liquor (CSL), ammonia, sulfuric acid, nutrients, water, and product.

Area 800: Combustor, boiler, and turbogenerator. The solids from the filter press and WWT are combusted along with the biogas from anaerobic digestion and the tailgas from the hydrotreater PSA unit to produce high-pressure steam for electricity production and process heat. Most of the process steam demand is in the pretreatment reactor. The boiler produces excess steam that is converted to electricity for use in the plant and for sale to the grid.

Area 900: Utilities. This area includes a cooling water system, chilled water system, process water manifold, and power systems.

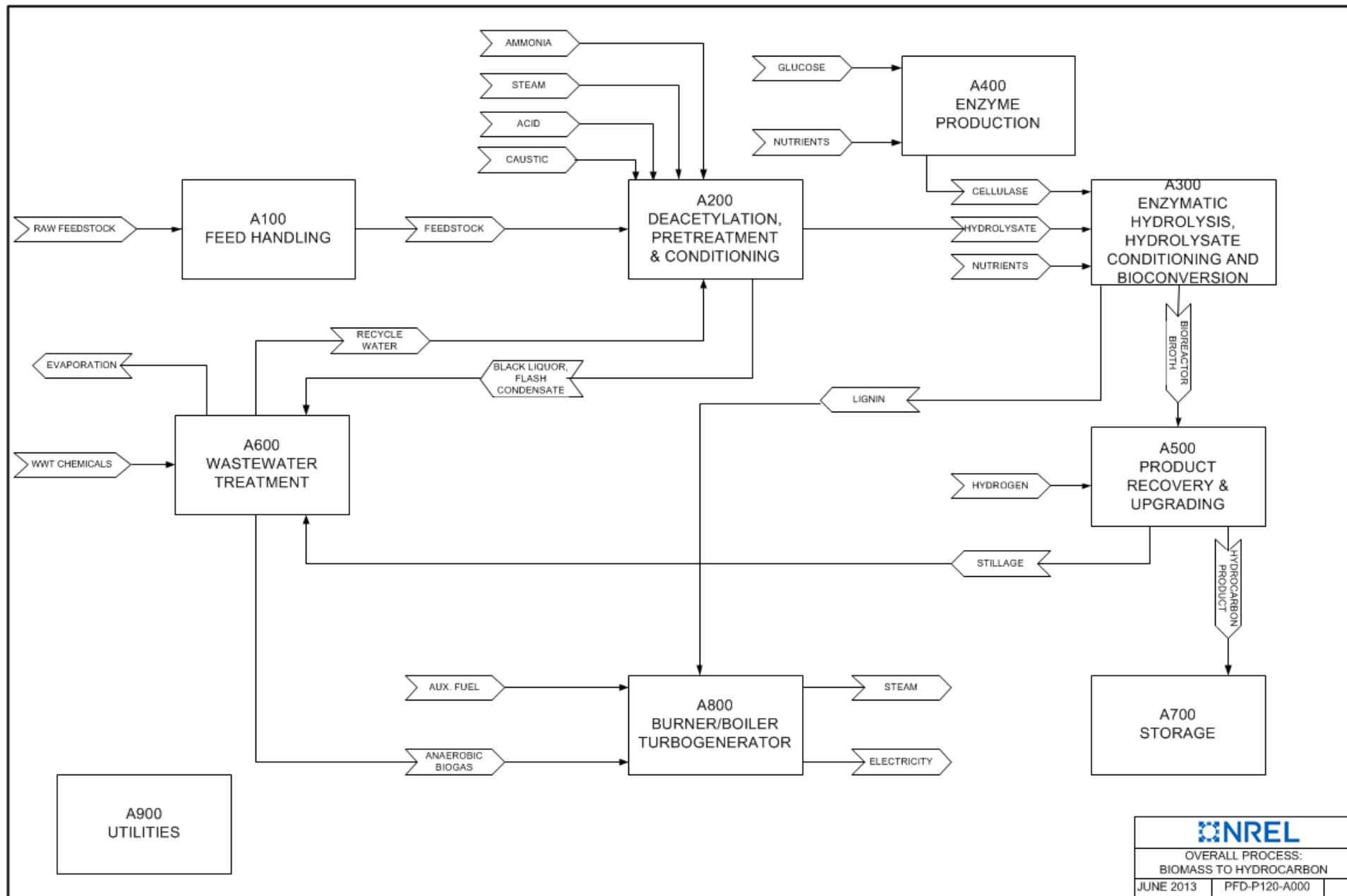


Figure 2. Simplified flow diagram of the overall process (key streams only; see Appendix E for more detailed schematic and process flow diagrams)

1.3 Techno-Economic Analysis Approach

Figure 3 describes the engineering approach used for modeling the conversion of biomass to biofuels, including process design, process modeling, and economic analysis. This approach was largely followed for this study as well, albeit under a condensed timeline and with additional external inputs from literature for areas of the process in which NREL does not yet have sufficient in-house data (primarily the microbial conversion step). As such, this report is less prescriptive in some sections than are previous reports, because of the early stage of understanding for new areas of the process and the somewhat more preliminary nature of the associated models.

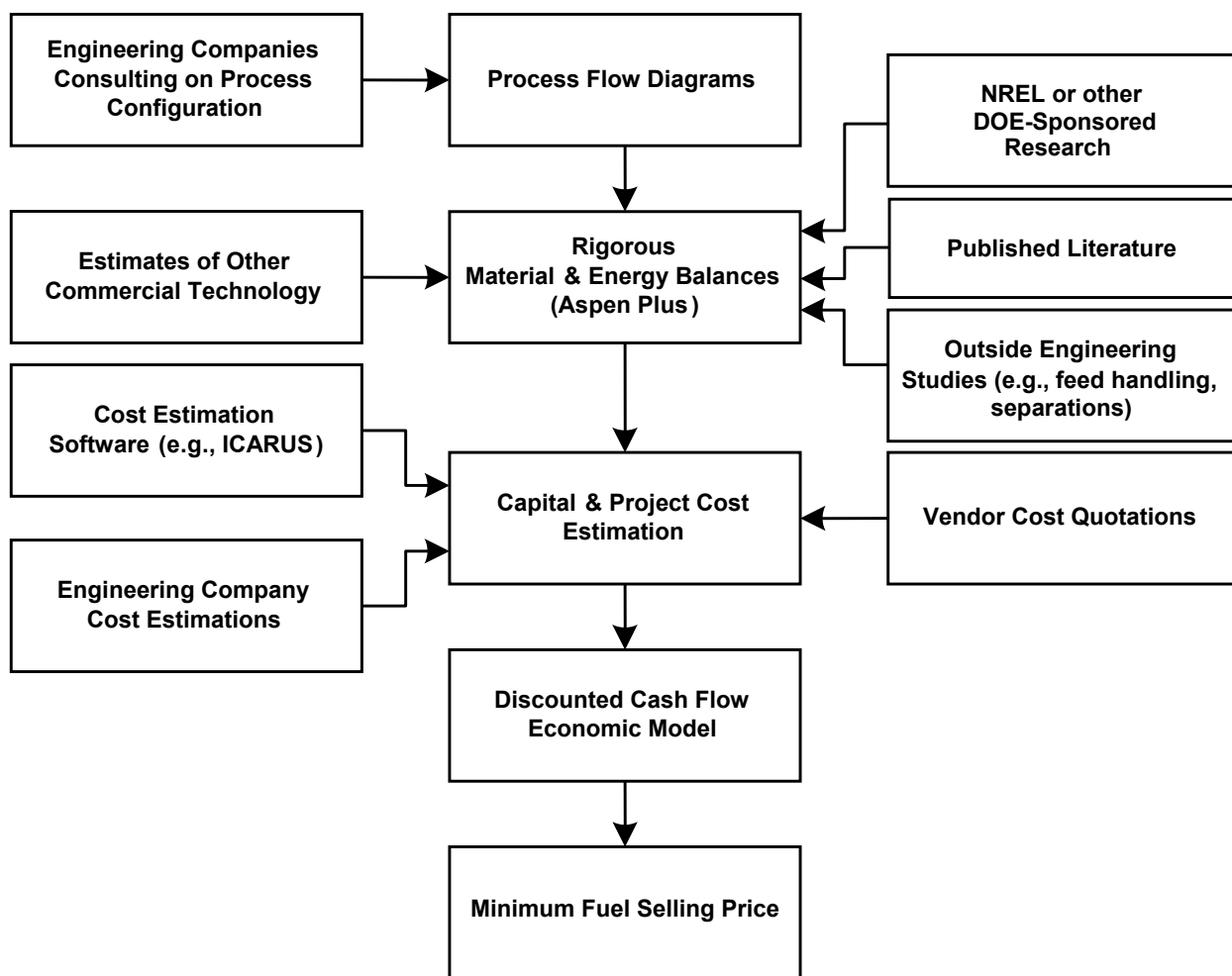


Figure 3. NREL's approach to process design and economic analysis

Starting from the general process flow diagram shown in Figure 2 and the more detailed diagrams contained in Appendix E, a process simulation is developed using Aspen Plus software [11]. This process model computes thermodynamically rigorous material and energy balances for each unit operation in this conceptual biorefinery.

The material and energy balance data from the Aspen simulation are next used to assist in determining the number and size of capital equipment items. As process conditions and flows change, baseline equipment costs are automatically adjusted in an Excel spreadsheet using a scaling factor. These baseline costs come from vendor quotes (a favored procedure for larger or nonstandard unit operations and packaged or skid-mounted subsystems) or from Harris Group's proprietary cost database (for secondary equipment such as tanks, pumps, and heat exchangers). Harris Group provided updated design and cost estimates based largely on vendor quotations for critical new or modified areas of the current process model, primarily deacetylation, sugar conditioning (lignin removal and sugar concentration), aerobic bioreactors, product separation, hydrotreating, and additional cost information on the pretreatment reactor. Final equipment costs for this report are tabulated in Appendix A.

Once equipment costs are determined, direct and indirect overhead cost factors (e.g., installation costs and project contingency) are applied to determine a total capital investment (TCI). The TCI, along with the plant operating expenses (also developed using flow rates from the Aspen model), is used in a discounted cash flow rate of return (DCFROR) analysis to determine a plant-gate price for refined renewable diesel blendstock (RDB) for a given discount rate. This plant-gate price is also called the minimum fuel selling price (MFSP, in \$/gallon), required to obtain a net present value (NPV) of zero for a 10% internal rate of return (IRR) after taxes.

The product of the analysis described above is a techno-economic model that reasonably estimates a product price for a pre-commercial process. The resultant MFSP is unique for the set of process conditions simulated, and it should be emphasized that a certain percentage of uncertainty always exists around these chosen conditions, as well as around the assumptions made for capital and raw material costs. Without a detailed understanding of the basis behind it, the absolute computed MFSP carries a risk of being taken out of context. While the MFSP can be used to assess the marketplace competitiveness of a given process, it is best suited for comparing technological variations against one another or for performing sensitivity analyses that indicate where economic or process performance improvements are needed.

1.4 About n^{th} -Plant Assumptions

The techno-economic analysis reported here uses what are known as " n^{th} -plant" economics. The key assumption implied by n^{th} -plant economics is that our analysis does not describe a pioneer plant; instead, it assumes several plants using the same technology have already been built and are operating. In other words, it reflects a mature future in which a successful industry of n plants has been established. Because the techno-economic model is primarily a tool for studying new process technologies or integration schemes in order to comment on their comparative economic impact, n^{th} -plant analysis avoids artificial inflation of project costs associated with risk financing, longer startups, equipment overdesign, and other costs associated with first-of-a-kind or pioneer plants, lest these overshadow the real economic impact of research advances in conversion or process integration. At the same time NREL also continues to work on quantifying economic factors associated with first-of-a-kind implementation. At the very least, these n^{th} -plant economics should help to provide justification and support for early technology adopters and pioneer plants.

The n^{th} -plant assumptions in the present model apply primarily to the factored cost model used to determine the total capital investment from the purchased equipment cost and to the choices

made in plant financing. The n^{th} -plant assumption also applies to some operating parameters, such as process uptime of 90%. These assumptions were agreed upon by NREL and DOE for this report and reflect our best estimates at the time of publication. It should be emphasized, however, that these assumptions carry a degree of uncertainty and are subject to refinement.

1.5 About the NREL Aspen Model

While Aspen Plus can be thermodynamically rigorous, such detail is not always warranted in the simulation, whether for lack of data or introduction of additional complexity for little gain in accuracy. Some unit operations, particularly solid-liquid separation and FFA product concentration, were modeled with a fixed performance determined by experimental testing or by standard engineering practices confirmed with vendors. Bioreactors were modeled using experimentally determined conversions of specific reactions (e.g., cellulose to glucose) rather than rigorous kinetics or rate expressions. This simple stoichiometric model still satisfies mass and energy balances.

The Aspen Plus simulation uses component physical properties internal to the software as well as property data developed at NREL or from the literature [12, 13]. Similar to the 2011 model, the current model does not rely on external property databanks and minimizes the number of custom-defined components within reason. A discussion of the components and properties used is given in Appendix D.

2 Design Basis and Conventions

2.1 Plant Size

The plant size in the present design is the same as that used in prior designs: 2,205 dry U.S. ton/day (2,000 metric tonne/day). With an expected 7,880 operating hours per year (90% uptime), the annual feedstock requirement is 724,000 dry U.S. ton/year. The present model assumes that feedstock is delivered under a uniform-format logistics system, which includes a blended feedstock consisting of multi-pass corn stover, single-pass corn stover, and switchgrass, to enable achieving cost and composition requirements set for 2017 targets by Idaho National Laboratory (INL) [14]. A strategy to reduce the cost of obtaining biomass is to “blend” or use numerous types of feedstocks to design an aggregated or formulated feedstock. This strategy assumes that the formulation of multiple feedstocks will perform as well as, or better than, a singular feedstock. There are research plans for FY 2014 to test various blended feedstocks in both bio-oil and sugar conversion pathways. Under the new uniform format system, opportunities may exist to justify a larger facility scale with an increased feed rate to the biorefinery, thus allowing for economy of scale advantages; however, the specifics are not yet defined and we retain the 2,000 dry tonne/day basis here.

2.2 Feedstock Composition

The conversion target feedstock composition remains the same as was assumed in the 2011 design basis; however, the biomass *supply* composition has been altered. As noted by INL, the previous requirements for feedstocks included volume and cost targets only. There were no quality requirements; further analysis indicated a mismatch on biomass characteristics and conversion in-feed specifications. Improved analysis highlighted the need to develop the technologies in the logistics supply chain that can address quality in addition to stability and densification requirements. The updated composition assumed in the 2011 design basis improved on the initial estimate in the 2002 basis document. This update further improves on the 2011 design basis and the associated price of \$58.50/dry ton (2007\$), which included a more uncertain grower payment, to a more reasonable target at an increased price of \$80/dry ton including grower payment (2011\$, used as the new basis here). This new price is more appropriate for a large commodity scale going beyond a “niche market” price.

As has been described in prior design reports, the feedstock composition (see Table 1) plays a critical role on overall process design and economics, primarily with respect to carbohydrate components (cellulose and hemicellulose), lignin, and increasingly acetate and ash, given modifications being made to the pretreatment strategy such as the use of deacetylation. The blended uniform-format feedstock composition assumed here for purposes of 2017 targets is shown below, with supporting details (in the context of corn stover compositional variability) described in the 2011 ethanol report [3]. Also consistent to the 2011 design, the moisture content for the delivered feedstock is 20%.

When converting the analytical composition to components used in the Aspen Plus model, the nonstructural component fractions from the compositional analysis were combined under “extractives.” The extractives component is assumed to be primarily organic, with an average composition of CH_2O , and consists primarily of sugars, sugar alcohols, and organic acids, as well as some nonstructural inorganics [15]. The presence of extractives in the biomass depends on the time of harvest and in part to how much microbial degradation of the material occurs after

harvest; the amount of extractives in a given sample may therefore be indicative of its age. Additionally, where the mass balance did not sum to 100%, the extractives component was used to close it by difference. Sucrose is another extractive component, but it is measured separately in laboratory analysis and has been added as a separate feedstock component in the present design. The amount of sucrose present in the biomass is dependent on harvesting and handling practices. In pretreatment, this sucrose is assumed to be fully hydrolyzed to glucose and fructose. The labile fructose is further converted to degradation products in pretreatment, but the less reactive glucose resists degradation and thus is available for fermentation [16].

Table 1. Delivered Feedstock Composition Assumed in the Present Design

Component	Composition (dry wt %)
Glucan	35.1
Xylan	19.5
Lignin	15.8
Ash	4.9
Acetate ^a	1.8
Protein	3.1
Extractives	14.7
Arabinan	2.4
Galactan	1.4
Mannan	0.6
Sucrose	0.8
<i>Total structural carbohydrate</i>	<i>59.0</i>
<i>Total structural carbohydrate + sucrose</i>	<i>59.8</i>
<i>Moisture (bulk wt %)</i>	<i>20.0</i>

^a Represents acetyl groups present in the hemicellulose polymer; converted to acetic acid in pretreatment.

In the present design, the lignin fraction ultimately will also become essentially of equal economic importance as the fermentable carbohydrates because of the need to improve overall carbon efficiency to product(s) in order to ultimately achieve the 2022 \$3/GGE target. This is described further in Section 6.

2.3 Updated Modeling Basis

A number of important adjustments were made to the model basis assumptions from an operational and a financial standpoint, relative to previous modeling efforts. These adjustments were made consistently to all new pathway models being developed under the DOE BETO Program to allow for slightly more conservative operational assumptions and to update the cost-year basis to a more recent and relevant timeframe [10, 17]. These updates are as follows:

1. Facility start-up time: 0.5 year (6 months) rather than previous 0.25 year (3 months)
2. Cost-year dollar basis: 2011 dollars rather than previous 2007 dollars (all cost results presented here will be in 2011-year dollars)
3. Facility on-stream time: 90% (7,884 hours/year) rather than 96% (8,406 hours/year); note, this is still intended to represent an “*n*th-plant” facility, but allows for slightly more operational downtime in part to reflect the increased process complexity of the new pathway model (e.g., sugar clarification and concentration steps, aerobic fed-batch conversion, hydrotreating, etc.) relative to the ethanol baseline.

Additionally, the feedstock cost for the biochemical pathway is updated from a previous basis of \$58.50/dry ton (2007\$) to \$80/dry ton (2011\$) for the 2017 target case, to reflect a more commercially relevant pricing model at a larger national scale (described in more detail below).

2.4 Design Report Conventions

2.4.1 Units

The Aspen Plus model we developed is, by legacy, based on the set of units required by Aspen for specifying custom component properties: kg, kmol, atm, °C for materials, and MMkcal (Gcal) for energy. Values in this report that were pulled directly from the Aspen model therefore tend to be reported in these units. Harris Group preferred to use U.S. standards (lb, Btu, °F, gal, etc.) when communicating with equipment vendors. Therefore, equipment specifications tend to be cited in these U.S. units.

Note that in the present report, certain quantities (e.g., yields and costs) are computed and reported in terms of “tons.” To avoid ambiguity, *tonne* will denote a metric tonne (1,000 kg) and *ton* will denote a short or U.S. ton (2,000 lb). In general, the U.S. ton is the standard for this document. *Ton* also appears in Section 3.9 in the context of refrigeration, but this usage should be clear from the discussion.

2.4.2 Total Solids Loading

The process described here converts a solid feedstock (corn stover blended with switchgrass) into a liquid product (FFA/RDB). Most material streams in the process therefore have a solid fraction and a liquid fraction. The relative amount of solids in a given stream is called its “solids loading.” Total solids (TS) loading is defined as the total weight percent of soluble solids (e.g., sugars and salts) and insoluble solids (IS; e.g., cellulose and lignin) in a given material stream. Where useful, the TS loading and the IS loading will be reported together. Note that in our convention, sulfuric acid, acetic acid, and ammonia are not considered soluble solids but ammonium acetate and ammonium sulfate are. Therefore, around some unit operations, e.g., hydrolysate conditioning, TS loading is not a conserved quantity.

2.4.3 Product Density and Heating Value

The results from this analysis are reported in terms of volume of product (RDB) produced: \$/gal, gal/yr, gal/ton, etc., as well as energy produced in gallons-gasoline-equivalent: \$/GGE, GGE/yr, GGE/ton, etc. As the final RDB product exiting the refining step is a mixture of more than one component, the blended product density as computed by Aspen Plus is utilized as the most accurate estimate for setting the RDB product volume flow rate. In the baseline model this density is computed as 0.769 kg/L at 20°C (68°F); this is a reasonable density value for a mixture of pentadecane and hexadecane (assumed to be produced stoichiometrically from the hydrotreating section under a simplifying scenario of palmitic acid upgrading) based on published literature values for each respective component [18, 19]. Similarly, component heating values were set at 10,047 KJ/mol and 10,699 KJ/mol (higher heating value [HHV] basis) for pentadecane and hexadecane, respectively [20, 21], for translating to an energy basis. An HHV basis was selected in this case as this is a more commonly published basis regarding heating values of the above-listed components (relative to lower heating value), thus minimizes room for error in translating to a GGE basis. To subsequently translate to a GGE basis, a conventional gasoline heating value of 124,340 Btu/gal (46.54 MJ/kg, HHV basis) was applied [22].

3 Process Design and Cost Estimation Details

The process design described in this study is based upon NREL's demonstrated performance during 2012 pilot-scale trials for ethanol production (specifically with respect to front-end steps for pretreatment and hydrolysis) to project plausible future improvements in these pertinent areas. For downstream operations, including bioconversion and microbial product secretion and purification, plausible targets are set based upon information presented in public literature as well as to consider the impact of similar performance targets originally set for ethanol (e.g., glucose, xylose, and arabinose utilization) to maintain consistency in translating to new hydrocarbon pathways. As noted previously, these targets are merely one set of conditions that would enable achieving the interim 2017 MFSP cost goal of \$5/GGE and will help to inform near-term research directions, but are not necessarily strict targets for NREL or other DOE biochemical research at this point. Additionally, given the scope and timeframe under which the present analysis effort was conducted, the report is more concise in some areas (such as detailed process flow diagrams and stream-level information), and summarizes rather than repeats in detail the process areas that were unchanged relative to the 2011 ethanol design basis. This section describes the process as modeled and discusses the influence of specific R&D goals in the decision-making process.

Two caveats are noted here in the context of process and cost estimates utilized in the present analysis. First, given the more preliminary scope and nature of the design models established here, the engineering support provided by Harris Group focused exclusively on the primary unit operations (e.g., reactors, separation and concentration equipment, upgrading operations, etc.), and did not cost out individual minor supporting equipment such as pumps, heat exchangers, and agitators (except for bioreactor agitators, as these are considered critical operations). For these minor equipment, Harris Group added a percentage factor to the provided cost estimate for the respective primary operations based on the associated costs in the 2011 ethanol design. Second, at the request of Harris Group who provided all vendor estimates for cost quotations, vendor company names associated with a particular unit operation will not be provided in this report. The equipment list in Appendix A may note vendors that have already been identified as discussed in the 2011 ethanol report; however, vendor names associated with new or modified operations for which estimates were provided for this design case are not shown.

3.1 Area 100: Feedstock Storage and Handling

3.1.1 Overview

Area 100 handles incoming biomass feedstock. For a biochemical conversion pathway, herbaceous biomass is the preferred feedstock. The present design assumes a blend of corn stover and switchgrass delivered according to the specifications detailed in the INL design report for the uniform-format feedstock supply system [23]. In this envisioned design, biomass is stored in a central depot and is preprocessed, densified, stabilized, and homogenized to a degree before delivery, such that the biorefinery receives feedstock with known, uniform-format specifications including particle size, ash content, and moisture content. All analysis and cost implications associated with Area 100, and with feedstock logistics in general, are outside the scope of the present effort focusing on the conversion biorefinery, but are summarized in the discussion below to convey information attributed to the updated feedstock cost of \$80/dry ton delivered to Area 200.

Feedstock logistics includes operations that take place after the biomass is produced in a field or forest, but before it is introduced into a conversion process. All activities related to feedstock logistics are directed at reducing the delivered *cost* of sustainably produced feedstock, improving and preserving the *quality* of harvested feedstock to meet the needs of biorefineries, and/or expanding the *volume* of feedstock materials accessible to the bioenergy industry. Feedstock logistics efforts are primarily focused on identifying, developing, demonstrating, and validating efficient and economic systems to harvest, collect, transport, store, and preprocess¹ raw biomass from a variety of crops to reliably deliver high quality, high volume, affordable feedstocks to biorefineries. Sustainably supplying the required quantities of quality, affordable feedstock to the emerging biorefining industry will be achieved through a transition from logistics systems that have been designed to meet the needs of conventional agriculture and forestry systems—termed “conventional” logistics systems—to more advanced, purpose-designed systems in the 2013 to 2022 timeframe, termed “advanced” logistics systems [24]. In the context of biochemical conversion using herbaceous feedstocks, the current focus is on the U.S. Midwest Corn Belt given its abundance of corn stover. However, future design cases will move away from the niche areas to areas with lower yields and more difficult logistic cost challenges.

As illustrated in Figure 4, the advanced Terrestrial Feedstock Processing Supply and Logistics System is envisioned to draw in presently inaccessible and/or underused resources via local biomass preprocessing depots that format biomass into a stable, bulk, densified, and flowable material. The formatted biomass will be transported to one or more networks of much larger supply terminals, where the material aggregated from a number of depots may be blended and/or further preprocessed to meet the specification required by each biorefinery conversion process (note that feedstock specifications may differ substantially, depending upon the actual conversion process). The advanced biomass logistics system design incrementally incorporates technology and other system improvements as the industry matures. This improved series of feedstock supply and logistics system designs will couple to, and build from, current systems and address science and engineering constraints that have been identified by rigorous sensitivity analyses as having the greatest impact on feedstock supply and logistics system efficiencies and costs. The introduction of advanced preprocessing operations and sequences, including the implementation of blending and formulation strategies, and preprocessing strategies, is critical to achieving feedstock cost, quality, and volume targets to meet BETO 2017 and 2022 goals.

¹ Note that some preprocessing research takes place under the conversion technology areas, while other research is funded under feedstock logistics.

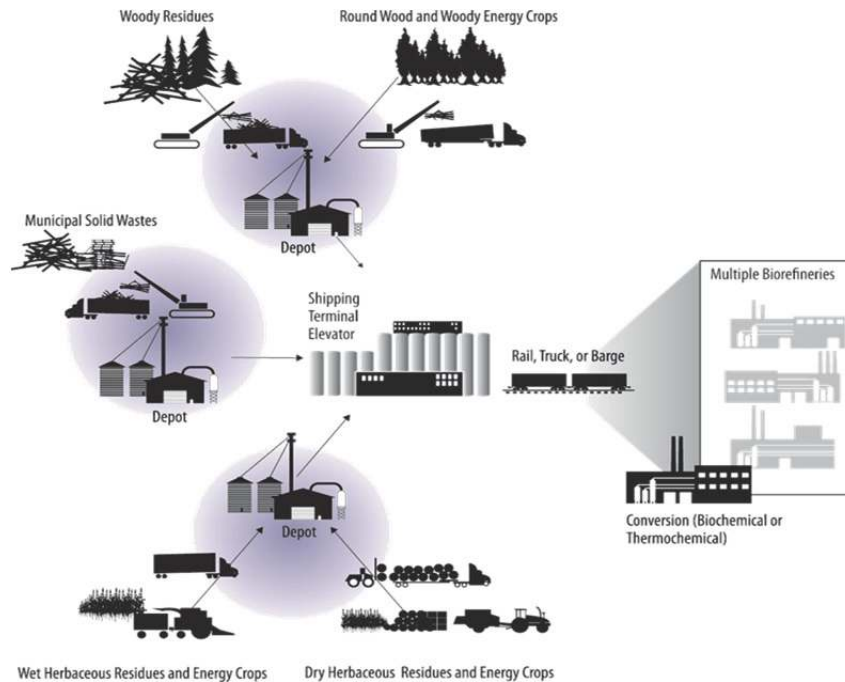


Figure 4. The depot concept behind the advanced Terrestrial Feedstock Processing Supply and Logistics System

To address the high cost of biomass procurement, lower cost resources could be supplemented from other regions, but this strategy would increase transportation costs. Another strategy to reduce the cost of obtaining biomass is to “blend” or use numerous types of feedstocks within a region to design an aggregated or formulated feedstock. This strategy assumes that the formulation of multiple feedstocks will perform as well as or better than a singular feedstock. To demonstrate this strategy, Figure 5 exemplifies farmgate price functions for three feedstocks in a region. At \$40/dry ton only around 250,000 tons of corn stover are accessible, but by including switchgrass and wheatstraw the available biomass at \$40/dry ton increases to 600,000 tons.

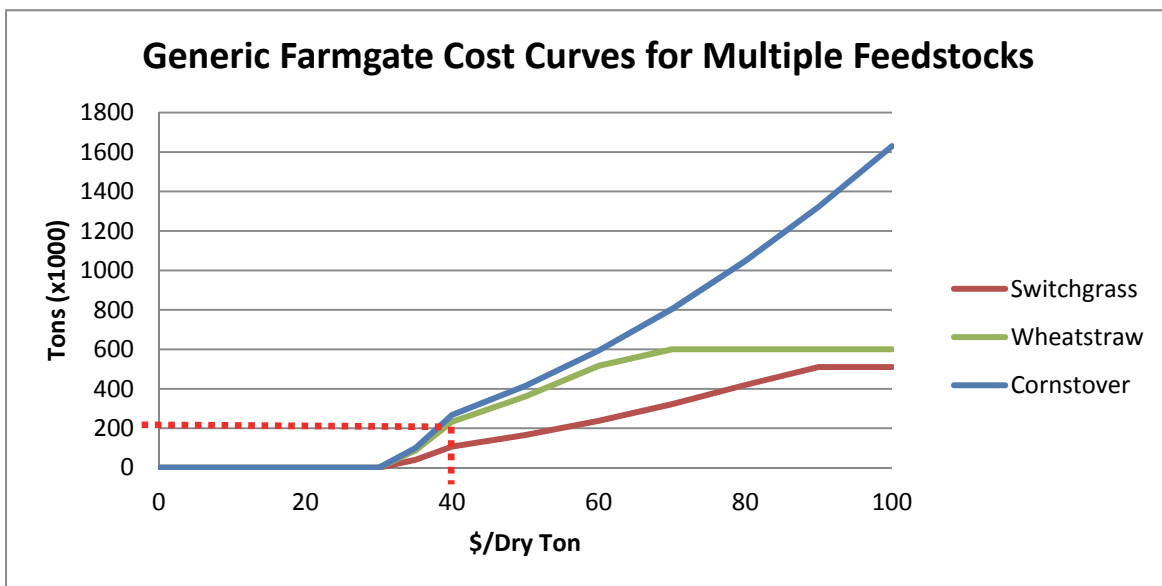


Figure 5. Typical farm gate price function for three feedstocks: corn stover, switchgrass, and wheatstraw, to demonstrate cost and/or scale advantages of feedstock blending (courtesy of INL)

Blending strategies could also improve overall feedstock quality to help meet biofuel quality specifications and conversion in-feed requirements. Quality targets can have a large impact on whether or not a particular feedstock is cost effective. One aspect of the inherent spatial and temporal variability of biomass resource quality is illustrated by the ash, xylan, and glucan distributions for biomass shown in Figure 6. Note: The distributions include not only biological variability but impacts from various field management, including different harvesting and collection practices such as single-pass and multi-pass harvesting, bar rake, wheel rake, etc. Formulation allows the use of low-cost, but typically low-quality, biomass blended with higher cost and quality biomass to achieve minimum conversion process quality specifications. The use of low-cost biomass allows the supply chain to implement additional preprocessing technologies that actively control feedstock quality and bring more biomass into the system.

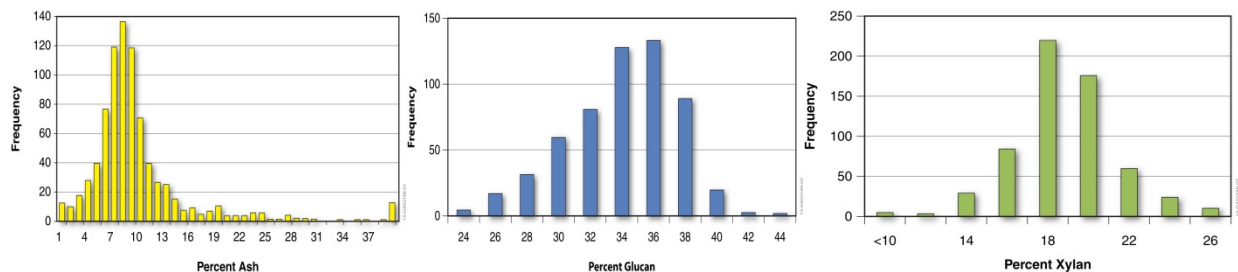


Figure 6. Example of the spatial and temporal variability of biomass characteristics

Preliminary results on feedstock supply chains delivering material to cellulosic biorefineries demonstrate that with the ability to blend multiple feedstocks and include some preprocessing operations, it is possible to acquire high volumes of material, reduce feedstock variability to meet biorefinery in-feed specifications, and meet the required price of feedstock material to the throat of the biorefinery. Much more research needs to be done on the performance of blended material and the blending strategies, as well as on other technologies incorporated into advanced designs. In addition, current pre-conversion systems are expensive, and reducing those costs is a significant barrier to meeting future cost targets. However, there is ongoing research at the national laboratories, universities, and industry to address these challenges.

3.1.2 Design Basis

In the new uniform-format feedstock supply system design, feedstock would be stored in a satellite depot location with delivery to the biorefinery occurring 6 days per week by truck, or possibly by rail. At the depot, material would be milled to a mean size of 0.15–0.25 in. (with a high content of fines), in order to achieve a mean bulk density of 9–11 lb/ft³ to maximize the biomass load per trailer. The incoming uniform format feedstock (corn stover/switchgrass blend) is assumed to have 20% moisture when it reaches the biorefinery; this is representative of a mixture of field-dried material having < 15% moisture and co-harvested material having > 20% moisture. Because the preprocessing operation is designed to lose very little dry matter and does not include any rinsing of biomass, it is assumed that the biomass composition discussed in Section 2.2 is valid for the delivered material.

The as-received feedstock requirement for a plant is 2,750 U.S. ton/day (104,200 kg/h; 229,700 lb/h) including moisture. In the projected design, refinery receiving operates on the same

schedule as the biomass depot: 24 hours per day, six days per week. Each truck trailer holds 10 U.S. tons of biomass. To satisfy production and storage requirements, the plant must receive 12 trucks every hour. Incoming trucks are weighed by electronic scale and unloaded using a whole-truck dumper capable of a 7–10 minute unloading time. The dumpers empty into dedicated hoppers that meter the biomass to a series of conveyors. The conveyors carry material from the truck tipper to short-term storage. The minimum receiving rate is 250 ton/h to maintain 110 ton/h of continuous processing. In order to process 250 ton/h, and assuming a relatively constant flow of trucks, a pair of scales (one inbound and one outbound) and two truck dumpers are required.

On-site storage is kept to a minimum of 72 hours to allow for a weekend buffer. Open piles are not favored due to concerns of fire, rodent infestation, and moisture degradation. Instead, the unloaded feedstock is stored in concrete domes. Two domes (each with a 36-hour capacity) are required so that one can be loaded while the other empties to the conversion process.

Conveyors connect the storage domes to the feedstock receiving bins on the pretreatment reactor in Area 200. A dust collection system integrated with the conveyors and domes handles airborne particles released during the unloading and conveying processes. No dry matter is assumed lost in Area 100.

3.1.3 Cost Estimation

The feedstock cost assumed in this report is \$80/dry ton (2011\$), a cost increase over the 2011 ethanol design that is attributed to the new uniform format logistics system described above. This cost comes from the Multi-Year Program Plan (MYPP) published by DOE-BETO [10]. This is a rolled-up cost which includes both grower payment as well as logistics considerations for all collection, processing, storage, and transportation costs between the field and the receiving bin on the pretreatment reactor (e.g., Table B-2 of the referenced MYPP document). It should be stressed that these costs are 2017 and 2022 DOE research targets, like the conversion performance targets used in the Aspen Plus model.

3.2 Area 200: Pretreatment and Conditioning

3.2.1 Overview

Pretreatment of biomass for biofuel production is a crucial step. Its primary role is to disrupt the matrix of polymeric compounds that are physically and chemically bonded within lignocellulosic biomass cell wall structures, including cellulose microfibrils, lignin, and hemicellulose.

Pretreatment has a significant impact not only on enzymatic hydrolysis, fermentation, and downstream processing [25], but also on overall process economics and sustainability. Acid-based pretreatments target hydrolysis of significant fractions of hemicellulose and small fractions of cellulose. The dilute acid pretreatment process converts most of the hemicellulose carbohydrates in the feedstock to soluble sugars (xylose, arabinose, galactose, and mannose) by hydrolysis reactions. Alkaline pretreatments break bonds between lignin and carbohydrates and disrupt lignin structure, making carbohydrates more accessible to enzymatic hydrolysis [25]. Dilute alkaline pretreatment normally results in better delignification than dilute acid pretreatment by cleaving lignin-hemicellulose linkages and swelling cellulose [26], with minimal hydrolysis of the cellulose or hemicellulose.

Due to complementary advantages of acid and alkaline pretreatment, a combination of both dilute acid and alkaline may reduce not only overall chemical loadings, but more importantly

provide high fermentable sugar yields for downstream bioconversion. The use of dilute alkaline deacetylation combined with low acid pretreatment process steps has shown improvements in ethanol yields and calculated MESP for cellulosic ethanol production [27, 28]. Acetyl groups in the hemicellulose are liberated and removed as acetic acid by sodium hydroxide during deacetylation, greatly reducing inhibition from acetate to improve hydrolysis and fermentation performance (in the context of ethanol production; implications for hydrocarbon production are noted below). Sugar degradation products such as furfural and 5-hydroxymethyl furfural (HMF) can be reduced using low severity acid pretreatment. These compounds can also have adverse effects on the fermenting organisms in sufficiently high concentrations.

In the present design, pretreatment reactions are catalyzed first using dilute sodium hydroxide, then using dilute sulfuric acid. This two-stage design results in a reaction severity that is milder than what has been modeled in previous designs. In the first step (deacetylation), biomass is soaked in dilute (~0.4%) sodium hydroxide solution (pH 8–10) at 20% TS and 80°C for 1 hour in a stirred tank. After deacetylation, the liquor is drained and the deacetylated biomass solid stream is charged with dilute sulfuric acid into a horizontal screw-feed reactor with a short residence time (5–10 minutes). A subsequent “oligomer conversion” step is no longer necessary in this design, as was utilized in the 2011 ethanol design basis. This is because deacetylation can significantly improve conversion of oligomeric to monomeric xylose, with one study showing a decrease in oligomeric xylose yield from 21%–23% for non-deacetylated corn stover to 7%–10% for deacetylated corn stover [28]. After the pretreatment reactors, the hydrolysate slurry is flash-cooled, vaporizing a large amount of water along with some of the acetic acid and furfural. The flash vapor is condensed and sent to the WWT area. The hydrolysate slurry is cooled by dilution water and sent to a conditioning reactor, where ammonia is used to raise its pH from 1 to 5. Figure 7 shows a simplified flow diagram of the pretreatment area. It bears noting that the two-step pretreatment process (deacetylation and dilute acid pretreatment) was a modification made relative to the 2011 ethanol design case as a more optimized approach for biomass deconstruction, and not a consequence of changing to a hydrocarbon product.

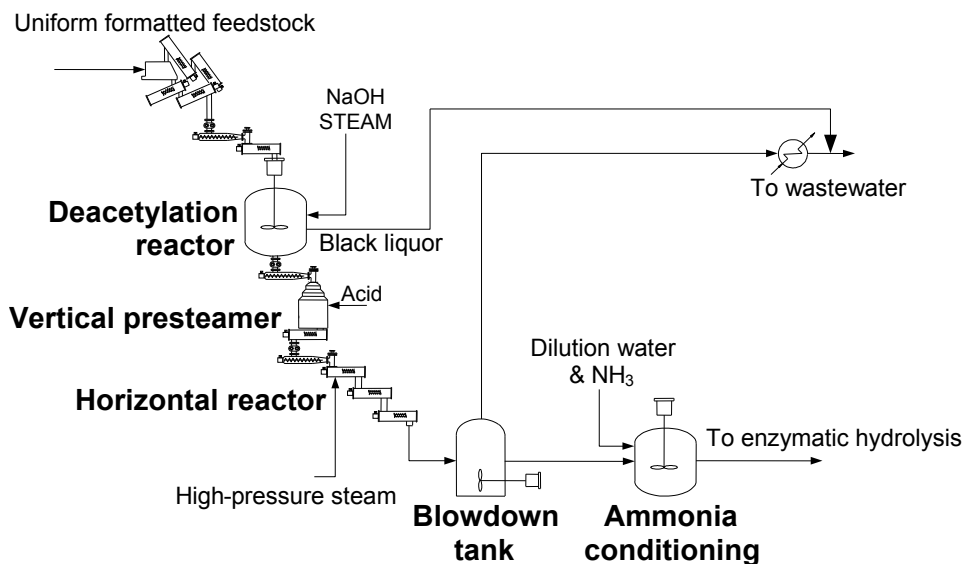


Figure 7. Simplified flow diagram of the deacetylation, pretreatment and conditioning process

3.2.2 Design Basis

Milled biomass (corn stover and switchgrass blend) is conveyed to the pretreatment area and treated with dilute sodium hydroxide (for deacetylation) and sulfuric acid catalyst at moderate to high temperature (see Table 2) to liberate the hemicellulose sugars and break down the biomass for enzymatic hydrolysis. Solids exiting the alkaline deacetylation step are sent on to dilute acid pretreatment, followed by ammonia conditioning to raise the pH of the whole pretreated slurry from ~1 to 5, which is then sent to enzymatic hydrolysis.

The deacetylation step uses a sodium hydroxide soaking process at 80°C for 1 hour, with a NaOH loading of 17 mg/g dry biomass. The deacetylated material is dewatered by draining through screens at the bottom of the deacetylation reactor. A vertical pressure vessel is used for the deacetylation tank with 316 stainless steel as the material of construction based on the reaction conditions. Three identical batch reactors are used with square trough live bottoms consisting of four 24-inch horizontal discharge screws each. Each tank volume is 44,000 gal with a total cycle time of 2.4 hours. The drained liquor, often referred to as “black liquor,” contains 20%–25% of the original dry biomass constituent material, including water extractives (100% solubilization), soluble ash constituents (75% ash solubilization), 20% of the lignin, 2% of the xylan, 50% of the sucrose, and 88% of the acetate that was originally present in the feedstock (dry basis). In addition to the benefit of reducing acetate inhibition during bioconversion, the removal of lignin, ash, and other primarily non-fermentable components provides an important secondary benefit of reducing the total flow rate to downstream operations, thereby reducing equipment size and cost. This black liquor stream is pumped to WWT (A600) in the baseline process design. The remaining biomass solids are discharged from the deacetylation reactor and transported to the acid pretreatment reactor system.

The acid pretreatment reactor system is described in detail in the 2011 ethanol design report, and will not be repeated in such detail here; in summary, this system includes a feedstock receiving system, followed by a vertical vessel with a long residence time for steam heating and potential acid impregnation of the biomass, followed by the horizontal pretreatment reactor, which operates at a higher pressure and a short residence time. The 26-inch plug screw feeder is a rugged, high-compression screw device designed to form a pressure-tight plug of material through axial compression. Dilute sulfuric acid is metered at the discharge spool of each plug screw feeder, shown in Figure 8. Feedstock drops from the plug screw discharge into a mixing and heating screw, which discharges the feedstock into the top of the presteamer. High-pressure steam is injected into this vessel to maintain temperature, while hot water is added at this point to control the pretreatment effluent at 30 wt% TS. The current model assumes operation of the presteamer at 100°C such that no significant hydrolysis reactions occur in this section. It can be used if additional hold up is required for acid hydrolysis. With a 2,205 U.S. ton/day throughput, the presteamer can add up to 10-minute retention time at 165°C, using a single vertical vessel. Feedstock flows downward through the vertical presteamer with uniform temperature throughout, discharging through a dual screw outlet device to two plug screw feeders. The plug screw feeders meter feedstock to the horizontal pretreatment reactor, with a horizontal reactor configuration chosen to allow tighter residence time distribution control than with a vertical reactor.

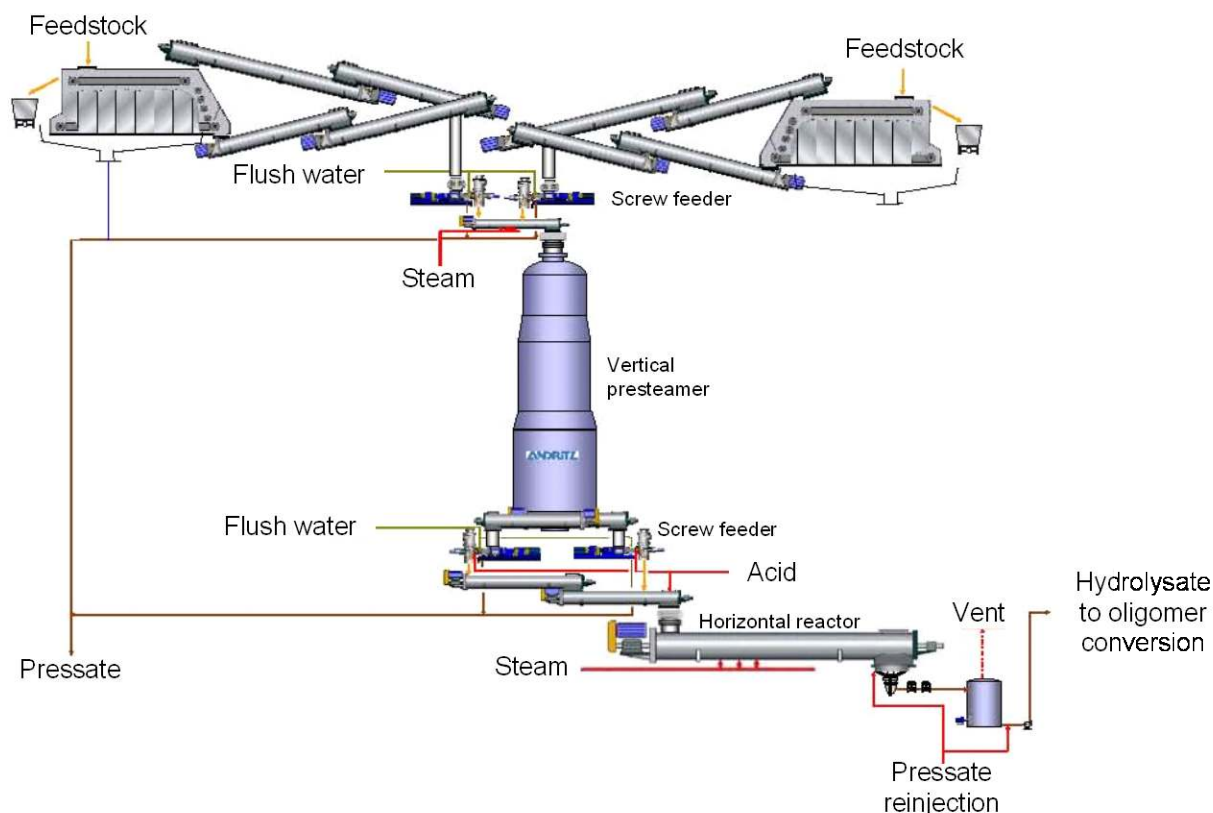


Figure 8. Horizontal acid pretreatment reactor design scheme

Upon deacetylation and solid-liquid separation by draining the black liquor, the actual sulfuric acid loading present in the horizontal acid pretreatment reactor is only 9 mg/g dry feedstock. The reactor pressure is held at the bubble point for the mixture. Heat losses from the reactor are not accounted for in the energy balance calculations. The residence time in the pretreatment reactor is nominally 5 minutes. The effective sulfuric acid concentration in the pretreatment reactor (estimated at 0.3–0.4 wt% after dilution by condensing steam is accounted for) may allow for the use of lower-cost metallurgies in the reaction zone (such as 904L or other duplex stainless alloys) instead of Incoloy-clad carbon steel, which could reduce pretreatment equipment costs. However, relevant corrosion data under these conditions are not available, so in the model, Incoloy-825 cladding is still conservatively assumed for the material of construction (consistent with the 2011 design report). The potential impact of lower-cost metallurgy and other pretreatment reactor cost savings is addressed below in the Sensitivity Analysis section.

The direct cost benefit of lower acid loading in pretreatment is the reduction of the amount of neutralization ammonia usage, along with reducing the formation of inhibitors (such as HMF and furfural) while maintaining effective pretreatment performance. Additionally, much less acetic acid is formed due to acetate removal during deacetylation, thus further reducing ammonia neutralization demand. Additional acid is used to pre-impregnate the deacetylated biomass (the cost of this usage is included in the purchased sulfuric acid cost in the techno-economic model), but much of this acid is removed in pilot plant operation upon dewatering of the impregnated biomass and does not enter the pretreatment reactor. Acid pre-impregnation and its associated dewatering step are not explicitly modeled in our design, but it is envisioned that these could

take place in the vertical presteamer, similar to the rationale in the 2011 design report [3]. The pretreatment reactor operating conditions are summarized in Table 2.

Table 2. Pretreatment Conditions Applied in the 2011 Design Model, Compared to This Design

Parameter	2011 design model	This design
Total sulfuric acid loading present in pretreatment reactor	22 mg/g dry biomass (includes 4 mg/g for oligomer conversion)	9 mg/g dry biomass
Residence time	5 minutes	5 minutes
Temperature	158°C	160°C
Pressure	5.5 atm	5.5 atm
Total solids loading	30 wt %	30 wt %

Table 3 summarizes the reactions and conversions that take place in pretreatment. Glucan contained in the hemicellulose is converted to glucose along with a small portion of the cellulose. Minor hemicellulose carbohydrates (arabinan and galactan) are assumed to have the same reactions and conversions as xylan. The xylan-to-xylose conversion is a total hydrolysis value, which also may include an enzymatic component that will be discussed later. The sucrose reaction to HMF and glucose reflects 100% hydrolysis of sucrose to fructose and glucose, followed by complete degradation of the fructose to HMF.

Table 3. Pretreatment Hydrolysis Reactions and Assumed Conversions

Reaction	Reactant	% Converted to Product
$(\text{Glucan})_n + n \text{ H}_2\text{O} \rightarrow n \text{ Glucose}$	Glucan	9.9%
$(\text{Glucan})_n + n \text{ H}_2\text{O} \rightarrow n \text{ Glucose Oligomer}^a$	Glucan	0.3%
$(\text{Glucan})_n \rightarrow n \text{ HMF} + 2n \text{ H}_2\text{O}$	Glucan	0.3%
$\text{Sucrose} \rightarrow \text{HMF} + \text{Glucose} + 2 \text{ H}_2\text{O}$	Sucrose	100%
$(\text{Xylan})_n + n \text{ H}_2\text{O} \rightarrow n \text{ Xylose}$	Xylan	90.0%
$(\text{Xylan})_n + m \text{ H}_2\text{O} \rightarrow m \text{ Xylose Oligomer}^a$	Xylan	2.4%
$(\text{Xylan})_n \rightarrow n \text{ Furfural} + 2n \text{ H}_2\text{O}$	Xylan	5.0%
$\text{Acetate} \rightarrow \text{Acetic Acid}$	Acetate	100%
$(\text{Lignin})_n \rightarrow n \text{ Soluble Lignin}$	Lignin	5.0%

^a Sugar oligomers are considered soluble but not fermentable.

The pretreatment reactor is discharged to a flash tank. The pressure of the flash is controlled to keep the temperature at 100°C (212°F). The flash is condensed and routed to WWT (Area 600), containing more than 30% of the furfural along with other volatile and potentially inhibitory organics from pretreatment. After the flash, the hydrolysate whole slurry containing 30% TS and 16% IS is sent to conditioning, namely neutralization by ammonia in stoichiometric quantities. Ammonia gas is mixed into dilution water to raise the hydrolysate pH to 5. The residence time for neutralization is 30 minutes and the dilution cools the slurry to 75°C (167°F). The slurry is diluted with water to slightly greater than 20 wt% TS to ensure miscibility through enzymatic hydrolysis and bioconversion. The composition of the stream at this point, and other major points throughout the process, is shown in the stream table information in Appendix E. The material from conditioning is conveyed to a saccharification storage tank.

3.2.3 Cost Estimation

Each deacetylation tank was quoted by Harris Group at \$890,000 for this design, including reactor tanks and conveyors. The acid pretreatment reactor design and cost basis is similar to that described in the 2011 ethanol design report; however, we have expanded the cost analysis in the present work to allow for a more robust cost estimate with higher flexibility in operational variables. Namely, an evaluation of pretreatment reactor pricing in terms of metallurgy, reactor conditions, and reaction residence time was conducted by Harris Group based on input from a vendor. In addition to the base case Incoloy-clad metallurgy used in the 2011 report and again here as the baseline assumption, a less costly stainless steel option was considered as an option. The stainless steels (duplex or 904) are acceptable for low-temperature and low-acid loadings only. Based on discussions with the vendor, stainless steel 904 may be acceptable in a temperature range of 135°–150°C with acid concentration below 0.5%. Duplex stainless steels may be acceptable if temperature is below 135°C and acid concentration is below 0.25%. An important outcome from this exercise is a quantified validation that acid concentration is not necessarily the primary factor for metallurgy selection, but rather the high temperature at the acid loadings considered here.

An additional outcome from the follow-up vendor consultation was a more detailed quantitative understanding of how the horizontal reactor cost may vary according to throughput and/or residence time. At issue is the fact that the horizontal reactors are discrete pieces of equipment that are additive in cost, rather than scalable, given a finite maximum capacity at the stipulated horizontal reactor design. As such, Harris Group worked with the vendor to establish cost boundaries for a low (2-minute) and high (20-minute) horizontal reactor residence time. Using the information provided, Harris Group then interpolated the resulting cost values to establish a single equation for total pretreatment reactor cost as a function of horizontal reactor residence time. The equations were further adjusted to the new pretreatment throughput basis of 1,516 dry tonne/day, which reflects the fractional biomass solubilization upstream during deacetylation from an initial feed rate of 2,000 dry tonne/day. The resulting equations are provided below, and will permit continued use of the same reactor quotation in our analyses as pretreatment severity and operating conditions change based on future research:

$$\text{Total Equipment Cost (2011 \$MM); Incoloy 825} = 16.4 + 7.4 \times m \quad (1)$$

$$\text{Total Equipment Cost (2011 \$MM); Duplex steel} = 16.8 + 3.9 \times m \quad (2)$$

Where, m = integer (minutes of resident time/3.3)

For the conditions used in this design, which are milder than earlier designs, the recommended metallurgy from the vendor continues to be Incoloy 825, with a total installed capital cost of approximately \$46.8MM (2011\$) for the system including feedstock receiving bin, pre-steaming, pressurized heating, reaction, and flash cooling. The reactor schematic is shown in Figure 8, and is similar to the configuration presented in the 2011 report.

Area 200 contributes about \$0.78/gal (or \$0.74/GGE) to the MFSP, including deacetylation, acid pretreatment, and conditioning. About 55% of the \$0.74/GGE contribution is attributed to capital cost, of which deacetylation and acid pretreatment equipment accounts for 96% of total capital expenses.

3.2.4 Achieving the Design Case

Table 4 shows demonstrated performance results achieved during NREL’s 2012 pilot-scale demonstration runs, as well as the 2011 ethanol report assumptions and the present 2017 conversion targets (i.e., those used in the current Aspen model) for the pretreatment area.

Table 4. Research Status and 2017 Targets in the Pretreatment Area

	2011 Design report	2012 SOT	2017 Targets
Pretreatment			
Solids loading (wt %)	30%	30%	30%
Xylan conversion to xylose (%)	90%	82%	90%
Xylan conversion to furfural (%)	5%	6%	5%
Conditioning			
Ammonia loading (g/L of hydrolysate)	4.8	1.6	1.6
Hydrolysate solid-liquid separation	no	no	no
Xylose sugar loss (% entering conditioning)	1%	0%	0%
Glucose sugar loss (% entering conditioning)	0%	0%	0%

As shown above, the 2017 target is 90% conversion of xylan to monomeric xylose with 5% loss to degradation products. Total xylan-to-xylose yield was demonstrated to range from 81%–88% in four out of five trials during NREL’s 2012 pilot demonstration runs, with a fifth run achieving 93% [29]. Thus, further room for improvement exists with a reasonable goal to achieve 90% conversion better and more consistently in a short timeframe by 2017 under mild pretreatment conditions. It is also noteworthy that NREL’s 2012 pilot runs demonstrated a higher xylose-to-ethanol yield, exceeding the 85% target in a number of cases, largely because of the addition of deacetylation which allowed for more complete sugar utilization. Another metric of note is the high arabinan-to-arabinose yields, but because of the small quantity of arabinan in the biomass there is more variability in demonstrated results. Nevertheless, an average arabinan-to-arabinose yield of 90% continues to be a reasonable assumption [29].

The deacetylation step also enables less sulfuric acid usage in pretreatment, resulting in lower furfural formation and less salt formation by requiring less ammonium hydroxide for neutralization, in addition to dramatically lowering acetic acid concentration and reducing total stream throughput in downstream operations. Thus, deacetylation is an important addition here, and the ability to achieve the deacetylation yields discussed above at reasonable conditions (primarily 17 mg/g caustic loading) will be another important performance metric. It is also recognized that a number of hydrocarbon-producing organisms may possess the ability to tolerate or even utilize acetate [30], thus negating inhibition concerns traditionally associated with ethanol fermentation, but the value gained in other benefits from deacetylation listed above (primarily reduction in non-fermentable biomass components and subsequent reduction in throughput and size for all downstream equipment) is expected to outweigh tolerance or utilization of acetate. This will be confirmed in further analysis moving forward.

Further research topics in the pretreatment area include optimizing deacetylation with acid pretreatment, additional size reduction after acid pretreatment and prior to enzymatic hydrolysis, and optimizing enzyme preparation and loading to accommodate deacetylated biomass. These

are aimed at overall process optimization for chemical loadings (alkaline, acid, and enzyme), process conditions (time, temperature, residence time) and other process steps to improve digestibility.

3.3 Area 300: Enzymatic Hydrolysis, Hydrolysate Conditioning, and Bioconversion

3.3.1 Overview

In this process area, cellulose is converted to glucose using cellulase enzymes. This process is known as enzymatic saccharification or enzymatic hydrolysis. A cellulase enzyme preparation is a mixture of enzymes (catalytic proteins) that work together to break down cellulose fibers into cellobiose and soluble gluco-oligomers and ultimately into glucose monomers. The resulting glucose and other sugars hydrolyzed from hemicellulose during pretreatment are then conditioned to remove insoluble solids, partially concentrated, and converted to hydrocarbon molecules (this final step is commonly referred to as “fermentation” and would be the analog to ethanol fermentation in the previous design case, however the process stipulated here is formally defined as aerobic respiration, thus we are avoiding the terminology “fermentation” here and instead using “bioconversion”).

The enzymatic hydrolysis portion of this process area follows the same fundamental process schematic described in the 2011 ethanol report; namely carrying out hydrolysis at elevated temperature (which provides higher enzyme activity) so the reaction proceeds faster and requires lower enzyme loading, with hydrolysis split between two sequential reactions: a high-solids continuous flow reactor followed by batch hydrolysis in a stirred tank. Bioconversion of the released sugars occurs separately at lower temperature and in separate vessels, thus the process configuration is akin to separate hydrolysis and “fermentation” (SHF).

After hydrolysis is complete, the hydrolysate material containing soluble sugars and insoluble residual solids (primarily lignin) is sent to a solid-liquid separation step where the insoluble fraction is removed using a vacuum filter press to enable more efficient gas-liquid mass transfer downstream in the aerobic bioreactors. This operation includes a wash step to recover soluble sugars carried over into the solids fraction. The washed lignin-rich solids fraction is then sent to the boiler for combustion. An important implication of this added solid separation step is that enzymes will also be removed prior to bioconversion, thus negating additional hydrolysis activity that could take place during bioconversion. A portion of the liquid fraction exiting the filter press is sent directly to the bioconversion step, which is carried out in fed-batch mode, while the majority of the stream is sent to an evaporator system to concentrate the sugars. The concentrated sugars are then cooled and fed to the bioreactors as the conversion reaction proceeds through the batch cycle. The bioreactors are inoculated with the conversion organism from an inoculum seed train, and the bioconversion process proceeds for approximately 2.9 days until the target conversion of sugars to FFA product is achieved. The product broth from the bioreactors is emptied to a storage tank before being pumped to purification. Figure 9 shows a simplified flow diagram of the enzymatic hydrolysis, conditioning, and bioconversion process.

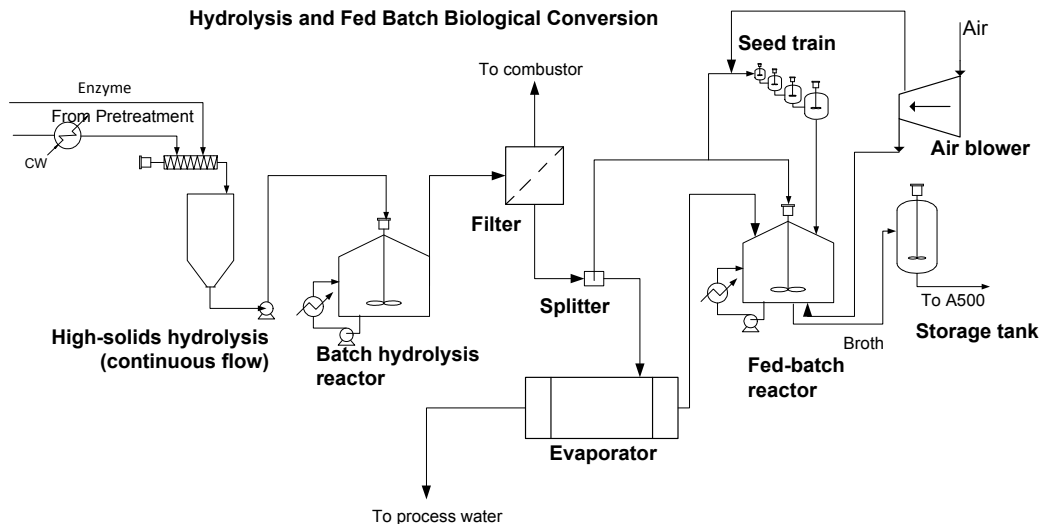


Figure 9. Simplified flow diagram of the enzymatic hydrolysis, hydrolysate conditioning, and bioconversion process

3.3.2 Design Basis

The process and design basis for enzymatic hydrolysis is the same as described in the 2011 ethanol report, thus will only be briefly summarized here. In short, enzymatic hydrolysis is initiated in a continuous, high-solids vertical tower reactor with the slurry flowing down the reactor by gravity; this first step is required as the feed material at 20% solids (or more) is not pumpable until the cellulose has been partially hydrolyzed. After mixing in the cellulase enzyme, the total solids loading entering the continuous column reactor is 20 wt% (12.2 wt% insoluble) and the temperature is 48°C (118°F). The residence time in the continuous reactor is 24 hours. After this point, the slurry is pumpable and is batched to one of six 1 MM gal vessels (950,000 gal working volume), where enzymatic hydrolysis continues for another 60 hours. The batch reactors are agitated and temperature controlled at 48°C using a pump-around loop with cooling water heat exchange.

The amount of enzyme used (the enzyme loading) is determined based on the amount of cellulose present in the hydrolysate and the specific activity of the enzyme. In the 2011 design report, the enzyme loading was set to a 2012 target of 20 mg enzyme protein/g cellulose to achieve a 90% conversion to glucose. During NREL's 2012 state of technology demonstration runs, both the enzyme loading target and the cellulose conversion target were achieved independently, although not at the same time: two runs at 19 mg/g enzyme loading resulted in 78% and 82% cellulose to glucose conversion, while a third run at 26 mg/g enzyme loading resulted in 89% cellulose conversion, very near the 90% target [5]. These particular results translated to a tradeoff in calculated MESP nearly identical to each other for all three runs, indicating that the increase in glucose yield paid for the higher enzyme loading in the latter case.

Moving forward to 2017, this metric will be targeted to aggressively improve to a loading of 10 mg/g cellulose while maintaining a 90% conversion target. Given ongoing advancements in enzyme preparations, discussions with enzyme manufacturers suggest this is not an unreasonable projection. Furthermore, new enzyme cocktails with increasing xylanase activity may become available to allow for a greater degree of xylan-to-xylose conversion during enzymatic

hydrolysis, taking some of the burden off the pretreatment section to achieve extremely high levels of xylan deconstruction to xylose (potentially allowing milder pretreatments at reduced cost). This tradeoff has not been considered here for lack of specifics to set quantitative targets, but may be considered in future state of technology cases or design updates. The target design conditions for enzymatic hydrolysis are summarized in Table 5.

Table 5. Enzymatic Hydrolysis Conditions

Temperature	48°C (118°F)
Initial solids loading	20 wt % total solids (12.2% insoluble/7.8% soluble)
Residence time	3.5 days total (84 h)
Number and size of continuous vessels	8 @ 950 m ³ (250,000 gal) each
Number and size of batch vessels	6 @ 3,600 m ³ (950,000 gal) each
Cellulase loading	10 mg protein/g cellulose

The reactions and conversions taking place during enzymatic hydrolysis are listed in Table 6. As noted above, although the use of more advanced enzymes may achieve some xylan conversion during enzymatic hydrolysis, for modeling purposes all xylan conversion is assumed to be achieved upstream during dilute acid pretreatment.

Table 6. Enzymatic Hydrolysis Reactions and Assumed Conversions

Reaction	Reactant	% Converted to Product
$(\text{Glucan})_n \rightarrow n \text{ Glucose Oligomer}$	Glucan	4.0%
$(\text{Glucan})_n + \frac{1}{2}n \text{ H}_2\text{O} \rightarrow \frac{1}{2}n \text{ Cellobiose}$	Glucan	1.2%
$(\text{Glucan})_n + n \text{ H}_2\text{O} \rightarrow n \text{ Glucose}$	Glucan	90.0%
$\text{Cellobiose} + \text{H}_2\text{O} \rightarrow 2 \text{ Glucose}$	Cellobiose	100%

Once sugar production is complete, the hydrolysate is processed through a series of conditioning steps to purify and concentrate the sugars prior to conversion. This represents a deviation from the ethanol design case where the sugars are immediately converted to ethanol by reducing temperature and initiating fermentation in the same vessels that were used for enzymatic hydrolysis, without any intermediate conditioning. The first conditioning operation is a solid-liquid separation step to remove lignin and other residual insoluble solids from the hydrolysate. As discussed in NREL's recent technical report, *Biological Conversion of Sugars to Hydrocarbons Technology Pathway*, unlike anaerobic ethanol fermentation, the conversion pathway modeled here is aerobic and the solids may adversely interfere with necessary gas-liquid oxygen mass transfer and limit oxygen uptake rates (OURs), and may also impede complete hydrocarbon product recovery and purification [31, 32]. However, the requirement for removing solids as a prerequisite to aerobic bioconversion is not yet fully understood. The relatively limited literature on hydrocarbon metabolic pathways focuses almost exclusively on using glucose or standard commodity hexose-based sugars (e.g., sugarcane juice, corn syrup) [33]; thus, performance with lignocellulosic hydrolysate, also including pentose sugars and solubilized lignin-derived compounds, is not yet quantified. From a cost standpoint it may be preferential to allow solids to pass through the bioconversion step to be removed downstream (as in the case of the ethanol process), as this may allow for the use of a lower-cost separation system and ultimately increase yield by avoiding sugar losses that are incurred in the upstream

separation; however, a tradeoff could be incurred by increasing the complexity of downstream product recovery in such a scenario. Namely, the hydrophobic lignin material may more readily partition into the hydrocarbon phase than the aqueous phase, potentially confounding downstream product recovery costs and/or efficiencies.

The design of the solid separation step was set based on extrapolating from NREL experimental data as well as input from Harris Group and vendors. NREL has evaluated the potential process and economic tradeoffs between three hydrolysate clarification technologies in the context of post-enzymatic hydrolysis material, namely a pressure belt filter, vacuum belt filter, and basket centrifuge [34]. Each option exhibits differences in capacity, sugar recovery, energy efficiency, and cost. Between the filter options, the vacuum belt filter was shown to accommodate a larger solids processing capacity (thus requiring lower total filtration area), but the pressure filter allowed for slightly higher retention of sugars (i.e., lower carryover loss of sugar into the solid stream) at a given wash ratio. The centrifuge exhibited similar sugar retention efficiency as the pressure filter, but at considerably lower capacity and increased cost than either filter press option; therefore, the centrifuge option was not explored further.

Based on the preliminary NREL data and Harris Group estimates, it was determined that the vacuum filter option would provide the most cost-efficient processing operation for hydrolysate clarification, while maintaining reasonably high sugar recovery (up to 99% at a wash ratio of 2.5 L water/L of liquor remaining in the filter cake). Although this is a relatively high wash ratio and incurs a cost penalty accordingly, the stipulation for 99% sugar recovery is also fairly aggressive, and not yet well understood in the context of separating solids in post-saccharification slurries, which is more challenging than prior to saccharification. The economic impact incurred by varying the assumption around sugar recovery is considered below in the Sensitivity Analysis section. Alternatively, to achieve good solids separation in this step after 90% hydrolysis of cellulose to glucose, additional filter area could plausibly be required relative to the baseline assumption. The cost impact associated with varying the vacuum filter capital cost (attributed to varying the total filtration area) is also investigated in the Sensitivity Analysis section. The design and performance metrics assumed for the vacuum belt filter are summarized in Table 7.

Table 7. Vacuum Belt Filter Specifications for Hydrolysate Solids Separation

Number of stages	2
Wash ratio	2.5:1 (L water : L liquor in filter cake)
Capacity (Insoluble Solids basis)	20 kg/hr-m ² (IS basis)
Soluble sugar recovery	99.0%
Maximum unit size	170 m ²
Power demand	490 KW (660 hp) per unit

As described in NREL’s recent technical memo on biological hydrocarbon production [32], following solids removal, the sugar stream may be sent directly to the biological conversion step or may be further processed to concentrate the sugars by evaporation or other means (e.g., reverse osmosis or nanofiltration). While utilizing dilute (100–150 g/L) sugars is the approach taken in the 2011 ethanol design model, concentrated commodity sugars (≥ 500 g/L) are utilized in many literature reports on hydrocarbon biofuels production [35]. Different processing schemes for the biological conversion step also require different optimum sugar concentrations, with

higher sugar concentrations being more conducive to fed-batch operation versus batch operation [36, 37]. Although overall bioreactor volumes can be similar in either case if volumetric productivities (i.e., g/L/h) are similar, there are additional impacts to downstream unit operations within the context of an integrated process if concentrated sugars are used; for example, employing an evaporation step prior to bioconversion will allow the evaporated water to be recycled directly as a high-purity water source, thus reducing total water feed rate to and cost of WWT.

The present model utilizes a fed-batch mode of operation in the bioreactors (described below), thereby favoring inclusion of a sugar concentration step prior to bioconversion. The process design detailed here assumes that 30% of the clarified hydrolysate material (13.8 wt% total sugar concentration) is sent directly to the bioreactors, which are filled to a 50% initial fill level (including inoculum addition) to commence bioconversion. After the sugar bioconversion step has been initiated, concentrated sugars (46.3 wt% concentration) are continuously fed to the bioreactors; fed-batch operation maintains high product titers and better control over the reaction [36, 37]. Sugar consumption and product formation then continue through the production cycle. Hydrolysate concentration is thus utilized for the 70% of the clarified hydrolysate stream fed into the production bioreactors during fed-batch mode. Moving forward further tradeoffs will be investigated in hydrolysate concentration, for example concentrating the entire clarified hydrolysate without first initiating bioconversion or seed growth with a dilute fraction.

The concentration step utilizes mechanical vapor recompression (MVR) evaporators. MVR evaporators were deemed to be preferable over standard thermal (steam)-driven evaporators given preliminary heat and power balance information, where MVR evaporators are primarily electricity-driven rather than steam-driven. Four effects are required to concentrate the sugars from 14% to 46% (i.e., reduce water content to 50%). While further concentration to 60%–70% may more closely replicate commodity sugar streams such as corn syrup, such a high concentration could become detrimental in the context of cellulosic-derived sugars as other impurities such as salts and inhibitors would also become more concentrated. Thus, the model conservatively concentrates to only 46% for lack of more quantitative in-house data at this time. To avoid the possibility of sugar degradation at high temperatures [38], the evaporators are assumed to be operated under slight vacuum to keep the maximum temperature below 80°C (176°F). The vapor exiting the evaporation system is nearly all water (~99.9% purity) and can be recycled directly to the process water manifold after being condensed by air cooling. This has an added benefit of reducing the total water flow rate to the WWT section (A600), which reduces cost for WWT units, which are dependent on the hydraulic flow rate. The vendor-provided evaporation system design specifications are summarized in Table 8.

Table 8. Hydrolysate Evaporator Specifications

Feed sugar concentration	14 wt%
Product sugar concentration	46 wt% (50% water, 4% other solubles)
Maximum operating temperature	80 °C
Evaporator technology	MVR
Number of effects	4
Electricity usage	3,600 KW (4,830 hp)
Steam usage (low-pressure steam)	1,550 kg/hr (0.8 MM kcal/hr)

The inoculum seed train design was assumed to be similar to that described in the 2011 ethanol report, with the addition of aeration to produce the conversion organism. To summarize, 10% of the hydrolysate stream (here, the clarified and concentrated hydrolysate) is diverted to seed production. Each inoculum production train consists of five reactors in series operating in batch mode with a 24-hour batch time and an additional 12-hour turnaround time. The seed reactors are cooled with chilled water from Area 900 to maintain the temperature at 32°C (90°F). The first vessel (40 gallons) is inoculated with a seed culture from the lab. Its broth is used to inoculate a larger reactor, and so on. After five iterations, the cell mass from the last vessel (200,000 gallons) is sufficient to inoculate the production vessel. Two parallel seed production trains are utilized as described in the 2011 design. Batch sequencing calculations were performed to verify adequate seed train capacity. These calculations confirmed that the seed production train does have enough capacity to accommodate the given bioreactor operational assumptions, with two seed trains and sizing/operational conditions as shown in Table 9. However, this must be re-evaluated as different operational factors such as volumetric productivity and bioreactor vessel size are introduced in the bioreactors.

Unlike prior designs for ethanol where the conversion organism (ethanologen) was known, namely *Zymomonas mobilis*, the current design intentionally avoids selecting a specific organism, as this would introduce a level of subjectivity given that the current design is intended strictly to establish a *representative* biochemical pathway to hydrocarbons from sugars without getting ahead of NREL or other DOE research, which has not yet publicly settled on a specific metabolic pathway, production host organism, or product (this is described more below). As such, *Z. mobilis* is maintained in the current design exclusively for purposes of satisfying mass and element balances, but is intended to serve as a placeholder that will be modified as additional specifics for targeted research become known. It is recognized that *Z. mobilis* may not be a realistic choice organism for an aerobic pathway, and a number of important caveats are noted further below recognizing the differences in metabolic demands for aerobic production organisms. While the fundamental design aspects for the seed train remain the same as the 2011 basis (e.g. consecutively larger vessels as described above), an important modification was made to introduce aeration for aerobic seed growth. Consistent with the early nature of the representative pathway model evaluated here (agnostic of organism selection and metabolic specifics), oxygen demands for seed growth were set by translating the same aeration demand on a volumetric basis (volume [of gas] per volume [of liquid] per minute or VVM) as was established for the main FFA production bioreactors (discussed below), with aeration for both the seed and main production vessels provided by a common air blower.

Table 9 summarizes the seed train design specifications. Similar to the 2011 design basis, 0.1% (w/v) sorbitol is used in the final seed fermentor to improve cell viability at high sugar concentrations [39, 40].

Table 9. Seed Train Specifications

Inoculum level	10 vol % of production vessel size
Batch time	24 h
Vessel turnaround time	12 h
Number of trains	2
Number of vessel stages	5
Maximum vessel volume	200,000 gal (757 m ³); 80% maximum working volume (160,000 gal)
Aeration rate	0.4 VVM (based on total seed train working volume; supplied by air blower shared with production bioreactors, see discussion below)
Corn steep liquor (CSL) loading	0.50 wt %
Diammonium phosphate (DAP) loading	0.67 g/L broth (whole slurry)

Table 10 gives the reactions and conversions used to describe the microorganism growth and sugar metabolism in the seed vessels, providing a comparison against assumptions employed in the 2011 model for anaerobic seed growth for ethanol production. As described in the 2011 report, the fraction of sugar converted to cell mass for anaerobic *Z. mobilis* inoculum for ethanol was quite small as is typical for this organism, namely 4% conversion of both glucose and xylose (of the 10% sugar stream diverted to seed growth; i.e., 0.8% diversion of total monomeric hydrolysate sugars to biomass seed growth), with a high ethanol yield even in the seed step at 90% conversion of glucose and 80% conversion of xylose to ethanol. However, because species such as *E. coli* or yeast could be expected to consume more sugar resulting in cell mass yields roughly 2 times higher than *Z. mobilis* under anaerobic conditions [3, 41], and because of the switch to aerobic production, the total sugar diversion to biomass growth during seed culture propagation is likely to be higher than in the ethanol case. Indeed, an excellent analysis of the subject by Huang and Zhang notes that sugar diversion to biomass growth in semi-aerobic systems may be at least 4–6 times higher than for anaerobic ethanol production by way of *Z. mobilis* due to increased energetic (ATP) demands for metabolism [41]. In a commercial system this will require strict control of reaction conditions, namely dissolved oxygen, to control cell growth (this may also be achieved by biological engineering and/or process configuration).

To account for increased cell mass production (assumed for modeling purposes to primarily occur in the seed train), a much larger fraction of glucose and xylose is diverted toward organism production in the current model, as shown below. These assumptions translate to a diversion of 8% of total glucose and 4% of total xylose in the original hydrolysate material being consumed for biomass organism growth, relative to 0.4% of each in the 2011 design basis. Combined with the cell growth assumed to occur downstream in the main bioreactor stage, these values result in a cell mass-to-total feed sugar ratio of 0.064 g/g, and a cell mass-to-FFA product ratio (exiting the bioreactors) of 0.226 g/g (for reference, the 2011 ethanol design report values are 0.017 g/g sugars and 0.038 g/g ethanol respectively). The model conservatively assumes no FFA production in the seed train, as the reactions in Table 10 are intended to account for the majority of all cell growth. This large diversion of substrate, which detracts from ultimate fuel yields, will be an important issue to better understand and quantify moving forward, and also represents a potential area for future improvement to incorporate possible cell recycling methods.

Table 10. Seed Train Reactions and Assumed Conversions

Reaction	Reactant	% Converted to Product	
		2011 design	2013 design
Glucose → Ethanol/FFA product (<i>stoichiometry varies</i>)	Glucose	90.0%	0%
Glucose + 0.047 CSL ^a + 0.018 DAP → 6 <i>Z. mobilis</i> + 2.4 H ₂ O	Glucose	4.0%	80.0%
Glucose + 2 H ₂ O → 2 Glycerol + O ₂	Glucose	0.4%	0.4%
Glucose + 2 CO ₂ → 2 Succinic Acid + O ₂	Glucose	0.6%	0%
Xylose → Ethanol/FFA product (<i>stoichiometry varies</i>)	Xylose	80.0%	0%
Xylose + 0.039 CSL + 0.015 DAP → 5 <i>Z. mobilis</i> + 2 H ₂ O	Xylose	4.0%	40.0%
3 Xylose + 5 H ₂ O → 5 Glycerol + 2.5 O ₂	Xylose	0.3%	0.3%
Xylose + H ₂ O → Xylitol + 9.5 O ₂	Xylose	4.6%	4.6%
3 Xylose + 5 CO ₂ → 5 Succinic Acid + 2.5 O ₂	Xylose	0.9%	0%

^a Corn steep liquor (CSL) and diammonium phosphate (DAP) are both nitrogen sources required for *Z. mobilis* growth. The stoichiometry shown above is only used to balance the compositions assumed for nonstandard components such as cell mass.

Sugar may be lost to side products by contaminating microorganisms in addition to being converted to cell mass and hydrocarbon (FFA) product. Sugar contamination losses were set consistent with the 2011 report basis, namely modeling a diversion of 3% sugar losses to lactic acid upstream of the production bioreactors. These contamination reactions are shown in Table 11. While it is recognized that sterility is more problematic in aerobic bioconversion systems with increased risk of contamination than for anaerobic fermentation, the assumption of similar contamination losses as for the ethanol design case is reasonable as an “*n*th-plant” target assuming a robust microbe may be developed to accommodate these values. Additionally, the vessel turnaround time is increased considerably longer than for the ethanol design case to account for more cleaning time between runs (discussed below). The cost impact for varying the contamination loss is considered below in the Sensitivity Analysis section.

Table 11. Bioreactor Contamination Loss Reactions

Reaction	Reactant	% Converted to Product
Glucose → 2 Lactic Acid	Glucose	3.0%
3 Xylose → 5 Lactic Acid	Xylose	3.0%
3 Arabinose → 5 Lactic Acid	Arabinose	3.0%
Galactose → 2 Lactic Acid	Galactose	3.0%
Mannose → 2 Lactic Acid	Mannose	3.0%

Bioconversion of sugars to product occurs in a system of 264,000 gal (1 MM L) stirred-tank aerated vessels. The design and operation of these vessels represents an important change from the 2011 anaerobic ethanol fermentation basis, which utilized simpler, larger vessels of 1 MM gal capacity (950,000 gal working volume). As noted previously, ethanol is produced by anaerobic fermentation (via organisms such as *Z. mobilis* as per NREL’s research). Long-chain hydrocarbon biofuel precursors such as farnesene, fatty alcohols, or fatty acids are typically produced by *aerobic* bioprocesses, although anaerobic pathways to hydrocarbons also exist [42, 43]. Such anaerobic processes likely require longer research timeframes, however, to achieve performance required for economic viability within the context of fuels. Thus, this representative model pathway focuses on aerobic bioconversion.

In aerobic processes, oxygen is a nutrient used by microorganisms for cell growth, maintenance, and metabolite production. Scarcity of dissolved oxygen negatively impacts process performance and reduces product yields. Molecular oxygen (O_2) has low solubility in aqueous media and the solubility also decreases with elevated temperature and increases in broth osmolarity and viscosity [44]. These factors create new challenges beyond those observed for cellulosic ethanol production, primarily related to economically scaling up oxygen mass transfer to a commercial level sufficient for biofuels applications. As noted in NREL's recent technical memo cited previously [32], it is anticipated that the ability to maintain effective gas-liquid mass transfer (i.e., sufficiently high volumetric oxygen transfer rates [OTRs]) will ultimately limit the size at which microbial fuel production can be operated to considerably smaller volumes than are possible for anaerobic processes. For example, the largest bioreactor scale reported publicly for biological upgrading of sugars to hydrocarbons is approximately 500,000 L (130,000 gal) [45], although it is expected that with further process optimization and continued scale-up it will be possible to increase maximum vessel size beyond this value (even the smaller A400 section enzyme aerobic bioreactors are sized at 300,000 L, discussed below). Thus to establish a baseline, the production bioreactors were assumed to be 1 MM L (264,000 gal); a reasonable, if not conservative, extrapolation to a commercial scale that provides economy of scale and still allows for good control of system and reaction parameters.

Fed-batch operations are commonly used for large-scale bioprocesses whereby the vessels are inoculated and filled to an initial level, and substrate is continuously fed to the bioreactors over the course of the batch cycle as sugars are continuously consumed [46] (the enzyme bioreactors also operate in fed-batch mode as described below). Fed-batch operation of aerobic bioprocesses can help balance the carbon feed rate to limits set by the maximum OTR [47]. In the present model the bioreactors are filled to a 50% initial level (including inoculum), using the clarified dilute sugar material obtained after solids separation (representing 30% of the total hydrolysate liquor). After this point, as the reaction proceeds the remaining 70% of the hydrolysate liquor is delivered to the bioreactors after first being concentrated through the sugar evaporation step described previously. This fed-batch delivery of concentrated sugars enables a high product titer and less downstream purification/concentration demand. A maximum fill level of 80% is specified to ensure adequate head space for vapor-liquid disengagement and to mitigate foaming issues associated with the aerobic nature of the process. Thus, to calculate the number of required bioreactors, an average vessel working volume of 65% (650,000 L) is assumed over the duration of the fed-batch cycle. In a realistic system the initial, final, and average working volume set-points are more complex, with dependencies on detailed bioreactor design including number and location of draws, draw volumes, gas holdup, etc.; however, these design details are currently beyond the scope of this analysis.

The agitation and aeration rates for the production bioreactors were set based on vendor feedback via Harris Group, using a calculated oxygen uptake rate (OUR, mmol/L-h), which was set stoichiometrically from the FFA production rate (similar to the basis for setting OUR in the A400 enzyme section). The vendor evaluated estimates for multiple stirred tank vessel sizes. All sizes evaluated were set at a maximum liquid height-to-diameter ratio of near 1:1, which tends to minimize agitator cost as well as blower cost and power demand relative to increased liquid heights (pressure head), albeit at the expense of aeration efficiency (degree of oxygen solubilization) relative to increased aspect ratios. This design assumption will continue to be evaluated in further detail moving forward to better quantify appropriate design optimization,

including to consider bubble columns and stirred tank vessels of higher aspect ratios relative to the 1:1 basis utilized here. For the vessel sizes evaluated by the equipment vendor, the quoted agitation power demand varied between roughly 0.2–0.4 hp/1,000 gal of working volume (based on the average working volume of 65% for any given vessel size); while already an order of magnitude higher than the anaerobic ethanol fermentor agitator in the 2011 design report (0.03 hp/1,000 gal), during external peer review of this report it was decided that such an agitation power may still likely be optimistically low for submerged aerobic systems. Thus, the agitation power was conservatively increased from the vendor basis up to 1.0 hp/1,000 gal (200 W/m³) of working volume, or 0.65 hp/1,000 gal of total bioreactor vessel volume for the 1 MM L (264,000 gal) vessel size (41 ft height × 33 ft diameter, maximum liquid level of 33 ft). This value is applicable during vessel operation only, but not during vessel downtime for turnaround (draining, cleaning, and refilling). This mixing power is roughly 20 times higher than the anaerobic ethanol model on a working volume basis, but is to be expected given that agitation is required merely to maintain bulk mixing of the slurry in the ethanol case, while it is an important aspect of achieving necessary oxygen gas-liquid mass transfer in the present design.

In addition to agitation demands, aeration rate is another critical design parameter in aerobic systems, as this sets air compressor cost and power, both of which can be significant [48]. Required aeration rate is a function of OTR, which is the product of the volumetric mass transfer coefficient k_1a (h⁻¹) and the log mean oxygen concentration gradient (the difference between the saturated dissolved oxygen concentration and the desired dissolved oxygen concentration) at the top and bottom of the bioreactor operating volume:

$$\text{OTR} = k_1a \frac{(C_b^* - C_D) - (C_t^* - C_D)}{\ln\left(\frac{C_b^* - C_D}{C_t^* - C_D}\right)}$$

where C_b^* and C_t^* are the saturated dissolved oxygen concentrations (mmol/L) at the bottom and top of the vessel, respectively, and C_D is the desired dissolved oxygen concentration. The volumetric mass transfer coefficient and dissolved oxygen concentration values are in turn dependent on gas solubilities, pressures, agitator power consumption, and vessel working volume; these parameters have been described in detail in the 2011 ethanol design report for the A400 enzyme section [3] and will not be repeated in such detail here, suffice it to reiterate the inter-dependencies that design considerations such as vessel size, agitation power, and oxygen transfer rate exhibit on each other, all of which are dependent on specific oxygen uptake rates and metabolic needs for a given product pathway.

Using the combination of the stoichiometric reactions for the bioreactor shown below in Table 14, as well as the assumed FFA volumetric productivity of 1.3 g/L/h (discussed below), the resulting stoichiometric OUR for FFA production would be relatively low at approximately 5.0 mmol/L-h as an average over the course of the fed-batch cycle (based on 65% average working volume), with a minimum of 4.1 at maximum working volume of 80% and maximum of 6.6 at minimum (initial) working volume of 50%. When setting OTR to this OUR value, the aeration demand required to achieve this value would be relatively low, e.g. < 0.1 VVM (volume air/working broth volume/minute) of air, which is less than what may be practical for commercial scale aerobic systems operating in a range of 0.3–0.5 VVM (a range which was confirmed during peer review of this report). Thus, the aeration rate was increased to 0.4 VVM

based on average working volume of the bioreactors (0.3 at maximum working volume and 0.5 at initial fill volume). This is delivered by air blowers operating at a pressure of 15 psig (2 atm) based on a maximum vessel liquid height of 33 ft (with a common air blower supplying the main bioreactors as well as the seed train, also operating on a basis of 0.4 VVM). It is recognized that the OTR is realistically governed by the complex operational parameters described above, and that the achieved OTR will in turn set achievable FFA volumetric productivity; however, the combination of the OTR, agitation power, and vessel design (1:1 aspect ratio) originally provided by the vendor appeared overly-optimistic, thus agitation and aeration were increased as described above. Relative to the 2011 ethanol design report with a total power demand of 2.6 MW for the A300 section, the new A300 power demand has increased by an order of magnitude to 20.0 MW, primarily due to bioreactor agitation and aeration power demands. The cost impact associated with varying the aeration rate is explored below in the Sensitivity Analysis section.

Unlike the ethanol system which contained significant amounts of ethanol in the fermentor vent gas (caused by ethanol's relatively high volatility), which in turn required the use of a vent scrubber to recover the volatilized ethanol, the hydrocarbon product targeted here has much lower volatility so there is nearly no FFA product in the vent gas and a scrubber is not required. Heat exchange assumptions are maintained the same as for the ethanol case, namely cooling the bioreactors using a pump-around loop with the chiller system, with cooling demands calculated in the Aspen model to maintain the reactors at 32°C (96°F). While reasonable for anaerobic ethanol production, this pump-around arrangement could plausibly be detrimental to the aerobic organism, either by damaging the organism itself or by introducing a contamination point. Moving forward, alternative cooling arrangements may be considered such as cooling coils or vessel jackets. Aerobic reactions typically produce more heat than anaerobic fermentation, with a published rule of thumb presented as 110 kcal of heat produced per mole of oxygen consumed [49], considering only the heat of reaction itself; this compares to 194 kcal/mol estimated in the Aspen model, although this includes other factors beyond strictly the reaction (e.g. aeration, etc.); in addition, the heat generated during agitation adds another 33 kcal/mol to this value in the model. Finally, to mitigate potential foaming issues associated with the aerobic nature of the present system, a corn oil antifoam agent is added to the bioreactors at a basis of 890 mg/L of clarified hydrolysate feed to the bioreactors (1 mL/L at 0.89 kg/L corn oil density). Table 12 provides a summary of bioreactor design parameters utilized in this design.

Table 12. Guiding Bioreactor Design Basis Assumptions

Operating mode	Fed-batch
Temperature	32°C (96°F)
Reactor size	1 MM L (264,000 gal) operating at 50% initial working volume, 80% final working volume
Reactor height	12.5 m (41 ft)
Reactor diameter	10 m (33 ft)
Agitation power	110 KW each; 2,110 KW total (150 hp each, 2,830 hp total)
Average aeration rate	0.4 VVM (based on average working volume)
Inoculum level	10 vol %
Corn steep liquor (CSL) level	0.25 wt %
Diammonium phosphate (DAP) level	0.33 g/L broth (whole slurry)
Corn oil antifoam level	890 mg/L (1 mL/L) of hydrolysate feed to bioreactors

A number of potential metabolic pathways and products exist for biological conversion of sugars to long-chain hydrocarbons. Such products include isoprenoids, fatty acids, triglycerides, and paraffins [41, 50-52]. Each pathway exhibits varying theoretical yields, dictated by underlying metabolic mass and energy yields. Based on a survey of literature, a summary of theoretical metabolic yields to the product classes noted above is provided in Table 13.

As evidenced in Table 13, ethanol remains a superior product for bioconversion of sugars in the context of fuel molecules, exhibiting a much higher theoretical metabolic mass yield (e.g., weight of product relative to sugar), but also a higher energy yield (e.g., heating value of product relative to sugar), with the energy yield for hydrocarbon products closer to that of ethanol, but still 5%–24% lower. This demonstrates the increased burden placed on the present approach to achieve cost targets for hydrocarbon pathways relative to ethanol. These example products are all diesel-range molecules; however, products in the gasoline or jet-range (e.g., isobutanol, C6-C10 alcohols, etc.) generally compare similarly to the energy yields below [33, 52].

Table 13. Theoretical Metabolic Yields for Various Product Pathway Classes Compared to Ethanol [41, 50–53]

	Mass yield	Carbon yield	Energy yield (HHV basis)
Ethanol	51%	67%	98%
Pentadecane	29%	62%	88%
Farnesene (DXP pathway)	29%	64%	85%
Farnesene (MVA pathway)	25%	56%	74%
Fatty Acid (Palmitic acid)	36%	67%	89%
FAEE (Ethyl palmitate)	35%	67%	90%
Fatty Alcohol (Hexadecanol)	34%	67%	93%

It is worth repeating here that the present technology pathway is generally in a much earlier state of development and understanding relative to ethanol, which has a number of decades of research and experience to pull from (both internal and external to NREL research) in developing detailed process and economic models. As there is not yet a single pathway, organism, or product selected at NREL or DOE for targeted research in biological hydrocarbon production (nor will there necessarily be a single such pathway selected in the near term as “the best” option, given the constantly evolving efforts in metabolic engineering in the field), the intention here is to select what may be viewed as a *representative* product pathway to provide quantitative insight as to technical and economic challenges and future potential of the general “biological sugar conversion” technology approach. As such, the FFA product pathway was selected for evaluation here, primarily because (a) it exhibits a potential metabolic energy yield (an indicator of ultimate GGE fuel yield) toward the middle of the range shown in Table 13, thus serving as a reasonable mid-point proxy for the general product suite discussed above, and (b) fatty acid biosynthesis (e.g., in *E. coli*) is a fundamental pathway that has been extensively investigated [54–56]. A high-level sensitivity analysis to product selling price associated with a number of alternative product pathways is presented and described below in the Sensitivity Analysis section.

FFAs have desirable properties such as high energy density and low water solubility. FFAs are precursors of lipids and they play a vital role in cell physiology. FFAs are typically used within

the cell to form phospholipids for incorporation into cellular membranes, or to form triacylglycerides (TAGs) for energy storage. Many bacteria and some plants synthesize fatty acids through the highly conserved type II fatty acid synthase system. Biosynthesis of fatty acids is energy intensive and carefully regulated.² Regulation is required to ensure that cells do not accumulate excess, energy-rich lipids. Any excess lipids are rapidly degraded by oxidative cleavage to acetyl-CoA. These regulatory mechanisms need to be overcome in order to over-produce free fatty acids. Microbes tend to predominantly produce palmitate, a C₁₆ fatty acid. Palmitate and other FFAs can be modified *ex vivo* to produce alkanes; i.e., by esterification, reduction to fatty alcohols, decarboxylation to olefins, or hydrotreating.

The type II fatty acid synthesis system in bacteria begins with the enzyme catalyzed formation of a three-carbon intermediate, malonyl-CoA, by carboxylation of acetyl-CoA. The elongation of fatty acid molecules progresses through the iterative addition of two-carbon units derived from malonyl-CoA with the elimination of CO₂. The process is generally complete when the chain length reaches 16 carbons (i.e., palmitate). However, other longer or shorter fatty acids may also be formed, with varying degrees of saturation. Palmitate (palmitic acid, C₁₆H₃₂O₂) is assumed in the present model to be the representative FFA component produced during the bioconversion step for purposes of setting mass balances and energy yields. It is recognized that in reality, a mixture of saturated and unsaturated FFA components would be produced without targeted organism manipulation (which would also lower the net melting point of the combined FFA hydrocarbon mixture to the point that hydrocarbon-phase processing is not expected to be problematic, thus special measures are not taken in the present model to address FFA congealing issues).

Hydrocarbon components produced by biological pathways may be present as intracellular products (for example, many heterotrophic algae species), or may be secreted into the broth [57]. Intracellular production typically requires a dedicated extraction step to disrupt cells and extract stored hydrocarbon/oil product, and this step has been shown in the literature to incur significant energy and/or cost penalties [41], which is consistent with preliminary NREL modeling of each pathway option. For this reason, a secreted FFA product is assumed in this baseline model pathway to permit easier product recovery and post-conversion processing (described further below).

Aside from engineering and design challenges, from a process standpoint the primary cost drivers for the conversion stage are product yield (dictated by sugar conversions) and volumetric productivity (g/L/h of product being produced). The present design case model assumes conversion performance targets for glucose, xylose, and arabinose consistent with the 2011 ethanol design case, shown in Table 14. Additionally, the batch time in this process is set by translating from volumetric productivity, which is targeted at a basis that is also consistent with the ethanol design case at 1.3 g/L/h (based on average working volume for the FFA bioreactors). This translates to a batch time of 69 hours, with an additional turnaround time of 10 hours for draining, cleaning, and refilling, requiring 19 bioreactor vessels (see Table 15). Important implications around these assumptions are discussed in Section 3.3.4. The turnaround time

² Biosynthesis of one palmitate requires 7 ATP and 14 NADPH

assumed here is considerably longer than in the anaerobic ethanol case (2 hours), even with smaller bioreactors, primarily to account for increased cleaning time associated with typical requirements to maintain a higher level of sterility for most aerobic bioconversion systems relative to anaerobic fermentation.

Table 14. Bioconversion Reactions and Assumed Conversions

Reaction	Reactant	% Converted to Product
4 Glucose + O ₂ → 1 Palmitate (FFA) + 8 CO ₂ + 8 H ₂ O	Glucose	95.0%
Glucose + 0.047 CSL ^a + 0.018 DAP → 6 <i>Z. mobilis</i> + 2.4 H ₂ O	Glucose	2.0% ^b
4.8 Xylose + O ₂ → 1 Palmitate (FFA) + 8 CO ₂ + 8 H ₂ O	Xylose	85.0%
Xylose + 0.039 CSL + 0.015 DAP → 5 <i>Z. mobilis</i> + 2 H ₂ O	Xylose	2.0%
4.8 Arabinose + O ₂ → 1 Palmitate (FFA) + 8 CO ₂ + 8 H ₂ O	Arabinose	85.0%
Arabinose + 0.039 CSL + 0.015 DAP → 5 <i>Z. mobilis</i> + 2 H ₂ O	Arabinose	2.0%

^a Corn steep liquor (CSL) and diammonium phosphate (DAP) are both nitrogen sources required for *Z. mobilis* growth. The stoichiometry shown above is only used to balance the compositions assumed for *Z. mobilis* cell mass. Nutrient demands have not been optimized and a minimal, low-cost nutrient formulation has yet to be defined.

^b Additional sugar diversion to biomass (represented as *Z. mobilis*) is assumed to occur at high rates in the seed train step, although some of the biomass growth modeled in the seed train may instead occur in the product bioreactors

Table 15. Bioconversion Productivity and Impacts on Bioreactor Vessels

FFA Volumetric productivity	1.3 g/L-hr (based on average working volume)
Bioconversion residence time	69 hours
Vessel turnaround time	79 hours
Number of vessels required	19 (1 MM L vessels, 65% average working volume)

3.3.3 Cost Estimation

For equipment which remains the same as the 2011 ethanol design case, as well as new equipment that was modified or added in the present analysis, the material of construction for most operations in this section remains 304SS, which is the most cost-effective material for fermentation service. The design and cost basis assumptions for all enzymatic hydrolysis equipment were left unchanged from the 2011 ethanol case, namely empty towers for the continuous hydrolysis reactor based on a vendor quotation for flat-bottomed plug-flow reactors with a 10:1 height:diameter ratio; as well as 1 MM-gal batch hydrolysis reactors and agitators. It is worth noting that the required number of batch hydrolysis vessels has decreased from 8 in the 2011 ethanol design case (i.e., 8 of the 12 1 MM-gal vessels were for the hydrolysis portion of the operation in the combined hydrolysis/fermentation step) to 6 in the present model, due to a reduction in total volumetric throughput into the hydrolysis section associated with the addition of up-front deacetylation to solubilize and remove a portion of non-fermentable biomass components.

The vacuum belt filter design and cost information was provided by a vendor, who provided a design basis of 170 m² maximum filtration area per individual filter, with filter sizing based on a filtration rate of 20 kg/h m² based on insoluble solids. The cost includes a two-stage countercurrent water wash step at a wash ratio of 2.5 L/L liquor in the filter cake. A filtered hydrolysate storage tank with a residence time of 20 minutes is included to provide intermediate

storage for filtrate from the belt filter. The sugar concentration (evaporation) equipment was also based on vendor-provided design and cost estimates. As noted above, the system utilizes MVR evaporators in a series of four effects to concentrate a fraction (70%) of the filtered hydrolysate from 14 wt% to 46 wt% (reducing water content to 50%). A concentrated sugar storage tank with a residence time of 20 minutes is included downstream of the evaporator.

The bioreactor vessels (using stirred tank agitators) were costed by scaling down from the previous vendor estimate for 1 MM-gal ethanol fermentation vessels, an approach that Harris Group confirmed to be reasonable for the bioreactor vessels themselves (i.e., not including new agitation and aeration considerations, to be included separately). As described above, the aerobic bioreactor vessels were selected to be sized at 1 MM L (264,000 gal, rather than 1 MM gal) as a reasonable extrapolation from the understanding of current, non-commercial scale capacity for similar service operations while restricting the size from becoming too large to enable effective oxygen mass transfer and uptake. Thus, while the cost basis for the large 1 MM-gal ethanol tanks was applied for scaling to the smaller 264,000-gal bioreactor vessel size, the smaller size loses economy-of-scale benefits, which results in a cost per reactor volume higher than that exhibited in the ethanol design (\$370/thousand L purchased cost per vessel versus \$240/thousand L in 2011\$ for larger 1 MM-gal tanks). Blower and agitator costs were scaled from information provided by Harris Group based on vendor quotations. The vendor indicated that for applications requiring higher air flow rates than those estimated here, more costly specialized impellers with a parabolic blade design would be required to achieve good dispersion; however, the air flow rate considered here is sufficiently low that conventional agitator blades were deemed appropriate. The cost and design bases for the seed train equipment were left unchanged from the 2011 ethanol design. Finally, a 1.2 MM-gal storage tank is provided downstream of the bioreactors.

Harris Group also provided cost estimates for bubble column reactors as a plausible alternative to standard stirred-tank reactors, but based on a preliminary analysis of power and cost implications for these units, the stirred tank basis was deemed more cost-effective. Thus, bubble columns are not utilized here in the design base case, but will be evaluated in more detail moving forward to better understand tradeoffs in design details, OTR demands, agitation/air compression power, and maximum plausible vessel size for either vessel option. Another anticipated benefit of bubble columns would be to negate the need for dedicated agitators, as the bubbles may provide the necessary mixing in-situ.

3.3.4 Achieving the Design Case

For the enzymatic hydrolysis and bioconversion area, Table 16 shows the 2011 design case ethanol target assumptions, the 2012 State of Technology demonstrated values, and the new target values used here for production through the FFA intermediate product.

Table 16. 2017 Targets for Enzymatic Hydrolysis and FFA Production, Compared to 2012 Targets and State of Technology Results for Ethanol

	2012 Targets (Ethanol)	2012 State of Technology (Ethanol)	2017 Targets (FFA)
Total solids loading (wt %)	20%	20%	20%
Enzymatic hydrolysis substrate	Whole-slurry	Whole-slurry	Whole-slurry
Hydrolysis time (days)	3.5	3.5	3.5
Enzyme loading (mg/g cellulose)	20	19	10
Bioconversion time (days)	1.5	1.5	2.9
Combined <i>cellulose-to-glucose</i> × <i>glucose-to-product</i> conversion (through hydrolysis and bioconversion,%) ^a	85.5%	74%	85.5%
Total xylan to xylose conversion (%)	90%	81%	90%
Xylose to product conversion (%)	85%	93%	85%
Arabinose to product conversion (%)	85%	54%	85%

^a Assumes 95% glucose-to-product conversion (product = ethanol or FFA respectively).

Note, this was previously stated as “overall cellulose-to-product (ethanol)” conversion; however the metric is strictly a combination of fractional cellulose conversion to glucose multiplied by fractional glucose conversion to product, and does not include losses to fermentation, cell mass growth, or processing inefficiencies (i.e., the amount of glucose ultimately available for conversion to product is less than the amount of glucose produced from upstream cellulose conversion)

3.3.4.1 Biomass Deconstruction (Pretreatment + Enzymatic Hydrolysis)

During NREL’s 2012 ethanol demonstration runs, the addition of deacetylation improved the performance of a number of downstream unit operations, namely pretreatment (milder conditions via reduced acid loading), hydrolysis, and fermentation (increased yields caused by reduced inhibition in both steps). However, a number of operations did not quite achieve the 2012 targets or the performance observed in prior SOT demonstrations, namely glucose yield during enzymatic hydrolysis, which had been performed on a washed-solids substrate rather than whole-slurry prior to 2012. Xylan-to-xylose yield was also somewhat below the target, but this was offset by a higher xylose-to-ethanol yield such that overall xylan-to-ethanol yield was similar to the target. Arabinose-to-ethanol conversion was low, and is an area for continued research moving forward, albeit for a different product pathway.

Biomass deconstruction to sugars is an important research area that will continue to progress by further improving monomeric sugar yields at increasingly less severe conditions (e.g., milder pretreatment and lower enzyme loadings). The FFA target production pathway stipulates 90% xylose yield from xylan, which may be observed from a combination of reduced severity pretreatment (combined with the use of deacetylation) as well as new advanced enzyme cocktails with xylanase activity to further reduce the burden on hemicellulose deconstruction exclusively in pretreatment. The target model also assumes that the stipulated solubilization of non-fermentable components will be achieved during deacetylation while maintaining xylan loss to no more than 2%. There is early indication that this is a reasonable set of targets for deacetylation, but will require further optimization of deacetylation conditions. The FFA target

pathway also stipulates 90% glucose yield at 50% of the enzyme loading (10 mg/g) relative to current 2012 performance, with constant enzymatic hydrolysis batch time. As evidenced by the lower glucose yield observed in the 2012 SOT demonstration even at higher (19 mg/g) enzyme loading, this will be an aggressive improvement, but again based on discussions with NREL researchers and enzyme companies, is a reasonable target for a 2017 timeframe given performance recently observed using the latest enzyme preparations.

3.3.4.2 *Bioconversion*

There remains considerable room for improvement in the efficiency of sugar conversion to fuel, particularly for utilization of pentose sugars, across a variety of hydrocarbon-producing microorganisms [58-60], as well as in improving specific productivity rates (g product/g cell/h), targeting a lower diversion of sugar to microbial cell growth and/or engineering ways to recover and reuse microbial cells (e.g., cell retention or cell recycle bioreactor configurations) and mitigate potential hydrocarbon product toxicity effects [50]. Likewise, volumetric productivities also solicit much room for improvement beyond publicly-demonstrated performance. Recent literature suggests that the current state of technology for microbial conversion to hydrocarbon components includes product titers ranging from 0.1- 24 g/L of long-chain hydrocarbons [35, 52, 61-63], with times for batch or fed-batch production of 2–7 days [59]. Relative to ethanol fermentation with demonstrated productivities of 1.2–1.6 g/L/h or higher, maximum reported productivities for long-chain hydrocarbons are on the order of 0.11–0.19 g/L/h for fatty acids (the highest rates were achieved using a fed-batch process) [61] [64, 65], and less than 0.1 g/L/h for other components such as fatty acid ethyl esters or isoprenoids [33, 51]. Even after adjusting for differences in theoretical metabolic yields, these productivities leave much room for improvement compared to established ethanol performance. This point is recognized by DOE-BETO as well, as microbial catalyst development is identified as a critical technical R&D barrier in the May 2013 MYPP [66].

While this information is strictly a subset of published literature values, and does not include NREL in-house data (which has not yet been established for the conversion step), it begets a question regarding the timeframe required to achieve organism performance targets. The most direct response to this point is that the intent of the present report is to document a transparent, quantitative path to achieve an RDB selling price of \$5/GGE based on rigorous process modeling, which is in fact achieved via the combination of process targets described here. We feel it is not our place to comment on the “state of the industry” (which includes a number of commercial entities that have already made significant progress in developing an organism and product pathway, which may or may not reflect similar values to those presented here from literature), to make an authoritative judgment call regarding specific timing of out-year achievements of such targets and how closely these achievements correlate between published literature and private industry. Additionally, moving forward as more detailed technical targets are developed, validated, and refined, if certain targets are not met in a given timeframe by NREL or other partners, the shortfall may be compensated for by achievements in other areas; for example, progress demonstrated for fractional conversion of lignin to value-added coproducts (which is considered for the time being in the ultimate “2022” path to \$3/GGE below in Section 6, but not here in the \$5/GGE model). Alternatively, a cell recycling step could plausibly be added, which could potentially increase per-pass sugar conversions as well as reduce the amount of sugar diversion to cell mass growth relative to FFA production. The cost impacts associated

with variations in both the sugar conversion efficiencies as well as volumetric productivity are considered below in the Sensitivity Analysis.

Advances in systems biology and metabolic engineering have enabled the development of microbes to produce hydrocarbon biofuels with properties similar to petroleum-based fuels. A variety of hosts, including microalgae, bacteria, and fungi, are available to produce biofuels. The discussion below focuses on *E. coli* as a model organism for the bioconversion of cellulosic sugars to free fatty acids. Figure 10 shows a comparison of the concentration, reported yield, and volumetric productivity of several hydrocarbon biofuel products produced by *E. coli* with those for ethanol as reported in literature and summarized in [33]. The figure illustrates that even with a well-understood microbe such as *E. coli*, further work is needed to put the production of hydrocarbons on par with ethanol. A brief description of those opportunities follows, but it is with the acknowledgment that other microbes such as oleaginous yeast or ethanologens such as *Z. mobilis* can be more productive than *E. coli* [67–70].

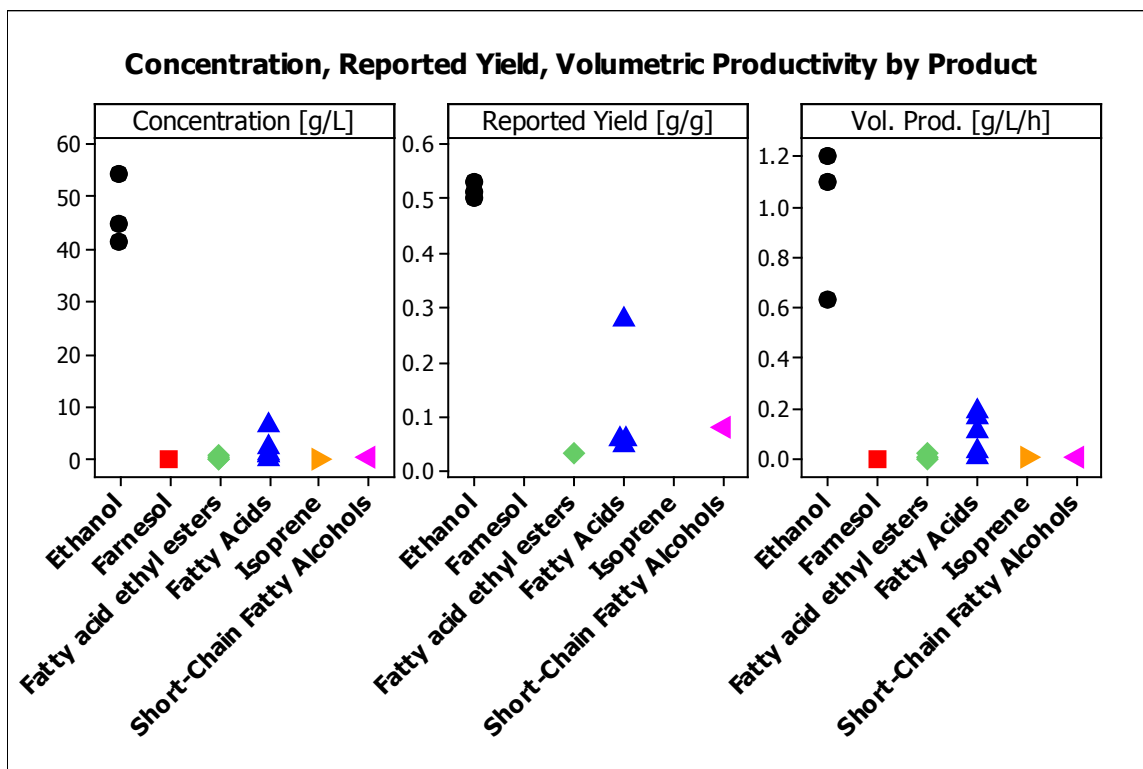


Figure 10. Comparison of titer, sugar utilization, and volumetric productivity for ethanol versus selected hydrocarbon products produced by *E. coli*, as reported in [33]

Knowledge of transcriptional and translation regulation of fatty acid biosynthesis is incomplete [71]. Approaches to producing fatty-acid derived fuel from *E. coli* require overcoming regulation of fatty acid biosynthesis, and upgrading fatty acids to meet fuel-grade specifications [51]. There have been a number of publications detailing approaches to increasing the production and quality of fatty acids from *E. coli*:

- The composition of fatty acids from *E. coli* has been modified by heterologous expression of plant thioesterases [72]. This enables the production of fatty acids at a variety of chain lengths and degrees of unsaturation—an important step to producing fuel-compatible FFAs.
- A multi-step metabolic engineering approach has shown encouraging results. Production of FFAs was increased by knocking out fatty acid degradation, expression of plant thioesterase, increasing malonyl-CoA production, and decreasing feedback inhibition by over-expressing an endogenous thioesterase [73–75]. When combined, these modifications resulted in a 19-fold increase in total fatty acid production compared to the original strain (0.048 g FA/g glycerol). Subsequent studies have mimicked this approach and the results were summarized by Lennen and Pfleger [71]. Zhang et al. reported one of the higher yield results from this approach at 0.19 g FA/g glucose [76].
- A promising result was reported by Dellomonaco et al. where they engineered the reversal of the beta-oxidation pathway that normally degrades fatty acids [61]. The advantage of this approach is that it eliminates the need to consume ATP when synthesizing malonyl-CoA. The result was an increase in product yields to 0.23 g FA/g glucose.

Lennen and Pfleger summarized four additional opportunities to improve fatty acid production [71]. First, increase FFA export rates. No transporter has been identified to export FFAs from within *E. coli*. Genetic engineering can improve export rates once transporters are identified. Second, regulate membrane saturation. Thioesterase can improve FFA yields but it can also impact cell physiology. Thioesterase can alter the relative amounts of saturated and unsaturated FFAs. The result is that cell membranes incorporate more saturated phospholipids that are found in a normal cell, decreasing cell viability. Third, address metabolic and regulatory bottlenecks. The barriers to prevent FFA production to reach near-theoretical yields remain unknown. Further work is needed, particularly on developing anaerobic production of FFAs to remove the operating costs associated with aeration. Fourth, additional structural, biochemical, and genetic studies are required. Basic science studies are needed to support metabolic engineering efforts, including enzyme kinetics, enzyme structure, and translational/transcriptional regulation.

In addition to organism performance factors driven by sugar utilization efficiency and volumetric productivity to hydrocarbons, a number of additional process issues will also be important in demonstrating achievement of the design case in the bioconversion area. These include:

- a. Bioconversion performance and tolerance to cellulosic hydrolysate impurities. This includes salts, acetate, lignin, and other byproducts formed upstream. As noted above, most public data on biological conversion of sugars to hydrocarbons focuses on glucose or other clean commodity sugars. Today's organisms may require such clean sugars, which in the present context could require even more hydrolysate conditioning equipment; e.g., further purification through ion exchange or other similar costly techniques. Additionally, little is known about the specific degree to which lignin and other insoluble solids impede oxygen mass transfer and bioconversion performance. Economically it may be preferable to remove lignin solids after bioconversion rather than before to allow for a lower-cost separation system and to avoid minor losses of sugars when employing this step prior to bioconversion. Furthermore, while acetate is a known inhibitor to ethanol fermentation, it may be tolerated or utilized by some hydrocarbon-

producing organisms. Much of the design of Area 200 is focused on deacetylation and the resulting acetate is sent to WWT. If acetate could be used as a carbon source for bioconversion to hydrocarbons, it could enable further optimization and cost reduction in upstream processes.

- b. Effective secretion of the FFA or other hydrocarbon product(s) outside the cell membrane. While a secretion pathway is selected as the baseline approach in the current model given inherent energy and cost savings rather than extraction of intracellular product, the effectiveness of such an approach warrants validation through continued research. Additionally, it will be important to quantify impurities such as polar membrane lipids or factors that may lead to emulsions as the targeted product is secreted across the membrane cell and into the surrounding broth, as this will have impacts on downstream processing/purification needs.
- c. Consideration of anaerobic pathways. Although most hydrocarbon-producing pathways occur aerobically, not all such pathways must inherently proceed this way. For example, as proof of concept, NREL researchers have demonstrated using anaerobic fermentation in the lab to produce low quantities of hydrocarbon fuel using engineered *Z. mobilis* [42]. Additionally, many anaerobic conversion pathways to produce intracellular and extracellular hydrocarbon products and intermediates exist in various bacteria and yeast microorganisms [43]. Making a switch to anaerobic bioconversion would allow for the use of larger, simpler equipment without the need for costly aeration capabilities, albeit likely requiring longer timeframes to achieve performance required for economic viability within the context of fuels.

3.3.4.3 Low-Cost Media

In keeping with the 2011 ethanol design case, corn steep liquor (CSL) is again assumed as a nutrient source for the seed and product bioconversion steps. While NREL does not use CSL in routine laboratory or pilot plant experiments, its use is assumed in the techno-economic model as a placeholder for a low-cost source of nitrogen and trace minerals. CSL, a by-product of the corn wet milling process, is high in protein, vitamins, and minerals and is usually mixed with the corn fiber by-product and sold as gluten feed [77]. On its own, CSL is used as a nutrient source in many fermentation industries, including wet-mill corn ethanol, pharmaceuticals, and industrial enzyme production. Because CSL is a wet mill by-product, and the corn starch business is relatively static, there is in effect a fixed amount of CSL available in the United States. Finding another low-cost and scalable nutrient source will be a continued subject of future research and TEA. Additionally, different nutrient demands and feeding strategies may be incurred for different types of organisms; for example, oleaginous yeast and heterotrophic algae may perform most optimally with replete nitrogen availability for organism growth, then switched to nitrogen depletion (starvation) to trigger lipid/product accumulation.

3.4 Area 400: Cellulase Enzyme Production

3.4.1 Overview

This process area produces cellulase enzyme that is used in Area 300 to hydrolyze cellulose into glucose. Cellulase refers to a mixture of enzymes (catalytic proteins) that includes: (1) endoglucanases, which attack randomly within the cellulose fiber, reducing polymer chain length rapidly; (2) exoglucanases, which attack the ends of highly crystalline cellulose fibers; and (3) β -glucosidase, which hydrolyzes the small cellulose fragments (cellobiose, a glucose dimer) to

glucose. Cellulase is produced industrially using (among other microorganisms) *Trichoderma reesei*, a filamentous fungus that secretes high levels of cellulase enzymes when grown aerobically in the presence of cellulose or other cellulase inducers.

The present analysis maintains consistency with the fundamental assumptions for enzyme production and cost estimation as detailed in the 2011 ethanol report, first and foremost being the use of on-site enzyme production rather than a purchased-enzyme model. As stipulated in the 2011 ethanol report, again we note that by including an on-site enzyme production section, NREL and DOE are not making a judgment about whether or not the cellulosic biofuel industry should align to this mode of enzyme distribution. Rather, the model on-site enzymes section is intended to improve transparency in determining the true cost of cellulase enzymes for large-scale cellulosic biofuel production.

As in the 2011 basis, the present design considers submerged aerobic cultivation (“aerobic fermentation”) of a *T. reesei*-like fungus on a feedstock of glucose and fresh water. Producing cellulase enzymes with glucose is not straightforward, because the absence of cellulose does not encourage the microorganism to secrete cellulase enzymes. Here, we have assumed a media preparation step where a small fraction of glucose is converted to sophorose, a powerful inducer of cellulase, using a small amount of the cellulase enzyme itself. When grown on this substrate, *T. reesei* has been shown to productively secrete cellulase [78]. Using glucose as the substrate is not necessarily more expensive than using hydrolysate slurry from pretreatment because the expected enzyme titer is significantly higher with glucose, reducing the capital and utility costs compared with using hydrolysate. Figure 11 is a simplified flow diagram of the enzyme production section.

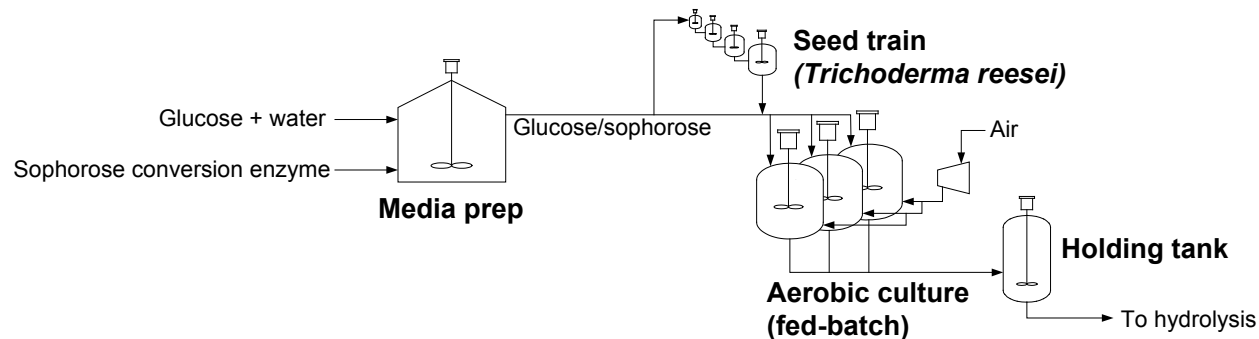


Figure 11. Simplified flow diagram of the enzyme production process

3.4.2 Design Basis

The design for the enzyme production operations is described in detail in the 2011 ethanol report, and will not be repeated in such detail here. In summary, the design for the system was based in part on the claims in U.S. Patent 4,762,788 (Example 5) [79] [80] in combination with a number of reasonable assumptions to develop a rudimentary process that is adequate for our needs. The key assumptions used in the current design are summarized in Table 17.

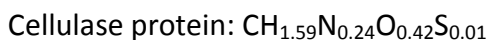
Table 17. Area 400 Guiding Design Basis Assumptions

Parameter	Assumption
Protein loading to enzymatic hydrolysis	10 mg protein/g cellulose
Reactor size	300,000 L @ 80% final working volume
Enzyme titer at harvest	50 g/L
Mass yield of enzyme from glucose	0.24 kg enzyme/kg glucose
Enzyme production cycle time	120 h online, 48 h offline, 168 h total

The assumed cellulase loading to enzymatic hydrolysis is reduced in the present pathway model to 10 mg of enzyme protein per g of cellulose, from 20 mg/g in the 2011 ethanol report. The rationale for this decision (keeping in mind this is a target for 2017) is described above in Section 3.3.2. “Protein” here refers to the total amount of high molecular weight protein in the enzyme broth as determined by assay; not all of this protein is active cellulase. The total protein demand was thus calculated to be 260 kg/h (570 lb/h). An additional 10% is produced to account for the slipstream provided to the media preparation tank to make the glucose/sophorose mixture. The size of the cellulase production vessels was set at 300 m³ (80,000 gal) with a height-to-diameter ratio (H/D) of 2. Fermentation is assumed to be a fed-batch process starting at 50% working volume and ending at 80%. Over one week, each bioreactor will see a 24-hour cell growth period, a 96-hour protein production period, and a 48-hour offline period for draining, cleaning, and refilling. With a one-week total cycle time and the production parameters listed in Table 17, one bioreactor is capable of producing 12,000 kg of protein in a week, or 71.4 kg/h (157 lb/h). The equivalent enzyme volumetric productivity is 0.30 g protein/L-h. Five reactors were therefore required to deliver the 260 kg/h of protein needed for enzymatic hydrolysis.

The reactors are loaded initially with the glucose/sophorose carbon source and nutrients including CSL, ammonia, and SO₂. After the initial cell growth period, additional substrate is added to maintain protein production. The bioreactors are sparged with compressed and cooled air and corn oil is added as an antifoam. The reactors are temperature-controlled by chilled water flowing through internal coils.

Aeration and agitation requirements for the production bioreactors are functions of OTR and OUR, which have been discussed above in Section 3.3.2 and in more detail in the 2011 ethanol report. Thus, the details and governing principles for these metrics will not be repeated again here. In the modeled bioreactors, the reaction stoichiometry balances the reactions of substrate, oxygen, ammonia, and SO₂ to cell mass and enzyme (plus CO₂ and water) using an elemental composition for commercial cellulase provided by Novozymes [80]. The composition of cell mass was taken as the average of a generic cell mass composition [81] and the enzyme composition, with the assumption that cell mass includes some unreleased protein.



In the production bioreactors, it is assumed that 90% of the carbon source is converted via the protein reaction and 10% is converted via the cell mass reaction. In the seed reactors, 85% of the carbon is converted via the cell mass reaction and 5% via the protein reaction, with 10%

unreacted. This represents an overall molar selectivity of glucose to 31% protein, 4% cell mass, and 65% CO₂, yielding 0.24 kg enzyme protein/kg glucose. The average aeration rate to the bioreactors remains the same as in the 2011 basis at 0.83 standard m³/s (including two days of offline time), as does the average impeller power *P* at 260 kW (350 hp), with a maximum of 600 kW (800 hp). The final specifications for the enzyme production reactors are shown in Table 18.

Table 18. Specifications of the Enzyme Production Bioreactors

Total volume	300 m ³ / 80,000 gal
Maximum working volume	80%
H/D ratio	2
Height	11.5 m
Diameter	5.75 m
Operating pressure	1 atm
Operating temperature	28°C (82°F)
Material	316SS
Agitator	800 hp
Total electricity demand per kg protein (air compressors, agitators, chillers, pumps)	9 kWh/kg

Four trains of three seed fermentors provide inoculum to the production bioreactors. Each vessel in the seed trains is run batchwise on the same substrate as the production vessels. Air is also sparged through each of the seed vessels, which are cooled with chilled water. The seed bioreactors are each sized at 10% of the next bioreactor volume, i.e., 0.3 m³, 3 m³, and 30 m³. The aeration demand is assumed to be 10% of the production aeration rate. Four trains were chosen because each production fermentor has a total cycle time of 7 days; each seed fermentor should have a cycle time of 2 days (including cleaning and sterilization) to get through the cell growth phase only.

Like the oxygen uptake rate, the glucose demand is also computed stoichiometrically from the required protein production rate. Ammonia and SO₂ are fed to the reactors stoichiometrically and CSL, trace nutrients, and antifoam (corn oil) are added to the substrate based on flow rate. The required nutrient concentrations are based on Schell et al. [82] and remain the same as presented in the 2011 ethanol report. Glucose, the carbon source for cell mass and protein, is the most significant enzyme production expense in this model. The cost for glucose was maintained consistently with the 2011 ethanol design case (after adjusting to 2011\$), but may be revisited moving forward as it may err slightly on the conservative side. Electricity also remains a significant contributor due to the power requirements of air injection, agitation, and refrigeration. Total electricity demand for these operations is shown in Table 18.

3.4.3 Cost Estimation

The cost estimation for all equipment in A400 was left unchanged from the basis values provided in the 2011 ethanol report. Most equipment in this area is stainless steel. The air compressor and some of the nutrient delivery equipment items are specified as carbon steel. Quotes for the production bioreactors, internal cooling coils, production agitators and motors, skid-mounted seed fermentors, and air compressor were provided by vendors through Harris Group, which developed costs for the pumps in this area using their internal database.

Not included in the enzyme production model are any costs for concentration, stabilization, or transportation of the enzyme to the plant. At the very least, one expects to have to pay licensing fees for the cellulase production microorganism, but these costs are not included because we lack information on what they might be (though an educated guess might be \leq \$0.05/gal of RDB product). Additionally, while the design and cost assumptions for the enzyme production vessels themselves were left unchanged from those described in the 2011 ethanol report, the 300,000 L vessel size could potentially be on the large side for realistic commercial operation of a highly viscous system such as that for *T. reesei*. The implications for variations in assumed vessel size (e.g., capital cost) are considered below in the Sensitivity Analysis section. The enzyme production system is also sized strictly to provide the amount of enzyme required for the hydrolysis step, for example, is not oversized to accommodate occasional poor-yielding runs. A reasonable backup measure for this risk would be to either over-design the enzyme system or to add supplemental purchased enzyme capacity. These strategies are not considered here for consistency with the n^{th} -plant approach taken elsewhere (e.g., avoiding over-design of equipment operations), but may be considered in future analyses exercising this design model.

3.4.4 Enzyme Cost Discussion

Based on the economics of the on-site enzyme section described above, the predicted cost of enzymes to the facility is \$0.39/gal of RDB. This is broken down as shown in Figure 12, and follows a very similar fractional breakdown in cost contributions as presented in the 2011 ethanol report, with small variations due to different rates of escalation for capital and material costs when translating to 2011 dollars. The carbon source (glucose) makes up 55% of the cost of the enzyme, i.e., \$0.22/gal of the \$0.39/gal is just for glucose. We can back out the unit cost of the enzyme from \$0.39/gal by multiplying by the RDB production rate and dividing by the enzyme flow rate, which works out to \$5.38/kg protein. On an absolute cost basis, this is higher than the cost of \$4.24/kg presented in the 2011 ethanol report primarily due to the adjustments made to underlying TEA assumptions, namely updating to 2011 dollars and reducing on-stream operating factor to 90% (7,884 hours/year).

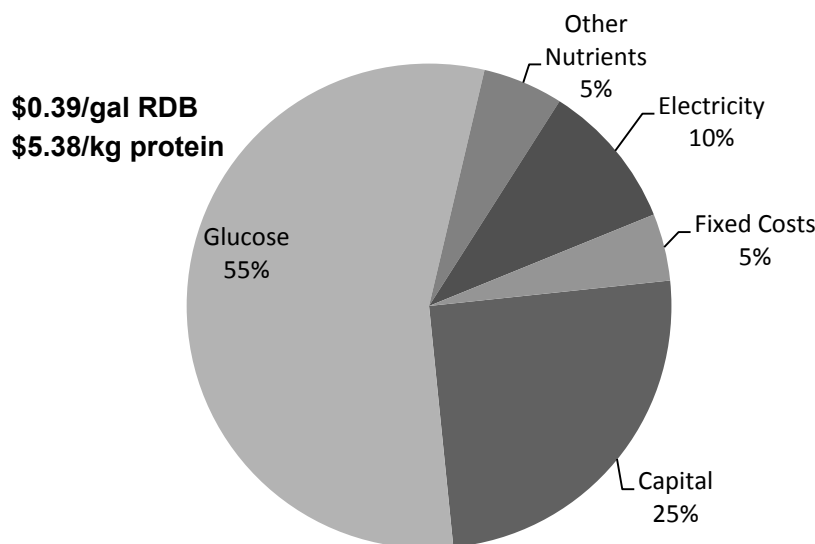


Figure 12. Enzyme production cost breakdown

While the fundamental process and design aspects of the enzyme production and enzymatic hydrolysis steps remain the same as stipulated in the 2011 ethanol report (e.g., size and cost of enzyme production and hydrolysis equipment, 3.5 day total hydrolysis time, etc), an important factor in achieving the \$5/GGE 2017 target for the present hydrocarbon pathway model is a reduction in required enzyme loading to 10 mg/g cellulose while maintaining cellulose-to-glucose yield at 90%. This is predicated on continued improvement in advanced enzyme formulations to achieve such an aggressive reduction in loading and concomitant increase in activity, but as noted previously this does not appear to be an unreasonable target for a 2017 timeframe, based on feedback from NREL researchers and enzyme companies. If enzyme loading of 20 mg/g were used in this design case, the resulting MFSP would be \$5.45/GGE of RDB product. Additional discussion regarding enzyme loading implications is provided below in the “Sensitivity Analysis” section.

As noted previously, advanced enzyme preparations may increasingly exhibit levels of xylanase activity to enable fractional increases in xylose yield during hydrolysis rather than exclusively in pretreatment, thus removing some of the burden for xylan conversion during pretreatment and potentially allowing for more mild pretreatment conditions (acid loading, temperature, and/or residence time) at lower cost. This benefit is not explicitly targeted in the present design, but may be considered in future iterations of the model as additional information becomes available to assist in setting associated targets.

The caveat discussed in the 2011 ethanol report bears repeating that the enzyme cost contribution modeled here is lower than one would expect for an enzyme preparation purchased from a separate, non-adjacent production facility. Transportation of the enzyme to the biorefinery facility could add \$0.09–\$0.18/kg of product, even if formulation costs could be avoided. Furthermore, by lumping the enzyme production equipment in with the biorefinery, some key items are inherently shared; e.g., the land and buildings, cooling tower, and utilities infrastructure. Overhead and fixed costs, especially labor and management, would also be higher for a standalone facility. Eliminating the shared aspects between the enzyme unit and the biorefinery could easily add another \$0.05/gal of RDB to the enzyme contribution. Additionally, an external enzyme production facility would probably demand a higher rate of return than the 10% IRR assumed for the biorefinery plant because it is a higher-risk and lower-volume business. Including all these extra costs would likely bring the total enzyme cost contribution in line with numbers cited publicly (on the order of \$0.50/gal for ethanol under today’s loading near 20 mg/g as demonstrated in NREL’s 2012 SOT work, which could translate to \$0.50–\$1.00/gal of RDB for 10–20 mg/g loading, respectively). Such differences between off-site and on-site production make an argument for eventual integration and on-site production; however, it is more likely that cellulosic biorefineries (whether targeting sugars, ethanol, or hydrocarbons) will purchase enzyme from an external supplier with an organization dedicated to improving enzyme performance and reducing costs.

3.5 Area 500: Product Recovery and Upgrading

3.5.1 Overview

Area 500 separates the bioreactor broth from A300 into a hydrocarbon (FFA) phase and an aqueous phase containing water, soluble solids (including unconverted sugars), and organism biomass. Aside from the bioconversion organism, the suspended solids fraction of the broth is

small as the lignin and other insoluble solids were already removed upstream (see Figure 13). The relatively high immiscibility of the FFA material is exploited to utilize simple phase separation to purify and concentrate the FFA product from the aqueous broth, rather than requiring cost- and energy-intensive distillation and dehydration steps as were required in the ethanol design model. Following phase separation, the concentrated FFA material is sent directly to on-site hydrotreating to upgrade the material into diesel-range RDB product.

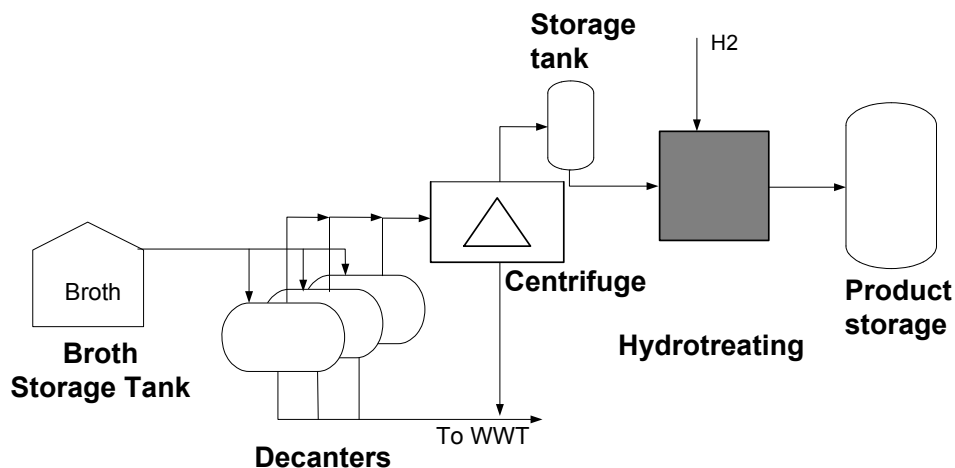


Figure 13. Simplified flow diagram of product recovery and upgrading

3.5.2 Design Basis

The broth from the bioconversion area contains approximately 9 wt% FFA (a function of sugar feed concentration as well as sugar utilization efficiencies described previously). As noted above, the FFA material is assumed for modeling purposes to consist of palmitate (palmitic acid), a fully saturated 16-carbon fatty acid; in reality, the FFA material will likely consist of a mixture of saturated and unsaturated fatty acids in the diesel carbon number range (C12–C20) [83]. These components will largely exhibit similar properties as palmitic acid, namely low density relative to water (palmitate density = 0.86 kg/L) and essentially immiscible with water. Thus, it is anticipated that this material will readily phase-separate from the rest of the fermentation broth using standard equipment such as decantation or centrifugation. For lack of in-house data currently available on the subject, this is a point that will require experimental validation to confirm, and that liquid-liquid mixing behavior or the formation of emulsions will not pose insurmountable problems requiring alternative purification techniques to those assumed here.

Under guidance from Harris Group with input from a vendor knowledgeable in processing of similar material (e.g., biodiesel processing), a standard biodiesel-type oil water separation decanter was selected for primary concentration of the hydrocarbon phase; subsequently to the engineering design conducted by Harris Group, it was also decided to follow the decanter purification step with centrifugation. Both Harris Group and the vendor felt comfortable with the use of decanters to achieve primary oil separation/purification, assuming the separation behaves similarly to ideal fatty acid/fatty acid methyl ester (FAME, i.e. biodiesel) processing. However, given uncertainties listed above regarding the possible presence of other impurities, emulsions, or lysed cells which may complicate the separation process, secondary centrifuge purification was also included to increase the likelihood of achieving desired separation performance (namely high oil recovery and purity).

The gravity decanter vendor estimated that a 15- to 30-minute residence time would be adequate for the decantation operation; however, based on Harris Group's experience in similar applications this was extended to a 60-minute residence time to err on the conservative side, particularly in ensuring high FFA product recovery, which was set to 97% (3% product carryover loss into the aqueous phase, combined between the decantation and centrifugation steps). Based on the flow rate provided, this resulted in four decanter vessels operating in parallel to process the full bioreactor broth stream, concentrating the material from approximately 9% to 34% (fourfold concentration factor). At this outlet concentration, the flow rate of the light liquid phase containing the partially concentrated FFA material is roughly 200 gal/min. This phase is then sent to a disk stack centrifuge with a maximum capacity of 250 gal/min (based on vendor feedback) for final concentration to > 99%. The aqueous stream from both unit operations, which contains cell biomass, unconverted sugars, ammonium sulfate salts, and excess nutrients, is routed to the WWT section (A600) for cleanup and energy recovery. The combination of decantation and centrifugation is assumed to achieve > 99% product purification with 97% product recovery. The cost impact associated with varying the assumed product recovery is investigated below in the Sensitivity Analysis section.

As noted above, depending on specific fatty acid components or impurities present in the secreted FFA product, additional processing considerations could be required to allow for effective handling or further purification of the product. For example, fully saturated fatty acids in the C12–20 range exhibit melting points between 45°–75°C, but introducing even one degree of unsaturation (one double bond) reduces these melting points to less than 25°C [84, 85]. As such, the present model assumes that special conditions such as elevated temperature to maintain a liquid FFA state are not required. Alternatively, if the secreted FFA product were to include carryover of significant levels of impurities such as polar lipids (present in the cell membrane) or binding with extracellular proteins, a separate cleanup step such as product bleaching and degumming or washing to remove such impurities could be required prior to hydrotreating; such impurities could also lead to emulsions making further purification more difficult. Dedicated cleanup or washing steps are not assumed to be required currently, but the question of impurities or emulsions will be an important subject of future research and quantification.

Following FFA product concentration, the material is upgraded in a hydrotreater to refine the oxygenated intermediate material into saturated paraffin components suitable for blending as a diesel blendstock. Harris Group consulted with a number of vendors, including catalyst suppliers and process licensors, to obtain budgetary estimates for a hydrotreating facility that may be expected to process a high-FFA feed as modeled here into deoxygenated diesel-range paraffins. A number of cost estimates were provided for such a facility, but the vendors declined to provide specifics without confidentiality restrictions regarding associated process and design conditions (e.g., reactor sizing dictated by space velocities, operating temperatures and pressures, hydrogen partial pressure, etc). Thus, to estimate reasonable process conditions for modeling purposes, a combination of literature and Harris Group estimates were applied. Namely, a prior NREL study for hydrotreating triglycerides was leveraged [86], which in turn was based in large part on a report jointly authored by UOP, NREL, Pacific Northwest National Laboratory, and Michigan Technological University [87]. This report described relatively mild hydrotreating temperature and pressure conditions at 350°C (660°F) and 35 atm (500 psig), but a high hydrogen feed ratio at 6,000 standard cubic feet/barrel of feed (this translates to a hydrogen partial pressure of approximately 460 psig at reactor inlet). As confirmed by Harris Group, high hydrogen feed is

necessary in part to provide a quench to control the large exotherm attributed to deoxygenation. A reasonable liquid hourly space velocity associated with this process would likely be in the range of 0.9–1.4 h⁻¹ [87], which was confirmed by an estimated value of 1.2 from Harris Group.

A schematic diagram of the FFA concentration and hydrotreating process operations is shown in Figure 14. This diagram includes an assumption of a two-stage hydrotreater, with the first stage including a guard bed for metals, as well as a possible mechanism for handling the high acid (total acid number [TAN]) content that may be expected to be present in a concentrated FFA feedstock (based on vendor feedback). Additionally, a cost estimate was also included for a pressure swing adsorption (PSA) unit in the hydrotreater gas recycle loop, primarily to remove CO₂ formed by decarboxylation reactions in the hydrotreater (discussed below). The design and cost estimates for the PSA unit were also provided by vendor input. In the Aspen model, the gas recycle feed stream to the PSA consists primarily of H₂ and CO₂ (after cooling the reactor effluent and knocking out most of the produced water, which is routed to WWT). Given this gas composition, the PSA vendor provided a cost estimate for a patented PSA unit which utilizes a zeolite-based sorbent to provide a high expected hydrogen recovery: the expected hydrogen loss noted by the vendor was only about 1%. As this recovery is higher than standard PSA operations (even if based on a more novel PSA technology), and given the relative uncertainty inherent to the early status of the model including details around product and recycle gas compositions, the hydrogen loss in the PSA tailgas was conservatively increased to 5% (95% recovery). The overall economic sensitivity to this assumed PSA hydrogen recovery is evaluated below in the Sensitivity Analysis section. The PSA tailgas, containing approximately 54 vol% H₂ and 46 vol% CO₂, is split to provide the necessary heat to the hydrotreater furnace (thus avoiding external natural gas to drive this operation), with the remainder sent to the boiler (A800).

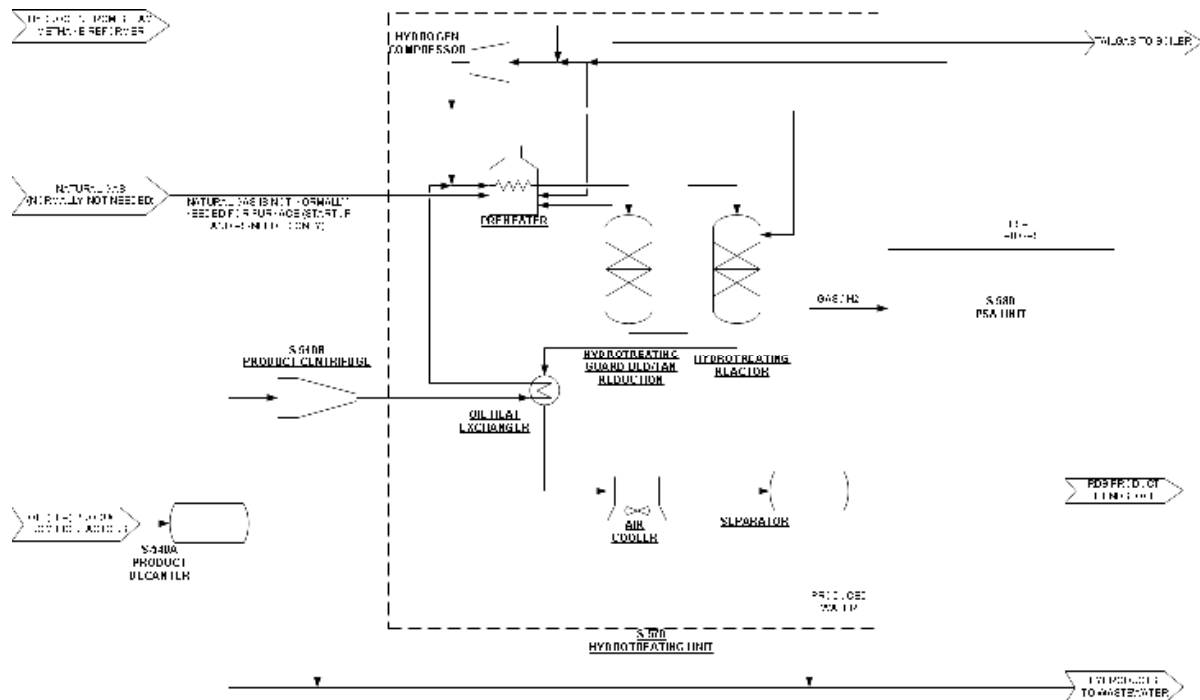


Figure 14. Schematic diagram of hydrotreating operations included in vendor design estimate (Note: vendor cost estimate includes distillation column for product separation, but present design model produces only diesel-range hydrocarbons)

Oxygen removal from the FFA feed may occur by way of hydrodeoxygenation (HDO) or decarboxylation (DCO) reactions in the hydrotreater. The relative degree of one reaction pathway over another may be tailored by catalyst and reaction conditions, with a tradeoff exhibited between higher hydrogen consumption to reject oxygen as water via HDO (this carries important implications particularly on the life cycle assessment (LCA)/sustainability metrics of the system when sourcing hydrogen from conventional fossil sources) and decreased carbon yields to reject oxygen as CO₂ via DCO (with decreased product yield translating directly to cost impacts). Again for lack of more specific details selected at this stage on targeted product pathways and reaction conditions consistent with the emphasis on a *representative* technology pathway, the oxygen removal mechanism is assumed to be split evenly between HDO and DCO reactions. A more likely scenario may be for the HDO versus DCO reactions to favor one reaction pathway over another (for example, 80/20 split favoring one reaction or another); however, again for purposes of setting a representative approach, and given that some potential pathway products (e.g., farnesene or other isoprenoids) are not even oxygenated in the first place, a 50/50 split is reasonable at this stage. Thus, the governing equations employed in the model for FFA upgrading are provided in Table 19.

Table 19. Governing Stoichiometry Assumed for Hydrotreating Reactions

Reaction	Reactant	% Converted to Product
1 Palmitate (FFA) + 3 H ₂ → 1 C ₁₆ H ₃₄ + 2 H ₂ O (<i>HDO reaction</i>)	FFA	50%
1 Palmitate (FFA) → 1 C ₁₅ H ₃₂ + 1 CO ₂ (<i>DCO reaction</i>)	FFA	50%

As shown in Table 19, the hydrotreating reactions were assumed to occur stoichiometrically to remove oxygen in the palmitate feedstock equally by HDO and DCO mechanisms, producing hexadecane and pentadecane in equimolar amounts. These reactions also set the hydrogen consumption across the hydrotreater, with additional hydrogen losses primarily in the recycle gas PSA unit (5% loss into the PSA tailgas). For the present preliminary model, no overcracking is assumed to light gases or naphtha-range material aside from the two reactions presented above. Thus, for modeling and mass balance purposes, the product is assumed to be composed of hexadecane and pentadecane, both straight-chain paraffins with high cetane value, making them valuable as diesel-range blendstocks. It is recognized that to produce a stand-alone final fuel product meeting ASTM diesel specifications, the straight-chain paraffinic product from hydrotreating would require further isomerization to address potential cloud point issues [88] however, the high cetane and low sulfur content expected to be exhibited by the RDB product is expected to make such a product valuable for diesel blending purposes, and the removal of oxygen during hydrotreating suffices to meet DOE requirements consistent across other technology pathways for a finished product [10]. The assumptions discussed above for the FFA hydrotreating section are summarized in Table 20.

Table 20. Summary of Hydrotreating Process Assumptions

FFA feed rate	99,540 gal/day (377 m ³ /day)
Average reaction temperature	660 °F (350 °C)
Pressure	500 psig (35 atm)
Hydrogen partial pressure	460 psig (32 atm) / 6,000 SCF/bbl
Reactor LHSV	~1.2 hr ⁻¹ (estimated) ^a
Hydrogen loss across recycle PSA	5%
Makeup hydrogen rate	2.2 MM SCFD (59,030 Nm ³ /day)
RDB product rate	95,400 gal/day (361 m ³ /day)

^a Reactor LHSV is not used in the present model (total hydrotreater facility cost was used based on vendor feedback, which implicitly includes hydrotreater sizing which was not provided by vendor)

3.5.3 Cost Estimation

The gravity decanter units for FFA concentration consist of horizontal cylindrical vessels with internal baffles that improve product separation by making flow more laminar. Each vessel is sized at 9,840 gal (96 in. × 35 ft) to provide one-hour residence time. The vendor-supplied cost estimate for each vessel is \$560,000 for equipment purchase. The centrifuge purchase cost is based on a previous vendor-supplied estimate of \$450,000 per unit with maximum unit capacity of 250 gpm [89], thus only one unit is required in the present design at a basis of 200 gpm exiting the decanters. The centrifuge is assumed to operate at a vendor-supplied power demand of 0.2 KW/gpm processed.

The hydrotreating facility cost is an “inside battery limits” (ISBL) cost estimate, including costs for reactors, makeup and recycle gas compressors, fired heater, separation vessels, and distillation (which is included to reflect a slate of products which may be produced from hydrotreating, although only pentadecane and hexadecane are assumed to be produced in the current model which both fall into the diesel range and would not require distillation under this simplistic scenario). Additionally, catalyst replacement cost is not explicitly specified, but one vendor noted that catalyst would be an insignificant part of the total cost estimate for this particular system, at a typical catalyst lifetime of two years and the given FFA feed specification.

Two vendor cost estimates were provided for the hydrotreating section, which varied considerably in magnitude, in part due to the preliminary nature of the modeling and the lack of specificity regarding FFA feed characteristics (more detailed FFA composition, presence of impurities, acid level, etc.); as such, it is important to emphasize that at this stage the cost estimate for the hydrotreating system is most appropriately viewed as an order-of-magnitude estimate, and should be treated as such in drawing conclusions as to the cost that may be incurred for upgrading the FFA material or other similar mildly oxygenated products from biological conversion pathways. Indeed, the uncertainty range associated with the cost estimate which was selected (\$23MM installed cost) was listed as -50% /+100%. The overall cost impact associated with this given range of uncertainty in the hydrotreating cost estimate is evaluated below in the Sensitivity Analysis section. Even with such a relatively high margin of uncertainty in the hydrotreating cost estimate, we feel it is more prudent to leverage this information than attempting a cost estimate on our own (e.g., using cost estimation software) as the vendor estimates bring valuable insight as to important considerations such as reactor design, number of stages, and operating conditions.

The lower vendor cost estimate of \$23MM installed cost was selected here over a second, higher estimate of \$62MM as the lower estimate appeared to be supported more by what might be reasonably predicted both based upon literature as well as Harris Group's expertise borrowing primarily from conventional petroleum hydrotreating, under an expectation of a relatively clean FFA feed stream low in impurities. While supporting detail behind the two vendor estimates was sparse, a primary reason for such a large cost discrepancy may be in how the acidity is addressed in a high-TAN feedstock such as FFA material. The vendor who provided the higher cost estimate indicated the necessity for exotic metallurgy to handle expected TAN content, while the vendor providing the lower cost number indicated a capability to deal with this issue through careful catalyst selection including an upstream guard bed, and specifically mentioned that exotic metallurgy was not required. Given the relatively mild hydrotreating conditions listed in Table 20, which are in line with a relatively high-quality material as would be expected to be produced through most biological pathways (e.g., fatty acids, fatty acid esters, isoprenoids, etc.), both Harris Group and NREL felt comfortable utilizing the \$23MM estimate as the baseline here.

The PSA unit was provided as a separate cost item, as this is not a typical unit operation in conventional hydrotreating systems, but is required here primarily to remove CO₂ formed during hydrotreating (e.g., via the DCO reaction which diverts carbon away from product yields to produce CO₂). The cost estimate for this operation was provided by a PSA vendor. As noted above, the design basis for this operation was based on a patented zeolite sorbent system, allowing for high expected hydrogen recoveries. Harris Group also evaluated the cost for an amine system as an alternative CO₂ removal option, and found that this alternative may be more cost effective relative to the PSA option, but this also is likely to exhibit a higher heat demand for amine regeneration. As more definition becomes available for the biological production pathway, intermediate product characterization, and hydrotreating specifics, the options for CO₂ removal in the recycle gas line may be revisited.

3.6 Area 600: Wastewater Treatment

3.6.1 Overview

All the wastewater generated in the conversion process is sent to the wastewater treatment system in Area 600. The treated water is assumed clean and fully reusable by the process, which reduces both the fresh makeup water requirement and discharge to the environment. In 2010, NREL placed a subcontract with Harris Group and Brown and Caldwell (a WWT technology vendor) to design a treatment system capable of handling wastewater material associated with NREL's 2011 biochemical ethanol design report model. The emphasis of the collaboration was primarily to ensure that the wastewater design could accommodate the large volume, high-salt/high-nitrogen material generated at the specific process conditions used in the design report model. Following this effort, a new subcontract was placed in 2012 to consult directly with Brown and Caldwell to revisit the WWT design and cost estimates, primarily to address process modifications being implemented. These modifications primarily included the addition of deacetylation and new black liquor stream to WWT, as well as the move to lower severity acid pretreatment, resulting in lower nitrogen and salt levels reaching the WWT section. We felt this second subcontract was necessary as the earlier 2010 subcontract provided very specific design and cost estimates associated with the design report basis conditions, and the basis for scaling all WWT equipment was established as the total kg/h feed rate to WWT; such a basis does not allow for accurately capturing cost impacts associated with different WWT feed characteristics such as

nitrogen or chemical oxygen demand (COD) loading. The 2012 subcontract also provided more flexibility in this regard, costing out equipment on a more individual basis with associated scaling factors provided based both on hydraulic rate as well as COD load. The updated simplified flow diagram is shown in Figure 15; the process schematic itself is similar to the previous design used in the 2011 ethanol report, but a number of unit-level costs and design assumptions are different. A key factor behind the updated wastewater equipment design provided by Brown and Caldwell was the use of actual representative material generated in the pilot plant to accurately characterize the WWT feed to be treated, forming a better-informed basis from which cost and design estimates are scaled in the present analysis.

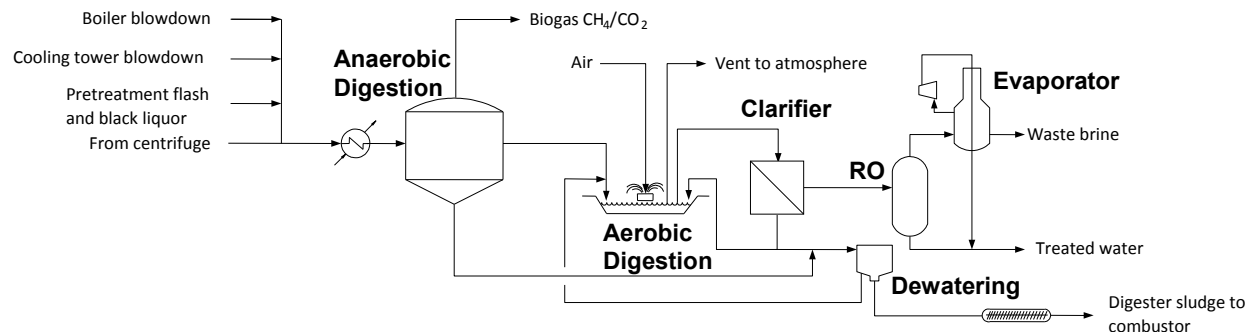


Figure 15. Simplified flow diagram of the WWT process

Condensed pretreatment flash vapor, black liquor from deacetylation, boiler blowdown, cooling tower blowdown, and the bioreactor broth water streams are mixed together. The combined wastewater stream is processed in A600 consisting of anaerobic and aerobic digestion, membrane filtration, reverse osmosis, evaporation, dewatering, and gravity belt thickening. Each process component and its function are summarized in Table 21. Anaerobic digestion produces a biogas stream that is rich in methane, so it is fed to the combustor. The aerobic system utilizes a membrane bioreactor which is essentially an aeration tank followed by an ultrafiltration membrane system with biomass recycle. The effluent of the membrane system is of sufficient quality to feed a reverse osmosis system directly (i.e., without additional filtration). The dewatered sludge and biogas are sent to the boiler in A800. The dewatering process for the anaerobic sludge is centrifugation. The aerobic sludge is thickened by gravity belt thickeners (GBTs) prior to centrifugation in order to reduce the number of centrifuges required. In general, centrifugation provides higher solids capture and a drier biomass cake compared to other dewatering systems thus reducing the size of the biomass burner system. It also provides a margin of safety against changes in sludge quality which could impact dewatering processes relying upon filtration (e.g., belt filter press). Reverse osmosis is required to remove dissolved salts, so that cleaned water can be recycled to upstream processes while mitigating salt accumulation.

This process produces a relatively clean water stream that can be reused in the process. The water stream is routed to the common process water header (A900) to be used in other process areas, such as dilution water in pretreatment or enzymatic hydrolysis.

Table 21. Process Components and Functions in Area 600

Process Component	Functions
Anaerobic Treatment	Organic load reduction, Biogas generation
Aerobic treatment	Organic load reduction
Membrane Filtration	Total suspended solids removal
	Colloidal organic material removal
	Protection of reverse osmosis system
Reverse Osmosis	Removal of dissolved inorganic salts
Evaporation	Volume reduction of reverse osmosis reject flow
	Reduction of heat needed in boiler
Gravity Belt Thickener	Biological sludge thickening prior to centrifugation
Centrifugation	Biological sludge dewatering
	Reduction of heat needed in biomass boiler

3.6.2 Design Basis

The WWT system was designed by and Brown and Caldwell under the 2012 subcontract mentioned above. The design includes anaerobic digestion, aerobic digestion, sludge dewatering, reverse osmosis, evaporation, and centrifugation. The relevant design parameters of the wastewater system are summarized in Table 21, based on actual material generated in the pilot plant in 2012.

Evaporated water from the sugar concentration step is of high purity (> 99.5% water), and thus is not routed to A600 for further cleanup but is recycled directly for process water use. This helps reduce the total hydraulic flow and cost of a number of WWT unit operations. The deacetylation black liquor, condensed pretreatment flash vapor, bioreactor aqueous phase after FFA separation, boiler blowdown, and cooling tower blowdown are mixed together and pumped through a heat exchanger and cooled to 35°C before being sent to the anaerobic digester.

The total COD entering anaerobic digestion in the current design case is approximately 120 g/L (30,700 kg/h). This COD concentration represents an increase from both the 2011 and 2012 WWT designs, primarily because of increased diversion of sugars to bioconversion cell mass, with a lower total volume flow caused by upstream sugar concentration and water removal. As noted above, the updated subcontract design/cost basis now allows for costing unit operations on a hydraulic load and COD basis (as appropriate), so these variations from the design are accurately captured in the cost estimates. Low-rate Bulk Volume Fermentors (BVF reactors) are used as the anaerobic digester vessels, capable of removing 89% of incoming COD. 85% of the COD is converted to biogas (methane and carbon dioxide) and 5% is converted to cell mass. Methane is produced from the organic matter at 238 g/kg COD removed. Carbon dioxide is also produced at a nearly equimolar rate to methane, such that the biogas from the digester is 51% CH₄/49% CO₂ on a dry molar basis; this ratio is lower than typical digester biogas at 60%–70% CH₄, but is consistent with the vendor suggestions. Cell mass is produced at a yield of 48 g cell mass per kg COD removed. Biogas blowers pull a negative pressure to remove the produced gas.

The preferred use of the biogas is in the on-site combustor for combined heat and power benefits. However, economic factors may drive the sale of the gas via pipelines. In either case, an

emergency biogas flare is required and designed into the process to burn the biogas in case of a process upset in the combustor. Sulfate is converted to hydrogen sulfide (H₂S) and leaves the system in the biogas. Since the COD-to-sulfate ratio in the design basis is ~2000, the methane-producing organisms will out-compete the sulfate-reducing organisms, so upstream removal of sulfate is unnecessary. The H₂S and any other sulfur species in the biogas are converted to SO₂ downstream in the combustor, which is mitigated using flue gas desulfurization (FGD) (Area 800).

Table 22. WWT System Design Basis

	2011 WWT design (used as basis for cost estimates in 2011 ethanol report)	2012 WWT design (used as scaling basis for cost estimates here)	This design (all values estimated by Aspen)
Hydraulic load	2.15 MMgal/d	2.7 MMgal/d	1.6 MMgal/d
Wastewater inlet temperature	50°C	60°C	60°C
Inlet pH	5.2	7.8	-
Total COD	87 g/L	66 g/L	120 g/L
Soluble COD	85 g/L	66 g/L	-
Total solids	68 g/L	33 g/L	130 g/L
Total suspended solids	1500 mg/L	56 g/L	27 g/L
Total alkalinity	2,750 mg/L as CaCO ₃	0 mg/L as CaCO ₃	-
Ammonia-N	1,060 mg/L	0 mg/L	-
Total Kjeldahl N	1,200 mg/L	404 mg/L	724 mg/L
Sulfate	4,400 mg/L	36 mg/L	-
Silica	1,600 mg/L	754 mg/L	-
Potassium	500 mg/L	1060 mg/L	-
Phosphate	805 mg/L	3260 mg/L	-

The liquid from the anaerobic digester is pumped to the aerobic activated-sludge basin with surface aerators. In the concrete and steel basin, 96% of the remaining soluble organic matter is removed, with 74% producing water and carbon dioxide and 22% forming cell mass. With the 89% COD reduction in anaerobic digestion followed by 96% reduction of the remaining COD in aerobic digestion, the total COD reduction is 99.6%. It is estimated by Brown and Caldwell that a non-degradable COD of 1,300 mg/L would be generated in the effluent of the aerobic basin. The fully digested material is pumped to a membrane bioreactor for clarification. The membrane unit removes additional COD along with colloidal particles (especially silica). Coarse- and ultra-filtration upstream of the membrane unit separate the aerobic biomass sludge. The sludge is pumped to a dewatering device to reduce the sludge volume and water content to the boiler. Typically, a centrifuge is used for dewatering. A GBT was evaluated by Brown and Caldwell as a pre-dewatering step prior to the centrifuge in order to reduce of the number of centrifuges required. In this design, the GBT produces sludge with a solid content of 4%. The centrifuge units are then periodically operated to provide a solids capture rate of 95% and a cake concentration of 20%. The centrate flow is recycled with polymer addition to the activated sludge aerobic system. Most of the dewatered sludge is recycled to the aeration basin to maintain a high cell mass loading. The remaining portion is removed to a holding tank, where it is mixed with sludge from anaerobic digestion. Dewatered sludge is then routed to the combustor in A800. The sludge solid is primarily cell mass and unconverted biomass components.

The treated water is pumped to a reverse osmosis (RO) membrane system for salt removal. RO produces a brine (217 gpm) containing primarily sodium nitrate along with all remaining ions and organics. The brine is further concentrated in a mechanical-vapor-recompression evaporator to 50% solids and the condensate is also recycled to the process. We do not further process the brine in our model at this time, and it is assumed waste.

3.6.3 Cost Estimation

Brown and Caldwell estimated the cost for the wastewater system, drawing on support from technology vendors. Unlike the previous study by Harris Group and Brown and Caldwell, which was utilized in the 2011 ethanol design basis and scaled all WWT costs according to total mass flow rate into the WWT system, the cost estimation provided in the updated analysis from Brown and Caldwell allows for greater detail to adjust individual unit costs either based on hydraulic flowrate or by COD, thus resulting in improved accuracy (e.g., to accommodate differences in COD concentration even at similar total hydraulic flow rate). This is an important improvement given the relatively high cost of the WWT system.

The anaerobic system is scaled based on total COD and the installed cost in this design is \$30.9MM, shown in Table 23. For the aerobic digestion step, liquid volume per basin is 4.2 MM gal, recommended by Brown and Caldwell. The total size of the aerobic basins is determined by hydraulic flow rate and mean cell residence time, which is set at 15 days by Brown and Caldwell and installed capital of the aeration basin is estimated at \$7.5MM here, including capital costs for the surface aerators. The membrane bioreactor, dewatering units, reverse osmosis system, and evaporators are also scaled based on hydraulic flow rate, and their capital costs are shown in Table 23, in comparison with the 2011 design report, based on 2011-dollars. It can be seen that although some cost savings are realized here, such as the centrifuge, which is less costly because of a reduction in hydraulic load as well as the addition of GBT dewatering prior to centrifugation (included here in the “other costs”), other costs have increased, namely the anaerobic and aerobic systems, both of which have cost elements which depend on COD loading (the entire anaerobic system cost, as well as the blowers for the aerobic system); these units were also both re-costed in the updated Brown and Caldwell subcontract effort, so a direct comparison as shown below is somewhat artificial.

Table 23. Equipment Capital Costs for WWT (A600), in Comparison With 2011 Design

Equipment	WWT Installed cost (\$MM; 2011\$)	
	2011 Design Model	Present Case
Evaporator System	4.2	5.9
Membrane Bioreactor	5.7	4.8
Reverse Osmosis System	2.4	2.6
Centrifuge	7.1	2.0
Anaerobic Digester	29.6	30.9
Aeration Basin	5.1	12.0
Others (pumps, conveyer, etc.)	1.0	2.0
Total WWT	55.1	60.2

Influent Total Kjeldahl Nitrogen (TKN) was analyzed at 404 mg-N/L in the 2012 wastewater sample, and it is 724 mg-N/L in this design estimated by Aspen Plus simulation. Both TKN numbers are low enough that a nitrification step is no longer needed in this design, as it was in the 2011 design basis (which was based on a TKN level of 1,200 mg/L). This is due to the shift toward increasingly more mild pretreatment conditions and acid loading (with subsequent lower ammonia neutralization demand), beyond the basis established in the 2011 report. Thus, caustic which was required in the 2011 design for pH adjustment during nitrification is no longer utilized in the WWT section here, resulting in a considerable operating cost savings. Instead, supplemental ammonia would be needed to make up for a slight nitrogen *deficit* now present in the model to meet the optimum nitrogen demand (1,055 mg-N/L) for microorganisms to metabolize organic compounds in the aerobic digestion unit. The resulting ammonia demand in the aerobic basin is calculated to be 140 kg/h. In addition, polymer is added to the centrifuge to increase dewatering efficiency. Polymer requirements are set at 9 lb/ton total solids feeding into the aeration basin, estimated at 3 kg/h in the present model. The replacement of caustic in the 2011 design with a smaller amount of ammonia and polymer in the present design results in a net variable operating cost savings of \$2.3 MM/yr (2011\$), with operating expenses discussed in more detail in Section 4.

3.7 Area 700: Product and Feed Chemical Storage

3.7.1 Overview

This portion of the plant provides bulk storage for process chemicals and the RDB product. The chemicals stored in this area include ammonia, CSL, sulfuric acid, sodium hydroxide, and purchased glucose for enzymes. Water for fire suppression is also stored here.

3.7.2 Design Basis

Table 24 shows the major storage requirements for the present design. The design and cost bases for all tanks maintained in the current design were left unchanged, and are scaled to a new cost if needed. The only exception is the product storage tank (RDB product, formerly the ethanol storage tank), which is cut by 50% to only require one tank for seven days of storage as the total volumetric product rate has decreased by nearly 50% relative to the ethanol design basis.

Table 24. Storage Requirements

Material	Size (size basis maintained from 2011 ethanol basis)
RDB product	Sufficient to contain 7 days of production: 1 carbon steel tank @ 750,000 gal
Sulfuric acid (93%)	1 carbon steel tank @ 12,600 gal
Caustic (as pure)	Duplicated from sulfuric acid tank: 1 carbon steel tank @ 12,600 gal
Ammonia	2 SA-516-70 tanks @ 28,000 gal. Ammonia is stored anhydrous at 250 psig
Fire water	4 hours of fire suppression @ 2,500 gpm: 1 glass-lined carbon steel tank @ 600,000 gal
Corn steep liquor	1 glass-lined carbon steel tank @ 70,000 gal
Glucose syrup for A400	Duplicated from CSL tank: 1 glass-lined carbon steel tank @ 70,000 gal
Diammonium phosphate (DAP)	1 SS304 tank @ 12,800 gal

Other supplemental tanks and pumps were left unchanged relative to the 2011 ethanol design basis, with more details provided in the 2011 report.

3.7.3 Cost Estimation

The costs for the A700 storage section were left unchanged relative to the 2011 ethanol design basis (with the exception of the main product tank as noted above), and costs are scaled according to new material flow rates to estimate new tank prices if applicable.

3.8 Area 800: Combustor, Boiler, and Turbogenerator

3.8.1 Overview

The purpose of the combustor, boiler, and turbogenerator subsystem is to burn various organic byproduct streams to produce steam and electricity. Combustible byproducts include all of the lignin and the unconverted cellulose and hemicellulose from the feedstock, biogas from anaerobic digestion, biomass sludge from WWT, and PSA offgas from the hydrotreating unit. Burning these byproduct streams to generate steam and electricity allows the plant to be self-sufficient in energy (“thermal-neutral”), reduces solid waste disposal costs, and generates additional revenue through sale of excess electricity. Sulfur oxide (SO_x) emissions are mitigated from the combustor via flue-gas desulfurization.

The fuel streams are fed to a combustor capable of handling the wet solids. A fan moves air into the combustion chamber. Treated water enters the heat exchanger circuit in the combustor and is boiled and superheated to high-pressure steam. A multistage turbine and generator are used to generate electricity. Steam is extracted from the turbine at two different conditions for use in the process. In the final stage of the turbine, the remaining steam is taken down to a vacuum and condensed with cooling water for maximum energy conversion. The condensate is returned to the boiler feed water system along with condensate from the various process heat exchangers. The steam turbine turns a generator that produces AC electricity for all users in the plant. The balance of electricity is assumed to be sold back to the grid, providing a co-product credit.

3.8.2 Design Basis

For the A800 section equipment, the fundamental design and cost basis assumptions as provided by a boiler vendor employed in the 2011 ethanol design report were maintained in the present model. Thus, details of the boiler and turbogenerator design will not be repeated here, but can be found in the 2011 report. To briefly summarize, the combustor system features a live-bottom grated fuel bin to ensure drying and complete combustion of the wet solid fuel, with a boiler efficiency near 80%. Flue gas from the combustor preheats the entering combustion air then enters a spray dryer for flue gas desulfurization (FGD) (with the majority of sulfur entering the boiler system in the form of ammonium sulfate salt introduced upstream during pretreatment and conditioning operations). Although the ammonium sulfate salt level has decreased in the present model relative to the 2011 design case because of lower acid and ammonia loadings upstream, the FGD capital cost was included as part of the original quoted overall boiler cost, thus is not decoupled here to reflect a cost differential for lower FGD demands (although the FGD lime operating cost is reduced here to reflect less SO₂ in the boiler flue gas). Ash is removed in a baghouse and disposed to a landfill. Finally, the boiler raises steam at 875 psig, which is superheated and then sent through a multistage steam turbine with two extraction ports and a final condenser.

While the design and cost bases for the boiler and turbogenerator system have not changed, a number of process parameters are somewhat different from the 2011 bases. Primarily, the moisture content of the combined solid feed to the combustor has increased from 44% in the 2011 ethanol model to 60% in the current model. This is primarily due to the new lignin removal step, which is now placed upstream of the bioreactors. This necessitates the use of a solids wash step to recover carryover losses of sugars into the solids material from the filter press. This wash step adds more water to the lignin stream, which diverts more heat toward drying and reduces the amount of heat generated in the combustor. This is somewhat offset by the addition of the new offgas stream from the hydrotreater PSA unit, although this is a relatively small stream. The net result is a decrease in steam cycle flow rate of 1% from 235,000 kg/hr to 233,000 kg/hr. However, the net power generation in the steam cycle is *increased by 29%* relative to the 2011 basis (from 41.3 MW to 53.1 MW) because heat demand and thus turbine steam extraction has decreased substantially. While the fraction of steam removed from the first turbine extraction point for feeding to the pretreatment reactor is similar to the 2011 basis, the fraction of steam subsequently removed in the second turbine extraction point (at a pressure of 125 psig or 9.5 atm) is much less at roughly 2.5% rather than 35% in the 2011 basis. In the 2011 ethanol model, the steam extracted at this stage was required in large part to drive the distillation reboilers, which are no longer required in this pathway model (instead using simple phase separation for product purification). A small new stream is taken off at this extraction point to provide supplemental heating for the sugar evaporator system, but as this is an MVR evaporation unit, it is driven primarily by electricity rather than heat; thus, the steam requirement is fairly low at 1,550 kg/h. After the intermediate extraction point, the remainder of the steam is sent through a final turbine stage to vacuum pressure, and is condensed at -13 psig (0.1 atm) and pumped back to the boiler. The turbine generator efficiency is assumed to be 85% as in the 2011 basis. The resulting power generation is 53 MW. The process uses 43 MW, leaving about 10 MW to be sold to the grid.

3.8.3 Cost Estimation

The cost basis for the A800 equipment remains the same as described in the 2011 ethanol report. Namely, the combustor/boiler system is based on a vendor quote and includes the boiler feed water preheater, FGD spray dryer, and baghouse. For the baghouse, bag replacement appears as a periodic charge in the cash flow worksheet. The turbogenerator is also based on a vendor quote for an industrial generator which remains suitable for this project. Harris Group also obtained quotes from a third vendor for support equipment including the deaerator, chemical injection system, tanks, and pumps.

3.9 Area 900: Utilities

3.9.1 Overview

Area 900 contains the utilities required by the RDB production facility (except for steam, which is provided by Area 800). Area 900 tracks cooling water, chilled water, plant and instrument air, process water, and the clean-in-place (CIP) system. In the model, Area 900 also tracks the electricity usage throughout the plant.

The process water manifold in Area 900 mixes fresh water with treated wastewater and condensate from the sugar evaporation system (assumed suitable for all plant users) and provides this water at a constant pressure to the facility. Water is provided to the cellulase production unit,

boiler and cooling tower makeup, the CIP system, and the wash for the lignin filter press. Fresh water is also mixed with some internally-recycled water for dilution before pretreatment and enzymatic hydrolysis. The plant and instrument air systems provide compressed air for general use (pneumatic tools and clean-up) and instrument operation. Larger users of compressed air, namely the cellulase system and aerobic bioreactors, have their own compressors specified. The CIP system provides hot cleaning and sterilization chemicals to hydrolysis, bioconversion, and the enzyme production section.

3.9.2 Design Basis

The cooling water system is designed for a 28°C supply temperature with a 9°C temperature rise in coolers throughout the facility. This is an assumed average rise; the actual cooling water rises across each exchanger are not explicitly modeled in Aspen. The primary cooling water users in this process are listed in Table 25. The percentage of cooling duty contributed by each user is shown in Figure 16. Compared to the 2011 ethanol design basis, the total cooling water demand has increased by 34% from 97 to 130 MMkcal/h, due primarily to increased steam turbine condenser duty for a larger steam flow reaching the condensing turbine (due in turn to lower facility steam/heat demand), the addition of the bioconversion air compressor cooler, and the addition of a water-cooled exchanger to cool the sugar evaporator condensate. This is discussed and analyzed in further detail below in Section 5.

Table 25. Cooling Water Users

M-811	Condenses the steam turbine exhaust at a vacuum.
M-908	The chilled-water loop requires cooling water to condense the refrigerant. The cooling water duty to M-908 is set equal to the total load on the chilled-water loop.
H-301	Cools the pretreated slurry to enzymatic hydrolysis temperature (48°C).
F-300	Before bioconversion is initiated, the slurry must be cooled to bioreactor temperature. It is assumed that cooling water would be used for the initial drop from 48°C to 32°C and that chilled water would afterward be substituted to sustain this temperature.
QC-EVCND	Provides cooling of the sugar evaporator condensate.
M-401	Uses cooling water to cool the compressed air used in enzyme production.
QC-AIRCL	Uses cooling water to cool the compressed air used in bioreactor aeration.
H-244	Condenses residual pretreatment flash vapor before it enters WWT. Most of the vapor is condensed by heat exchange with the incoming dilution water and boiler feed water.

As was the case in the 2011 ethanol model, the largest user of cooling water is the condensing turbine. Aspen computes the cooling tower evaporation rate based on a temperature drop from 37°C to 28°C. It was assumed that windage would be 0.005% of the total flow to the tower. The tower blowdown was assumed to be 0.15% of the flow leaving the tower basin.

Chilled water is provided by two 2,350-ton Trane centrifugal chillers. Per the chiller spec sheet, the compressor electricity demand for the chiller was estimated at 0.56 kW/ton of refrigeration. The cooling water demand for the chiller system was assumed to be equal to the heat removed in the chilled-water loop. The chiller provides cooling to the bioreactors in Area 300 and Area 400.

Total = 130 MMkcal/hr (516 MM BTU/hr)

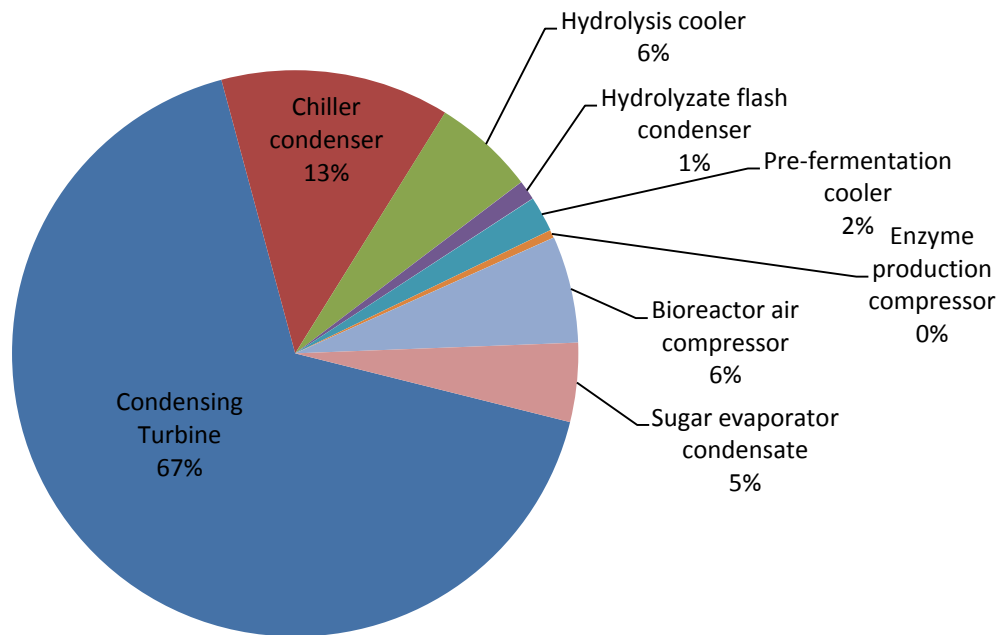


Figure 16. Cooling water heat duty distribution between major users

Fresh water is assumed to enter the facility at 13°C and is used to cool the wastewater entering Area 600 to digestion temperature before entering the process water tank. The fresh water is mixed with the treated wastewater effluent and the evaporation condensate in the process water tank (T-914) and then split several ways. Clean water must be provided to biomass dilution in the front end, to the cellulase production unit, to lignin filter press wash step, and to the boiler and cooling tower water makeup. The process water tank is designed for an 8-hour residence time. The process water pump (P-914) pumps water from the tank into the facility and is designed to handle 1.5 times the process water flow requirement.

The plant and instrument air systems provide compressed air for pneumatic tools and clean-up and instrument operation (not including major air demands such as enzyme and product bioreactors). The plant air compressor is sized for 400 SCFM at 125 psig. An instrument air dryer and surge tank were designed to provide clean dry air at a consistent pressure to the instrument air system. The surge tank was sized at 3,800 gal.

About 80% of the electricity generated by the boiler in Area 800 is used throughout the plant to power pumps, agitators, compressors, etc. The surplus is sold to the grid for credit. The distribution of total plant power utilization among all areas is shown in Figure 17. Note that the cost of the power required by Area 100 is already assumed to be included in the feedstock cost but must be subtracted from the plant's electricity export. This is reflected in the economics by an operating cost credit equal to this amount of electricity.

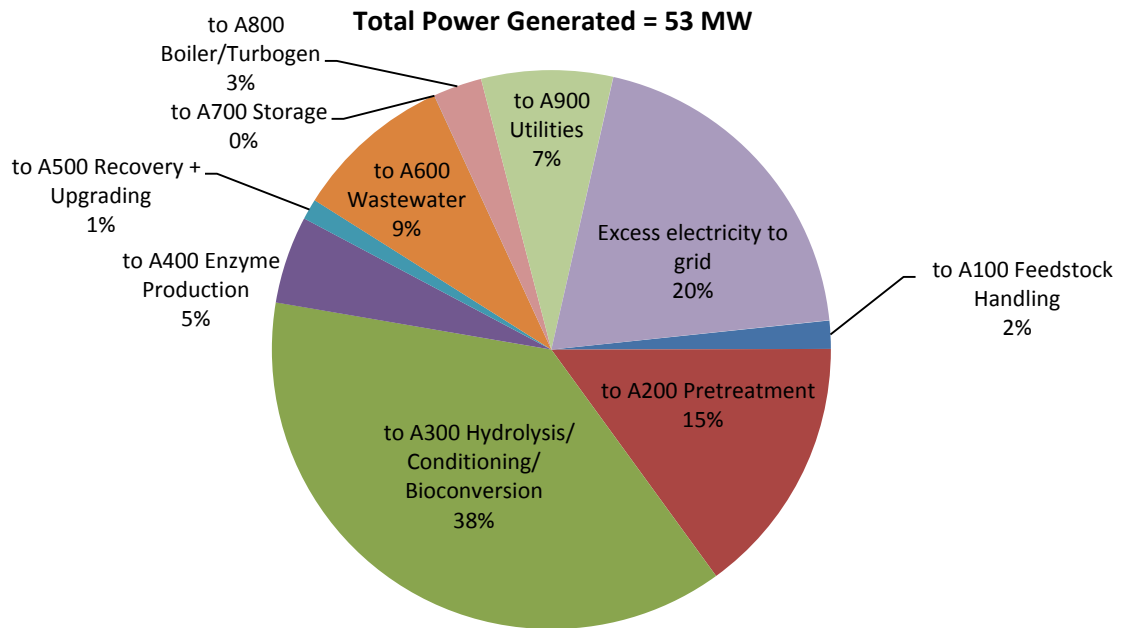


Figure 17. Distribution of plant electricity utilization by process area

3.9.3 Cost Estimation

All cost estimates for the utility equipment in A900 were maintained consistent with the basis values used in the 2011 report. To summarize, the cooling tower was based on a cost estimate from a vendor for a fiberglass cooling tower capable of handling 44,000 gpm; this cost is scaled to the increased cooling water throughput estimated here. Harris Group had estimated costs for the cooling water circulation and makeup pumps using their internal database. The material of construction for the cooling water loop is carbon steel. The cost for the chiller came from a recent quote for a similarly-sized system. Harris Group had also used their internal database to estimate costs for the remaining equipment: the process water tank and pump; the plant/instrument air compressor, dryer, and surge tank; and the CIP system.

4 Process Economics

The ultimate purpose for developing such a detailed process design, simulation model, and cost estimate is to determine the economics of biofuel production. This information is used either as an absolute cost to assess the product's potential in the marketplace or as a relative cost that can be used to guide research by examining the change in production cost associated with a process modification or other core research activity.

The total capital investment (TCI) is first computed from the total equipment cost. Next, variable and fixed operating costs are determined. With these costs, we use a discounted cash flow analysis to determine the minimum fuel selling price (MFSP) required to obtain a zero net present value (NPV) with a finite internal rate of return (IRR). This section summarizes the assumptions made in completing the discounted cash flow analysis, with more details and supporting description available in the 2011 ethanol report for assumptions that are unchanged. Our analysis does not take into account any policy factors such as subsidies, mandates, or carbon credits, because these would be purely speculative. The purpose of this analysis is to demonstrate the process requirements needed to achieve specific DOE cost targets which are set from the top-down, and to demonstrate how the technology pathway described here is able to achieve such targets on its own merits (through bottom-up TEA modeling) and, if it cannot, to give policymakers a sense of the magnitude of incentive required to make it so.

4.1 About Cost-Year Indices

The cost-year of 2011 was chosen for this analysis to provide more updated and relevant cost output information relative to the 2007-year basis which had been consistently utilized for a number of years in prior analyses [3, 90]. This new basis is being applied consistently across all DOE-BETO platforms for which similar “design case target” reports are being established during 2013–2014 efforts, and it is expected that performance goals and TEA outputs will remain in 2011\$ through 2017 to permit comparison of future feedstocks, conversion technologies, and other alternative scenarios. However, the present equipment costs were obtained in 2012\$ or 2013\$ for new pieces of key equipment which were added or replaced in the current design model (as part of the subcontract with Harris Group), and in 2009\$ or 2010\$ for unit operations that were previously provided by Harris Group and vendors in support of NREL's 2011 ethanol design report, and are still maintained in the present model. Cost-years for chemicals range from 1999 to 2012.

The methods used for determining MFSP in another year's dollar value and for scaling capital, operating, and labor cost estimates to a desired target year remain the same as described in the 2011 ethanol report. Thus, the details will not be repeated here, but will be summarized briefly. Capital costs provided in a year other than 2011\$ were adjusted using the Plant Cost Index from *Chemical Engineering Magazine* [91] to a common basis year of 2011. The final cost index for a given year is generally not made available until the spring of the following year. Therefore, for the small number of equipment items that were quoted in 2013\$, we assumed the same Plant Cost Index value from 2012 (all cost quotes which fall in this category were provided in the first half of 2013). Similarly, for chemical costs we used the Industrial Inorganic Chemical Index from SRI Consulting [92]. Employee salaries were maintained from 2009\$ and were scaled using the labor indices provided by the U.S. Department of Labor Bureau of Labor Statistics [93]. The general formula for year-dollar back-casting is:

$$2011 \text{ Cost} = (\text{Base Cost}) \left(\frac{2011 \text{ Cost Index}}{\text{Base Year Index}} \right)$$

Since NREL’s biochemical ethanol report was released in 2011 (which included cost estimates and analysis collected between 2009 and 2011), the cost indices have remained more stable than during the five-year period between 2005 and 2008, which experienced a significant run-up in the price of materials such as steel and petroleum, as well as the considerable fluctuation that ensued between 2008 and 2011. Thus, the indexing that takes place to discount costs back to 2011\$ from 2012\$ or 2013\$ for the newest price estimates utilized in the present report does not introduce large price differences for these specific years. To maintain consistency with the 2011 ethanol report, capital costs and material prices for items which were unchanged in the present analysis were not modified except to update to 2011-year dollars. The only new “feed materials” that were added to the present design that were not required in the ethanol case were hydrogen and WWT chemicals, whose assumptions on delivery and pricing are described below. The electricity export price, taken to be the average wholesale price as determined by the North American Electric Reliability Corporation, was left unchanged from the ethanol report, set at \$0.0572/kWh. This corresponds to roughly 84% of the EIA 2011 average industrial retail price for electricity of \$0.068/kWh [94], which is consistent with published values for wholesale electricity as a fraction of retail prices [95].

4.2 Total Capital Investment

Section 3 of this report describes the details of the conceptual process design and how the purchased cost of the equipment was determined. The next step is to determine the installed cost of that equipment. The installation cost can be determined by performing a detailed study of everything required to install the necessary equipment and make it operational (e.g., foundation, piping, and wiring). This type of detail is not warranted at this level of analysis, and a factored approach in which multipliers are applied to the purchased equipment cost is considered satisfactory. The methodology and rationale for applying unit-level installation costs remain the same as described in the 2011 ethanol report, and again further detail can be found there that will not be repeated here. In summary, each type of equipment utilizes a different installation factor to scale the given direct equipment purchased cost to a final installed cost, with these factors generally varying between 1.5 and 3.0. A complete list of the equipment is provided in Appendix A, along with equipment purchased and installed costs. As described in the 2011 ethanol report, Harris Group obtained many package quotes for recent cost estimates, in which a given unit operation and all of its support equipment were quoted under one price. The installation factor for such packages can be relatively low because most of the engineering is already included in the price. Additionally, equipment designed as a pre-fabricated skid generally has a lower construction cost. Also, components that are more highly machined and have higher quality metallurgy tend to be more expensive per unit mass and therefore have a lower installation factor as a function of purchase price than a less sophisticated component does.

The purchased cost for a given component reflects a baseline equipment size. As changes are made to the process, the equipment size required may be different than what was originally designed. Instead of re-costing in detail, an exponential scaling expression was used:

$$\text{New Cost} = (\text{Base Cost}) \left(\frac{\text{New Size}}{\text{Base Size}} \right)^n$$

In this equation, the scaling exponent n varies depending on the type of equipment to reflect economy-of-scale dependencies (more detail on reasonable scaling values for different types of equipment is provided in the 2011 ethanol report). The basis for scaling is typically some characteristic of the equipment related to production capacity, such as flow or heat duty. Some equipment does not follow such a scaling-factor approach, namely when the capacity for a given operation is exceeded and requires multiple units in parallel (thus losing economy of scale benefits which are captured in the exponential expression above). A good example of this is the new pretreatment reactor cost information discussed in Section 3, which has resulted in a modified cost estimate to utilize multiple discrete sections of the horizontal portion of the pretreatment reactor (e.g., the portion which is in contact with acid) to allow for variations in residence time through this section of the reactor.

Once the total equipment cost has been determined in the year of interest, we must add several other direct and indirect costs to determine the total capital investment (TCI). Site development and warehouse costs are based on the inside-battery-limits (ISBL) equipment costs (Areas 200, 300, 400, and 500) and are considered part of the total direct cost (TDC). Beyond ISBL Areas 200–500, the other process areas are considered outside-battery-limits (OSBL) including Areas 100 (rolled up into feedstock costs) and 600-900. Project contingency, field expenses, home-office engineering and construction activities, and other costs related to construction are computed relative to the TDC and give the fixed capital investment (FCI) when summed. The sum of FCI and the working capital for the project is the TCI. Table 26 summarizes these categories and additional factors. The values assumed for each respective factor were maintained consistently with those discussed in the 2011 ethanol report.

Table 26. Additional Costs for Determining TCI

Item	Description	Amount
Additional direct costs		
Warehouse	On-site storage of equipment and supplies.	4% of ISBL ^a
Site development	Includes fencing, curbing, parking lot, roads, well drainage, rail system, soil borings, and general paving. This factor allows for minimum site development assuming a clear site with no unusual problems such as right-of-way, difficult land clearing, or unusual environmental problems.	9% of ISBL
Additional piping	To connect ISBL equipment to storage and utilities outside battery limits.	4.5% of ISBL
Indirect costs		
Prorateable costs	This includes fringe benefits, burdens, and insurance of the construction contractor.	10% of total direct cost (TDC)
Field expenses	Consumables, small tool and equipment rental, field services, temporary construction facilities, and field construction supervision.	10% of TDC
Home office and construction	Engineering plus incidentals, purchasing, and construction.	20% of TDC
Project contingency	Extra cash on hand for unforeseen issues during construction.	10% of TDC
Other costs	Start-up and commissioning costs. Land, rights-of-way, permits, surveys, and fees. Piling, soil compaction/dewatering, unusual foundations. Sales, use, and other taxes. Freight, insurance in transit, and import duties on equipment, piping, steel, instrumentation, etc. Overtime pay during construction. Field insurance. Project team. Transportation equipment, bulk shipping containers, plant vehicles, etc.	10% of TDC

^a ISBL = installed cost of equipment inside battery limits (A200,300,400,500)

Table 27. Project Cost Worksheet Including TDC and TCI

Process Area		Purchased Cost	Installed Cost
Area 100: Feedstock handling ^a		\$ 15,800,000	\$ 26,900,000
Area 200: Deacetylation + Pretreatment		\$ 33,900,000	\$ 51,400,000
Area 200: Conditioning		\$ 1,100,000	\$ 2,200,000
Area 300: Enzymatic hydrolysis/conditioning/bioconversion		\$ 58,100,000	\$ 75,400,000
Area 400: Enzyme production		\$ 7,300,000	\$ 12,400,000
Area 500: Recovery + Upgrading		\$ 16,300,000	\$ 26,600,000
Area 600: Wastewater		\$ 43,700,000	\$ 60,100,000
Area 700: Storage		\$ 1,900,000	\$ 3,400,000
Area 800: Boiler		\$ 42,000,000	\$ 76,000,000
Area 900: Utilities		\$ 5,100,000	\$ 8,800,000
Totals (excl. Area 100)		\$ 209,300,000	\$ 316,300,000
Warehouse	4.0% of ISBL		\$ 6,700,000
Site development	9.0% of ISBL		\$ 15,100,000
Additional piping	4.5% of ISBL		\$ 7,600,000
Total Direct Costs (TDC)			\$ 345,700,000
Prorateable expenses	10.0% of TDC		\$ 34,600,000
Field expenses	10.0% of TDC		\$ 34,600,000
Home office & construction fee	20.0% of TDC		\$ 69,100,000
Project contingency	10.0% of TDC		\$ 34,600,000
Other costs (start-up, permits, etc.)	10.0% of TDC		\$ 34,600,000
Total Indirect Costs			\$ 207,400,000
Fixed Capital Investment (FCI)			\$ 553,200,000
Land			\$ 1,800,000
Working capital	5.0% of FCI		\$ 27,700,000
Total Capital Investment (TCI)			\$ 582,700,000
Lang Factor (FCI/purchased equip cost) ^b			3.2
TCI per annual gallon 2011 dollars			\$18.59/gal

BC1307A

^a Feedstock handling not included in this calculation.

^b Area 600 not included in Lang Factor.

4.3 Variable Operating Costs

Variable operating costs, which include raw materials, waste handling charges, and byproduct credits, are incurred only when the process is operating. Quantities of raw materials used and wastes produced were determined using the Aspen material balance. Table 28 documents the costs and sources of chemicals used in the process, and Table 29 summarizes the variable costs on a per-year and per-gallon-of-RDB basis.

As noted above, the cost basis for all material costs in the present model which were also used in the 2011 ethanol model were left unchanged, except to update to 2011\$. The only new materials in this list are WWT chemicals (polymer), which was added during NREL's subcontract with Brown and Caldwell in 2012, corn oil antifoam (added to the A300 bioreactors to mitigate foaming due to aeration and product secretion) and hydrogen, which was assumed here to be purchased as a product from standard natural gas-derived steam methane reforming (SMR). This

approach for hydrogen sourcing was taken given the relatively small hydrogen demand for hydrotreating this particular FFA material, as well as to maintain consistency with the intention of evaluating a *representative* pathway model (with different hydrogen demands to be required for upgrading different products other than the FFA pathway), so to not place too much burden on an alternative on-site hydrogen production system without more definition on a specific product pathway and associated upgrading requirements. Moving forward, NREL will evaluate implications in cost and sustainability metrics associated with producing the required hydrogen internally (e.g., from anaerobic digestion biogas or other internal sources) rather than sourcing from natural gas off-site. Hydrogen price was set based on a recent DOE Hydrogen Program report, which presented a current price for natural gas-based SMR hydrogen of \$1.57/kg (assumed in 2012\$) associated with a natural gas price of \$4/MM Btu [96]. This price is likely to err on the conservative side, as the associated report was for forecourt production (smaller scale distributed systems rather than large central production), and today's U.S. industrial natural gas price is even lower at \$3.54/MM Btu in 2012 [97] (while the 2011 natural gas price was higher at \$4.70/MM Btu [97], the \$4/MM Btu basis is a reasonable average of the two most recent years). The overall cost sensitivity to the assumed hydrogen price is presented below in the Sensitivity Analysis section, using a reasonable maximum and minimum hydrogen cost range as presented in the referenced DOE report, namely \$1.10–\$2.00/kg associated with a natural gas price range of \$2–\$7.37/MM Btu, respectively. Prices for other new and repeated materials are summarized below.

Table 28. Chemical Costs and Sources

Component	Cost (2011\$)	Source
Biomass uniform-format feedstock	\$0.0320/lb	2013 MYPP, \$80/dry ton @ 20% moisture [10]
Sulfuric acid, 93%	\$0.0499/lb	Basic Chemical of Omaha via Harris Group
Ammonia	\$0.2496/lb	Terra Industries via Harris Group
Corn steep liquor	\$0.0316/lb	Corn Products via Harris Group
Diammonium phosphate	\$0.5492/lb	Ronas Chemicals via Harris Group
Corn oil (antifoam)	\$0.6077/lb	SRI Chemical Economics Handbook (CEH)
Sorbitol	\$0.6269/lb	Coast Southwest via Harris Group
Glucose	\$0.3230/lb	USDA ERS [98]
SO ₂	\$0.1690/lb	SRI Chemical Economics Handbook (CEH)
Enzyme nutrients	\$0.4570/lb	SRI CEH (See 2011 design report for details)
Hydrogen	\$0.6838/lb	DOE report, SMR H ₂ @ \$4/MM BTU NG [96]
Caustic	\$0.0832/lb	Brown and Caldwell 2011 WWT design [99]
Polymer for WWT	\$2.4806/lb	Brown and Caldwell 2012 WWT design [100]
Lime	\$0.1109/lb	Harris Group
Boiler chemicals	\$2.7788/lb	2002 Design Report [2]
Cooling tower chemicals	\$1.6653/lb	2002 Design Report [2]
Fresh water	\$0.0001/lb	Peters & Timmerhaus [101]

Table 29. Variable Operating Costs

Process Area	Stream Description	Usage (kg/h)	Usage (lb/h)	Cost (\$/ton)	\$/hour	MM\$/yr (2011\$)	Cent/Gal RDB (2011\$)
Raw materials							
N/A	Feedstock (wet)	104,167	229,688	64.00	7,350.00	57.95	184.90
A200	Sulfuric acid, 93%	2,240	4,940	99.85	246.62	1.94	6.20
	Caustic (as pure)	1,406	3,101	166.42	258.02	2.03	6.49
	Ammonia	260	574	499.27	143.38	1.13	3.61
A300	Corn steep liquor	1,404	3,095	63.24	97.86	0.77	2.46
	Diammonium phosphate	127	279	1,098.38	153.40	1.21	3.86
	Corn oil antifoam	122	269	1,215.42	163.77	1.29	4.12
	Sorbitol	18	40	1,253.71	25.04	0.20	0.63
A400	Glucose	1,213	2,675	645.94	863.86	6.81	21.73
	Corn steep liquor	83	182	63.24	5.75	0.05	0.14
	Corn oil antifoam	7	15	1,215.42	8.98	0.07	0.23
	Ammonia	58	127	499.27	31.75	0.25	0.80
	Host nutrients	34	75	913.94	34.05	0.27	0.86
	Sulfur dioxide	8	18	338.08	3.07	0.02	0.08
A500	Hydrogen	221	488	1,367.51	333.84	2.63	8.40
A600	Ammonia	173	381	499.27	95.08	0.75	2.39
	Polymer	3	6	4,961.25	14.97	0.12	0.38
A800	Boiler chems	<1	1	5,557.64	1.40	0.01	0.04
	FGD lime	191	420	221.90	46.64	0.37	1.17
A900	Cooling tower chems	3	7	3,330.66	11.51	0.09	0.29
	Makeup water	217,059	478,615	0.29	68.95	0.54	1.73
Subtotal					9,889.19	78.51	250.51
Waste disposal							
A800	Disposal of ash	4,542	10,015	35.39	177.22	1.40	4.46
Subtotal					177.22	1.40	4.46
By-products and credits							
	Grid electricity	10,490	kW	\$0.0572/kWh	599.71	4.73	15.09
	Area 100 electricity	859	kW	\$0.0572/kWh	49.13	0.39	1.24
Subtotal					648.84	5.12	16.32
Total variable operating costs					9,417.57	74.79	238.64

4.4 Fixed Operating Costs

Fixed operating costs are generally incurred in full whether or not the plant is producing at full capacity. These costs include labor and various overhead items. The assumptions on fixed operating costs were maintained consistently from the 2011 design basis (after updating to 2011\$), which in turn were based in large part on the 2002 ethanol design report [2] and/or Peters and Timmerhaus [101].

Table 30 shows the recommended number of employees and associated salaries. The number of employees was estimated by considering the likely degree of automation for each area and adding a reasonable number of management and support employees. Details behind the assumed number of employees and associated salaries are provided in the 2011 ethanol report. Because the model feedstock is predominately corn stover, salaries were estimated for rural regions of the U.S. Midwest (Iowa, Missouri, etc.). These estimates may vary depending on location.

Table 30. Fixed Operating Costs

Position	2011 Salary	# Required	2011 Cost	MM\$/yr (2011\$)	Cent/Gal RDB (2011\$)
Labor and supervision					
Plant manager	155,400	1	155,400		
Plant engineer	74,000	2	148,000		
Maintenance supervisor	60,257	1	60,257		
Maintenance technician	42,286	12	507,429		
Lab manager	59,200	1	59,200		
Lab technician	42,286	2	84,571		
Lab tech-enzyme	42,286	2	84,571		
Shift supervisor	50,743	4	202,971		
Shift operators	42,286	20	845,714		
Shift operators-enzyme	42,286	8	338,286		
Yard employees	29,600	4	118,400		
Clerks and secretaries	38,057	3	114,171		
Total salaries			2,718,971	2.72	8.68
Labor burden (90%)			2,447,074	2.45	7.81
Other overhead					
Maintenance	3.0%	of ISBL	5,039,796	5.04	16.08
Property insurance	0.7%	of FCI	3,872,126	3.87	12.36
Total fixed operating costs				14.08	44.92

A 90% labor burden is applied to the salary total and covers items such as safety, general engineering, general plant maintenance, payroll overhead (including benefits), plant security, janitorial and similar services, phone, light, heat, and plant communications. The 90% estimate is the median of the general overhead range suggested in the 2008 PEP Yearbook produced by SRI Consulting [92]. Annual maintenance materials were estimated as 3% of the installed ISBL capital cost and property insurance and local property tax were estimated as 0.7% of the fixed capital investment, based on the 1994 Chem Systems report described in NREL’s 2011 ethanol report. These factors are all consistent with those used in the 2011 ethanol report.

4.5 Discounted Cash Flow Analysis and the Minimum Selling Price of Fuel

4.5.1 Discount Rate

For this analysis, the discount rate (which is also the IRR in this analysis) was set to 10% and the plant lifetime was set to 30 years. The discount rate was also used in previous design reports and was based on the recommendation in Short et al. [102] on how to perform economic evaluations of renewable energy technologies for DOE. His view was that, “In the absence of statistical data on discount rates used by industrial, transportation and commercial investors for investments with risks similar to those of conservation and renewable energy investments, it is recommended that an after tax discount rate of 10%...be used.”

4.5.2 Equity Financing

For this analysis, it was assumed that the plant would be 40% equity financed. The terms of the loan were taken to be 8% interest for 10 years. The principal is taken out in stages over the 3-year construction period. Interest on the loan is paid during this period, but principal is not paid back. (This is another n^{th} -plant assumption, which says that this cash flow comes from the parent company until the plant starts up.) This is all consistent with the assumptions used in the 2011 ethanol report. Figure 18 illustrates the sensitivity of MFSP to the percentage of equity financing and the after-tax discount rate (the IRR).

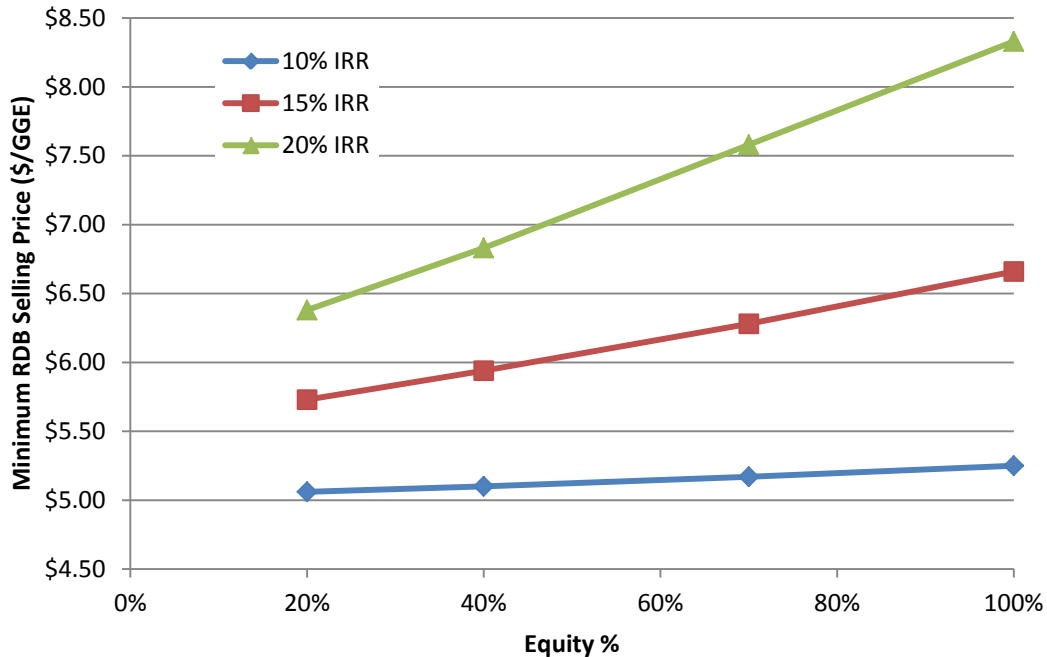


Figure 18. Sensitivity of MFSP to IRR and % equity (8% interest on a 10-year loan)

4.5.3 Depreciation

To determine the capital depreciation amount for the calculation of federal taxes to be paid, we used the IRS Modified Accelerated Cost Recovery System (MACRS). Within the MACRS system is the General Depreciation System (GDS), which allows both the 200% and 150% declining balance (DB) methods of depreciation. This offers the shortest recovery period and the largest tax deductions. According to IRS publication 946 [103], a cellulosic biorefinery plant would fall under Asset Class 49.5, “Waste Reduction and Resource Recovery Plants.” This class uses a 7-year recovery period, not including the steam plant equipment, which has a 20-year recovery period (Asset Class 49.13). IRS publication 946 contains a special provision for cellulosic biofuels plants that allows them to write off 50% of the capital investment in the first year. This was not implemented in our cost model because it does not ultimately affect the MFSP. (Although the provision affects the cash flow in the first few years of the analysis, it does not change the year in which the plant goes into the black and must start paying taxes.)

4.5.4 Taxes

The federal corporate tax rate used in our analysis is 35%. Income tax is averaged over the plant life and that average is calculated on a per-gallon basis. The amount of income tax to be paid by a potential fuel producer varies annually due to changes in the volume of product produced and the allowable depreciation deduction. In fact, no income tax is paid in the first eight years of operation because the depreciation and loan interest deductions are greater than the net income. State taxes are not considered, primarily because the location of the plant has not been determined and tax rates vary from state to state (from 0% to 12%).

4.5.5 Construction Time

The construction time is important to the cash flow analysis because no income is earned during construction, but huge sums of money are being expended. Construction time assumptions were left unchanged from the 2011 ethanol basis. Perry and Green [31] indicate that small projects (less than \$10 million investment) can be constructed in fewer than 18 months and that larger projects can take up to 42 months. An overview of petroleum refining economics indicates that large refineries (on the order of \$1.5 billion investment) can be constructed in 24 months [104]. Certainly this FFA/RDB process is much smaller than a petroleum refinery, so using a construction time of 24 months fits within these references, although an important difference between this type of facility and a refinery is the large number of field-erected vessels. These are constructed on-site and have a longer construction time than if the tanks were delivered finished. Table 31 summarizes the schedule for construction and the cash flow during that time. Twelve months are added before construction for planning and engineering.

Table 31. Construction Activities and Cash Flow

Project Start Month	Project End Month	Activity Description	% of Project Cost
0	12	Project plan and schedule established; conceptual and basic design engineering, permitting completed. Major equipment bid packages issued, engineering started on selected sub-packages, P&IDs complete, preliminary plant and equipment arrangements complete.	8%
12	24	All detailed engineering including foundations, structure, piping, electrical, site, etc. complete; all equipment and instrument components purchased and delivered; all site grading, drainage, sewers, rail, fire pond, foundation, and major structural installation complete; 80% of all major process equipment set (all except longest-lead items), all field fabricated tanks built, and the majority of piping and electrical materials procured.	60%
24	36	Complete process equipment setting, piping, and instrumentation installation complete; all electrical wiring complete; all building finishing and plumbing complete; all landscaping complete; pre-commissioning complete; and commissioning, start-up, and initial performance test complete.	32%
TOTAL			100%

Note: The above assumes no utility or process equipment orders placed prior to month seven. Expenditures based on typical 60 MMgal/yr grain-to-ethanol facility.

4.5.6 Start-Up Time

Perry and Green [31] indicate that for a moderately complex plant, start-up should be about 25% of the construction time, or 6 months in this case. While the 2011 ethanol model assumed a start-up time of 3 months under an n^{th} plant assumption, this is extended back to 6 months in the present analysis. The start-up period is not completely wasted, however. We expect that an average of 50% production could be achieved during that period while incurring 75% of variable expenses and 100% of fixed expenses.

4.5.7 Working Capital

Peters and Timmerhaus [101] define working capital as money available to cover (1) raw materials and supplies in inventory, (2) finished product in storage, (3) accounts receivable, (4) cash on hand for monthly payments such as wages and maintenance supplies, (5) accounts payable, and (6) taxes payable. The present analysis applies the same basis for working capital as was used in the 2011 ethanol report, namely 5% of FCI; this translates to a slightly higher working capital cost value given the increased direct capital costs and FCI in the present model.

Table 32 summarizes the parameters used in the discounted cash flow analysis. Using these parameters, plus the cost information in Table 27, Table 29, and Table 30, the resulting MFSP of pure RDB is \$5.35/gal or \$5.10/GGE (2011\$). Table 33 summarizes the yields and conversion costs for the present design. According to the methodology of Cran [105], the expected accuracy of the TCI analysis is 25%. If we apply this uncertainty to the TCI, the impact on the cost of RDB is \pm \$0.65/gal (\$0.61/GGE). The complete discounted cash flow summary worksheet is shown in Appendix B. The MFSP can be further broken down into the cost of each process area. Figure 19 illustrates the contribution to the overall cost by process area and capital, operations, and fixed costs. (The bar for feedstock + handling reflects the single feedstock cost of \$80.00/dry U.S. ton delivered to pretreatment and has not been decomposed.)

Table 32. Discounted Cash Flow Analysis Parameters

Plant life	30 years
Discount rate	10%
General plant depreciation	200% declining balance (DB)
General plant recovery period	7 years
Steam plant depreciation	150% DB
Steam plant recovery period	20 years
Federal tax rate	35%
Financing	40% equity
Loan terms	10-year loan at 8% APR
Construction period	3 years
First 12 months' expenditures	8%
Next 12 months' expenditures	60%
Last 12 months' expenditures	32%
Working capital	5% of fixed capital investment
Start-up time	6 months
Revenues during start-up	50%
Variable costs incurred during start-up	75%
Fixed costs incurred during start-up	100%

Table 33. Summary of Yields, Rates, and Conversion Costs

Feedstock rate	2,205 dry U.S. ton/day
On-line time	7,884 h/yr (90% on-line factor)
FFA intermediate yield	0.162 ton/dry ton feedstock (68% theoretical based on feedstock carbohydrates)
RDB yield	43.3 gal/dry U.S. ton feedstock (45.4 GGE/ton)
RDB production rate	31.3 MMgal/yr (32.9 MM GGE/yr)
Total equipment cost	\$316MM
Total capital investment (TCI)	\$583MM
TCI per annual gallon	\$18.59/gal
Minimum Fuel Selling Price	\$5.35/gal (\$5.10/GGE)
Feedstock contribution	\$1.85/gal (\$1.76/GGE)
Enzyme contribution	\$0.39/gal (\$0.37/GGE)
Non-enzyme conversion contribution	\$3.11/gal (\$2.96/GGE)

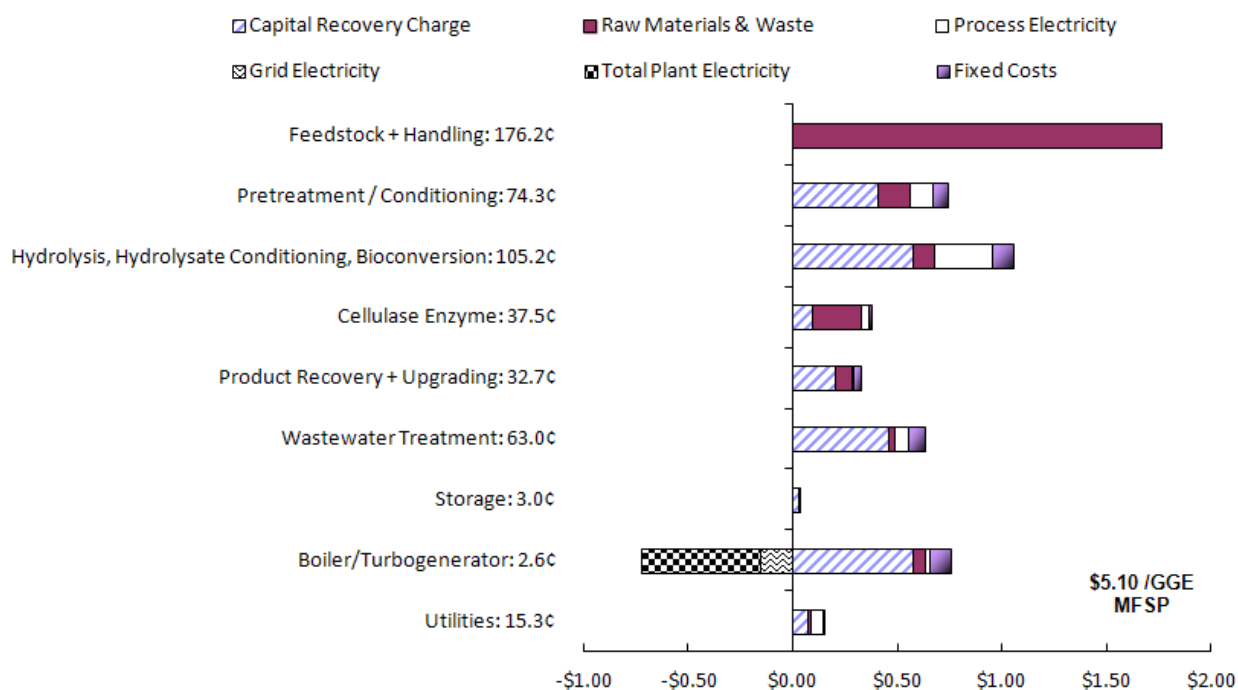


Figure 19. Cost contribution details from each process area (per GGE RDB product)

It is worth drawing a comparison here between the results presented above and those shown in the 2011 ethanol report. Both cases utilize similar assumptions regarding sugar yields (albeit at improved process conditions such as reduced enzyme loading) and subsequent sugar utilization efficiencies (90% glucose, 85% xylose, and 85% arabinose of the total sugars fed to the bioreactors and converted to product), but the MFSP cost is considerably increased here; the ethanol MESP would be \$3.61/GGE when updated to 2011\$ (all other variables held constant; the original ethanol MESP was \$3.27/GGE in 2007\$). This difference is primarily due to:

- a. Higher facility capital costs (TCI = \$583 MM versus \$471MM for ethanol when updated to 2011\$): Due primarily to increased complexity in A300 (hydrolysate conditioning and aerobic bioreactors) and the addition of hydrotreating in A500
- b. Lower yields (45.4 GGE/dry ton versus 52.0 GGE/dry ton for ethanol): Due to lower metabolic energy efficiency for FFA relative to ethanol (Table 13), higher diversion of sugars to biomass propagation (Table 10), thus a lower fraction of total sugars amenable to conversion to the desired FFA product, and additional yield losses across the hydrotreater for FFA upgrading to the RDB product
- c. Higher feedstock cost (\$80/dry ton versus \$58.50/dry ton in the ethanol case): At the yields presented here, the feedstock cost contributes \$1.76/GGE to the MFSP, compared to \$1.13/GGE in the ethanol case
- d. Decreased facility on-line time (7,884 h/yr vs 8,410 h/yr in the ethanol case): This parameter was adjusted externally to allow for a slightly more conservative n^{th} plant assumption, intended to be applied consistently across all new hydrocarbon pathways in the DOE-BETO platform work.

At the same time, other costs have decreased relative to the 2011 ethanol basis. Namely, the 2017 targeted enzyme loading has been reduced by 50% to 10 mg/g cellulose, relative to the 2012 ethanol target of 20 mg/g; this results in a considerable reduction in total enzyme cost contribution to the MFSP, which is traditionally a very large economic driver at historical enzyme loadings of 20 mg/g or higher. Indeed, allocated enzyme cost shown in Figure 19 is now the fifth-largest contributor to MFSP of the nine facility process areas, while it was second only to feedstock cost in the 2011 ethanol report.

While the analysis presented here demonstrates a viable and realistic path to achieve DOE's intermediate 2017 target of \$5/GGE via biological conversion, additional improvements will be needed to achieve the final 2022 target of \$3/GGE for this pathway. Although it is premature to establish a design case in the same level of detail as described in this report for the 2017 (\$5/GGE) pathway, a high-level discussion of such improvements is provided below in Section 6.

5 Analysis and Discussion

5.1 Carbon and Water Balances

Table 34 shows the overall flow of carbon inputs and outputs, with a carbon balance closure very near unity. As shown in the table, > 98% of all carbon in the process enters in the biomass feed, with small amounts of additional carbon coming from glucose (for enzyme production) and bioconversion nutrients such as CSL. Given the reduced enzyme loading relative to the 2011 ethanol report, the glucose contribution to total input carbon flow was reduced from 2.5% to 1.3%.

Table 34. Biorefinery Overall Carbon Balance

Stream	Carbon Flow (kmol/hr)	% of Carbon Flow
Carbon inlets		
Biomass feedstock	3,117	98.1%
Glucose	40	1.3%
A300/400 nutrients	19	0.6%
Total	3,176	100.0%
Carbon outlets		
RDB product	818	25.8%
Combustion exhaust	1,796	56.5%
Ash	10	0.3%
WWT brine	33	1.0%
Aerobic lagoons	58	1.8%
A400 vent	27	0.9%
A300 vent	438	13.8%
Hydrotreater furnace flue gas	10	0.3%
Total	3,189	100.4%

Of the carbon inputs to the process, 26% of carbon atoms leave as RDB after the inclusion of hydrotreating, which rejects a portion of the carbon in the FFA intermediate to additional CO₂ by way of decarboxylation. Major exit points for the balance of carbon (accounting for 70%) are the combustor stack and bioreactor vent. We expect the amount of carbon exiting in the combustion exhaust to be rather large because most byproducts (lignin, etc.) of this process are burned to form CO₂. The majority of the carbon exiting the bioreactor vent is also in the form of CO₂ inherent to the bioconversion process.

Only the carbohydrate components of the biomass are assumed to be convertible to product by bioconversion. Of the carbon in the feed stream, 1,857 kmol/h (59.6%) is carbohydrates (glucan, xylan, arabinan, mannan, galactan, and sucrose); converting all of this carbon to RDB represents the theoretical yield. According to Table 34, 1,256 kmol/h of the feed stream carbon is actually converted by the RDB pathway (carbon in the product plus CO₂ in the bioreactor vent), so the actual yield is 68% of the theoretical yield. This has decreased from the 2011 ethanol basis of 76% due to (a) minor losses of sugars attributed to the solid-liquid separation step now being placed before bioconversion, (b) additional diversion of sugars to biomass organism propagation

inherent to aerobic bioconversion, and (c) loss of carbon to CO₂ via decarboxylation for oxygen removal during hydrotreating. Carbon efficiency to the RDB product from initial hydrolysate sugars is 50%, dictated by a metabolic yield of 0.284 kg FFA intermediate/kg total sugars reaching the bioconversion step (79% of the theoretical metabolic yield, 0.36 kg FFA/kg).

The overall flow of water throughout the model is presented below in Table 35. The primary point of entry for dedicated process water demand is the “makeup water” stream, shown in the current model to be 217,100 kg/h or 14.4 gal/gal RDB product. This is considerably higher than the 2011 ethanol demand of 147,100 kg/h (5.4 gal/gal), primarily because of increased cooling water demands and associated cooling tower evaporation losses, as well as the reintroduction of a solid-liquid separation unit which requires a washing step to recover soluble sugars. Cooling tower evaporation accounts for 85% of the total process makeup water demand, and has increased in magnitude attributed to a cooling demand of 130 MMkcal/h in the present design versus 97 MMkcal/h in the 2011 ethanol design; this in turn is due to considerably increased flow of steam through the condensing stage of the steam turbine cycle, higher chiller condenser duty (primarily due to increased heat removal for the bioreactors), and an added exchanger to cool the sugar evaporator condensate material for recycle purposes. A lignin filter press with a dedicated washing step was utilized in the 2002 ethanol design report for pretreatment conditioning, but removed in the 2011 ethanol design report and replaced with a lignin press on the beer stillage after fermentation (with no washing required). In the present design, a vacuum filter press is utilized after hydrolysis to remove lignin and other insoluble solids for downstream bioconversion, which again requires a wash step to recover lost sugars; this wash step results in a lignin material with considerably higher moisture content, and thus water loss, as described previously.

Table 35. Biorefinery Water Balance

Inputs	kg/hr	gal/gal	Outputs	kg/hr	gal/gal
Moisture in feedstock	20,833	1.38	Water in fuel product	30	0.00
Water in glucose syrup	214	0.01	Cooling tower evap.	184,167	12.23
Water in raw chemicals	1,442	0.10	Stripped in enzyme aeration	388	0.03
Generated in enzyme prodn.	648	0.04	Bioreactor vent	13,042	0.87
Generated in bioconversion	8,750	0.58	Consumed in Pretreatment	2,394	0.16
Generated in WWT	-637	-0.04	Consumed in Enz. Hydr.	2,640	0.18
Generated in Combustor	26,968	1.79	WWT evap	2,857	0.19
Enzyme air intake	320	0.02	WWT Brine	3,767	0.25
Lignin cake dryer intake	0	0.00	Combustor stack	72,468	4.81
WWT air intake	2,878	0.19	Boiler blowdown vent	2,558	0.17
Combustion air intake	6,298	0.42	Upgrading flue gas	210	0.01
Makeup water	217,059	14.41	Upgrading produced water	917	0.06
Sum of Inputs	284,773	18.90	Sum of Outputs	285,407	18.95

Additional water enters the process via the feedstock and raw chemicals, both as free water and as “potential” water, i.e., the combustion product of lignin and unconverted sugars. Water is also consumed in hydrolysis reactions, and these are accounted for as well. As discussed in the 2011 ethanol report, again we note that describing water usage with the units of gallons of water per gallon of product (whether ethanol or RDB) can be somewhat misleading, because this quantity

obviously depends on product yield, and the unadjusted volumetric yield to RDB in the present design is about 45% lower than in the 2011 design to ethanol (43.3 gal RDB/ton versus 79.0 gal ethanol/ton). However much of this difference is artificial, due to differences in metabolic mass yield and product densities; a more consistent comparison of water consumption would be on a GGE basis, which would be 13.7 gal/GGE RDB or 8.2 gal/GGE ethanol for the biorefinery consumptive water use.

As noted above, utilities are responsible for a large majority of the water loss, with 85% of the net water loss due to cooling tower evaporation. Table 36 expresses the individual cooling water users (see Figure 16) in terms of their water loss responsibility in gal/gal.

Table 36. Individual Contributors to Cooling Water Evaporation

Cooling Water User	MMkcal/h	% of duty	gal/gal
Condensing Turbine	86.8	66.9%	8.18
Chiller condenser	16.9	13.1%	1.60
Hydrolysis cooler	7.5	5.8%	0.71
Hydrolysate flash condenser	1.5	1.1%	0.14
Pre-fermentation cooler	2.6	2.0%	0.25
Enzyme production compressor	0.6	0.5%	0.06
Bioreactor air compressor	7.9	6.1%	0.75
Sugar evaporator condensate	5.8	4.5%	0.55
Total	130.0	100%	12.23

The largest cooling water user is the condensing turbine, which is responsible for 8.2 gal/gal of water loss. A condenser on the turbine allows the steam to discharge from at a vacuum (about 0.1 atm) for maximum conversion of compressive energy to electricity. With the condensing turbine in place, the process generates enough electricity to supply all users in the plant plus a significant surplus, which is assumed to be sold to the grid. Without the ability to let the steam down to such low pressure (and temperature), the total amount of generated electricity may decrease to the point that either a power coproduct is no longer produced, or the plant no longer makes enough electricity to support all of its users and would have to purchase the balance from the grid (particularly given the increased facility electricity demand relative to the 2011 ethanol basis). The present design model presents an interesting comparison with the 2011 ethanol model, in that facility power demand has increased but heat demand has decreased; thus, considerably less steam is removed from intermediate turbine stages to supply facility heating demands (such as distillation which is no longer utilized here), resulting in a larger amount of steam ultimately reaching the final condensing turbine stage, resulting in a larger cooling water demand for this stage as previously noted. While this allows for increased electricity generation from the turbine (53.1 MW versus 42.3 MW in the ethanol case), the increased facility power demand (42.6 MW versus 28.5 MW in the ethanol case) results in a marginally higher amount of facility power use relative to generation (80% versus 69% in the ethanol case).

Moving forward, we will continue to evaluate ways to reduce the biorefinery consumptive water use. One promising possibility may be in direct air-cooled condensing of the steam turbine exhaust. The current conversion process employs largely wet evaporative cooling as the means of satisfying plant heat rejection requirements. The wet evaporative system is the most common

system used industrially. It requires a water-cooled surface condenser, a cooling tower, cooling tower basin, a circulating water system to carry cooling water to and from a cooling tower, and associated water treatment facilities. This system requires continuous makeup water to offset water lost through evaporation, drift, and blowdown (discharge). On the other hand, a direct air-cooled condenser is a completely closed-circuit heat exchange system in which the turbine steam is condensed on the inside of the tubes as a result of colder ambient air flowing across the outside of the finned tube surfaces. Because the heat rejection is achieved using only air, no water is consumed in the condensing process. A previous preliminary NREL study suggested that replacing the water cooler with an air-cooled condenser system on the steam turbine exhaust may effectively reduce the total consumptive water usage by about 50%, which in this model would reduce water consumption from 14 to 6 gal/gal RDB product. This improvement in water usage would not necessarily be at the expense of the RDB production cost. cursory analysis suggests that the higher capital investment for the air cooler is offset by a lower total variable operating cost. Further study is warranted to confirm that replacing the water-cooled steam turbine condenser with an air-cooled condenser (either in full or in part) to reduce consumptive water use is technically and economically feasible.

5.2 Sustainability Metrics for 2017 Base Model

Beyond the carbon and water balance considerations discussed above, an important aspect of evaluating biomass-derived fuel processes is the quantification of life cycle resource consumption and environmental emissions. Life cycle assessment (LCA) provides a framework from which the environmental sustainability of a given process may be quantified and assessed. This section presents the salient sustainability metrics of the current conceptual process at the conversion stage. Direct CO₂, NO₂, and SO₂ emissions, consumptive water use (discussed above), and other process-related metrics were derived from the integrated process model.

SimaPro v.7.3 software [106] was used to develop and link units quantifying life cycle impacts as previously documented by Hsu et al. [107]. Ecoinvent v.2.0 [108] and the U.S. Life Cycle Inventory (LCI) [109] processes were used to fill the data gaps. The Ecoinvent processes were modified to reflect U.S. conditions (e.g., replacing the default European electricity mix with the U.S. electricity mix), and the U.S. LCI processes were adapted to account for embodied emissions and fossil energy usage. The LCI of the conversion step captures the impacts of input raw materials, and outputs, such as emissions and waste as predicted by the process model, as shown in Table 37.

**Table 37. Input and Output Data for Biorefinery Processing
2,000 Dry Metric Tonnes of Biomass per Day**

Products	Production rate		
	kg/hr	gal/hr	MJ/hr (HHV)
RDB	11576	3975	492812
Grid electricity	10490	kW	
Resource Consumption	Flow rate	Per gal fuel	Per MJ fuel
	kg/hr	kg/gal	kg/MJ
Feedstock (corn stover)	104167	26.20	0.21
Sulfuric acid (93%)	2240	0.56	4.5E-03
Caustic (as pure)	1406	0.35	2.9E-03
Ammonia	491	0.12	1.0E-03
Corn steep liquor	1486	0.37	3.0E-03
Diammonium phosphate	127	0.03	2.6E-04
Corn oil	129	0.03	2.6E-04
Sorbitol	18	4.6E-03	3.7E-05
Glucose	1213	0.31	2.5E-03
Host nutrients	34	0.01	6.9E-05
Sulfur dioxide	8	2.1E-03	1.7E-05
Hydrogen	221	0.06	4.5E-04
Polymer	3	6.9E-04	5.6E-06
Boiler chemicals	2.3E-01	5.7E-05	4.6E-07
FGD lime	191	0.05	3.9E-04
Cooling tower chemicals	3	8.0E-04	6.4E-06
Makeup water	217059	54.60	0.44
Air demand	469468	118.10	0.95
Air Emissions			
Water (H ₂ O)	296665	74.63	0.60
Nitrogen (N ₂)	366641	92.23	0.74
Oxygen (O ₂)	142388	35.82	0.29
Carbon dioxide (CO ₂)*	102227	25.72	0.21
Methane (CH ₄)	2.0	5.1E-04	4.1E-06
Nitrogen dioxide (NO ₂)	76	0.02	1.5E-04
Carbon monoxide (CO)	67	0.02	1.4E-04
Sulfur dioxide (SO ₂)	11	2.9E-03	2.3E-05
Waste Streams			
Disposal of ash	4542	1.14	0.01
Wastewater (Brine)	7531	1.89	0.02

* Direct carbon dioxide (CO₂) emission is 100% biogenic CO₂.

In addition to the primary hydrocarbon RDB product, the process also produces an excess amount of electricity from lignin combustion (described in detail above). Electricity produced exceeds the on-site power demand for the biorefinery and is assumed in the TEA model to be sold back to the grid for a co-product credit. Given the large impact that electricity co-production exhibits on greenhouse gas (GHG) and fossil energy profiles, we evaluate the sustainability metrics both with and without consideration of the excess electricity co-product credits for

avoided GHG emissions and fossil energy consumption. This exported electricity is treated as an avoided product using the product displacement method [110]. Co-product displacement (also termed system boundary expansion) is based on the concept of displacing the existing product with the new product. The excess electricity co-product displaces an equivalent amount of grid electricity, thus avoiding a significant amount of GHG emissions as well as fossil energy consumption, assuming an average U.S. electricity grid mixture. The GHG and fossil energy consumption credits attributed to the displacement of an average U.S. electricity grid mixture is 0.78 kgCO_{2-eq}/kWh and 9.1 MJ/kWh, respectively, as defined by Ecoinvent. The associated breakdown of the average U.S. electricity grid mix as utilized in Ecoinvent are as follows: coal (47%), natural gas (17%), oil (3.3%), nuclear power (20%), biomass (1.1%), wind (0.35%), solar (0.015%), hydroelectric (8.2%), and others (2.5%).

Details of contributions to GHG emissions and fossil energy consumption at the conversion stage are presented in Table 38, which corresponds to the information in Table 37. GHG emissions associated with the conversion stage for the cases with and without electricity co-product displacement credits are estimated to be 0.07 kg CO_{2-eq}/GGE and 2.02 kg CO_{2-eq}/GGE, respectively. Thus, the electricity co-product is responsible for a GHG offset of 1.95 kg CO_{2-eq}/GGE. There is minimal contribution to GHG emissions directly from the biorefinery. Direct CO₂ emission from the conversion process (shown in Table 37) is biogenic CO₂ (i.e., CO₂ absorbed from the atmosphere and incorporated as biomass during the feedstock production phase, which is then re-released through lignin combustion, bioconversion to CO₂, etc.). With its biomass origin, biogenic CO₂ does not contribute to the increase of GHG in the atmosphere [111] and is not considered in the IPCC global warming methodology [112]. Hence, the contributions to GHG at the conversion stage are solely from the associated underlying processes (e.g., material inputs/outputs to and from the facility to support process operations).

Table 38. Conversion Process GHG Emissions and Fossil Energy Consumption per Unit of RDB Product

	GHG Emission		Fossil Energy Input	
	kg CO _{2-eq} /GGE		MJ/GGE	
Electricity credit	No	Yes	No	Yes
Direct refinery emission	0.012	0.012	0.00	0.00
Pretreatment chemicals	0.522	0.522	5.73	5.73
Ammonia conditioning	0.136	0.136	2.60	2.60
Bioconversion (nutrients)	0.200	0.200	2.32	2.32
Infrastructure	0.0164	0.0164	0.172	0.172
Enzyme production	0.834	0.834	9.5	9.5
Hydrogen	0.089	0.089	9.9	9.9
Boiler water chemicals	8.62E-05	8.62E-05	1.06E-03	1.06E-03
Flue gas desulfurization chemicals	0.036	0.036	0.198	0.198
Wastewater treatment chemicals	0.1602	0.1602	3.07	3.07
Cooling tower Chemicals	1.63E-03	1.63E-03	1.84E-02	1.84E-02
Waste disposal	0.00827	0.00827	0.213	0.213
Electricity credit	0.00	-1.95	0.00	-22.8
Total	2.02	0.07	33.60	10.79

Table 38 also shows the fossil energy consumption for the biorefinery conversion process. Fossil energy consumption associated with the conversion stage for the cases with and without electricity co-product displacement credits are estimated to be 10.8 MJ/GGE and 33.6 MJ/GGE, respectively. Thus the electricity co-product is responsible for a fossil energy offset of 22.8 MJ/GGE. Because the current biorefinery in the base case does not require any direct fossil energy input such as natural gas or fossil-derived electricity from the grid, the fossil energy consumption is entirely associated with the underlying process material inputs and outputs.

Table 39 summarizes the key sustainability metrics for the process both including and excluding electricity co-product displacement credits. On the basis of RDB energy content, the GHG emissions at the conversion stage are 15.9 kg CO_{2-eq}/GJ without co-product credits and 0.5 kg CO_{2-eq}/GJ with co-product credits. Similarly, the fossil energy consumption is 0.27 MJ/MJ without co-product credits and 0.09 MJ/MJ with co-product credits. Clearly, the GHG and fossil energy metrics for the biological conversion pathway are strongly influenced by the co-product credit gained through the export of excess electricity, which provides considerable reductions in these metrics when assumed to displace the current U.S. electricity grid mix which is relatively carbon-intensive attributed in large part to coal usage.

In addition to GHG emissions and fossil energy consumption discussed above, consumptive water use, total fuel efficiency (e.g. yield), and carbon-to-fuel efficiency are also repeated for reference in Table 39. As described previously, the total RDB product yield is 43.3 gal/dry ton and the corresponding carbon-to-product efficiency is determined to be 26.2%. The net water consumption (i.e., makeup water) for the biorefinery is 14.4 gal/gal. The U.S. Geological Survey defines consumptive water use as “water that is evaporated, transpired, incorporated into products or crops, consumed by humans or livestock, or otherwise removed from an immediate water environment” [113]. Biorefinery consumptive use may occur through incorporation into the product, and evaporation from cooling and heating processes. Based on this definition, the consumptive water use for the conversion process is equal to the makeup water to the plant, described previously to be 14.4 gal/gal RDB (13.7 gal/GGE), with implications discussed above.

Table 39. Summary of Sustainability Metrics for the Baseline Process

Electricity credit	No	Yes
GHG emissions (kg CO _{2e} /GJ)	15.9	0.5
Consumptive water use (m ³ /day)	5209	5209
Consumptive water use (gal/GGE)	13.7	13.7
Total fuel efficiency (gal/dry ton)	43.3	43.3
Carbon-to-fuel efficiency (C in fuel/C in biomass)	26.2%	26.2%
Net fossil energy consumption (MJ/MJ)	0.27	0.085

5.3 Cost Sensitivity Analysis

5.3.1 Single-Point Sensitivity Analysis

A single-point sensitivity was performed on the Aspen model using the variables and limits shown in Table 40. The baseline for all variables used in the design case is described previously in this report. Reasonable minima and maxima for each variable were chosen to understand and quantify the resulting cost impact on overall MFSP. Each variable was changed to its maximum

and minimum value with all other factors held constant. The sensitivities of (a) MFSP and (b) product yield are displayed as tornado charts in Figure 20.

The variation of xylose-to-product yield during bioconversion, volumetric productivity during bioconversion, uncertainty in capital costs resulting from the factored approach we used ($\pm 25\%$), and enzyme loading (mg protein/g cellulose) have the largest impact to MFSP. Enzyme loading plays a less critical role in overall cost impacts at a 10 mg/g basis than in the 2011 ethanol report at 20 mg/g, but still carries a higher cost impact over the loading range evaluated than the remainder of the parameters evaluated here.

Conversion-related parameters have the largest (and only) impacts on RDB yield; to simplify the yield plot, all other parameters considered in the cost sensitivity plot that did not have an impact on the yield sensitivity plot were excluded from the latter plot. Conversion parameters also factor heavily into production cost, because these parameters not only affect product final yield, but also affect capital and other operating costs. We note that this is an imperfect comparison because the TCI bar represents a true uncertainty while the other bars are more accurately called a risk, in the sense that they represent a range of results that we might expect to see in future pilot-scale demonstration runs.

Table 40. Assumptions Varied in the Sensitivity Analysis

	Assumption Name	Min	Baseline	Max
Pretreatment	Deacetylation xylan loss	0%	2%	10%
	PT reactor metallurgy	Stainless Steel	High Alloy	
	PT residence time	2	5	10
	PT acid loading (mg/g)	5	9	20
	PT temperature °C	150	158	170
	PT xylan to xylose	80%	90%	95%
	PT xylan to furfural	3%	5%	8%
	PT glucan to glucose	6%	10%	12%
Enz hydrolysis + conditioning	EH % solids	17.5%	20%	25%
	EH cellulose to glucose	75%	90%	95%
	EH enzyme loading mg/g	5	10	20
	EH time (d)	2	3.5	6
	Sugar loss in S/L separation	-	1%	5%
	S/L separation capex	-50%	-	+50%
Enz production	A400 capex	-50%	-	+50%
Bioconversion	CONV contamination losses	0%	3%	6%
	CONV xylose to FA	50%	85%	90%
	CONV arabinose to FA	50%	85%	90%
	CONV productivity (g/L/hr)	0.4	1.3	3.0
	Aeration (VVM)	0.1	0.4	1.0
	FFA product recovery	95%	97%	99%
Upgrading	Catalytic upgrading capital	-50%	-	+100%
	H2 price (\$/kg)	1.10	1.57	2.00
	PSA H2 Recovery	85%	95%	99%
Capital	Total capital investment	-25%	-	25%

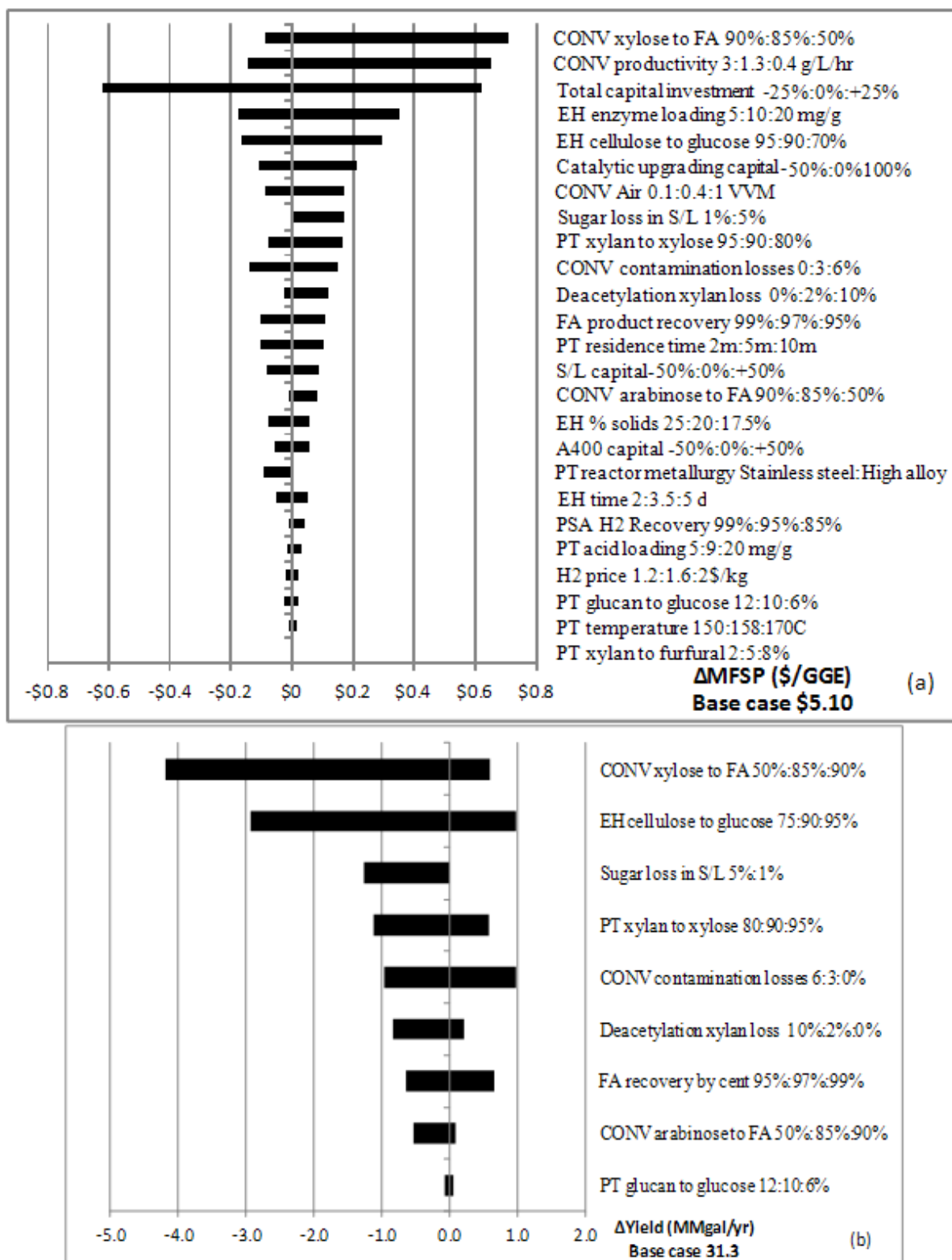


Figure 20. Single-point sensitivity tornado charts for (a) MFSP and (b) production yield

5.3.2 Evaluation of Alternative Metabolic Pathways

The diversity of biological pathways presents a challenge in regard to the selection of which molecules or which pathway may best serve as the “representative” baseline for the general biological conversion technology platform. Fatty acids are assumed in the base-case model to be a representative molecule (using palmitic acid as the representative component) for purposes of setting mass balances and energy yields. For comparison we evaluated six pathways for four molecules for a preliminary cost sensitivity analysis to account for variations on the governing metabolic yields and carbon efficiencies, shown in Table 41. The theoretical metabolic yield and carbon efficiency information are repeated from the discussion above shown in Table 13, based on a survey of literature [41, 50, 52, 53, 114, 115]. To compare with the base case using common assumptions, the bioconversion yield of glucose-, xylose-, and arabinose-to-product are set at 95%, 85%, and 85% respectively, with all other operational assumptions also held constant (e.g. aeration rate, batch time, etc.). While such aggressive yield data have not yet been reported publicly for any pathway to the best of our knowledge, this assessment stands to serve primarily as a consistent comparison across metabolic pathways and subsequent product upgrading demands.

The pathway for pentadecane production exhibits a moderate theoretical metabolic yield, in comparison with other pathways listed in Table 41. However, since pentadecane itself is a finished fuel blendstock and does not need any further upgrading, the resulting MFSP (per GGE basis) is lower than the \$5.10/GGE base case. There are two metabolic pathways leading to the production of the precursor farnesene; the mevalonic acid (MVA) pathway and the more recently characterized deoxyxylulose-5-phosphate (DXP) pathway, which is also known as the methylerythritol phosphate (MEP) pathway [116]. Additionally, we have also modeled a hypothetical anaerobic pathway to farnesene, to reflect early research conducted at NREL on anaerobic farnesene production, and to understand potential process and cost savings in switching from the aerobic baseline. Thus, this study considers farnesene production via MVA, DXP, and anaerobic pathways.

Table 41. Sensitivity Analysis for Various Pathways to Hydrocarbons, Based on Sugar Conversion Efficiencies Consistent With the Baseline FFA Model

Pathway	Theoretical metabolic mass yield	Theoretical carbon efficiency	MFSP (\$/gal)	MFSP (\$/GGE)	Production (MMgal/yr)	Production yield (gal/dry ton biomass)
Pentadecane	0.29	0.63	\$5.19	\$4.96	30.0	41.4
Farnesene (MVA)	0.25	0.56	\$6.25	\$5.97	27.0	37.3
Farnesene (DXP)	0.29	0.64	\$5.44	\$5.20	31.1	43.0
Farnesene (Anaerobic)	0.32	0.71	\$4.61	\$4.41	34.8	48.0
Fatty ester (palmitate ethyl ester)	0.35	0.67	\$5.83	\$5.55	28.9	40.0
Fatty acid (palmitate, base case)	0.36	0.67	\$5.35	\$5.10	31.3	43.3
Fatty alcohol (hexadecanol, anaerobic)	0.34	0.67	\$4.94	\$4.70	32.3	44.5

The hypothetical anaerobic farnesene pathway exhibits the lowest MFSP, also shown in Figure 21, not only because of its reduced cost for anaerobic fermentation, but also because of its high metabolic mass yield. In comparison with aerobic conversion, anaerobic fermentation enables reduced capital cost for the bioreactor vessels (e.g., 1 MM-gal anaerobic fermentors versus 1 MM-L aerobic systems), as well eliminating the need for air compression and associated compressor power demand. Among all three farnesene pathways, the hypothetical anaerobic pathway has the highest metabolic mass yield and carbon efficiency. Farnesene or other isoprenoids may also possess additional advantages in allowing for a more simplistic hydrotreating reactor and/or lower hydrogen demands, as these molecules only require saturation and not oxygen rejection; such nuances are not captured here in this high-level comparative analysis. Fatty alcohol (hexadecanol as the representative molecule) also may proceed anaerobically, so the resulting MFSP for this pathway is the second lowest under this assumption. The metabolic mass yield for fatty alcohol is lower than that of the anaerobic farnesene pathway. The farnesene production route via the MVA pathway exhibits the highest MFSP due to considerably lower theoretical energy yields than most other pathways considered. The fatty ester (palmitate ethyl ester) pathway also exhibits a cost on the upper range of those considered here. Although carbon efficiency from the biological conversion step is reasonably high for this pathway, carbon loss to carbon dioxide as well as rejection of the ethyl group to ethane in the catalytic upgrading step reduces the overall product yield.

Since the sugar to product utilization efficiency is fixed constant for each evaluated pathway, the MFSP is closely correlated with metabolic mass yield. The correlation, however, is found to be nonlinear, given other tradeoffs in system design and cost (e.g., aerobic versus anaerobic bioconversion) as well as upgrading demands in hydrotreating (e.g. additional carbon losses during FAEE conversion, no deoxygenation demand for farnesene, and no hydrotreating demand at all for pentadecane). Additionally, while all process performance metrics such as sugar utilization efficiencies and volumetric productivity were held constant to isolate the economic implications for different theoretical metabolic pathways, in reality most anaerobic pathways to long-chain hydrocarbons proceed considerably more slowly today than aerobic pathways which are better developed [32]; this translates to lower practical volumetric productivities and increased bioreactor capital costs, which are not reflected in this theoretical exercise with such factors held constant. Figure 21 also validates the intended rationale for the selection of FFA as a *representative* mid-point on an overall MFSP cost basis, relative to other potential product pathways.

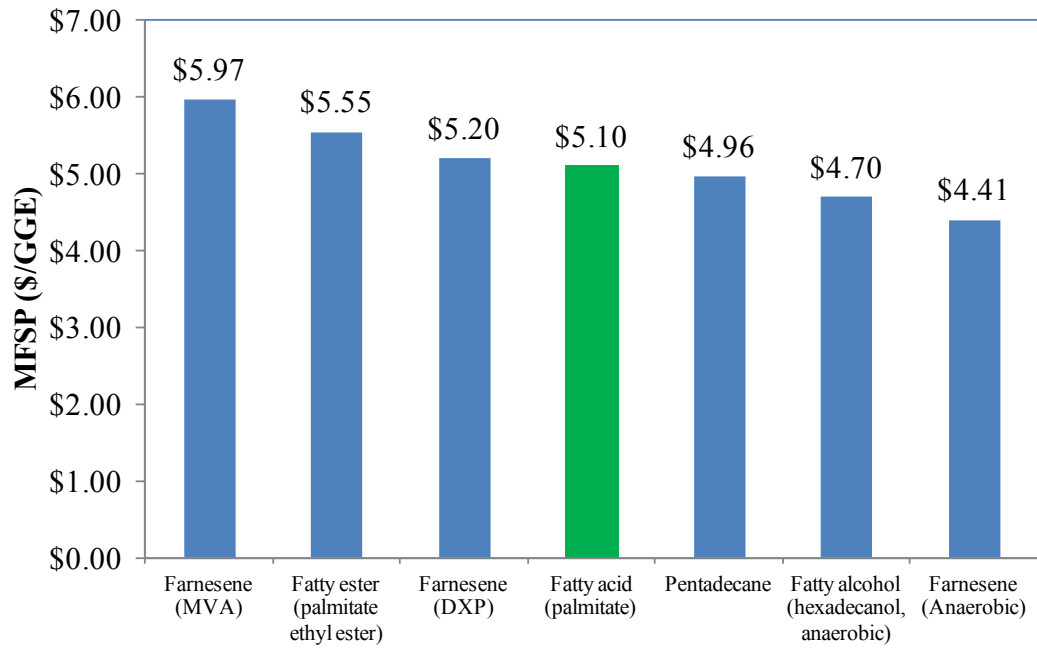


Figure 21. MFSP (\$/GGE) estimates for alternative pathways

6 Paths Forward to \$3/GGE

To meet future 2022 cost target goals of \$3/GGE for this pathway, further cost reductions from the 2017 design case baseline will be needed. One potential route for economic improvement is to maximize the overall carbon efficiency by converting underutilized fractions of the biomass. As detailed in this section, finding routes for converting lignin from biomass to value added commodity chemicals and fuels with large global markets has the potential to meet and surpass the \$3/GGE cost target goals.

In addition to the conversion of lignin to chemicals and fuels, there are other opportunities that are not explored in detail here to achieve the \$3/GGE cost target goals, for example by reducing the overall carbohydrate conversion costs. As highlighted in the 2017 design case, the sugar production metrics are tied to pretreatment and enzymatic hydrolysis. Reductions in sugar costs will continue to be important areas for further R&D and may be achieved through the use of alternative or milder pretreatment options and/or improved enzyme performance (higher conversion yields and/or lower enzyme doses or cost), including the incorporation of new enzyme classes and enzymatic hydrolysis mechanisms [50]. Developing methods to utilize biomass-derived intermediates beyond monomeric sugars could also help to improve overall carbon conversion efficiencies in the process. Tailoring the hydrolysate stream to the microorganism tolerance will be essential for improving overall yields and lowering production costs. Another potential pathway to optimize process integration is “direct microbial conversion” (also known as consolidated bioprocessing), whereby enzymatic hydrolysis and bioconversion occur in a single step without the need for externally added enzymes. Given the still relatively high cost of enzyme addition, this approach also warrants continued evaluation and research.

Reduction of hydrolysate conditioning costs could also be realized through a better understanding of the tolerance of hydrocarbon-producing microbes to lignin and other cellulosic sugar substrate impurities, including organic acids, salts, and other potential inhibitors. The current 2017 design basis is potentially a conservative design approach that is informed by the majority of literature sources for hydrocarbon production by utilizing clean, solids-free sugar sources. The performance and cost tradeoffs between sugar stream concentration and purity and microbial hydrocarbon production must be quantified to be able to develop optimal process designs. These tradeoffs are complex and will vary for different microbes, product pathways, and hydrocarbon production process configurations.

Furthermore, reductions in bioconversion costs may be possible through the production of hydrocarbon biofuels by anaerobic microbial conversion (e.g., anaerobic fermentation). Reducing the need to incorporate more complex and costly aeration capabilities into bioreactor systems should also be considered in parallel to improve process economy. The demonstration and development of organisms that can produce hydrocarbons at high rates and yields via anaerobic pathways would be a breakthrough for this field.

The remainder of this section is intended to provide more details on technical context, as well as TEA and sustainability implications, specifically around the opportunity for lignin co-product utilization and upgrading to value-added materials, primarily to demonstrate quantitatively one potential path which could ultimately achieve the \$3/GGE target. However, it is recognized that there are additional areas of potential improvement as discussed immediately above, and

although not considered explicitly here, they will be important areas to continue evaluating moving forward, both from a research and a modeling standpoint.

6.1 Lignin Utilization: Technical Context

As mentioned above, lignin utilization is of paramount importance for the biological conversion of sugars to hydrocarbons pathway to meet the 2022 cost target of \$3/GGE. Here, we briefly discuss several options and technical considerations concerning lignin utilization in the context of this pathway. We also highlight potential benefits and drawbacks of well-known options for isolating lignin from carbohydrate streams, many of which will require further research and development to quantify their impact on the overall process via TEA and LCA. The upgrading of lignin is also briefly discussed, which is an area of significant research need for the economic viability of this conversion pathway.

Lignin is a heterogeneous, alkyl-aromatic polymer comprised of three phenylpropanoid monomers that are primarily thought to polymerize via radical coupling reactions during plant cell wall formation [117], as illustrated in Figure 22. Lignin is connected by a diverse collection of C-C and C-O bonds, including linkages to hemicellulose, and possesses a broad range of reactivity to thermochemical environments and chemical and biological catalysts.

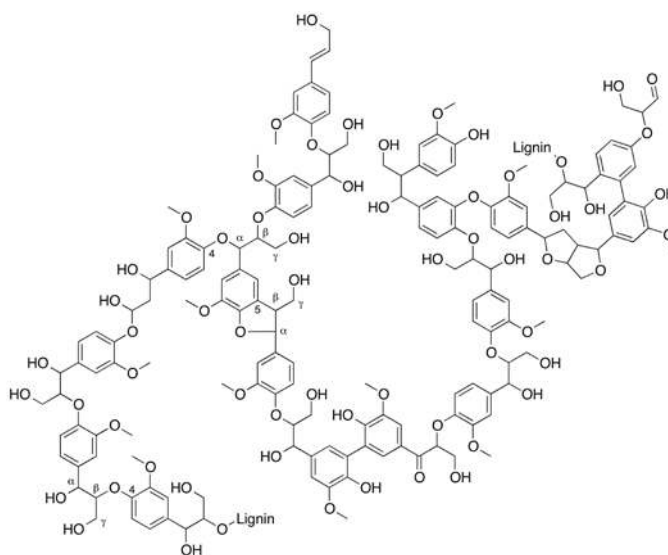


Figure 22. Illustration of an intact lignin bio-polymer, taken from Kim et al. [118]

The heterogeneous nature of lignin significantly imparts the two primary challenges associated with its utilization in the context of this pathway: namely (1) separation of lignin from biomass without negatively impacting carbohydrate yields, and (2) conversion of lignin from a heterogeneous feedstock to a product of substantial purity, quality, and/or quantity, depending on the fuel, chemical, material, or product of interest. These challenges, coupled to the need for lignin utilization to approach economic viability for hydrocarbon production, require a co-design approach for carbohydrate and lignin utilization. Lignin isolation is currently feasible at multiple process locations (illustrated in Figure 23), including:

- Prior to carbohydrate deconstruction, as an *in situ* lignin deconstruction step utilizing an alkaline catalyst that partially removes lignin and acetate, followed by dilute acid pretreatment and enzymatic hydrolysis for the stream primarily comprised of carbohydrates (this scenario was used as the design basis for the model developed here)
- As a single fractionation step that utilizes a pretreatment catalyst that can (partially) remove lignin and (partially) solubilize hemicellulose into separate liquid-phase process streams, for example, using an Organosolv or acid pulping approach
- After carbohydrate deconstruction by recovering and either deconstructing the recovered solid, lignin-rich residue remaining after processing via, e.g., base-catalyzed depolymerization or catalytically with a method such as hydrogenolysis, or utilizing this lignin-rich residue as a structural material.

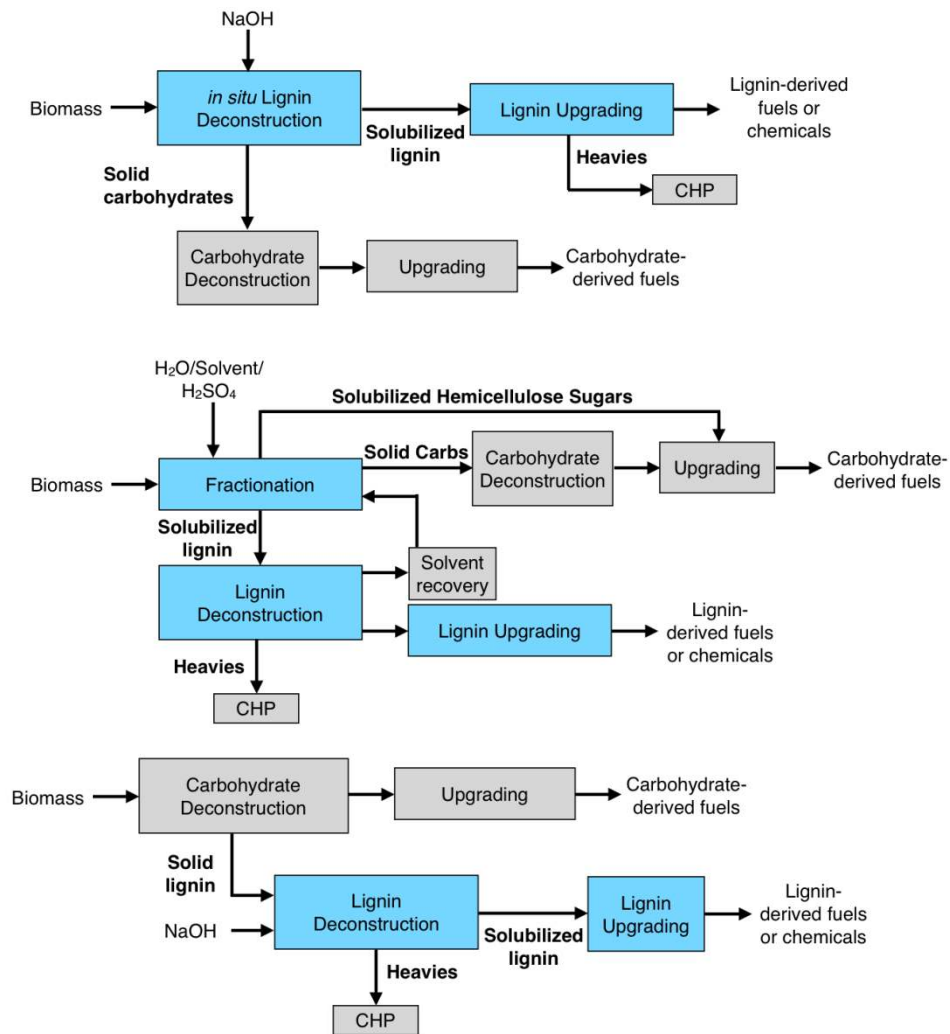


Figure 23. There are multiple options for selective lignin utilization. (Top) Lignin can be deconstructed to a soluble, separable stream with, for example, sodium hydroxide, and the remaining carbohydrate solid can be converted subsequently. (Middle) Lignin can be fractionated from the carbohydrate fractions for subsequent deconstruction and upgrading in a parallel fashion to carbohydrate conversion with organic solvents and an acid catalyst. (Bottom) The lignin-rich residue after carbohydrate deconstruction can be isolated and upgraded to products of interest.

There are myriad approaches within each of the aforementioned general options for isolating or removing lignin from biomass, and likely others that are not adequately captured in those generic isolation options. Regardless of the specific technology, catalyst, and processing conditions chosen for obtaining lignin in an upgradeable form, virtually all processing options will affect lignin chemistry, structure, and degree of polymerization. Additionally, the form of lignin necessary for upgrading to the desired fuel, material, chemical, or product of interest will also necessitate consideration of the entire process, as the nature of the lignin-enriched stream will likely dictate yield and product quality.

Regarding lignin removal or fractionation before or concomitantly with carbohydrate deconstruction, there are many processing options available for this type of work, including biological pretreatment [119-125], alkaline or acid-based pulping-like processes [120, 126], numerous Organosolv processes [127-130], and use of novel solvents such as ionic liquids [131-133]. Regardless of the upstream lignin isolation strategy, there may be significant changes to the carbohydrate fraction of the biomass, including potential carbohydrate loss to the resulting lignin stream, which will impact yields and thus MFSP. Conversely, significant reductions in cellulase enzyme loadings may be feasible with lower lignin content in the carbohydrate stream. This additionally may warrant further cocktail engineering for these carbohydrate streams that vary from those described as the basis of this specific design case (i.e., not derived from dilute-acid pretreatment). Moreover, there are additional potential benefits to lignin removal upstream for the carbohydrate train, including a lower mass flow through the pretreatment and enzymatic hydrolysis units [134], which was paramount in meeting the 2012 ethanol cost target, resulting from the deacetylation step.

Alternatively, for lignin conversion processes that follow carbohydrate deconstruction, such as pretreatment and enzymatic hydrolysis, the nature of the pretreatment process will likely impact the lignin chemistry significantly. For example, high severity dilute acid pretreatment is thought to catalyze aryl-ether (C-O) bond cleavage in lignin and promote recondensation of C-C linkages, likely rendering lignin more recalcitrant [135, 136]. Thus, the nature of the upstream pretreatment chemistry intended to (in some cases) remove hemicellulose, redistribute lignin, and render biomass more digestible by enzymes should be considered in light of the intended downstream lignin conversion process. Multiple types of processes have been considered, beyond combustion of residual lignin for heat and power, for converting lignin to value-added molecules after carbohydrate removal. For example, pyrolysis and gasification of lignin-enriched streams following pretreatment and enzymatic hydrolysis have been examined at length, but both strategies exhibit significant technical hurdles primarily around feeding lignin to high-temperature reactors [137]. Beyond this, a plethora of catalysts and processing technologies have been demonstrated for depolymerization of biomass-derived lignin such that lignin deconstruction products can then be subsequently upgraded to fuels and chemicals. These include (but are not limited to) depolymerization in the presence of catalysts in aqueous or organic media [138], in high severity alkaline environments [139-144], and via hydrogenolysis over hydrogen-activating catalysts in the presence of high pressures of H₂ or a hydrogen donor molecule [145-147]. These processes are typically followed by further catalytic upgrading and/or finishing to value-added chemicals. Other means for lignin utilization may involve retaining the natural or modified polymeric structure of lignin. Instead of needing to overcome the heterogeneity of lignin, it can be utilized directly or with some modifications in multiple materials applications [148]. Essentially, many process options have been examined in the

context of lignin conversion technologies, and as with carbohydrate utilization, the appropriate technology for lignin utilization will depend on both the upstream processing of lignin and the desired value-added molecules.

To that end, there are multiple potential product classes for lignin utilization, many of which are reviewed in the seminal review products-from-lignin report [148]. A general approach of this integrated design for a standalone lignin upgrading process is illustrated in Figure 27, starting with examples of the heterogeneous lignin deconstruction product slate through upgrading to potential products from lignin. The variety of products from lignin allows for potential process flexibility and a design focus in line with the BETO programmatic goals toward displacing the whole barrel of oil. The largest—and perhaps most scale-relevant—is the conversion of lignin to fuels, likely as gasoline-range aromatics [148]. Given the heterogeneity of resulting lignin deconstruction products, this will likely require significant efforts into development of selective deoxygenation chemistries across multiple functional groups, as shown in Figure 27 as a “catalytic defunctionalization” step. This challenge is similar to that faced in bio-oil conversion pathways, and it is likely that work therein can be leveraged and adapted for lignin utilization. Additionally, it may be possible with sufficient hydrogenation and severity to obtain ring-opened products, which could expand the range of fuel types to distillates with more desirable fuel properties.

On a smaller scale, there are many opportunities to develop commodity and specialty chemical streams from lignin, as reviewed in detail [148]. Upgrading lignin to chemicals is a challenge that many groups have examined over prior years, with limited and small-scale success to date. To make a broad slate of chemicals from lignin, the development of “catalytic defunctionalization” methodologies will be essential to reduce the heterogeneity of the lignin-derived streams. In terms of target molecules, aromatics such as phenol, benzene, toluene, xylenes, terephthalic acid, cumene, and other functionalized aromatics are significant in the commodity chemicals market, and are primary targets from lignin. Additionally, ring-opened chemicals that have developed routes already from aromatics, such as adipic acid as examined in the design case reported here and recently reviewed [149], will likely be a component of the renewable chemical portfolio derived from lignin. Further, there are novel chemical conversion routes to specialty chemical products from lignin that with further research and development have the potential to grow the market in renewable chemical products, including polymer precursors and advanced materials such as carbon fibers. Generally, however, the development of processes to produce a specific molecule will hinge on the ability to control and tune the lignin-derived feedstock and lignin upgrading chemistry to obtain the desired product yields and required product purity.

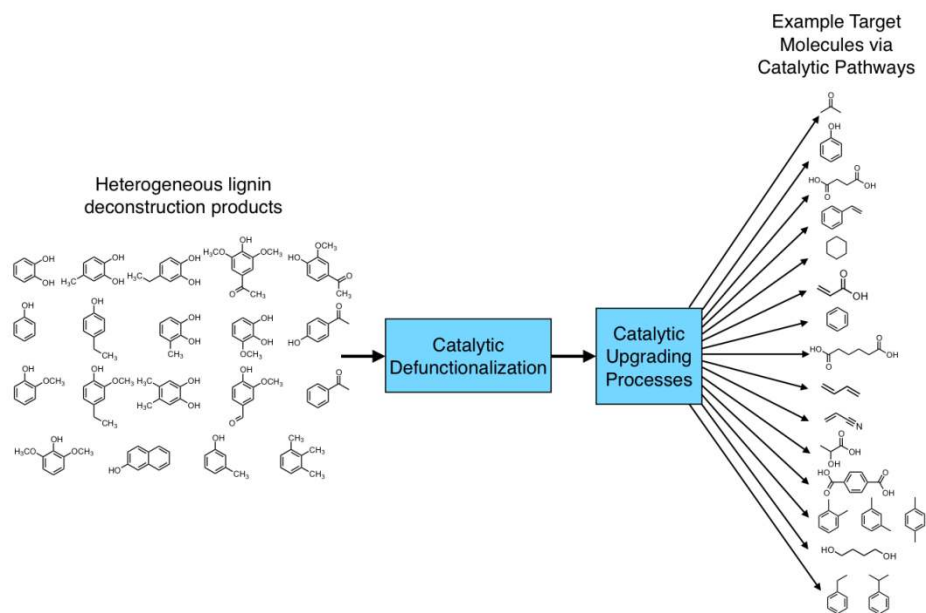


Figure 24. There are multiple options for selective lignin upgrading to fuels and chemicals via standalone lignin upgrading processes. Many of these pathways will require intense research, development, and deployment going forward to demonstrate pathway viability and TEA/LCA efforts to understand the economic and sustainability tradeoffs between them.

6.2 Lignin Utilization: TEA Modeling/Analysis

It should be noted that the lignin utilization process design is in an early stage of development and understanding. This outlined design is meant to serve as a representative, preliminary pathway to provide insight for the potential economic and sustainability impacts for lignin conversion to commodity chemicals and fuels, as well as to highlight key bottlenecks, design uncertainties, and data gaps for future research and development.

The conceptual design basis for lignin conversion is a multistep process. A high-level block flow diagram of the process is shown in Figure 25, which highlights the three key conversion areas: lignin deconstruction, lignin upgrading to chemicals, and product recovery and purification.

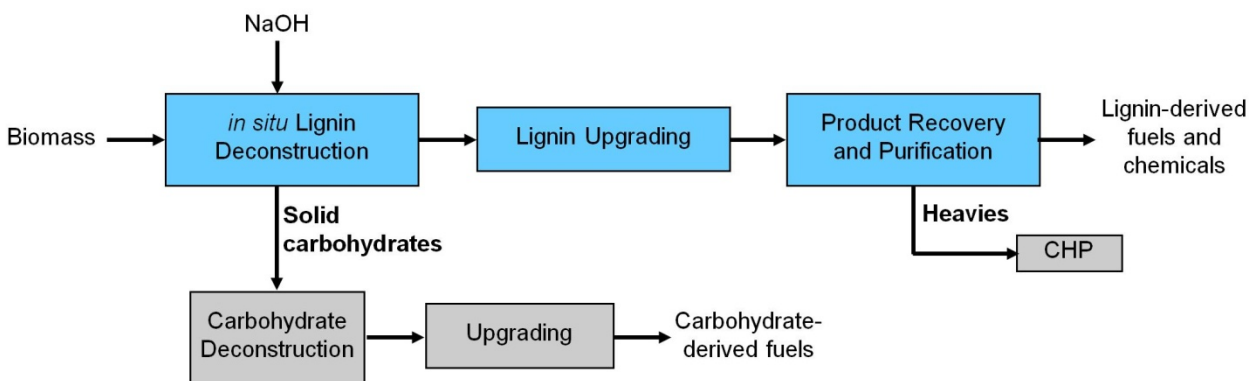


Figure 25. Schematic diagram for lignin deconstruction/upgrading pathway utilized for TEA analysis

In the current design basis, the lignin deconstruction process is an alkaline pretreatment approach. The alkaline pretreatment process modeled here is a direct extension of the deacetylation biomass pre-conditioning process, and was chosen for the initial economic analysis to be in line with the 2017 target base design. For the alkaline pretreatment step, the biomass is conveyed into the pretreatment reactor and mixed with sodium hydroxide. Medium pressure steam is introduced into the batch reactor system to reach the targeted 130°C temperature. The reaction conditions and process yields are summarized in Table 42 and are based on current conditions and yields from ongoing NREL research efforts and literature data [120]. To minimize loss of the carbohydrate biomass fraction, anthraquinone is added at a loading of 0.5 mg/g dry biomass to the pretreatment process. Anthraquinone has been shown to catalytically inhibit carbohydrate loss due to peeling reactions when added in low dosages to alkaline pulping processes, such as in soda pulping [120]. The slurry is agitated in the batch alkaline pretreatment reactor for 30 minutes. Solubilized lignin is then drained from the residual carbohydrates streams, consistent with the previously outlined deacetylation process. The solid carbohydrate stream continues to dilute acid pretreatment and upgrading consistent with the 2017 target base design as previously outlined. The solubilized lignin stream is sent to the catalytic lignin upgrading process.

As highlighted in the overview of the lignin section, there are a multitude of routes for the deconstruction of biomass that results in delignification. Both experimental work and detailed TEA are under development at NREL for alternative lignin deconstruction processes, and the most promising technologies will be carried forward for further research and development.

Table 42. Comparison of Deacetylation and Alkaline Pretreatment Processing Conditions

	Deacetylation	Alkaline pretreatment
Process Details		
Temperature (°C)	80	130
Time (hr)	1	0.5
NaOH loading (mg/g dry biomass)	17	39.6
Anthraquinone loading (mg/g dry biomass)	0	0.5
Solids loading (wt%)	20	20
Process Results		
Xylan loss (wt%)	2	9
Acetate removal (wt%)	88	88
Extractives removal (wt%)	100	100
Sucrose removal (wt%)	50	100
Ash removal (wt%)	75	75
Lignin solubilized (wt%)	20	80

The solubilized lignin stream is sent to catalytic upgrading to produce commodity chemicals and fuels. In the current design, it is assumed that minimal preprocessing steps are required prior to upgrading. However, depending on the tolerance of the catalyst to any poisons in the lignin deconstruction stream, further preprocessing will likely be necessary and will be an important consideration in future designs.

As described in Figure 24, there are multiple products possible from the upgrading of lignin to fuels and chemicals. A subset of four commodity products was selected as representative of this large slate of possible products, with lower cost hydrocarbon products and higher valued oxygenated commodity chemicals included in the evaluation. These specific products, outlined in Table 43, have significant global market demand and positive projected market growth. The product prices utilized in this analysis are based on recent cost information and care was taken to ensure that these prices were not the high point of recent commodity market curves but more mid-range estimates. The goal of this analysis is to understand both the economic and sustainability tradeoffs for each product. The catalytic upgrading to produce commodity chemicals and fuels from the solubilized lignin deconstruction product is an ongoing research and development project at NREL. The specific pathways and detailed yields are currently being characterized.

Table 43. Summary of Lignin Upgrading Products Considered Here [92, 150–155]

Product	World Production (thousand tons/year)	Price (\$/ton)	Projected growth rate	Primary Usage
1,3 Butadiene	>12,000	3200	5%	Synthetic rubber
1,4 Butanediol	>1,000	3170	5%	Tetrahydrofuran, specialty chemicals
Adipic Acid	>3,000	1700	4-4.5%	Nylon-6,6
Cyclohexane	>5,700	1000	2.5%	Nylon-6,6 precursors

The upgraded lignin products and residual unconverted products are sent to product recovery and purification. A minimum product purity specification of 95% was utilized for each of the products. There is a high degree of uncertainty around this purification specification as the preliminary process models have focused on a small slate of model components for the lignin deconstruction products. Further research is needed to better understand and quantify the ability to meet the high purity specifications of these commodity products. Furthermore, even more stringent product purification specifications can be required for commodity products and future work should consider any required higher product purity specifications and the subsequent process intensification and cost impacts.

Harris Group provided preliminary capital cost estimates for the lignin utilization process configuration by considering the costs of the major process units. Harris Group provided cost estimates for the alkaline pretreatment reactor with a design a 127 m³ vertical pressure vessel similar to the pre-steaming section of the pretreatment reactor. The lignin upgrading process is estimated to cost \$67MM for the total installed capital cost. The pretreatment reactor accounts for ~37% of the overall cost, the lignin upgrading process is ~43% of the overall cost, and the remaining ~20% of costs are associated with the product separations processes.

Applying this estimate for capital costs and high-level process models, a preliminary TEA estimate was developed to understand the economic and sustainability drivers associated with the conversion of lignin to commodity products. Figure 26 summarizes this preliminary economic analysis to illustrate the potential for the conversion of lignin to meet the program DOE BETO cost target goals of \$3/GGE. This diagram illustrates the MFSP for the four commodity chemical products as a function of the percentage of lignin converted to the product. As highlighted in this

figure, the addition of the capital and operating costs associated with inserting the new lignin process train increases the base-case MFSP from \$5.10 to \$5.57/GGE, assuming no lignin conversion to products; this increase is driven primarily by increased cost of caustic, new cost of anthraquinone, and added capital cost. As seen in Figure 26, there are a number of product pathways that show promise to meet and potentially surpass the overall economic targets, including adipic acid and 1,4 butanediol. Both of these products are oxygenated species with high market value. Based on the preliminary analysis, the lower cost hydrocarbon products such as cyclohexane will not be able to achieve the \$3/GGE target goal.

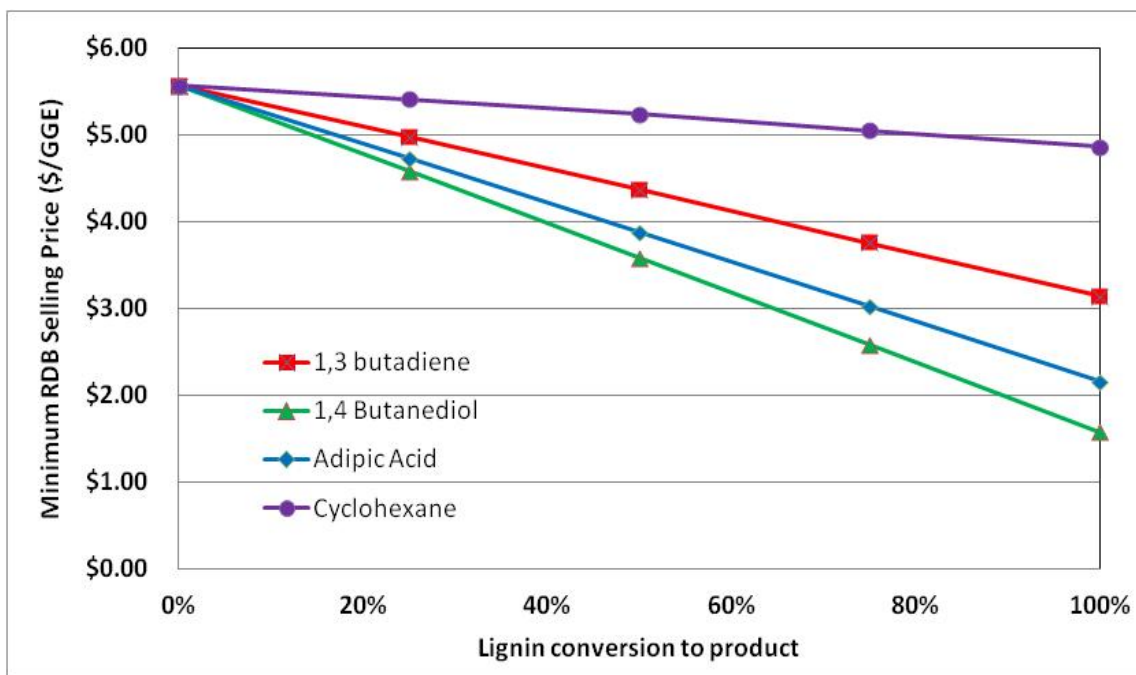


Figure 26. Minimum RDB selling price as a function of lignin conversion to selected coproducts

To begin to identify key cost drivers for the lignin utilization process design, a series of sensitivity analyses were performed on the \$3/GGE adipic acid design (as outlined in Figure 27). To capture the price fluctuations of the commodity chemicals market, the high point and low point of the adipic acid cost curve were considered. As shown in Figure 27, at the lowest cost of adipic acid in the past 15 years, the MFSP would increase by \$0.67/GGE while at the highest cost point, the MFSP would decrease by more than \$0.27/GGE. The preliminary capital cost provided by Harris Group was an AACE Class 5 analysis with capital cost uncertainty ranging from -20% to +100%. If capital costs associated with the lignin utilization design doubled, the MFSP would increase by \$0.45/GGE. Further, it should be noted that a mid-range price point from recent price quotes from Harris Group was utilized for this overall analysis. Key process targets for anthraquinone loadings and xylose loss are also shown. Anthraquinone loadings have a significant impact if loadings are raised to 2 mg/g. If xylose losses are increased by more than double, the impact on the MFSP is \$0.06/GGE.

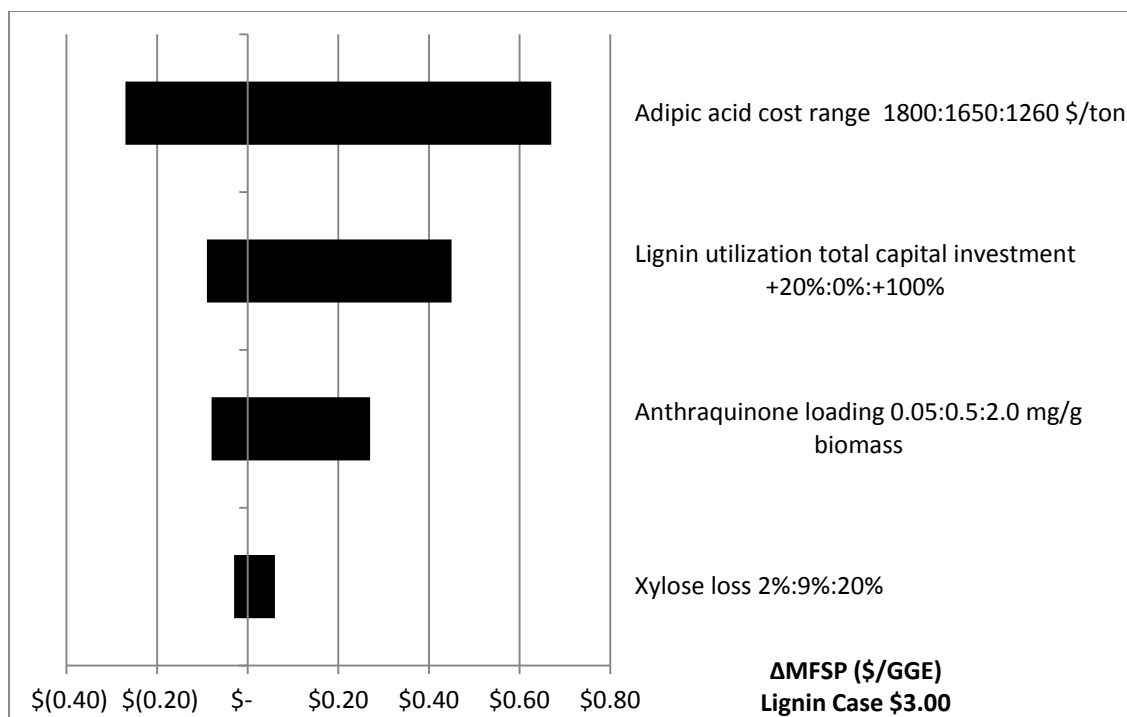


Figure 27. Cost sensitivity analysis for a range of uncertainties in the preliminary TEA estimate for lignin deconstruction and conversion to adipic acid; base case = \$3/GGE RDB

Further opportunities exist for cost reductions when investigating the integrated design of a biorefinery that co-utilizes carbohydrates and lignin. For example, similar to deacetylation, it is expected that the alkaline pretreatment will help break down the biomass structure and has the potential to further reduce the required severity of the dilute acid pretreatment process and overall process costs. Additionally, it is well established that lignin removal will aid in the digestibility of polysaccharides, and thus it is likely that reductions in enzyme loadings could be realized through significant up-front lignin removal in conjunction with engineering of new cellulase cocktails. Alternative lignin deconstruction routes are under investigation and could also lead to improvements to the overall cost of lignin conversion. Additionally, in this feasibility-level analysis we focus only on conversion of lignin in the alkaline pretreatment liquor stream; however, additional carbon utilization could be gained through conversion or recovery of acetate and “lost” carbohydrate species that are also fractionated into this stream.

6.3 Lignin Utilization: Sustainability Analysis

To understand the sustainability drivers associated with lignin conversion to commodity products, GHG emissions associated with the processes described above for lignin deconstruction and conversion to coproducts are quantified using SimaPro as described in Section 5.2. As with exported electricity, lignin-derived co-products (adipic acid, 1,3 butadiene, 1,4 butanediol, and cyclohexane) are treated as avoided products using the product displacement method [110], e.g. co-products are assumed to displace the equivalent existing material produced by conventional methods (largely derived from petroleum), thus avoiding a degree of GHG emissions as well as fossil energy consumption. The displacement credits for the lignin-derived co-products are summarized in Table 44.

Table 44. GHG Emissions and Fossil Energy Consumption for Traditional Production of Petroleum Based Co-products as Well as Average U.S. Grid Electricity, as Modeled in SimaPro and Defined by Ecoinvent

	GHG emissions	Fossil energy	Displacement ratio
Adipic acid	26.2 kg CO ₂ -eq./kg	134.6 MJ/kg	1 kg of adipic acid from biorefinery displaces 1 kg of the same from petroleum
1,3-Butadiene	1.16 kg CO ₂ -eq./kg	65.04 MJ/kg	1 kg of 1,3-Butadiene from biorefinery displaces 1 kg of the same from petroleum
1,4-Butanediol	5.05 kg CO ₂ -eq./kg	92.92 MJ/kg	1 kg of 1,4-Butanediol from biorefinery displaces 1 kg of the same from petroleum
Cyclohexane	2.40 kg CO ₂ -eq./kg	74.35 MJ/kg	1 kg of cyclohexane from biorefinery displaces 1 kg of the same from petroleum
Average U.S. electricity mix*	0.78 kg CO ₂ -eq./kWh	9.1 MJ/kWh	1 kWh of electricity from biorefinery displaces 1 kWh of US average grid electricity

* U.S. grid mix: Coal (47%), natural gas (17%), Oil (3.3%), nuclear power (20%), biomass (1.1%), wind (0.35%), solar (0.015%), hydroelectric (8.2%), and others (2.5%).

Figure 28 shows the GHG emissions profile as a function of lignin conversion associated with the specific lignin coproduct pathways evaluated for economic potential above. These processes utilize a lignin deconstruction step followed by a lignin conversion step and in turn require additional input of resources, including anthraquinone, hydrogen, and eventual import of electricity (upon becoming power limited), the latter of which comes into consideration as more lignin is diverted away from the boiler and toward the given coproduct. The GHG emissions associated with the production of these inputs are accounted for. Additionally, the co-products displace an equivalent amount of the same products derived from petroleum, and the resulting GHG emissions associated with the displacement are credited. Thus, the net GHG emissions are shown to increase for some products and decrease for others as a result of the interplay between electricity (imported/exported) and hydrogen consumption, as well as the magnitude of the individual lignin-derived co-product GHG credits (see Figure 29).

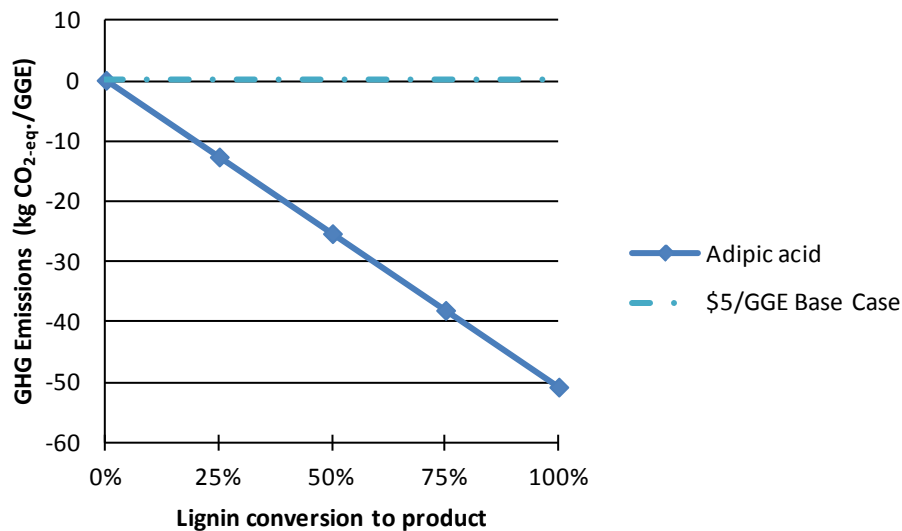
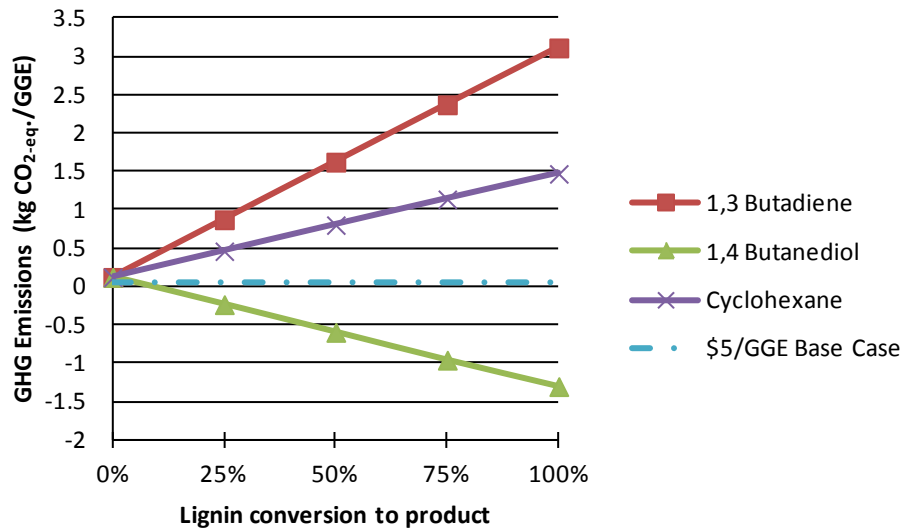


Figure 28. Comparison of GHG Emissions versus percent lignin conversion to co-products. The dashed line represents the GHG emissions for the \$5/GGE base case (0.07 kg CO₂-eq./GGE) which assumes combustion of lignin and conversion to power coproduct. The 0% lignin conversion represents the case with lignin deconstruction but without any conversion to chemical coproducts.

Figure 28 shows that the GHG emissions for the \$5/GGE base case (without utilizing lignin conversion to commodity products) is 0.07 kg CO₂-eq./GGE. When the lignin deconstruction step is included but not subsequent conversion to chemical coproducts (i.e., 0% lignin conversion point), the GHG emissions is found to be comparable to the \$5/GGE baseline, as the increased GHG emissions associated with the addition of anthraquinone and the increase of caustic during lignin deconstruction is offset by increased power generation due to more carbon and less water reaching the boiler (demonstrated in Figure 29).

Increasing the yields of adipic acid and 1,4 butanediol both translate to a decrease in GHG emissions. While more resources are required to achieve higher lignin co-product yields (simultaneously reducing electricity co-product credit), the high chemical co-product displacement credits outweigh the additional GHG emissions associated with the underlying processes, including hydrogen and electricity import. In other words, the conventional production techniques for adipic acid and 1,4 butanediol are more carbon-intensive and offer greater coproduct offset credits than the equivalent amount of standard U.S. grid electricity displaced when converting the same amount of lignin to either the chemical product or electricity.

Adipic acid is considerably more GHG-intensive to produce by conventional methods than all other products considered here, and thus exhibits the highest co-product displacement credit, 26.2 kg CO_{2-eq}/kg. Consequently, the GHG emissions at the conversion stage for the adipic acid pathway are significantly below the GHG profile of the \$5/GGE base case. Similarly, the GHG emissions for the conversion of lignin to 1,4 butanediol also show the potential to be lower than the \$5/GGE base case, and continue on this trend as additional lignin is converted to coproduct. Conversely, because of the relatively low co-product displacement credits, both 1,3 butadiene and cyclohexane exhibit GHG emissions increasingly higher than the \$5/GGE case as additional lignin is diverted to either product, and thus do not offer the same GHG benefits over lignin combustion.

Figure 29 reveals in further detail the tradeoffs between the minimization and eventual loss of excess power co-production as more lignin is diverted away from the boiler towards alternate co-products (resulting in the import of electricity), and the GHG profile of the specific co-product which is being displaced. It is noted here that given the very large GHG offset associated with the adipic acid pathway (more-so than all other products evaluated), to maintain a reasonable scale for the plot, the adipic acid coproduct GHG credits are multiplied by a factor of 0.1; thus, a reading on the y-axis of “-2” kg CO_{2-eq}/GGE is actually -20 for this specific coproduct.

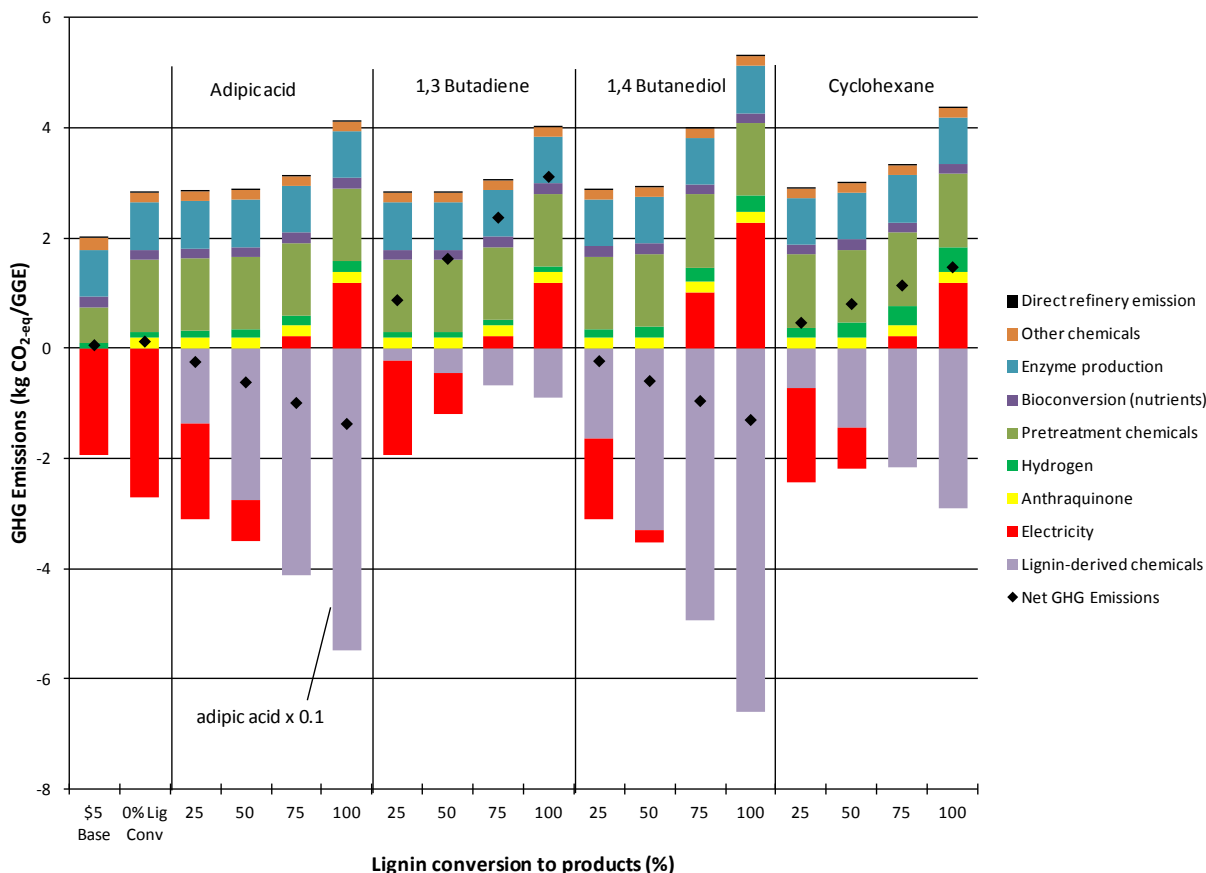


Figure 29. GHG emissions contributions versus percent lignin conversion to coproducts. The \$5/GGE case is the base case with excess electricity credit and without lignin deconstruction or conversion. The 0% case adds lignin deconstruction but no lignin conversion. Note: For the adipic cases, the co-product credits are multiplied by a factor of 0.1 to maintain a reasonable scale in the plot alongside the other products.

While the estimates discussed here for TEA and sustainability analyses are preliminary in nature and certainly do not consider an exhaustive list of all potential coproducts which may be produced from lignin (and should not be taken as such), the primary point to emphasize here is that credible, realistic pathways exist to further decrease economics from the \$5/GGE base case to a final \$3/GGE target by way of increasing overall biomass carbon efficiency via utilization of biomass components that are not amenable to traditional carbohydrate-based bioconversion. A number of important tradeoffs exist between economics and sustainability for specific lignin conversion coproduct options, and it will be critical to be mindful of such tradeoffs as further data become available for these coproduct pathways. The market sustainability (e.g., market volume) of such products will also play a key role in the practicality of a given coproduct pathway; we have performed an early high-level analysis for market volume of the given subset of coproducts evaluated here to ensure that sufficient market volumes exist to warrant their consideration, but will continue to evaluate this important issue moving forward.

7 Concluding Remarks

7.1 Summary

The present report establishes a plausible case for achieving an intermediate 2017 cost goal of \$5/GGE of upgraded renewable diesel blendstock via biological production, based on a single set of process R&D metrics and associated cost estimates. Namely, the pathway discussed here assumes continued improvements are made in the biomass deconstruction areas, including deacetylation, dilute-acid pretreatment, and enzymatic hydrolysis, beyond performance demonstrated during NREL's 2012 State of Technology trials. This includes demonstrating high removal of acetate and other non-fermentable components at low loss of fermentable components under reasonable conditions during deacetylation, high xylose and arabinose yields under mild acid loading and other process conditions during pretreatment, and high glucose yields at low enzyme loadings during hydrolysis. These front-end unit operations leverage NREL expertise and prior work in these areas, and will continue to be important areas of future research for continued improvement.

In addition to biomass deconstruction to sugars, the design also sets targets for sugar upgrading to fuels, primarily sugar conversion (95% glucose, 85% xylose, and 85% arabinose) and FFA volumetric productivity (1.3 g/L/h). While these targets for bioconversion are consistent with NREL's 2011 ethanol design report targets, many of which were demonstrated at NREL in 2012 for ethanol, current literature suggests that today's state of technology is notably lower for these parameters in the context of biological hydrocarbon production, and thus still represents a reasonable set of targets to maintain for this new pathway by 2017. Even so, achieving this set of targets is anticipated to support an intermediate DOE cost goal of \$5/GGE, but additional improvements elsewhere will be required to achieve the ultimate goal of \$3/GGE. These include further integration and optimization to reduce process costs (e.g. direct microbial conversion or other options to reduce the number of processing steps) as well as increasing carbon yield likely beyond that achievable with the fermentable fraction of biomass alone (e.g. pursuing opportunities for value-added coproducts from lignin and acetate).

The end result of the techno-economic analysis was a predicted minimum fuel selling price (MFSP) of \$5.10/GGE (2011\$) at a final upgraded product yield of 45.4 GGE/dry ton of biomass. This reflects a \$1.76/GGE contribution from feedstock, a \$0.37/GGE contribution from enzymes, and a \$2.96/GGE contribution from the remainder of the conversion process. This modeled selling price is strictly representative of *n*th-plant assumptions regarding biorefinery design, operation, and financing, and is not intended to reflect first-of-a-kind or early-entry commercial facilities. While the yield presented here is notably lower than that presented in prior design reports for ethanol (even after adjusting for energy content), the technology pathway described in this report carries a distinct advantage of producing a molecule or mixture of components which may be directly utilized by the existing fuel infrastructure and blended into existing fuel markets (namely diesel in this case), likely with select desirable fuel properties such as cetane value.

Beyond the detailed modeling and analysis conducted to establish the \$5/GGE pathway, this report also describes viable improvements to ultimately achieve the \$3/GGE target by 2022. While the analysis for the latter case is not detailed, due to insufficient data available given the early status of work at NREL on lignin co-product utilization, a higher level analysis does indeed

suggest that lignin deconstruction and conversion to a small subset of many possible coproducts exhibits the potential to ultimately achieve the \$3/GGE target, while remaining within realistic limits for total carbon conversion efficiency.

In addition to providing an economic analysis, the present report also considers sustainability metrics for the baseline \$5/GGE and alternative \$3/GGE target scenarios, by tracking and reporting on greenhouse gas emissions, fossil energy demand, and direct consumptive water use at the modeled biorefinery facility. The sustainability analysis for the baseline scenario indicates a GHG profile of 0.07 kg CO_{2-eq}/GGE, fossil energy consumption of 10.8 MJ/GGE, and water demand of 13.7 gal/GGE. The GHG emissions profile shows the potential to either increase or decrease in the alternative \$3/GGE scenarios relative to the baseline \$5/GGE case, which is a function primarily of the tradeoff between the minimization and eventual loss of excess power co-production as more lignin is diverted away from the boiler towards alternate coproducts, and the GHG profile of the specific coproduct which is being displaced. Given these important results in both cost and sustainability implications for co-production of value-added products from lignin (or other potential carbon sources), NREL will continue to evaluate this scenario as further experimental data become available.

It is worthwhile to reiterate that cellulosic ethanol production via fermentative pathways is supported by decades of research and process understanding, both at NREL and elsewhere, thus carrying a level of certainty and credibility when making target projections for biochemical ethanol TEA modeling, as in the case of the 2011 and even 2002 ethanol design reports. In contrast, biological hydrocarbon production is a much newer and more novel approach to biological conversion of sugars, with doors that have only recently been opened to a number of product pathways given recent advances in metabolic engineering, which continues to be a rapidly evolving field in this context. Thus, the absolute cost values established here, as well as the timeframe required to achieve these outcomes, inherently carries a somewhat higher degree of uncertainty given the nascent stage of research as presented in the public domain.

7.2 Future Work

Moving forward, to ultimately achieve cost goals as well as reduce uncertainty in key areas for the biological conversion pathway, a number of important bottlenecks, uncertainties, and areas for further development are summarized below. These points are repeated from NREL's recent technical memo for biological hydrocarbon production [32]:

- **Investigate synergistic opportunities for sugar/intermediate production and process integration:** Tailoring the hydrolysate stream to the microorganism tolerance will be essential to improving yield and lowering production cost, and there continue to be further opportunities for synergistic improvement in combining unit operations or otherwise simplifying the fully integrated process.
- **Develop separation and conditioning requirements for hydrolysate:** A better understanding is needed of the tolerance of hydrocarbon-producing microbes to soluble lignin and other cellulosic sugar substrate impurities, including organic acids, salts, and other potential inhibitors. Improving this understanding would allow for a better optimized bioconversion process.
- **Optimize design and scale for aerobic fuel production:** While Harris Group has provided NREL with preliminary insight into process and design tradeoffs for submerged

aeration systems, including plausible vessel sizes, oxygen transfer rates, and agitation demands, more room for improvement exists to identify the most cost-effective engineering design for commercial-scale aerobic bioconversion operations.

- **Maximize sugar (and/or carbon) utilization and microbe metabolic performance:** There is currently a dearth of literature and high-quality data in the public domain on sugar uptake/conversion and microbial productivity, particularly with respect to production using cellulosic feedstock-derived substrates containing pentose sugars. Better understanding is needed regarding the productivity of the fuel production microorganism and the potential of genetic engineering to significantly increase metabolic production rates and yields, minimize side-product formation, mitigate substrate and/or product toxicity effects, and otherwise develop robust microbes [50].
- **Define product separation and final polishing/upgrading requirements:** Given the early status of the pathway model described here, further insight is needed as to the ease or difficulty in recovering products secreted directly into the aqueous broth, given potential challenges with retention of product on cell mass, the potential for emulsions, and phase separation. Furthermore, a more detailed quantification of the product components and impurities is required to better quantify upgrading requirements and associated costs to refine the intermediate product(s) into final fuel blendstocks.
- **Evaluate co-product opportunities:** To ultimately achieve cost targets, particularly a level of \$3/GGE to compete with petroleum fuels, co-products from lignin, acetate, or other non-fermentable components will become an increasingly important focus in the biological conversion pathway. These co-product opportunities must be carefully evaluated beyond strictly an economic context, including considerations for sustainability metrics as well as co-product market volumes and saturation potential.

Beyond the new focus on hydrocarbon fuel production by *biological conversion*, NREL is next planning to expand the analysis work to also consider an alternative route to hydrocarbons via *catalytic conversion* of sugars and other hydrolysate intermediates. This technology pathway brings a new set of advantages and challenges, as documented in [156]. NREL will work with DOE and other partners to define logistics for establishing the model and associated targets for the catalytic conversion pathway during FY 2014.

References

NREL milestone reports cited below cannot be accessed outside of NREL and DOE. Readers may contact the authors of the specific reference to determine if this information has been made public since publication of this design report.

1. Wooley, R.J., et al., *Lignocellulosic Biomass to Ethanol Process Design and Economics Utilizing Co-Current Dilute Acid Prehydrolysis and Enzymatic Hydrolysis Current and Futuristic Scenarios*, 1999.
2. Aden, A., et al., *Lignocellulosic Biomass to Ethanol Process Design and Economics Utilizing Co-Current Dilute Acid Prehydrolysis and Enzymatic Hydrolysis for Corn Stover*, in *Other Information: PBD: 1 Jun 2002*2002. p. Medium: ED; Size: 154 pages Available from: <http://www.nrel.gov/docs/fy02osti/32438.pdf>.
3. Humbird, D., et al., *Process Design and Economics for Biochemical Conversion of Lignocellulosic Biomass to Ethanol: Dilute-Acid Pretreatment and Enzymatic Hydrolysis of Corn Stover*, 2011 Available from: <http://www.nrel.gov/docs/fy11osti/47764.pdf>.
4. MYPP, *Biomass Program Multi-Year Program Plan - November 2011*, U.S.D.o. Energy, Editor 2011, Bioenergy Technologies Office Available from: http://www1.eere.energy.gov/biomass/pdfs/mypp_november_2011.pdf.
5. Schell, D., *Biochemical Processing Integration*, in *2013 DOE Bioenergy Technologies Office (BETO) Project Peer Review*2013: Alexandria, VA Available from: https://www2.eere.energy.gov/biomass/peer_review2013/Portal/Biochemical/#.
6. Davis, R., *Biochemical Platform Analysis*, in *2013 DOE Bioenergy Technologies Office (BETO) Project Peer Review*2013: Alexandria, VA Available from: https://www2.eere.energy.gov/biomass/peer_review2013/Portal/Biochemical/#.
7. Humbird, D. and A. Aden, *Biochemical Production of Ethanol from Corn Stover: 2008 State of Technology Model*, 2008 Available from: <http://www.nrel.gov/biomass/pdfs/46214.pdf>.
8. Humbird, D., et al., *Economic Impact of Total Solids Loading on Enzymatic Hydrolysis of Dilute Acid Pretreated Corn Stover*. *Biotechnology Progress*, 2010. **26**(5): p. 1245-1251.
9. Humbird, D., *FY 2011 Biochemical Platform State of Technology Update*. 2011.
10. MYPP, *Biomass Multi-year Program Plan - May 2013*, U.S.D.o. Energy, Editor 2013, Bioenergy Technologies Office Available from: http://www1.eere.energy.gov/biomass/pdfs/mypp_may_2013.pdf.
11. ASPEN, *Release 7.2*, in *AspenPlus*2007, Aspen Technology Inc.: Cambridge MA Available from: www.aspentech.com.
12. Wooley, R.J., V. Putsche, and K. Ibsen, *Development of an ASPEN PLUS Physical Property Database for Biofuels Components*, 1999. p. 18.
13. Wooley, R.J. and V. Putsche, *Development of an ASPEN PLUS Physical Property Database for Biofuels Components*, in *NREL Technical Memo*1996, National Renewable Energy Laboratory: Golden, CO Available from: <http://biodev.nrel.gov/pdfs/3955.pdf>.
14. Muth, D., et al., *Feedstock Pathway for Cellulosic Sugar Conversion Pathway*, 2008, Idaho National Laboratory: Idaho Falls, ID.
15. Chen, S.F., et al., *Compositional analysis of water-soluble materials in corn stover*. *Journal of Agricultural and Food Chemistry*, 2007. **55**(15): p. 5912-5918.
16. Bower, S., et al., *Modeling sucrose hydrolysis in dilute sulfuric acid solutions at pretreatment conditions for lignocellulosic biomass*. *Bioresource Technology*, 2008. **99**(15): p. 7354-7362.

17. MYPP, *Biomass Multi-year Program Plan - November 2012*, U.S.D.o. Energy, Editor 2012, Bioenergy Technologies Office Available from:
http://www1.eere.energy.gov/biomass/pdfs/mypp_november_2012.pdf.
18. DDBST GmbH, *Density of Hexadecane*, Last visited 2013 Available from:
http://www.ddbst.com/en/EED/PCP/DEN_C516.php.
19. Chemical Book, *N-PENTADECANE*, 2010 Available from:
http://www.chemicalbook.com/ChemicalProductProperty_EN_CB4217947.htm.
20. NIST. *Hexadecane*. Material Measurement Laboratory [cited 2013 June 24, 2013]; Available from: <http://webbook.nist.gov/cgi/cbook.cgi?Name=hexadecane&Units=SI>.
21. NIST. *Pentadecane*. Material Measurement Laboratory [cited 2013 June 24, 2013]; Available from: <http://webbook.nist.gov/cgi/cbook.cgi?Name=pentadecane&Units=SI>.
22. U.S. DOE Hydrogen Analysis Resource Center. *Lower and higher heating values of hydrogen and fuels*. 2012; Available from:
http://hydrogen.pnl.gov/cocoon/morf/hydrogen/site_specific/fuel_heating_calculator.
23. Hess, J.R., *Uniform Format Design and Depot Preprocessing*, in *PNWER 2010 Annual Summit 2010*, Idaho National Laboratory: Calgary, Alberta Available from:
<http://www.pnwerarchive.org/LinkClick.aspx?fileticket=wAARiq9I5sl%3D&tabid=1892&mid=3531>.
24. Hess, J.R., et al., *Uniform-Format Solid Feedstock Supply System: A Commodity-Scale Design to Produce an Infrastructure-Compatible Bulk Solid from Lignocellulosic Biomass*, 2008, Idaho National Laboratory: Idaho Falls, ID Available from: www.inl.gov/bioenergy/uniform-feedstock.
25. Galbe, M. and G. Zacchi, *Pretreatment of lignocellulosic materials for efficient bioethanol production*, in *Biofuels*, L. Olsson, Editor. 2007. p. 41-65.
26. Shill, K., et al., *Ionic Liquid Pretreatment of Cellulosic Biomass: Enzymatic Hydrolysis and Ionic Liquid Recycle*. *Biotechnology and Bioengineering*, 2011. **108**(3): p. 511-520.
27. Tao, L., et al., *Improved ethanol yield and reduced MESP by modifying low severity dilute acid pretreatment with deacetylation and mechanical refining: 2) Techno-economic Analysis*. *Biotechnology for Biofuels*, 2012. **5**(69).
28. Chen, X., et al., *Improved ethanol yield and reduced Minimum Ethanol Selling Price (MESP) by modifying low severity dilute acid pretreatment with deacetylation and mechanical refining: 1) Experimental*. *Biotechnology for Biofuels*, 2012. **5**(1): p. 60.
29. Tao, L., et al., *FY 2012 Biochemical State of Technology Report 2012* Available from:
<https://biodev.nrel.gov/bcfcdoc/11106.pdf>.
30. NABC. *National Advanced Biofuels Consortium News Release: Amyris Successfully Makes Biofene from Cellulosic Hydrolysate*. 2012; Available from:
http://www.nabcprojects.org/pdfs/amyris_makes_biofene_from_cellulosic_hydrolysate.pdf.
31. Perry, R.H. and D.W. Green, *Perry's Chemical Engineers' Handbook* 7th Edition ed. 1997: McGraw-Hill.
32. Davis, R., et al., *Biological Conversion of Sugars to Hydrocarbons Technology Pathway*, 2013 Available from: <http://www.nrel.gov/docs/fy13osti/58054.pdf>.
33. Huffer, S., et al., *Escherichia coli for biofuel production: bridging the gap from promise to practice*. *Trends in Biotechnology*, 2012. **30**(10): p. 538-545.
34. Siever, D., L. Tao, and D. Schell, *Performance and Technoeconomic Assessment of Several Solid-Liquid Separation Technologies for Processing Dilute-Acid Pretreated Corn Stover*. To be submitted to *Bioresource Technology*, 2013.
35. Renninger, N.S. and D.J. McPhee, *Fuel Compositions Comprising Farnesane and Farnesane Derivatives and Method of Making and Using Same*, 2008.
36. Pandey, A., et al., *Biofuels - Alternative Feedstocks and Conversion Processes*. 2011: Elsevier.

37. Nag, A., *Biofuels Refining and Performance*. 2008: McGraw-Hill.
38. Fagerson, I.S., *Thermal degradation of carbohydrates; a review*. Journal of Agricultural and Food Chemistry 1969. **17**(4): p. 747-750.
39. Loos, H., et al., *Sorbitol Promotes Growth of Zymomonas-Mobilis in Environments with High-Concentrations of Sugar - Evidence for a Physiological-Function of Glucose-Fructose Oxidoreductase in Osmoprotection*. Journal of Bacteriology, 1994. **176**(24): p. 7688-7693.
40. Dowe, N., D. Humbird, and D. Schell, *Joule Milestone: Status Report on Overall Corn Stover to Ethanol Yield Improvement Effort*, 2009, National Renewable Energy Laboratory: Golden, CO Available from: <http://biodev.nrel.gov/bcfcdoc/10457.pdf>.
41. Huang, W.D. and Y.H.P. Zhang, *Analysis of biofuels production from sugar based on three criteria: Thermodynamics, bioenergetics, and product separation*. Energy & Environmental Science, 2011. **4**(3): p. 784-792.
42. Zhang, M., *Metabolic Engineering of Zymomonas mobilis for Hydrocarbon Fuels Production*. Presented at the 2012 SIMB Annual Meeting, 2012.
43. Ladygina, N., E.G. Dedyukhina, and M.B. Vainshtein, *A review on microbial synthesis of hydrocarbons*. Process Biochemistry, 2006. **41**(5): p. 1001-1014.
44. Garcia-Ochoa, F. and E. Gomez, *Bioreactor scale-up and oxygen transfer rate in microbial processes: An overview*. Biotechnology Advances, 2009. **27**(2): p. 153-176.
45. Solazyme. *Solazyme Successfully Scales Renewable Oil Fermentation to 500,000 Liters at ADM Clinton, Iowa Facility*. 2013 July 2013]; Available from: <http://solazyme.com/media/2012-12-13>.
46. Yang, S.-T., *Bioprocessing for Value-Added Products from Renewable Resources - New Technologies and Applications*. 2007: Elsevier.
47. Lidén, G., *Understanding the Bioreactor*. Bioprocess and Biosystems Engineering, 2002. **24**(5): p. 273-279.
48. Kollaras, A., et al., *Multiple Coproducts Needed to Establish Cellulosic Ethanol Industry*, in Ethanol Producer Magazine 2012.
49. Benz, G.T., *Bioreactor Design for Chemical Engineers*. Chemical Engineering Progress, 2011. **107**(8): p. 21-26.
50. Department of Energy, *Conversion Technologies for Advanced Biofuels*, 2012, Department of Energy, Office of the Biomass Program in the Office of Energy Efficiency and Renewable Energy, Conversion Technologies for Advanced Biofuels Workshop.
51. Liu, T.G. and C. Khosla, *Genetic Engineering of Escherichia coli for Biofuel Production*. Annual Review of Genetics, Vol 44, 2010. **44**: p. 53-69.
52. Rude, M.A. and A. Schirmer, *New microbial fuels: a biotech perspective*. Current Opinion in Microbiology, 2009. **12**(3): p. 274-281.
53. Dugar, D. and G. Stephanopoulos, *Relative potential of biosynthetic pathways for biofuels and bio-based products*. Nature Biotechnology, 2011. **29**(12): p. 1074-1078.
54. Magnuson, K., et al., *Regulation of Fatty-Acid Biosynthesis in Escherichia-Coli*. Microbiological Reviews, 1993. **57**(3): p. 522-542.
55. White, S.W., et al., *The structural biology of type II fatty acid biosynthesis*. Annual Review of Biochemistry, 2005. **74**: p. 791-831.
56. Fujita, Y., H. Matsuoka, and K. Hirooka, *Regulation of fatty acid metabolism in bacteria*. Molecular Microbiology, 2007. **66**(4): p. 829-839.
57. Westfall, P.J. and T.S. Gardner, *Industrial fermentation of renewable diesel fuels*. Current Opinion in Biotechnology, 2011. **22**(3): p. 344-350.
58. Zhou, H., et al., *Xylose isomerase overexpression along with engineering of the pentose phosphate pathway and evolutionary engineering enable rapid xylose utilization and ethanol production by Saccharomyces cerevisiae*. Metabolic Engineering, 2012. **14**(6): p. 611-622.

59. Zhang, F.Z., S. Rodriguez, and J.D. Keasling, *Metabolic engineering of microbial pathways for advanced biofuels production*. Current Opinion in Biotechnology, 2011. **22**(6): p. 775-783.
60. Hawkins, R.L., *Utilization of xylose for growth by the eukaryotic alga, Chlorella*. Current Microbiology, 1999. **38**(6): p. 360-363.
61. Dellomonaco, C., et al., *Engineered reversal of the beta-oxidation cycle for the synthesis of fuels and chemicals*. Nature, 2011. **476**(7360): p. 355-359.
62. Peralta-Yahya, P.P., et al., *Identification and microbial production of a terpene-based advanced biofuel*. Nat Commun, 2011. **2**: p. 483.
63. Steen, E.J., et al., *Microbial production of fatty-acid-derived fuels and chemicals from plant biomass*. Nature, 2010. **463**(7280): p. 559-U182.
64. Liu, T., H. Vora, and C. Khosla, *Quantitative analysis and engineering of fatty acid biosynthesis in E. coli*. Metabolic Engineering, 2010. **12**(4): p. 378-386.
65. Lu, X., H. Vora, and C. Khosla, *Overproduction of free fatty acids in E. coli: Implications for biodiesel production*. Metabolic Engineering, 2008. **10**(6): p. 333-339.
66. MYPP, *Biomass Multi-year Program Plan*, 2013 Available from: http://www1.eere.energy.gov/biomass/pdfs/mypp_may_2013.pdf.
67. Kosa, M. and A.J. Ragauskas, *Lipids from heterotrophic microbes: advances in metabolism research*. Trends in Biotechnology, 2011. **29**(2): p. 53-61.
68. Zhao, X., et al., *Medium optimization for lipid production through co-fermentation of glucose and xylose by the oleaginous yeast Lipomyces starkeyi*. European Journal of Lipid Science and Technology, 2008. **110**(5): p. 405-412.
69. Ageitos, J., et al., *Oily yeasts as oleaginous cell factories*. Applied Microbiology and Biotechnology, 2011. **90**(4): p. 1219-1227.
70. Althoff, K., *Commercializing Cellulosic Ethanol Technology*, 2010, Dupont Danisco Available from: <http://www.epoverviews.com/oca/althoff.pdf>.
71. Lennen, R.M. and B.F. Pfeleger, *Engineering Escherichia coli to synthesize free fatty acids*. Trends in Biotechnology, 2012. **30**(12): p. 659-667.
72. Voelker, T.A. and H.M. Davies, *Alteration of the Specificity and Regulation of Fatty-Acid Synthesis of Escherichia Coli by Expression of a Plant Medium-Chain Acyl-Acyl Carrier Protein Thioesterase*. Journal of Bacteriology, 1994. **176**(23): p. 7320-7327.
73. Davis, M.S., J. Solbiati, and J.E. Cronan, *Overproduction of acetyl-CoA carboxylase activity increases the rate of fatty acid biosynthesis in Escherichia coli*. Journal of Biological Chemistry, 2000. **275**(37): p. 28593-28598.
74. Cho, H.S. and J.E. Cronan, *Defective Export of a Periplasmic Enzyme Disrupts Regulation of Fatty-Acid Synthesis*. Journal of Biological Chemistry, 1995. **270**(9): p. 4216-4219.
75. Jiang, P. and J.E. Cronan, *Inhibition of Fatty-Acid Synthesis in Escherichia-Coli in the Absence of Phospholipid-Synthesis and Release of Inhibition by Thioesterase Action*. Journal of Bacteriology, 1994. **176**(10): p. 2814-2821.
76. Zhang, F.Z., J.M. Carothers, and J.D. Keasling, *Design of a dynamic sensor-regulator system for production of chemicals and fuels derived from fatty acids*. Nature Biotechnology, 2012. **30**(4): p. 354-U166.
77. *Ethanol Co-Products*. 2007 [cited 2013 June 1, 2013]; Available from: <http://ethanol-information.com/ethanol-coproducts.php>.
78. Meerman, H.J., A.S. Kelley, and M. Ward, *Advances in Protein Expression in Filamentous Fungi, in Protein Expression Technologies: Current Status and Future Trends.* , F. Baneyx, Editor. 2004, Horizon Bioscience: Norfolk, UK. p. 345.
79. Warzywoda, M., 1984.
80. Emme, B., *Personal communication*, D. Humbird, Editor 2009, Novozymes, Inc.

81. Wiseman, A., *Biochemical-Engineering and Biotechnology Handbook* - Atkinson, B, Mavituna, F. Chemistry in Britain, 1983. **19**(5): p. 423-424.
82. Schell, D., et al., *Technical and Economic Analysis of an Enzymatic Hydrolysis Based Ethanol Plant* 1991, Solar Energy Research Institute: Golden CO Available from: <http://biodev.nrel.gov/bcfcdoc/3892.pdf>.
83. Cuellar, M.C., J.J. Heijnen, and L.A. van der Wielen, *Large-scale production of diesel-like biofuels - process design as an inherent part of microorganism development*. *Biotechnol J*, 2013. **8**(6): p. 682-9.
84. Bart, J.C.J., N. Palmeri, and S. Cavallaro, *Biodiesel Science and Technology - From Soil to Oil*. 2010: Woodhead Publishing.
85. Altman, P.L. and D.S. Dittmer, *Biology Data Book*. Vol. 1-3. 1972-1974: Federation of American Societies for Experimental Biology.
86. Davis, R., A. Aden, and P.T. Pienkos, *Techno-economic analysis of autotrophic microalgae for fuel production*. *Applied Energy*, 2011. **88**(10): p. 3524-3531.
87. Marker, T.L., et al., *Opportunities for Biorenewables in Oil Refineries*, U.S.D.o. Energy, Editor 2005, UOP LLC Available from: <http://www.osti.gov/bridge/servlets/purl/861458-Wv5uum/861458.pdf>.
88. Dirks, G., J. McGowen, and P.T. Pienkos, *Sustainable Algal Biofuels Consortium*, in *2013 DOE Bioenergy Technologies Office (BETO) Project Peer Review* 2013: Alexandria, VA Available from: https://www2.eere.energy.gov/biomass/peer_review2013/Portal/Algae/#.
89. Davis, R., et al., *Renewable Diesel from Algal Lipids: An Integrated Baseline for Cost, Emissions, and Resource Potential from a Harmonized Model*, 2012 Available from: <http://www.nrel.gov/docs/fy12osti/55431.pdf>.
90. Dutta, A., et al., *Process Design and Economics for Conversion of Lignocellulosic Biomass to Ethanol, Thermochemical Pathway by Indirect Gasification and Mixed Alcohol Synthesis*, 2011, National Renewable Energy Laboratory.
91. *Chemical Engineering Magazine*, 2011, Chemical Engineering Magazine Plant Cost Index Available from: <http://www.che.com/pci/>.
92. SRI Consulting, *U.S. Producer Price Indexes – Chemicals and Allied Products/Industrial Inorganic Chemicals Index*. Chemical Economics Handbook, 2008 (Menlo Park, CA).
93. Bureau of Labor Statistics Data website, *National Employment, Hours, and Earnings Catalog, Industry: Chemicals and Allied Products, 1980-2009.*, 2009 Available from: <http://data.bls.gov/cgi-bin/srgate>.
94. U. S. EIA. *Electricity Retail Price to Consumers*. 2013 July 2013]; Available from: <http://www.eia.gov/electricity/data.cfm#sales>.
95. U. S. EIA, *Electricity Wholesale Market Data*, 2013 Available from: <http://www.eia.gov/electricity/wholesale/index.cfm>.
96. Dillich, S., T. Ramsden, and M. Melina, *DOE Hydrogen and Fuel Cells Program Record*, U.S.D.o. Energy, Editor 2012 Available from: http://www.hydrogen.energy.gov/pdfs/12024_h2_production_cost_natural_gas.pdf.
97. Administration, U.S.E.I., *U.S. Natural Gas Prices*, 2013 Available from: http://www.eia.gov/dnav/ng/ng_pri_sum_dc_u_nus_a.htm.
98. *Table 7—U.S. wholesale list price for glucose syrup, Midwest markets, monthly, quarterly, and by calendar and fiscal year*, in *USDA ERS - Sugar and Sweeteners Yearbook Tables*, USDA, Editor 2013 Available from: http://www.ers.usda.gov/datafiles/Sugar_and_Sweeteners_Yearbook_Tables/World_and_US_Sugar_and_Corn_Sweetener_Prices/TABLE07.XLS.

99. Brown Caldwell, *Process Design of Wastewater Treatment for the NREL Cellulosic Ethanol Model*, 2011, Brown and Caldwell for Harris Group Inc.
100. Brown Caldwell, *Process Design of Wastewater Treatment for the NREL Cellulosic Ethanol Model*, 2012.
101. Peters, M.S., et al., *Plant design and economics for chemical engineers*. 2003: McGraw-Hill New York.
102. Short, W., D.J. Packey, and T. Holt, *A Manual for the Economic Evaluation and Energy Efficiency and Renewable Energy Technologies*, 1995, National Renewable Energy Laboratory: Golden, CO.
103. Service, I.R., *How to Depreciate Property*, D.o.t. Treasury, Editor 2009: Washington, D.C. Available from: <http://www.irs.gov/pub/irs-pdf/p946.pdf>.
104. Gary, J.H. and G.E. Handwerk, *Petroleum refining : technology and economics*. 3rd ed. 1994, New York: M. Dekker. xii, 465 p.
105. Cran, J., *Improved factored method gives better preliminary cost estimates*. *Chemical Engineer*, 1981. **88**(7): p. 65-79.
106. SimaPro, *SimaPro, v.7.3; Product Ecology Consultants: Amersfoort, the Netherlands, 2011.*, 2011.
107. Hsu, D., Heath, G., Wolfrum, E., Mann, M.K., and Aden, A., *Life Cycle Environmental Impacts of Selected U.S. Ethanol Production and Use Pathways in 2022*. *Environ. Sci. Technol*, 2010: p. 5289–5297.
108. Ecoinvent, *Ecoinvent, v.2.2; Swiss Center for Life Cycle Inventories: Duebendorf, Switzerland, 2010.*, 2010.
109. LCI, *U.S. Life-Cycle Inventory, v. 1.6.0; National Renewable Energy Laboratory: Golden, CO, 2008.*, 2008.
110. Wang, M., H. Huo, and S. Arora, *Methods of dealing with co-products of biofuels in life-cycle analysis and consequent results within the US context*. *Energy Policy*, 2011. **39**(10): p. 5726-5736.
111. Biorecro, A.B., *Global Status of BECCS Projects 2010*. Canberra, Australia: Global CCS Institute., 2010.
112. Fischer, B.S., et al., *Issues related to mitigation in the long term context*. *Climate Change 2007: Mitigation. Contribution of Working Group III to the Fourth Assessment Report of the Intergovernmental Panel on Climate Change*. 2007: Cambridge: Cambridge University Press.
113. Shaffer, K.H., *Consumptive Water Use in the Great Lakes Basin, U.S. Geological Survey (USGS)*, <http://pubs.usgs.gov/fs/2008/3032/pdf/fs2008-3032.pdf>, 2008, U.S. Geological Survey (USGS) Available from: <http://pubs.usgs.gov/fs/2008/3032/pdf/fs2008-3032.pdf>.
114. Blanch, H.W., *Bioprocessing for biofuels*. *Current Opinion in Biotechnology*, 2012. **23**(3): p. 390-395.
115. Paap, S.M., et al., *Biochemical production of ethanol and fatty acid ethyl esters from switchgrass: A comparative analysis of environmental and economic performance*. *Biomass and Bioenergy*, 2013. **49**(0): p. 49-62.
116. Lange, B.M., et al., *Isoprenoid biosynthesis: The evolution of two ancient and distinct pathways across genomes*. *Proceedings of the National Academy of Sciences of the United States of America*, 2000. **97**(24): p. 13172-13177.
117. Boerjan, W., J. Ralph, and M. Baucher, *Lignin biosynthesis*. *Annual Review of Plant Biology*, 2003. **54**: p. 519-546.
118. Kim, S., et al., *Computational Study of Bond Dissociation Enthalpies for a Large Range of Native and Modified Lignins*. *The Journal of Physical Chemistry Letters*, 2011. **2**(22): p. 2846-2852.
119. Fernandez-Fueyo, E., et al., *Comparative genomics of *Ceriporiopsis subvermispota* and *Phanerochaete chrysosporium* provide insight into selective ligninolysis*. *Proceedings of the National Academy of Sciences of the United States of America*, 2012. **109**(14): p. 5458-5463.

120. Li, Q., et al., *Comparison of different alkali-based pretreatments of corn stover for improving enzymatic saccharification*. *Bioresource Technology*, 2012. **125**: p. 193-199.
121. Martinez, D., et al., *Genome, transcriptome, and secretome analysis of wood decay fungus *Postia placenta* supports unique mechanisms of lignocellulose conversion*. *Proceedings of the National Academy of Sciences of the United States of America*, 2009. **106**(6): p. 1954-1959.
122. Martinez, D., et al., *Genome sequence of the lignocellulose degrading fungus *Phanerochaete chrysosporium* strain RP78*. *Nature Biotechnology*, 2004. **22**(6): p. 695-700.
123. Salvachua, D., et al., *Fungal pretreatment: An alternative in second-generation ethanol from wheat straw*. *Bioresource Technology*, 2011. **102**(16): p. 7500-7506.
124. Archibald, F.S., et al., *Kraft pulp bleaching and delignification by *Trametes versicolor**. *Journal of Biotechnology*, 1997. **53**(2-3): p. 215-236.
125. Breen, A. and F.L. Singleton, *Fungi in lignocellulose breakdown and biopulping*. *Current Opinion in Biotechnology*, 1999. **10**(3): p. 252-258.
126. Kleppe, P.J., *KRAFT PULPING*. *Tappi*, 1970. **53**(1): p. 35-&.
127. Aziz, S. and K. Sarkanen, *Organosolv Pulping - A Review*. *Tappi Journal*, 1989. **72**(3): p. 169-175.
128. Johansson, A., O. Aaltonen, and P. Ylinen, *Organosolv Pulping - Methods and Pulp Properties*. *Biomass*, 1987. **13**(1): p. 45-65.
129. Bozell, J.J., et al., *Solvent fractionation of renewable woody feedstocks: Organosolv generation of biorefinery process streams for the production of biobased chemicals*. *Biomass & Bioenergy*, 2011. **35**(10): p. 4197-4208.
130. Bozell, J.J., *An evolution from pretreatment to fractionation will enable successful development of the integrated biorefinery*. *Bioresources*, 2010. **5**(3): p. 1326-1327.
131. Li, C.L., et al., *Comparison of dilute acid and ionic liquid pretreatment of switchgrass: Biomass recalcitrance, delignification and enzymatic saccharification*. *Bioresource Technology*, 2010. **101**(13): p. 4900-4906.
132. Swatloski, R.P., et al., *Dissolution of cellose with ionic liquids*. *Journal of the American Chemical Society*, 2002. **124**(18): p. 4974-4975.
133. Wang, H., G. Gurau, and R.D. Rogers, *Ionic liquid processing of cellulose*. *Chemical Society Reviews*, 2012. **41**(4): p. 1519-1537.
134. Tao, L., et al., *Improved ethanol yield and reduced minimum ethanol selling price (MESP) by modifying low severity dilute acid pretreatment with deacetylation and mechanical refining: 2) Techno-economic analysis*. *Biotechnology for Biofuels*, 2012. **5**.
135. Kobayashi, T., et al., *Molecular-Level Consequences of Biomass Pretreatment by Dilute Sulfuric Acid at Various Temperatures*. *Energy & Fuels*, 2011. **25**(4): p. 1790-1797.
136. Moxley, G., et al., *Structural changes of corn stover lignin during acid pretreatment*. *Journal of Industrial Microbiology & Biotechnology*, 2012. **39**(9): p. 1289-1299.
137. Nowakowski, D.J., et al., *Lignin fast pyrolysis: Results from an international collaboration*. *Journal of Analytical and Applied Pyrolysis*, 2010. **88**(1): p. 53-72.
138. Zakzeski, J., et al., *The Catalytic Valorization of Lignin for the Production of Renewable Chemicals*. *Chemical Reviews*, 2010. **110**(6): p. 3552-3599.
139. Shabtai, J., W. Zmierczak, and E. Chornet. *Conversion of lignin to reformulated gasoline compositions. 1. Basic processing scheme*. 1997. Elsevier.
140. Shabtai, J., et al., *Conversion of lignin. 2. Production of high-octane fuel additives*. *Prepr. Symp. - Am. Chem. Soc., Div. Fuel Chem.*, 1999. **44**(Copyright (C) 2013 American Chemical Society (ACS). All Rights Reserved.): p. 267-272.
141. Shabtai, J., et al. *Lignin conversion to high-octane fuel additives*. 1999. Elsevier Science.
142. Shabtai, J.S., W.W. Zmierczak, and E. Chornet, *Process for conversion of lignin to reformulated hydrocarbon gasoline*, 1999, The University of Utah Research Foundation, USA . p. 32 pp.

143. Vigneault, A., D.K. Johnson, and E. Chornet, *Base-catalyzed depolymerization of lignin: separation of monomers*. Can. J. Chem. Eng., 2007. **85**(Copyright (C) 2013 American Chemical Society (ACS). All Rights Reserved.): p. 906-916.
144. Miller, J.E., et al., *Batch microreactor studies of lignin and lignin model compound depolymerization by bases in alcohol solvents*. Fuel, 1999. **78** (Copyright (C) 2013 American Chemical Society (ACS). All Rights Reserved.): p. 1363-1366.
145. Macala, G.S., et al., *Hydrogen Transfer from Supercritical Methanol over a Solid Base Catalyst: A Model for Lignin Depolymerization*. Chemsuschem, 2009. **2**(3): p. 215-217.
146. Wang, X.Y. and R. Rinaldi, *Exploiting H-transfer reactions with RANEY (R) Ni for upgrade of phenolic and aromatic biorefinery feeds under unusual, low-severity conditions*. Energy & Environmental Science, 2012. **5**(8): p. 8244-8260.
147. Song, Q., et al., *Lignin depolymerization (LDP) in alcohol over nickel-based catalysts via a fragmentation-hydrogenolysis process*. Energy & Environmental Science, 2013. **6**(3): p. 994-1007.
148. Holladay, J., et al., *Top value-added chemicals from biomass volume II—results of screening for potential candidates from biorefinery lignin.*, 2007, Oak Ridge, TN, USA: Pacific Northwest National Laboratory.
149. Van de Vyver, S. and Y. Roman-Leshkov, *Emerging catalytic processes for the production of adipic acid*. Catalysis Science & Technology, 2013. **3**(6): p. 1465-1479.
150. ICIS Chemical Business, *5/14/2007, Vol. 271, Issue 19*, 2007. p. 43.
151. ICIS Chemical Business, *10/10/2011, Vol. 280, Issue 11*, 2011. p. 55.
152. ICIS Chemical Business, *2/28/2011, Vol. 279, Issue 8*, 2011. p. 43.
153. ICIS Chemical Business, *9/6/2011, Vol. 280, Issue 9*, 2011. p. 43.
154. ICIS Chemical Business, *10/1/2012, Vol. 282, Issue 9*, 2012. p. 34.
155. Chemical Week, *10/3/2011, Vol. 173 Issue 24*, 2011. p. 35 Available from: http://www.prweb.com/releases/adipic_acid_market/polyurethane_resins/prweb9410852.htm
156. Bidy, M.J. and J. SB, *Catalytic Upgrading of Sugars to Hydrocarbons Technology Pathway*, 2013 Available from: <http://www.nrel.gov/docs/fy13osti/58055.pdf>.
157. Keller and Heckmann LLP, *Assessment Plan for Corn Steep Liquor (CAS #66071-94-1) in Accordance with the USEPA High Production Volume Chemical Challenge Program*. 2006: Prepared for The Corn Refiners Association.
158. Verevkin, S.P., et al., *Biomass-Derived Platform Chemicals: Thermodynamic Studies on the Conversion of 5-Hydroxymethylfurfural into Bulk Intermediates*. Industrial & Engineering Chemistry Research, 2009. **48**(22): p. 10087-10093.
159. Lewis Sr., R.J., *Hawley's Condensed Chemical Dictionary*. 15th Edition ed. 2007, New York: Hawley's Condensed Chemical Dictionary.
160. Merrill, A.L. and B.K. Watt, *Energy Value of Foods: Basis and Derivation*, U.A.H. #74, Editor 1973 Available from: <http://www.ars.usda.gov/SP2UserFiles/Place/12354500/Data/Classics/ah74.pdf>.
161. Roels, J.A., *Energetics and Kinetics in Biotechnology*. 1983, Amsterdam: Elsevier Biomedical Press.
162. Bailey, J.E. and D.F. Ollis, *Biochemical Engineering Fundamentals*. 2nd Edition ed. 1986, New York: McGraw-Hill.

Appendix A. Individual Equipment Cost Summary

The following table shows abbreviated specifications, purchased cost and installed cost for each piece of equipment in this process design. Although each piece of equipment has its own line, many were quoted as part of a package. Updated or new equipment cost estimates provided from Harris Group for this analysis (beyond estimates that were utilized in the 2011 ethanol report) are highlighted in blue in the table below. NREL and Harris Group would like to acknowledge the equipment vendors who assisted us with the cost estimation effort for this design report.

REV 0	PROJECT: 30374.00 Mechanical Equipment List: Advanced Biofuels Engineering Design: Biochemical Conversion of Corn Stover						Scaled Installed Costs													
	5/1/2013																			
EQPT NO	EQUIPMENT TITLE	DESCRIPTION	HP	MATERIAL	NUM REQD	\$	Year of Quote	Purch Cost in Base Yr	Scaling Variable	Scaling Val	Units	Scaling Exp	Inst Factor	New Val	Size Ratio	Scaled Purch Cost	Purch Cost in Proj year	Inst Cost in Proj year		
C- 101	Transfer Conveyor	160 MTPH ea., enclosed, 60 in. x 65 ft.	20 hp	CS	2	\$5,397,000	2009	\$5,397,000	STRM.101	94697	kg/hr	0.60	1.7	104167	1.10	\$5,714,628	\$6,413,216	\$10,902,467		
C- 102	High Angle Transfer Conveyor	160 MTPH ea., enclosed, 72 in. wide	50 hp	CS	2	INCLUDED														
C- 103	Reversing Load-in Conveyor	320 MT / hr, enclosed, 84 in. wide	20 hp	CS	1	INCLUDED														
C- 104	Dome Reclaim System	100 MTPH ea.	45 kw	CS	2	\$3,046,000	2009	\$3,046,000	STRM.101	94697	kg/hr	0.60	1.7	104167	1.10	\$3,225,265	\$3,619,540	\$6,153,218		
C- 105	Reclaim Conveyor	100 MTPH ea., enclosed, 48 in. x 125	10 hp	CS	2	INCLUDED														
C- 106	High Angle Transfer Conveyor	100 MTPH, enclosed, 72 in. wide	20 hp	CS	1	INCLUDED														
C- 107	Elevated Transfer Conveyor	100 MTPH, enclosed, 48 in. x 200 ft.	10 hp	CS	1	INCLUDED														
C- 108	Process Feed Conveyor	70 MTPH ea., enclosed, 42 in. x 25 ft.	5 hp ea.	CS	1	INCLUDED														
M- 101	Truck Scale	10' x 70', 200,000 lb		CONCRETE	2	\$110,000	2009	\$110,000	STRM.101	94697	kg/hr	0.60	1.7	104167	1.10	\$116,474	\$130,712	\$222,211		
M- 102	Truck Dumper	70' x 55 ton x 63 degree	2 x 50 hp	CS	2	\$484,000	2009	\$484,000	STRM.101	94697	kg/hr	0.60	1.7	104167	1.10	\$512,485	\$575,134	\$977,727		
M- 103	Truck Dumper Hopper	3500 cu.ft. hopper w/ drag chain	50 hp	CS	2	\$502,000	2009	\$502,000	STRM.101	94697	kg/hr	0.60	1.7	104167	1.10	\$531,544	\$596,523	\$1,014,089		
M- 104	Concrete Feedstock Storage	98 ft. dia., 160 ft. high., 4000 MT		CONCRETE	2	\$3,500,000	2009	\$3,500,000	STRM.101	94697	kg/hr	0.60	1.7	104167	1.10	\$3,705,984	\$4,159,025	\$7,070,342		
M- 105	Belt Scale	Scale plus processor		CS	2	\$10,790	2009	\$10,790	STRM.101	94697	kg/hr	0.60	1.7	104167	1.10	\$11,425	\$12,822	\$21,797		
M- 106	Dust Collection System	8500 ACFM	25 hp	CS	6	\$279,900	2009	\$279,900	STRM.101	94697	kg/hr	0.60	1.7	104167	1.10	\$296,373	\$332,603	\$565,425		
Area 100 Totals																\$14,114,178	\$15,839,574	\$26,927,276		

Appendix C. Process Parameters/Operating Summary

Feedstock		Conditioning		Boiler/Turbogenerator	
Moisture Content	20%	Ammonia Loading (g/L hydrolyzate)	1.6	WWT sludge moisture %	54.3%
Pretreatment		Sugar Losses:		First effect lignin moisture %	
Acid Conc (wt%)	0.43	Xylose	0.0%	Combined boiler feed moisture	62.5%
Acid Loading (mg/g dry biomass)	9.0	Arabinose	1.0%	Boiler feed combustion energy MMkcal/hr	-182
Total Solids (wt%)	30.0%	Glucose	0.0%	% from lignin cake	36%
Insoluble Solids in (wt%)	26.0%	Galactose	1.0%	% from biogas	44%
Insoluble Solids out (wt%)	18.7%	Mannose	1.0%	Boiler feed heating value (kcal/kg)	-443
Temperature (°C)	158	Cellobiose	1.0%	Boiler feed heating value (Btu/lb)	-798
Pressure (atm)	5.7	Fermentation		Boiler efficiency (feed/steam)	
Conversions		Overall	Total Solids (wt%)	29.0%	79%
Cellulose to Glucolig	0.3%	Insoluble Solids (wt%)	1.5%	Steam loop flow (kg/hr)	232,711
Cellulose to Cellobiose	0.0%	Temperature (°C)	32	Total Generator Output (kW)	-53,057
Cellulose to Glucose	9.9%	Pressure (atm)	1.0	to A100 Feedstock Handling	859
Cellulose to HMF	0.0%	Residence Time (days)	2.9	to A200 Pretreatment	7,975
Xylan to Oligomer	2.4%	Conversions:		to A300 Hydrolysis/Conditioning/Bioconversion	20,009
Xylan to Xylose	90.0%	Glucose to FFA	95.0%	to A400 Enzyme Production	2,687
Xylan to Furfural	5.0%	Glucose to Zymo (cell mass)	2.0%	to A500 Recovery + Upgrading	633
Xylan to Tar	0.0%	Glucose to Glycerol	0.0%	to A600 Wastewater	4,861
Mannan to Oligomer	2.4%	Glucose to Succinic Acid	0.0%	to A700 Storage	9
Mannan to Mannose	90.0%	Glucose to Acetic Acid	0.0%	to A800 Boiler/Turbogen	1,490
Mannan to HMF	5.0%	Glucose to Lactic Acid	0.0%	to A900 Utilities	4,042
Galactan to Oligomer	2.4%	Xylose to FFA	85.0%	Excess electricity to grid	10,490
Galactan to Galactose	90.0%	Xylose to Zymo	2.0%	Electricity Used (kW)	42,566
Galactan to HMF	5.0%	Xylose to Glycerol	0.0%	Electricity Used (%)	80%
Arabinan to Oligomer	2.4%	Xylose to Xylitol	0.0%	Wastewater Treatment	
Arabinan to Arabinose	90.0%	Xylose to Succinic Acid	0.0%	NH3-N to Ferm mg/L	767
Arabinan to Furfural	5.0%	Xylose to Acetic Acid	0.0%	NH3-N out of Ferm mg/L	747
Arabinan to Tar	0.0%	Xylose to Lactic Acid	0.0%		
Acetate to Oligomer	0.0%	Arabinose to Zymo	2.0%		
Acetate to Acetic Acid	100.0%	Arabinose to Glycerol	0.0%	Hydraulic Load (L/hr)	251,777
Furfural to Tar	100.0%	Arabinose to Succinic Acid	0.0%	Hydraulic Load (gpm)	1,109
HMF to Tar	100.0%	Arabinose to Acetic Acid	0.0%	Hydraulic Load (MMgal/day)	1.6
Lignin to Soluble Lignin	5.0%	Arabinose to Lactic Acid	0.0%	Total COD (kg/hr)	31,019
Enzymatic Hydrolysis		Galactose to Zymo	0.0%	Total COD (g/L)	123.2
Enzyme Loading (mg/g cell)	10.0	Galactose to Glycerol	0.0%		
Total Solids (wt%)	19.9%	Galactose to Succinic Acid	0.0%	Hydraulic Load (L/hr)	251,777
Insoluble Solids (wt%)	12.2%	Galactose to Acetic Acid	0.0%	Hydraulic Load (gpm)	1,109
Temperature (°C)	32	Galactose to Lactic Acid	0.0%	Hydraulic Load (MMgal/day)	1.6
Pressure (atm)	1.0	Galactose to Zymo	0.0%	Total COD (kg/hr)	31,019
Residence Time (days)	3.5	Mannose to Zymo	0.0%	Total COD (g/L)	123.2
Conversions:		Mannose to Glycerol	0.0%		
Cellulose to Glucolig	4.0%	Mannose to Succinic Acid	0.0%	Biogas composition (Dry molar%)	
Cellulose to Cellobiose	1.2%	Mannose to Acetic Acid	0.0%	CH4	51%
Cellulose to Glucose	90.0%	Mannose to Lactic Acid	0.0%	CO2	49%
Glucolig to Cellobiose	0.0%	Contamination Loss	3.0%	methane produced (kg/kg COD)	0.239
Glucolig to Glucose	0.0%	FFA Out of Fermenters (wt%)	9.4%	cell mass	0.047
Cellobiose to Glucose	0.0%	Enzyme Production			
Xylan to Oligomer	0.0%	Glucose feed (kg/hr)	1,213		
Xylan to Xylose	0.0%	Protein produced (kg/hr)	290		
Xylose Oligomer to Xylose	0.0%	Protein yield (kg/kg substrate)	0.24		
Xylan to Tar	0.0%	Protein harvest titer (g/L)	40		
Arabinan to Oligomer	0.0%	Compressor electricity (kW)	706		
Arabinan to Arabinose	0.0%	Agitator electricity (kW)	1050		
Galactan to Oligomer	0.0%	Chiller system electricity (kW)	797		
Galactan to Galactose	0.0%	A400 total electricity (kW)	2687		
Galactose Oligomer to Galactose	0.0%	Electricity demand (kWh/kg protn)	9		
Mannan to Oligomer	0.0%	Production selectivity:			
Mannan to Mannose	0.0%	Selectivity to protein	31.3%		
Mannose Oligomer to Mannose	0.0%	Selectivity to cell mass	4.1%		
		Selectivity to CO2	67.6%		

Appendix D. Aspen Plus Properties

The table below is a list of the components used in the Aspen model. Previous versions of the model used custom property databanks created at NREL. Where possible in the new model, these components have been replaced with components from Aspen's native databanks. Property definitions for the few remaining custom components were moved into the model itself (i.e., inside the simulation file) and are discussed here.

The component CSL (corn steep liquor) used in previous models was removed. CSL streams are now modeled as 50% water, 25% protein, and 25% lactic acid [157].

Component	Property	Quantity	Units	Reference
H2O	-	-	-	Native Aspen component
GLUCOSE	-	-	-	Native Aspen component (dextrose)
GALACTOS	-	-	-	Duplicate of GLUCOSE
MANNOSE	-	-	-	Duplicate of GLUCOSE
XYLOSE	DHFORM	-216752.65	cal/mol	Native Aspen component (d-xylose) with DHFORM specified (5/6 of GLUCOSE DHFORM)
ARABINOS	-	-	-	Duplicate of XYLOSE
CELLOB	-	-	-	Cellobiose. Used native Aspen component sucrose
SUCROSE	-	-	-	Native Aspen component
GLUCOLIG	MW	162.1424		Glucose oligomers. Most properties from GLUCOSE; MW is GLUCOSE minus H2O
	DHFORM	-192875.34	cal/mol	Back-calculated to match ΔH_c of CELLULOS
GALAOLIG	-	-	-	Galactose oligomers. Duplicate of GLUCOLIG
MANOLIG	-	-	-	Mannose oligomers. Duplicate of GLUCOLIG
XYLOLIG	MW	132.11612		Xylose oligomers. Most properties from XYLOSE; MW is XYLOSE minus H2O
	DHFORM	-149412.58	cal/mol	Back-calculated to match ΔH_c of XYLAN
ARABOLIG	-	-	-	Arabinose oligomers. Duplicate of XYLOLIG
EXTRACT	-	-	-	Organic extractives. Duplicate of GLUCOSE
LGNSOL	-	-	-	Solubilized lignin. Native Aspen component vanillin (see note at LIGNIN)

Component	Property	Quantity	Units	Reference
HMF	MW	126.11		(5-hydroxymethylfurfural) Properties for HMF were estimated within Aspen using NIST TDE routines. Specify molecular structure, MW, TB and DHFORM. From [158].
	TB	532.7	K	
	DHFORM	-79774.53	cal/mol	
	DHVLWT-1	80550000	J/kmol	
	TC	731.012	K	NIST TDE
	PC	5235810	Pa	
	OMEGA	0.99364671		
	VC	0.3425	m ³ /kmol	
	RKTZRA	0.198177974		
FURFURAL	-	-	-	Native Aspen component
AACID	-	-	-	Native Aspen component (acetic acid)
LACID	-	-	-	Native Aspen component (lactic acid)
XYLITOL	-	-	-	Native Aspen component
GLYCEROL	-	-	-	Native Aspen component
SUCCACID	-	-	-	Native Aspen component (Succinic acid)
NH3	-	-	-	Native Aspen component
H2SO4	-	-	-	Native Aspen component
NH4SO4	-	-	-	Native Aspen component (ammonium sulfate)
NH4ACET	PLXANT/1	-1.00E+20	atm	Native Aspen component (ammonium acetate) forced non-volatile
DAP	-	-	-	Native Aspen component (diammonium phosphate)
HNO3	-	-	-	Native Aspen component
NANO3	-	-	-	Native Aspen component
NAOH	-	-	-	Native Aspen component
CNUTR	-	-	-	Cellulase nutrient mix. Duplicate of glucose
WNUTR	-	-	-	WWT nutrient mix. Duplicate of glucose
DENAT	-	-	-	Denaturant. Native Aspen component (n-heptane)

Component	Property	Quantity	Units	Reference
OIL	-	-	-	Corn oil antifoam. Native Aspen component (oleic acid)
O2	-	-	-	Native Aspen component
N2	-	-	-	Native Aspen component
NO	-	-	-	Native Aspen component
NO2	-	-	-	Native Aspen component
CO	-	-	-	Native Aspen component
CO2	-	-	-	Native Aspen component
CH4	-	-	-	Native Aspen component
H2S	-	-	-	Native Aspen component
SO2	-	-	-	Native Aspen component
CELLULOS	DHSFRM	-233200.06	cal/mol	Native Aspen component with specified heat of formation; back-calculated
GALACTAN	-	-	-	Duplicate of CELLULOS
MANNAN	-	-	-	Duplicate of CELLULOS
XYLAN	Formula	C ₅ H ₈ O ₄ (monomer)		
	MW	132.117		
	DHSFRM	-182099.93	cal/mol	From [13]. Assumes the ratio of ΔH_c of glucose:xylose is the same for cellulose:xylan.
ARABINAN	-	-	-	Duplicate of xylan
LIGNIN	-	-	-	Used native Aspen component vanillin (C ₈ H ₈ O ₃). The HHV of this compound (-23,906 Btu/kg) is very close to what we previously assumed for lignin as a custom component (-24,206)
ACETATE	-	-	-	Used native Aspen component acetic acid
PROTEIN	Formula	CH _{1.57} O _{0.31} N _{0.29} S _{0.007}		Wheat gliadin [159]
	MW	22.8396		
	DHSFRM	-17618	cal/mol	From literature value of gliadin ΔH_c [160]
	PLXANT/1	-1.00E+20	atm	Forces non-volatility

Component	Property	Quantity	Units	Reference
ASH	-	-	-	Native Aspen component CaO
ENZYME	Formula	$CH_{1.59}O_{0.42}N_{0.24}S_{0.01}$		Provided by Novozymes [3]
	MW	24.0156		
	DHSFRM	-17618	cal/mol	copied from PROTEIN
DENZ	-	-	-	Denatured enzyme. Duplicate of enzyme
ZYMO	Formula	$CH_{1.8}O_{0.5}N_{0.2}$		Z. mobilis cell mass. Average composition of several microorganisms In [161]
	MW	24.6264		
	DHSFRM	-31169.39	cal/mol	From [13] after [162]
TRICHO	Formula	$CH_{1.645}O_{0.445}N_{0.205}S_{0.005}$		T. reesei cell mass. Average of generic cell mass [81] and the ENZYME composition
	MW	23.8204		
	DHSFRM	-23200.01	cal/mol	Copied BIOMASS
BIOMASS	Formula	$CH_{1.64}O_{0.39}N_{0.23}S_{0.0035}$		WWT sludge.
	MW	23.238		
	DHSFRM	-23200.01	cal/mol	From [13] after [162]
TAR	-	-	-	Modeled as solid xylose
LIME	-	-	-	Native Aspen component (calcium hydroxide)
CASO4	-	-	-	Native Aspen component
C	-	-	-	Native Aspen component (graphite carbon)
N-TETRADECANOIC-ACID	Formula	$C_{14}H_{28}O_2$		Native Aspen component
ETHYL-PALMITATE	Formula	$C_{18}H_{36}O_2-N_2$		Native Aspen component
METHYL-OLEATE	Formula	$C_{19}H_{36}O_2$		Native Aspen component
N-PENTADECANE	Formula	$C_{15}H_{32}$		Native Aspen component
N-HEXADECANOIC-ACID	Formula	$C_{16}H_{32}O_2$		Native Aspen component
N-HEXADECANE	Formula	$C_{16}H_{34}$		Native Aspen component
HYDROGEN	Formula	H_2		Native Aspen component

Appendix E. Process Flow Diagrams

High-level stream table information from Aspen Plus modeling output follows, for key streams associated with each process operation area. This is followed by high-level PFDs for the associated process areas. Space for stream tables was limited; below is a key to lumped components. As the stream table information focuses primarily on the high-level overall process and does not include every individual modeled stream within each process area, mass balance closure around a given unit area may not be 100%.

Other sugars (SS)	arabinose, mannose, galactose, cellobiose, sucrose
Sugar oligomers (SS)	oligomers of glucose, xylose, and all minor sugars
Organic soluble solids (SS)	ammonium acetate, solubilized lignin, organic extractives, lactic acid, cellulase and WWT chemicals
Inorganic soluble solids (SS)	ammonium sulfate, diammonium phosphate, sodium hydroxide, nitric acid, sodium nitrate
Furfurals	furfural, HMF
Other organics	glycerol, gasoline denaturant, corn oil, sorbitol, succinic acid, xylitol
CO/SO _x /NO _x /H ₂ S	NO, NO ₂ , SO ₂ , CO, H ₂ S
Other struct. carbohydr. (IS)	arabinan, mannan, galactan
Protein (IS)	corn protein, cellulase, denatured cellulase
Cell mass (IS)	WWT sludge, <i>Z. mobilis</i> from biological conversion, <i>T. reesei</i> from cellulase production
Other insoluble solids (IS)	tar, ash, carbon, lime, gypsum

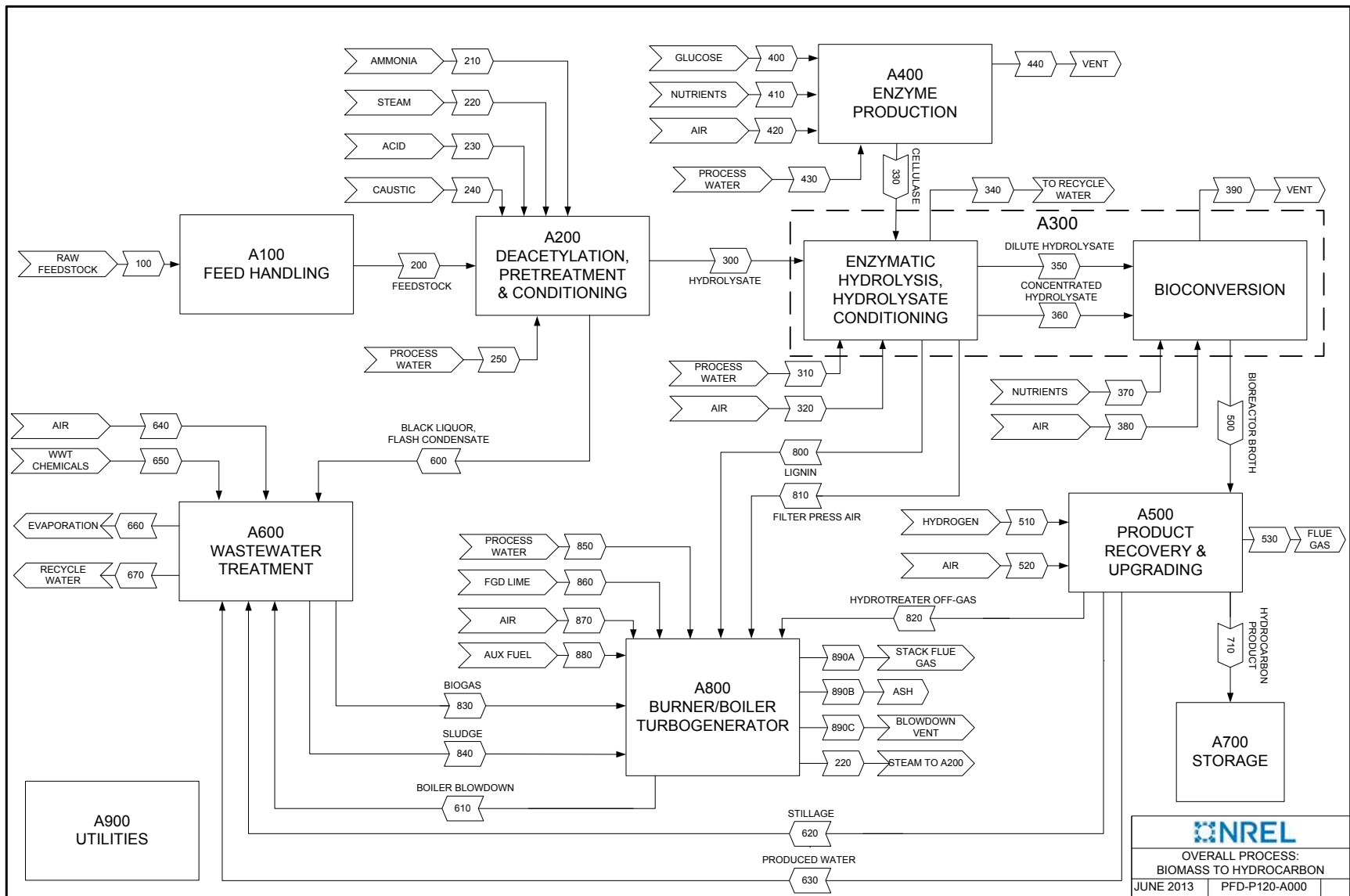


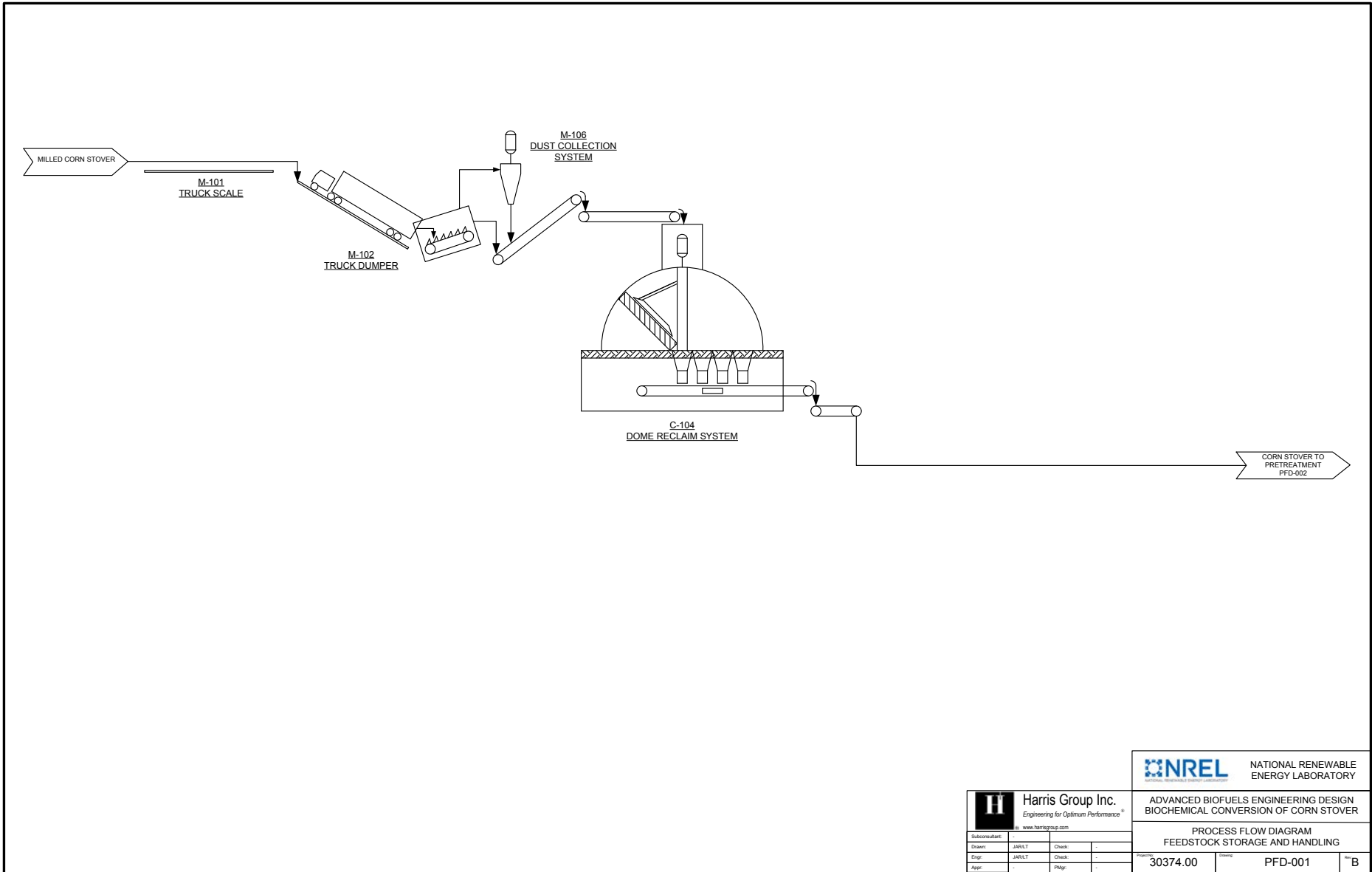
Figure 30. Overall process schematic for Aspen stream tables



Aspen Plus mass balance information for key stream tables:

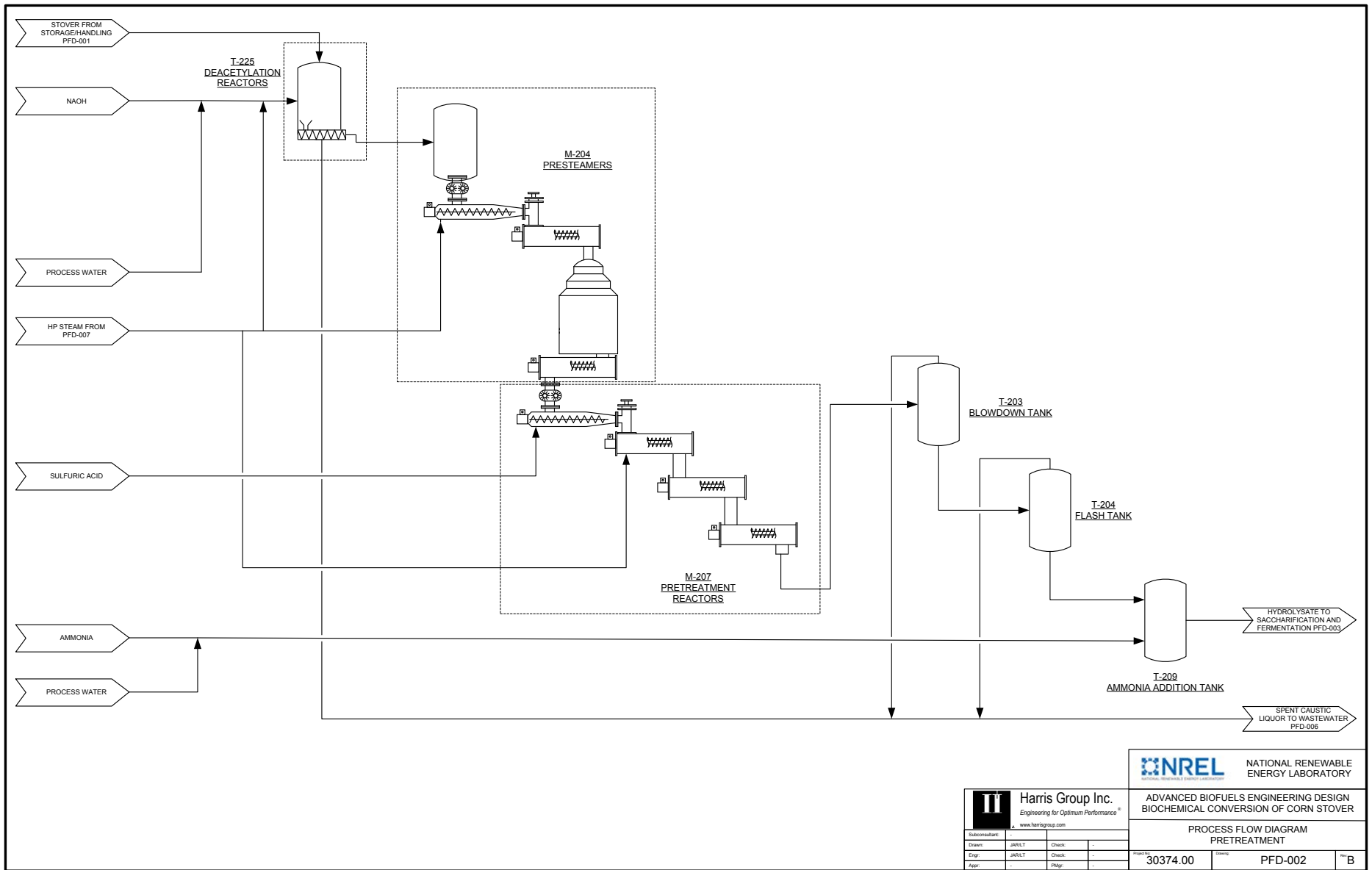
COMPONENT	UNITS	100	200	210	220	230	240	250	300	310	320	330	340	350	360	370	380
Total Flow	kg/hr	104,167	104,167	260	23,889	806	1,406	305,359	325,613	67,245	163	6,942	175,101	106,886	74,300	1,670	421,150
Insoluble Solids	%	67.7%	67.7%	0.0%	0.0%	0.0%	0.0%	0.0%	12.4%	0.0%	0.0%	5.3%	0.0%	0.0%	0.1%	0.0%	0.0%
Soluble Solids	%	12.3%	12.3%	0.0%	0.0%	0.0%	100.0%	0.0%	7.9%	0.0%	0.0%	0.3%	0.0%	14.8%	49.5%	0.0%	0.0%
Temperature	°C	25	25	20	268	20	20	33	76	20	25	29	35	43	63	20	25
Pressure	atm	1.0	1.0	9.0	13.0	3.4	1.0	5.0	7.8	1.0	1.0	1.7	1.0	1.0	1.0	1.0	1.0
Vapor Fraction		0.0	0.0	0.0	1.0	0.0	0.0	0.0	0.0	0.0	1.0	0.0	0.0	0.0	0.0	0.0	1.0
RDB	kg/hr																
FFA	kg/hr																
Water	kg/hr	20,833	20,833		23,889	56		305,359	259,103	67,245		6,549	174,843	90,917	37,298	705	
Glucose (SS)	kg/hr								3,381					8,793	20,518		
Xylose (SS)	kg/hr								16,310					4,844	11,303		
Other sugars (SS)	kg/hr	642	642						3,682					1,192	2,782		
Sugar Oligomers (SS)	kg/hr								559					477	1,114		
Organic Soluble Solids (SS)	kg/hr	12,208	12,208						699			20	38	210	451	347	
Inorganic Soluble Solids (SS)	kg/hr						1,406		1,011					276	645	127	
Ammonia	kg/hr			260													
Acetic Acid	kg/hr																
Sulfuric Acid	kg/hr					750											
Furfurals	kg/hr								504				220	150	130		
Other Organics	kg/hr											7		2	5	140	
Carbon Dioxide	kg/hr													0.1			
Methane	kg/hr																
H2	kg/hr																
O2	kg/hr										38						98,093
N2	kg/hr										125						323,057
CO/SOX/NOX/H2S	kg/hr																
Cellulose (IS)	kg/hr	29,205	29,205						26,226					2	4		
Xylan (IS)	kg/hr	16,273	16,273						415					1	1		
Other Struct. Carbohydr. (IS)	kg/hr	3,675	3,675						96					0.1	0.3		
Acetate (IS)	kg/hr	1,508	1,508														
Lignin (IS)	kg/hr	13,132	13,132						9,980					15	35		
Protein (IS)	kg/hr	2,583	2,583						2,583			311		4	10	351	
Cell Mass (IS)	kg/hr											54		0.1	0.2		
Other Insoluble Solids (IS)	kg/hr	4,108	4,108						1,064					2	4		

COMPONENT	UNITS	390	400	410	420	430	440	500	510	520	530	600	610	620	630	640	650
Total Flow	kg/hr	451,657	1,427	189	16,346	5,729	16,750	152,333	221	956	1,408	110,275	4,640	138,805	917	146,928	175
Insoluble Solids	%	0.0%	0.0%	0.0%	0.0%	0.0%	0.0%	2.2%	0.0%	0.0%	0.0%	3.1%	0.0%	2.5%	0.0%	0.0%	0.0%
Soluble Solids	%	0.0%	85.0%	0.0%	0.0%	0.0%	0.0%	6.5%	0.0%	0.0%	0.0%	16.2%	0.0%	7.1%	0.0%	0.0%	0.0%
Temperature	°C	32	28	20	25	33	28	32	25	32	380	85	100	33	39	25	20
Pressure	atm	1.0	1.0	1.0	1.0	5.0	1.0	1.0	1.0	1.0	1.2	1.0	5.4	6.0	1.1	1.0	1.0
Vapor Fraction		1.0	0.0	0.0	1.0	0.0	1.0	0.0	1.0	1.0	1.0	0.0	0.0	0.0	0.0	1.0	0.0
RDB	kg/hr																
FFA	kg/hr							13,946						418			
Water	kg/hr	13,042	214	41	320	5,729	388	124,630			210	88,640	4,640	124,630	917	2,878	
Glucose (SS)	kg/hr		1,213					784						784			
Xylose (SS)	kg/hr							1,945						1,945			
Other sugars (SS)	kg/hr							2,188				321		2,188			
Sugar Oligomers (SS)	kg/hr							1,592						1,592			
Organic Soluble Solids (SS)	kg/hr	8		54				2,381				16,169		2,381			175
Inorganic Soluble Solids (SS)	kg/hr							998				1,406		998			
Ammonia	kg/hr			58			0.2										
Acetic Acid	kg/hr																
Sulfuric Acid	kg/hr																
Furfurals	kg/hr	46						234				332		234			
Other Organics	kg/hr			7				221						221			
Carbon Dioxide	kg/hr	19,144					1,195	5			428			5			
Methane	kg/hr																
H2	kg/hr								221								
O2	kg/hr	96,363			3,733		2,873	1		223	37			1			33,552
N2	kg/hr	323,055			12,293		12,293	2		733	733			2			110,499
CO/SOX/NOX/H2S	kg/hr			8													
Cellulose (IS)	kg/hr							6						6			
Xylan (IS)	kg/hr							2				325		2			
Other Struct. Carbohydr. (IS)	kg/hr							0.5						0.5			
Acetate (IS)	kg/hr																
Lignin (IS)	kg/hr							50						50			
Protein (IS)	kg/hr			21				185						185			
Cell Mass (IS)	kg/hr							3,159						3,159			
Other Insoluble Solids (IS)	kg/hr							5				3,081		5			

COMPONENT	UNITS	660	670	710	800	810	820	830	840	850	860	870	880	890A	890B	890C
Total Flow	kg/hr	146,796	203,888	11,638	43,507	167	742	25,364	19,211	32,637	953	321,584	0	406,986	4,542	2,558
Insoluble Solids	%	0.0%	0.0%	0.0%	36.0%	0.0%	0.0%	0.0%	44.5%	0.0%	100.0%	0.0%	0.0%	0.0%	100.0%	0.0%
Soluble Solids	%	0.0%	0.0%	0.0%	1.4%	0.0%	0.0%	0.0%	1.0%	0.0%	0.0%	0.0%	0.0%	0.0%	0.0%	0.0%
Temperature	°C	25	27	40	29	29	40	37	30	33	25	25	25	156	0	100
Pressure	atm	1.0	1.0	1.1	1.0	1.0	30.6	1.0	2.0	5.4	1.0	1.0	1.0	1.0	1.0	1.0
Vapor Fraction		1.0	0.0	0.0	0.0	1.0	1.0	1.0	0.0	0.0	0.0	1.0	1.0	1.0	0.0	1.0
RDB	kg/hr			11,576												
FFA	kg/hr								19					0.2		
Water	kg/hr	2,857	203,888	30	27,194	4	2	815	10,423	32,637	763	6,298		72,468		2,558
Glucose (SS)	kg/hr				296				1							
Xylose (SS)	kg/hr				163				2							
Other sugars (SS)	kg/hr				40				45					0.4		
Sugar Oligomers (SS)	kg/hr				16				7							
Organic Soluble Solids (SS)	kg/hr				21			0.3	17					0.2		
Inorganic Soluble Solids (SS)	kg/hr	0.1			89				120					109		
Ammonia	kg/hr	0.1														
Acetic Acid	kg/hr															
Sulfuric Acid	kg/hr								24							
Furfurals	kg/hr				5			1	1							
Other Organics	kg/hr								0.3							
Carbon Dioxide	kg/hr	2,533		32			701	17,802	2					78,927		
Methane	kg/hr	2						6,738								
H2	kg/hr			0.2			38							0		
O2	kg/hr	30,899			0.2	38		2	0.1			73,435		12,216		
N2	kg/hr	110,496			0.4	125		4	0.1			241,850		243,119		
CO/SOX/NOX/H2S	kg/hr	9							1					146		
Cellulose (IS)	kg/hr				1,253				6							
Xylan (IS)	kg/hr				413				328							
Other Struct. Carbohydr. (IS)	kg/hr				95				0.5							
Acetate (IS)	kg/hr															
Lignin (IS)	kg/hr				9,930				50							
Protein (IS)	kg/hr				2,879				131							
Cell Mass (IS)	kg/hr				54				4,947							
Other Insoluble Solids (IS)	kg/hr				1,059				3,086		191				4,542	



 NREL <small>NATIONAL RENEWABLE ENERGY LABORATORY</small>		NATIONAL RENEWABLE ENERGY LABORATORY																							
 Harris Group Inc. <small>Engineering for Optimum Performance®</small> <small>www.harrisgroup.com</small>		ADVANCED BIOFUELS ENGINEERING DESIGN BIOCHEMICAL CONVERSION OF CORN STOVER																							
<table border="1"> <tr> <td>Subcontract</td> <td></td> <td></td> <td></td> </tr> <tr> <td>Drawn</td> <td>JARLT</td> <td>Check</td> <td>-</td> </tr> <tr> <td>Eng.</td> <td>JARLT</td> <td>Check</td> <td>-</td> </tr> <tr> <td>Appr.</td> <td></td> <td>PKP</td> <td>-</td> </tr> </table>		Subcontract				Drawn	JARLT	Check	-	Eng.	JARLT	Check	-	Appr.		PKP	-	<table border="1"> <tr> <td colspan="2"> PROCESS FLOW DIAGRAM FEEDSTOCK STORAGE AND HANDLING </td> </tr> <tr> <td> Project: 30374.00 </td> <td> Drawing: PFD-001 </td> </tr> <tr> <td></td> <td style="text-align: right;">B</td> </tr> </table>		PROCESS FLOW DIAGRAM FEEDSTOCK STORAGE AND HANDLING		Project: 30374.00	Drawing: PFD-001		B
Subcontract																									
Drawn	JARLT	Check	-																						
Eng.	JARLT	Check	-																						
Appr.		PKP	-																						
PROCESS FLOW DIAGRAM FEEDSTOCK STORAGE AND HANDLING																									
Project: 30374.00	Drawing: PFD-001																								
	B																								



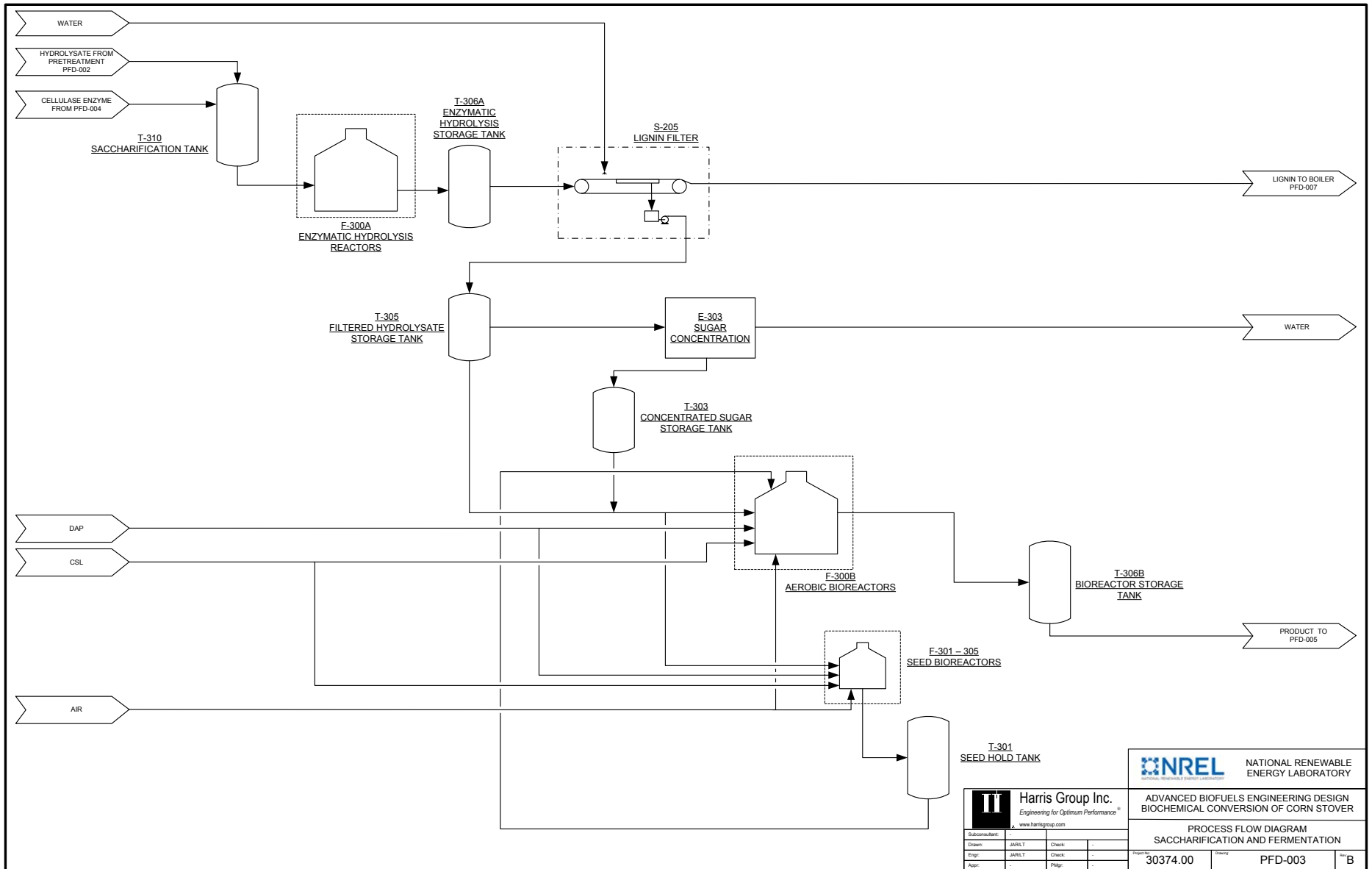
NREL NATIONAL RENEWABLE ENERGY LABORATORY

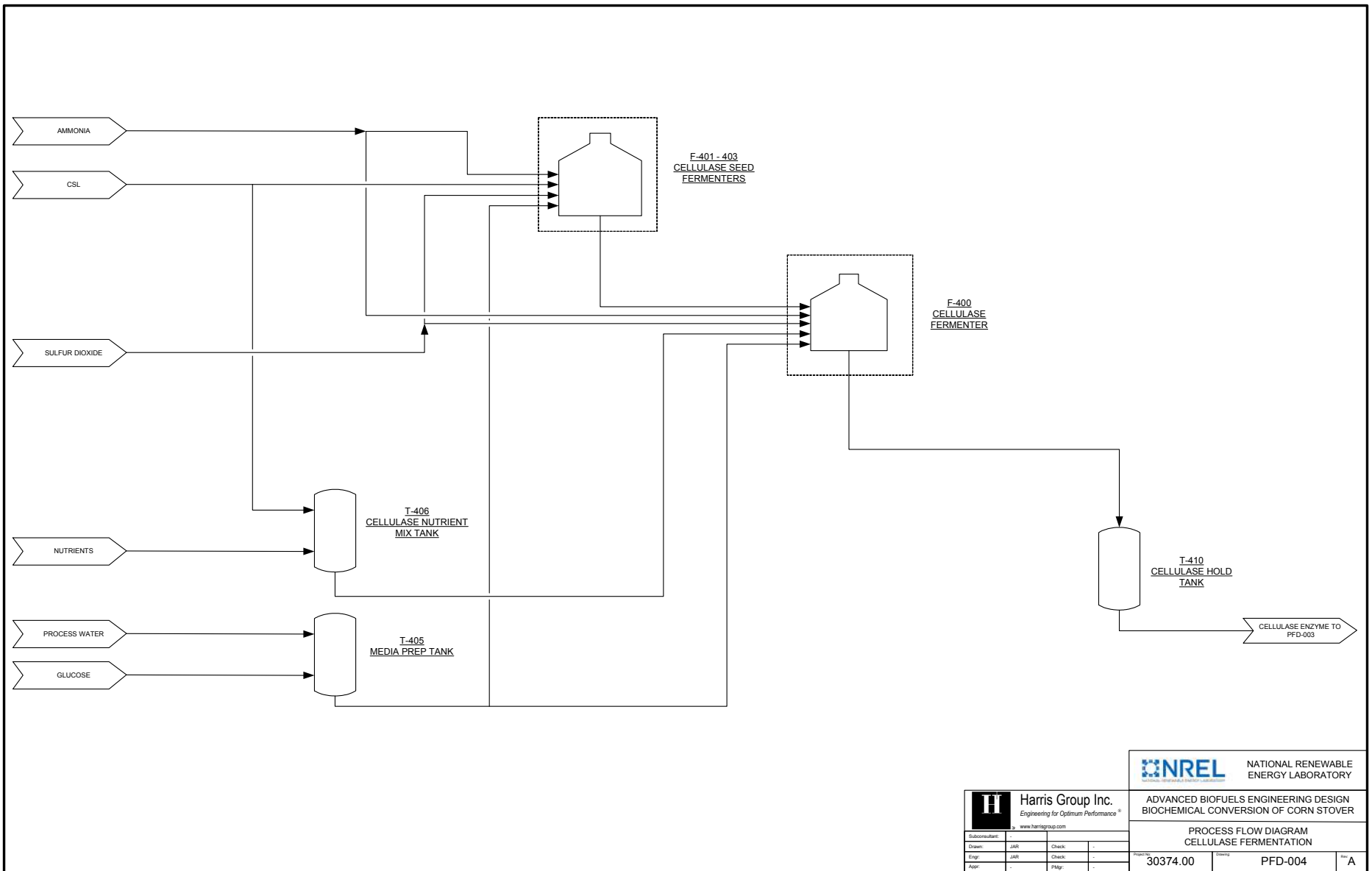
Harris Group Inc.
Engineering for Optimum Performance®
www.harrisgroup.com

ADVANCED BIOFUELS ENGINEERING DESIGN
BIOCHEMICAL CONVERSION OF CORN STOVER

Subcontractor			
Drawn	JARLT	Check	
Eng.	JARLT	Check	
Appr.		PKR	

PROCESS FLOW DIAGRAM PRETREATMENT	
Project No. 30374.00	Drawn PFD-002
	B





NREL NATIONAL RENEWABLE ENERGY LABORATORY

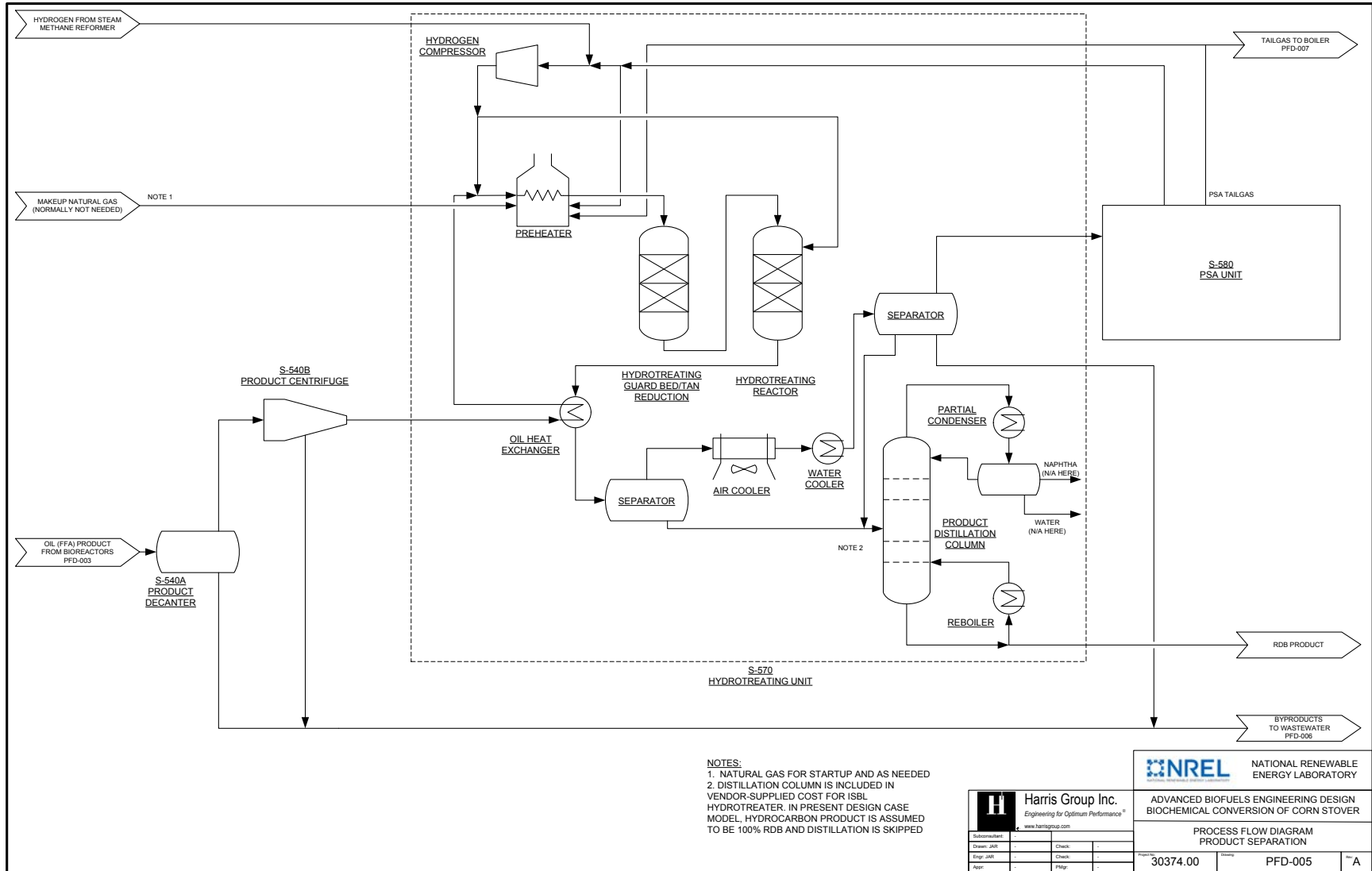
Harris Group Inc.
 Engineering for Optimum Performance®
 www.harrisgroup.com

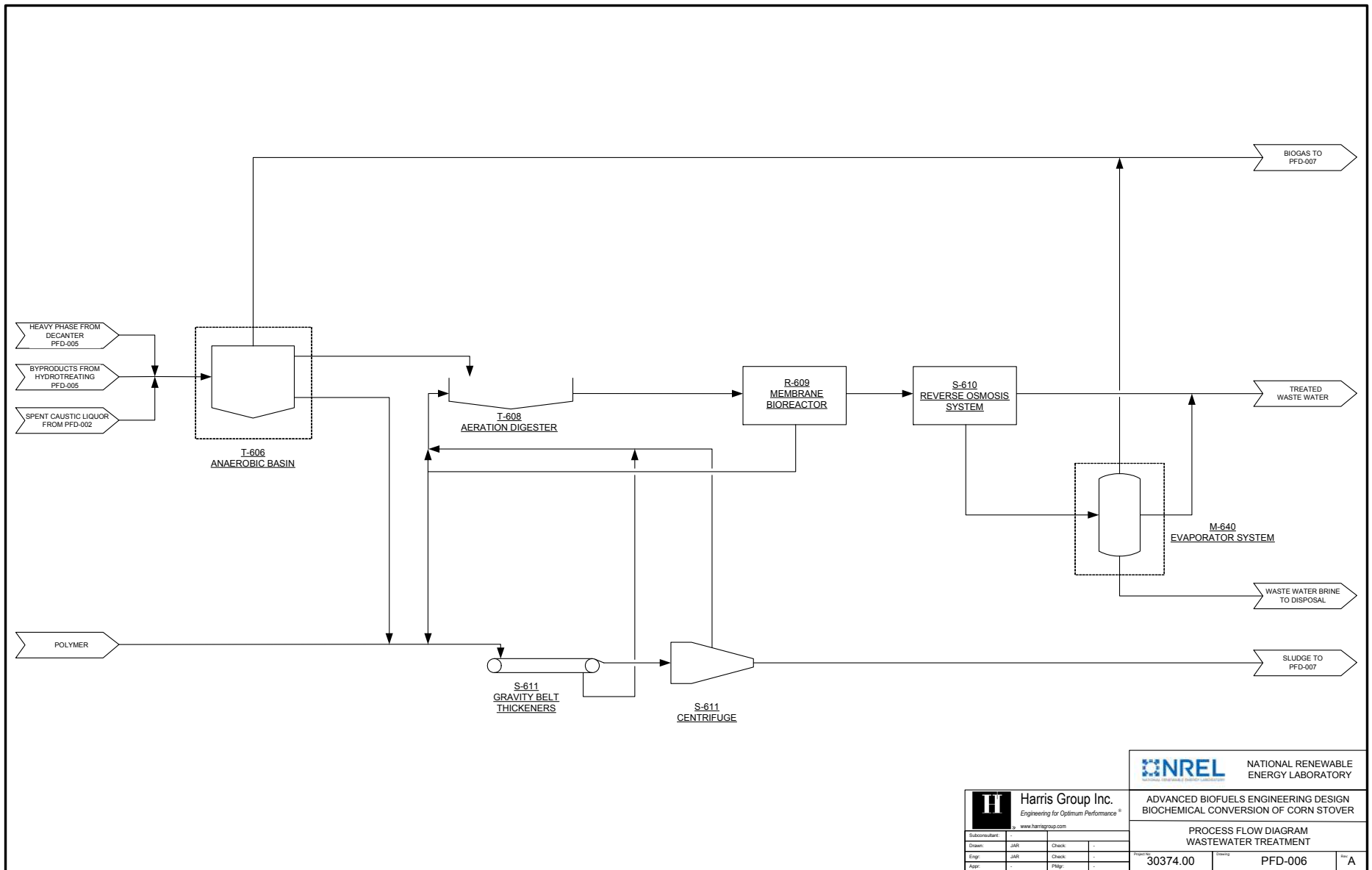
Subconsultant			
Drawn	JAR	Check	-
Eng.	JAR	Check	-
Appr.		INR	-

ADVANCED BIOFUELS ENGINEERING DESIGN
 BIOCHEMICAL CONVERSION OF CORN STOVER

PROCESS FLOW DIAGRAM
 CELLULOSE FERMENTATION

Project No.	30374.00	Sheet No.	PFD-004	Rev.	A
-------------	----------	-----------	---------	------	---





NREL NATIONAL RENEWABLE ENERGY LABORATORY

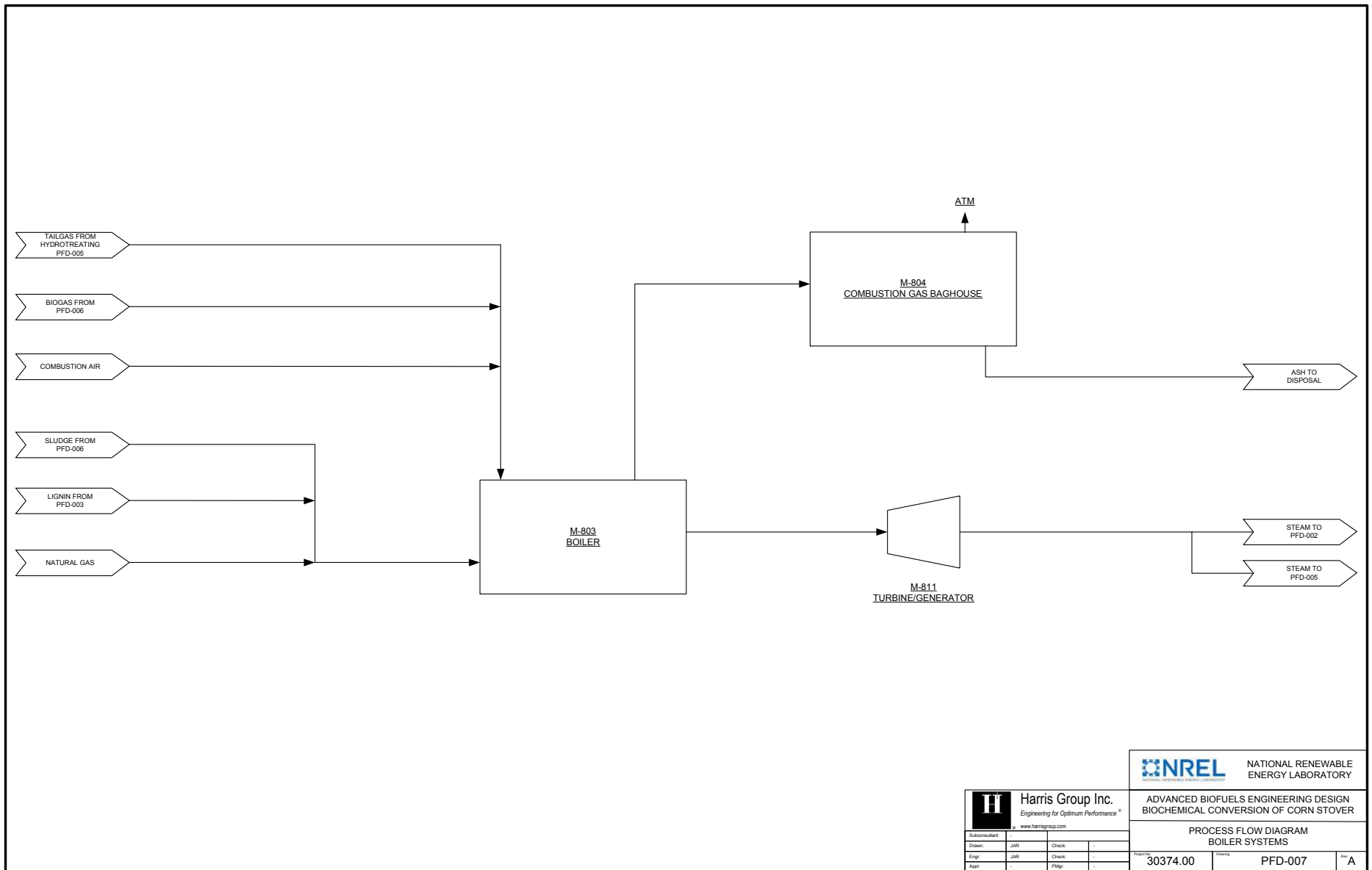
Harris Group Inc.
Engineering for Optimum Performance®
www.harrisgrp.com

ADVANCED BIOFUELS ENGINEERING DESIGN
BIOCHEMICAL CONVERSION OF CORN STOVER

PROCESS FLOW DIAGRAM
WASTEWATER TREATMENT

Subcontract				
Drawn	JAR	Check	-	
Engr.	JAR	Check	-	
Appr.		PKR	-	

Project: 30374.00 Drawing: PFD-006 Rev: A



NREL NATIONAL RENEWABLE ENERGY LABORATORY	
Harris Group Inc. Engineering for Optimum Performance®	
ADVANCED BIOFUELS ENGINEERING DESIGN BIOCHEMICAL CONVERSION OF CORN STOVER	
PROCESS FLOW DIAGRAM BOILER SYSTEMS	
Project: 30374.00	Drawing: PFD-007
Revision:	Sheet: A